Departamento de Biotecnología

Descifrando las funciones de la microbiota intestinal en la obesidad

Memoria de la tesis presentada por

Inmaculada López Almela

Para optar al grado de Doctor en Biotecnología por la Universidad Politécnica de Valencia

Directora: **Dra. Yolanda Sanz Herranz**

Codirectora: **Dra. Marina Romaní Pérez**

Valencia, Junio de 2021

La Dra Yolanda Sanz Herranz, Profesora de Investigación del CSIC, perteneciente al Instituto de Agroquímica y Tecnología de Alimentos (IATA) de Valencia.

CERTIFICA:

que la Graduada en Bioquímica y ciencias Biomédicas Inmaculada López Almela ha realizado bajo su dirección en el Instituto de Agroquímica y Tecnología de Alimentos el trabajo que lleva por título “Descifrando las funciones de la microbiota intestinal en la obesidad”, y autoriza su presentación para optar al grado de Doctor.

Y para que así conste, expido y firmo el presente certificado en Valencia, a 11 de Junio de 2021.

Dra. Yolanda Sanz Herranz

A las estrellas de mi vida

Resumen

En la actualidad, la obesidad es uno de los principales problemas de salud pública debido a su elevada prevalencia y a las comorbilidades asociadas, lo que se traduce en una reducción considerable de la calidad y esperanza de vida, además de un enorme gasto económico.

Se trata de una enfermedad que resulta del desequilibrio entre la ingesta calórica y el gasto energético, que conduce a un aumento del peso y la grasa corporal. Puesto que la obesidad es de origen multifactorial, incluyendo tanto factores genéticos como ambientales, el desarrollo de terapias efectivas para combatirla resulta complejo y se ha convertido en uno de los principales retos de la sociedad.

Se ha demostrado que la microbiota intestinal, mediante su comunicación con el organismo humano, ejerce un papel relevante en el mantenimiento del balance energético y salud metabólica. Por ello, las estrategias basadas en la modificación de la microbiota intestinal para, de forma beneficiosa, modular el metabolismo energético, son consideradas hoy en día potenciales alternativas para el manejo clínico de la obesidad. No obstante, la aplicación de estas estrategias con eficacia requiere un mayor conocimiento sobre cuáles son las especies bacterianas clave en el mantenimiento de la homeostasis energética del hospedador y su modo de acción.

El objetivo general de la tesis ha sido identificar nuevas estrategias basadas en la manipulación de la composición y funciones de la microbiota intestinal eficaces contra la obesidad, así como sus mecanismos de interacción con el hospedador.

El capítulo primero de la tesis se centra en estudiar los mecanismos de acción por los que *Bacteroides uniformis* CECT 7771 ejerce efectos protectores frente al desarrollo de la obesidad, tal y como nuestro grupo ha descrito en trabajos previos. A través de un estudio de 14 semanas en ratones con obesidad inducida por la dieta hemos demostrado que esta cepa reduce la disfunción metabólica a través de la modulación de la microbiota intestinal y las alteraciones inmunológicas. Los efectos inmunoreguladores más destacados de *B. uniformis* fueron la reducción de los niveles de células B, macrófagos totales y el balance de macrófagos pro y antiinflamatorios (M1/M2), así como un aumento en los niveles de linfocitos T reguladores y la citocina antiinflamatoria IL-10, tanto

en intenstino como en tejido adiposo epididimal. Además, en el tejido adiposo se incrementaron las citocinas TSLP e IL-33 que están involucradas en la activación de una respuesta antiinflamatoria. Todos estos efectos sobre el eje intestino-tejido adiposo parecen estar mediados por la activación de TLR5 en ambos tejidos.

En línea con el potencial anti-obesidad mostrado por *B. uniformis* CECT 7771, en otro estudio perteneciente al mismo capítulo, hemos desarrollado una estrategia similar a un simbiótico con el fin de incrementar la eficacia de esta bacteria administrándola a dosis menores. La formulación simbiótica se diseñó en base a trabajos previos del grupo demonstrando la preferencia de *B. uniformis* CECT 7771 por el salvado de trigo (WBE, enriquecido en oligosacáridos de arabinoxilano [AXOS]) como fuente de carbono en cultivos *in vitro*. Para demonstrar la eficacia *in vivo* de la administración conjunta de *B. uniformis* CECT 7771 y WBE hemos realizado una intervención en ratones con obesidad inducida por dieta en la que caracterizamos los beneficios inmuno-metabólicos de dicha combinación, en relación a los efectos individuales de cada componente. Además, con el fin de demostrar la aplicabilidad y ventajas del simbiótico, se estudiaron sus efectos utilizando una dosis inferior de *B. uniformis* CECT 7771 con respecto al primer estudio. Como resultados destacables, mientras que individualmente los componentes del simbiótico ejercieron efectos más modestos contra la obesidad, la combinación fue la intervención más eficaz al reducir el aumento de peso corporal y la adiposidad, al tiempo que mejoraron las rutas del metabolismo energético moduladas por insulina y la homeostasis inmunológica intestinal. En particular, la combinación restauró la reducción de la lipogénesis en el tejido adiposo epididimal y la glucogénesis hepática en obesidad. Además, reforzó la primera línea de defensa inmunológica al aumentar los niveles de butirato y restaurar los niveles de linfocitos intraepiteliales inducidos y las células linfoides innatas de tipo 3. Esta intervención también atenuó la inflamación hepática, causante de resistencia a la insulina en obesidad, a través de una mejora de la señalización de IL-22.

En el segundo capítulo de la tesis hemos llevado a cabo dos estudios preclínicos que describen los efectos de dos nuevas bacterias autóctonas del tracto gastrointestinal humano como potenciales probióticos para el tratamiento de la obesidad identificadas con posterioridad por el grupo.

El primer estudio, muestra los efectos antidiabéticos de *Holdemanella biformis* CECT 9752, una bacteria intestinal aislada de heces de humanos metabólicamente sanos, en un modelo animal de obesidad. La administración de esta cepa de *H. biformis* durante 13 semanas a ratones con obesidad inducida por la dieta redujo los niveles de glucosa en ayuno y mejoró la tolerancia oral a la glucosa de forma independiente a la insulina y asociado a mayores niveles plasmáticos de la hormona gastrointestinal GLP-1, necesaria para el mantenimiento de las variaciones postprandiales de glucosa y la sensibilidad a insulina. A nivel del contenido luminal del intestino grueso, la suplementación con la bacteria incrementó los niveles de ácidos grasos insaturados, lo que indica un aumento de los niveles preabsortivos de potenciales secretagogos lipídicos de GLP-1, como el ácido oleico y α-linoleico. A nivel del intestino delgado, la bacteria promovió la comunicación paracrina de GLP-1 con las inervaciones intestinales, pudiendo directamente incrementar la sensibilidad a GLP-1 de las neuronas vagales aferentes, mecanismo implicado en la comunicación intestino-cerebro que controla la producción endógena de glucosa. A nivel hepático, la suplementación con la bacteria redujo la gluconeogénesis y mejoró la sensibilidad a insulina.

En el segundo estudio hemos evaluado los efectos inmuno-metabólicos de *Phascolarctobacterium faecium* DSM 32890 en un modelo animal de obesidad inducido por dieta. Esta especie bacteriana consume succinato y produce propionato y la cepa fue aislada a partir de heces humanas de voluntarios metabólicamente sanos. La administración diaria de la bacteria al modelo de obesidad redujo el aumento de peso corporal y la ingesta de alimentos y mejoró la tolerancia oral a la glucosa. Estos beneficios se asociaron a un aumento sostenido de la hormona intestinal anorexigénica PYY en plasma y una prevención de la hipersecreción de GIP inducida por la dieta rica en grasa. Además, la bacteria normalizó la inmunidad intestinal alterada en la obesidad, reduciendo la proporción de los linfocitos intraepiteliales (ILC1 y TCRαβ), aumentando la de los macrófagos antiinflamatorios (M2) y mejorando la integridad de la barrera intestinal.

Resum

Actualment, l'obesitat és un dels principals problemas de salut pública a causa de la seua elevada prevalença i a les comorbilitats associades, la qual cosa es tradueix en una reducció considerable de la qualitat i de l'esperança de vida, a més d'una enorme despesa econòmica.

Es tracta d'una malaltia que resulta del desequilibri entre l'ingesta calòrica i la despesa energètica, que condueix a un augment del pes i del greix corporal. Pel fet que l'obesitat és d'origen multifactorial, incloent tant factor genètics com ambientals, el desenvolupament de teràpies efectives per combatre-les resulta complex i s'ha convertit en un dels principals reptes de la societat.

S'ha demostrat que la microbiota intestinal, mitjançant la comunicació amb l'organisme humà, exerceix un paper rellevant en el manteniment del balanç energètic i salut metabòlica. Per això, les estrategias basades en la modificació de la microbiota intestinal per, de manera beneficiosa, modular el metabolisme energètic, son considerades hui en dia potencials alternatives per al maneig clínic de l'obesitat. No obstant això, l'aplicació d'aquestes estratègies amb eficàcia requereix d'un major coneixement sobre quines son les espècies bacterianes claus al manteniment de l'homeòstasi energètica de l'hoste i la seua manera d'acció.

L'objectiu general de la tesi ha sigut identificar noves estratègies basades en la manipulació de la composició i funcions de la microbiota intestinal eficaces contra l'obesitat, així com els seus mecanismes d'interacció amb l'hoste.

El capítol primer de la tesi es centra en estudiar els mecanismes d'acció pels quals *Bacteroides uniformis* CECT 7771 exerceix efectes protectors enfront del desenvolupament de l'obesitat, tal com el nostre grup ha descrit previament. A través d'un estudi de 14 setmanes en ratolins amb obesitat induïda per la dieta hem demostrat que aquesta soca redueix la disfunció metabòlica a través de la modulació de la microbiota intestinal i les alteracions immunològiques. Els efectes immunoreguladors més destacats de *B. uniformis* van ser la reducció dels nivells de cèl.lules B, macròfags totals i el balanç de macròfags pro- i antiinflamatoris (M1/M2), així com un augment als nivells de limfòcits T reguladors i la citocina aniinflamatoria IL-10, tant a l'intestí com al teixit adipos epididimal.

A més, al teixit adipós va augmentar les citocines TSLP i IL-33 involucrades amb l'activació d'una resposta anti-inflamatòria. Tots aquests efectes sobre l'eix intestí-teixit adipós semblen estar mediades per l'activació de TLR5 en tots dos teixits.

D'acord amb el potencial antiobesitat mostrat per *B. uniformis* CECT 7771, a un altre estudi pertanyent al mateix capítol, hem desenvolupat una estrategia similar a un simbiòtic amb la finalitat d'incrementar l'eficàcia d'aquest bacteri administrant-la a dosis menors. La fomulació simbiòtica es va dissenyar basant-se en treballs previs del grup demostrant la preferència de *B. uniformis* CECT 7771 pel segó del blat (WBE, enriquit amb oligosacàrids de arabinoxilano [AXOS]) com a font de carboni en cultius *in vitro.* Per demostrar l'eficàcia *in vivo* de l'administració conjunta de *B. uniformis* CECT 7771 i WBE hem realitzat una intervenció en ratolins amb obesitat induïda per dieta en la qual caracteritzem els beneficis immuno-metabòlics d'aquesta combinació, en relació als efectes individuals de cada component. A més, amb la finalitat de demostrar l'aplicabilitat i avantatges del simbiòtic, es van estudiar els seus efectes utilitzant una dosi inferior de *B. uniformis* CECT 7771 respecte al primer estudi. Com a resultats destacables, mentre que individualment els components del simbiòtic van exercir efectes més reduïts contra l'obesitat, la combinació va ser la intervenció més eficaç en reduir l'augment de pes corporal i l'adiposita t, al mateix temps que van millorar les rutes del metabolisme energètic modulades per insulina i la homeòstasi immunològica intestinal. En particular, la combinació va restaurar la reducció de la lipogènesi en el teixit adipós epididimal i la glucogènes hepàtica a l'obesitat. A més, va reforçar la primera línia de defensa immunològica augmentant els nivells de butirat i restaurant els nivells de limfòcits intraepitelials induïts i de les cèl·lules limfoides innates de tipus 3. Aquesta intervenció també va atenuar la inflamació hepàtica, causant de resistència a la insulina en obesitat, a través d'una millora de la senyalització de IL-22.

Al segon capítol de la tesi hem dut a terme dos estudis preclínics que descriuen els efectes de dos nous bacteris autòctones del tracte gastrointestinal humà com a potencials probiòtics per al tractament de l'obesitat identificades amb posterioritat pel grup.

El primer estudi, mostra els efectes antidiabètics de *Holdemanella biformis* CECT 9752, un bacteri intestinal aïllat de femta d'humans metabòlicament sans, a un model animal d'obesitat. L'administració

d'aquesta soca de *H. biformis* durant 13 setmanes a ratolins amb obesitat induïda per la dieta va reduir els nivells de glucosa en dejú i va millorar la tolerància oral a la glucosa de manera independent a la insulina i associat a majors nivells plasmàtics de l'hormona gastrointestinal GLP-1, necessària per al manteniment de les variacions postprandials de glucosa i la sensibilitat a insulina. A nivell del contingut luminal de l'intestí gros, la suplementació amb el bacteri va incrementar els nivells d'àcids grassos insaturats, la qual cosa indica un augment dels nivells preabsortius de potencials secretagogos lipídics de GLP-1, com l'àcid oleic i α-linoleic. A nivell de l'intestí prim, el bacteri va promoure la comunicació paracrina de GLP-1 amb les innervacions intestinals, podent directament incrementar la sensibilitat a GLP-1 de les neurones vagals aferents, mecanisme implicat en la comunicació intestí-cervell que controla la producció endògena de glucosa. A nivell hepàtic, la suplementació amb el bacteri va reduir la gluconeogènesi i va millorar la sensibilitat a insulina.

En el segon estudi hem avaluat els efectes immuno-metabòlics de *Phascolarctobacterium faecium* DSM 32890 a un model animal d'obesitat induït per dieta. Aquesta espècie bacteriana consumeix succinat i produeix propionat i la soca va ser aïllada a partir de femta humana de voluntaris metabòlicament sans. L'administració diària del bacteri al model d'obesitat va reduir l'augment de pes corporal i l'ingesta d'aliments i va millorar la tolerància oral a la glucosa. Aquests beneficis es van associar a un augment sostingut de l'hormona intestinal anorexigénica PYY en plasma i la prevenció de la hipersecreció de GIP induïda per la dieta rica en greix. A més, el bacteri va normalitzar la immunitat intestinal alterada en l'obesitat, reduint la proporció dels limfòcits intraepitelials (ILC1 i TCRαβ), augmentant la dels macròfags antiinflamatoris (M2) i millorant la integritat de la barrera intestinal.

Abstract

Currently, obesity is one of the main public health problems due to its high prevalence and associated comorbidities, which results in a considerable reduction of the health-related quality of life and life expectancy, as well as in an overwhelming cost to global health economies.

Obesity results from an imbalance between caloric intake and energy expenditure that lead to an increase in weight and body fat. As obesity has a multifactorial origin, including both genetic and environmental factors, the development of effective therapies is complex and has become one of the main challenges for society.

It has been demonstrated that the gut microbiota, through its communication with the human gut, plays an important role in the maintenance of energy balance and metabolic health. Therefore, strategies based on gut microbiota modification to beneficially modulate energy metabolism are nowadays considered potential alternatives for the clinical management of obesity. However, the effective implementation of these strategies requires the identification of key bacterial species for the maintenance of host energy homeostasis as well as the better understanding of which mechanisms are behind of their effects.

The general objective of this doctoral thesis has been to identify new and effective strategies against obesity based on the manipulation of the gut microbiota composition and function, as well as their mechanisms of interaction with the host.

The first chapter of the thesis focuses on studying the mechanisms of action by which *Bacteroides uniformis* CECT 7771 induces protective effects against the onset of obesity, based on previous studies of our group. A 14-week intervention conducted in diet-induced obese mice, we have demonstrated that this strain reduces metabolic dysfunction through the modulation of the intestinal microbiota and immune players. Among the most notable immunoregulatory properties of *B. uniformis* we highlight its effect reducing B cells levels, the total macrophages and the balance of pro- and anti-inflammatory macrophages (M1/M2) as well as increasing the abundance of regulatory T lymphocytes and the anti-inflammatory cytokine IL-10, in both intestine and epididymal white adipose tissue. In

addition, in adipose tissue, *B. uniformis* increased TSLP and IL-33 cytokines, involved in the activation of an anti-inflammatory response. All these effects on the gut-adipose tissue axis appear to be mediated by TLR5 activation in both tissues.

In line with the anti-obesity potential shown by *B. uniformis* CECT 7771, in another study of the same chapter, we have developed a symbiotic strategy with the aim of increasing the *B. uniformis* anti-obesity efficacy at lower doses. The symbiotic formulation was designed based on previous investigations conducted by our group demonstrating the preference of *B. uniformis* CECT 7771 for wheat bran (WBE, enriched in arabinoxylan oligosaccharides [AXOS]) as a carbon source in *in vitro* cultures. To demonstrate the *in vivo* efficacy of the co-administration of *B. uniformis* CECT 7771 and WBE, we have carried out an intervention in diet-induced obese mice to characterize the immuno-metabolic benefits of the combination of the bacterium and the fiber compared with the individual effects of each component. In addition, in order to demonstrate the applicability and advantages of the symbiotic, its effects were studied using a lower dose of *B. uniformis* CECT 7771 compared to the first study. As remarkable results, while individually the components of the symbiotic had more modest effects against obesity, the combination was the most effective intervention in reducing body weight gain and adiposity, along with improving insulin-modulated energy metabolism pathways and intestinal immune homeostasis. In particular, the combination restored the reduced lipogenesis in epididymal adipose tissue and hepatic glycogenesis in obesity. In addition, the symbiotic formulation strengthened the first line of immune defence by increasing butyrate levels and restoring levels of induced intraepithelial lymphocytes and type 3 innate lymphoid cells. This intervention also attenuated hepatic inflammation, which causes insulin resistance in obesity, by enhancing IL-22 signaling.

In the second chapter of the thesis we have carried out two pre-clinical studies describing the effects of two new autochthonous bacteria of the human gastrointestinal tract as potential probiotics for the treatment of obesity identified later by the group.

The first study shows the antidiabetic effects of *Holdemanella biformis* CECT 9752, an intestinal bacterium isolated from the feces of metabolically healthy humans, in an animal model obesity. The administration of *H. biformis* for 13 weeks to mice with diet-induced obesity

reduced fasting glucose levels and improved oral glucose tolerance in an insulin-independent manner and associated with higher plasma levels of the gastrointestinal hormone GLP-1, which is required for the maintenance of postprandial glucose variations and insulin sensitivity. In the luminal content of the large intestine, the supplementation with the bacteria increased the abundance of unsaturated fatty acids, which indicates an increase of the pre-absorptive levels of potential GLP-1 secretagogues, such as oleic and α-linoleic acid. In the small intestine, the bacterium seems to enhance the paracrine communication of GLP-1 with intestinal innervations and could directly increase the GLP-1 sensitivity of vagal afferent neurons, a mechanism involved in the gut-brain communication to control hepatic endogenous glucose production. At the hepatic level, the supplementation with the bacteria reduced gluconeogenesis and improved insulin sensitivity.

In the second study we have evaluated the immuno-metabolic effects of *Phascolarctobacterium faecium* DSM 32890 in an animal model of diet-induced obesity. This bacterial specie consumes succinate and produces propionate and the strain was isolated from human feces of metabolically healthy volunteers. Daily administration of the bacteria to mice fed high fat high sugar diet reduced body weight gain and food intake and improved oral glucose tolerance. These benefits were associated with a sustained increase in plasma of the anorexigenic gut hormone PYY and a prevention of high-fat diet-induced GIP hypersecretion. In addition, the bacteria normalized the impaired intestinal immunity in obesity, reducing the proportion of intraepithelial lymphocytes (ILC1 and TCRαβ), increasing the abundance of anti-inflammatory macrophages (M2) and improving intestinal barrier integrity.

Índice

INTRODUCCIÓN

Introducción

1. Obesidad

1.1 Epidemiología

La obesidad es un importante desafío de salud mundial debido a su alta prevalencia y a las comorbilidades asociadas como la diabetes mellitus tipo 2, enfermedad del hígado graso, enfermedades cardiovasculares o varios tipos de cáncer, entre otras [1,2]. Las evidencias más recientes alertan de que la obesidad ha aumentado de manera exponencial en los últimos 30 años, tanto en los países desarrollados, como los que se encuentran en vías de desarrollo. Por este motivo la Organización Mundial de la Salud considera que la obesidad es una epidemia global [3]. Esta condición no solo afecta a la salud y al bienestar de la población, sino que supone un elevado coste para los sistemas de salud y protección social, y una reducción de la productividad económica. Por estas razones, la lucha contra la obesidad es una de las prioridades de la Agenda 2030 para el Desarrollo Sostenible adoptado por los Estados miembros de las Naciones Unidas [4]

1.2 Etiopatogenia

La obesidad es el resultado de un desequilibrio entre la ingesta calórica y el gasto energético, que tiene como resultado un aumento del peso corporal y una excesiva acumulación del tejido adiposo subcutáneo y/o abdominal. Se trata de una enfermedad de etiología compleja que resulta de la convergencia, tanto de factores genéticos, como ambientales, que conducen al desequilibrio energético [5].

El índice de masa corporal (IMC), relación del peso en kilogramos entre la altura en metros cuadrados (kg/m^2), es una medida antropométrica utilizada para diagnosticar el sobrepeso y la obesidad. La tasa de heredabilidad del IMC es alta y puede variar entre el 40-70% [6], indicando una elevada influencia del componente genético en la etiología

de la obesidad. De hecho, gracias a estudios de asociación a gran escala (GWAS*, Large-scale genome wide association studies*), se han descrito más de 300 locis relacionados con la obesidad [7]. En el caso del gen que codifica para la proteína de masa grasa asociada a la obesidad (FTO, *Fat mass and obesity-associated protein*), existen ciertos polimorfismos que aumentan el riesgo de padecer la enfermedad entre 1.2-1.32 veces [6,8]. Aunque en la mayoría de los casos la obesidad se debe a interacciones entre polimorfismos génicos y el ambiente, se han descrito algunas formas monogénicas, entre las que se encuentran las mutaciones en la leptina (*Lep*), el receptor de la leptina (*Lepr*), la pro-opiomelanocortina (*Pomc*), el receptor 4 de melanocortina (*Mc4r*), etc [9,10].

El aumento exponencial de la obesidad en los últimos años evidencia la fuerte influencia de diferentes factores ambientales como los socioeconómicos y los relacionados con el estilo de vida (ejercicio físico, dieta, uso de fármacos, etc), entre otros [1,11].

La interacción entre los genes y el medio ambiente regula el balance energético, mediante una red coordinada de mecanismos centrales y periféricos, entre los que se incluyen aquellos mediados por el sistema inmune, el sistema nervioso autónomo y el sistema endocrino.

La acumulación excesiva de grasa, tanto en el tejido adiposo, como de forma ectópica, está asociada con un estado proinflamatorio crónico de bajo grado, caracterizado por un perfil de citocinas circulantes alterado, infiltración de células inmunes en los tejidos y activación de vías de señalización proinflamatorias. De hecho, tanto en sujetos obesos como en modelos animales de obesidad, genéticos e inducidos por dieta hipercalórica (DIO, *diet-induced obesity*), se han descrito niveles elevados de diversas moléculas proinflamatorias a nivel sistémico como la interleuquina (IL)-1β, IL-5, IL-6, IL-8, IL-10, IL-12, IL-18, Interferón (IFN)γ, factor de necrosis tumoral (TNF)α y proteina quimioatrayente de monocitos (MCP)-1 [12–20].

Algunas de estas citocinas juegan un papel clave en la activación de las células inmunes, así, la IL-12 promueve la diferenciación de los linfocitos T *naïve* a linfocitos T efectores [21]; el IFNγ induce la polarización de los macrófagos hacia un fenotipo proinflamatorio o M1 activados clásicamente [22–24], mientras que las quimiocinas con motivo C-X-C (CXCL)-1 y MCP-1 median la migración de las células inmunes de

la médula ósea hacia los tejidos relacionados con el metabolismo energético [25,26].

La acumulación de células y citocinas proinflamatorias en estos tejidos se asocia con disfunción metabólica y obesidad, sobre todo cuando ocurre en el tejido adiposo, en donde se produce principalmente infiltración de macrófagos acompañada de la producción de citocinas y adipocinas inflamatorias (Ej. TNFα, IL-6, IL-1β y leptina). Este estado proinflamatorio induce la polarización de los macrófagos hacia un fenotipo pro-inflamatorio o M1 contribuyendo al desarrollo de resistencia a insulina [27] y, por tanto, a la disfunción de las rutas metabólicas bajo su control, como la lipólisis o la lipogénesis, entre otras [28].

La movilización excesiva de ácidos grasos en el tejido adiposo conduce a la acumulación ectópica de grasas que, junto con las moléculas proinflamatorias producidas por los adipocitos y las células inmunes infiltradas, podrían ser las responsables del inicio de la inflamación hepática a través de la vena porta [29]. Tanto macrófagos hepáticos residentes, conocidos como células de Kupffer, como macrófagos hepáticos reclutados (RHM*, recruited hepatic macrophages*), contribuyen a la inflamación hepática crónica y la resistencia a insulina, afectando por tanto a rutas metabólicas del hígado esenciales para la homeostasis energética, como la gluconeogénesis y/o la glucogenogénesis [30]. Además, la inflamación sistémica, iniciada en el tejido adiposo, puede progresar hacia otros tejidos como el músculo esquelético, el páncreas o las estructuras cerebrales implicadas en el control de la homeostasis energética, incluyendo el hipotálamo, y contribuyendo aún más a la desregulación del metabolismo [31].

Por otra parte, las aferencias vagales del sistema nervioso autónomo que inervan el intestino, componente neural del eje intestino-cerebro, transmiten información sensorial del contenido del lumen al cerebro [32]. Estas inervaciones convergen en el ganglio nodoso cuyas neuronas proyectan hacia el núcleo del tracto solitario (NTS), estructura del tronco cerebral que conecta con distintas áreas del cerebro, incluyendo el hipotálamo, donde se integra la información sensorial procedente del intestino para responder a las necesidades nutricionales y energéticas [33]. La transmisión de la información nutricional desde el intestino al cerebro regula el comportamiento alimentario, al modular la actividad de neuronas orexigénicas, estimulando el apetito a través del neuropéptido Y

(NPY) y la proteína relacionada con Agouti (AgRP), o neuronas anorexigénicas, que suprimen el apetito a través de la pro-opiomelanocortina (POMC) y el péptido regulado por la cocaína y la anfetamina (CART) [34]. Independientemente del control de la ingesta, los mismos núcleos hipotalámicos controlan el metabolismo energético a través de las eferencias simpáticas y parasimpáticas vagales que inervan tejidos relacionados con el metabolismo energético [35] y el tracto gastrointestinal, regulando la motilidad gástrica.

A nivel intestinal, el principal estímulo de las aferencias vagales son las hormonas gastrointestinales secretadas por las células enteroendocrinas (CEEs) en respuesta a la ingesta de alimentos. En general, la obesidad produce desensibilización de las neuronas vagales aferentes, lo que implica una reducción de los efectos inducidos por dichas hormonas y expresión constitutiva de marcadores orexigénicos que contribuyen a la hiperfagia [36]. Esta pérdida de sensibilidad, reducción general de la excitabilidad y disminución de la capacidad para disparar potenciales de acción, se ve reflejada en la actividad neuronal reducida en el NTS [37,38].

Las hormonas gastrointestinales, actuando por vía endocrina o paracrina sobre las aferencias vagales, juegan un papel clave en el mantenimiento de la homeostasis energética en respuesta a las necesidades nutricionales del organismo.

Las CEEs se localizan a lo largo del epitelio gastrointestinal y expresan quimiorreceptores en su superficie apical y basolateral, los cuales median la secreción hormonal a diferentes estímulos del lumen intestinal. Estudios in vivo e in vitro han demostrado la expresión de receptores de membrana que se unen a diversos componentes de la dieta como ácidos grasos de cadena larga (GPR120 y GPR40), monoacilgliceroles (GPR119) o glucosa (SGTL1) entre otros [39,40] o a metabolitos derivados de la interacción de las bacterias intestinales con la dieta, como son los ácidos grasos de cadena corta (GPR41 y GPR43), ácidos biliares secundarios (TGR5), indoles (AHR), etc. [41].

En función de su localización y tipo de hormona secretada, las CEEs pueden ser células X/A, localizadas en el estómago y secretoras de grelina y leptina principalmente; células I y K, que secretan colecistoquinina (CCK) y péptido insulinotrópico dependiente de la glucosa

(GIP), respectivamente, y abundantes en el intestino delgado proximal; y células L, localizadas principalmente en el íleon y colon, que secretan péptido similar al glucagón tipo 1 y tipo 2 (GLP-1 y GLP-2), péptido tirosina-tirosina (PYY) y oxintomodulina (OXM) [42]. Una vez secretadas, estas hormonas activan sus receptores de membrana por vía endocrina, en órganos distantes al lugar de secreción, o paracrina, al activar sus receptores presentes en las inervaciones aferentes intestinales del nervio vago [33], localizadas cerca del lugar de secreción.

El GLP-1 muestra una gran relevancia terapéutica debido a su capacidad de inducir la secreción de insulina por las células β del páncreas tras la ingesta y, por tanto, de mantener los niveles de glucosa postprandiales (efecto incretina) [43]. Además, inhibe la secreción del glucagón en las células α pancreáticas [41] y reduce el apetito, tanto al ser administrado a nivel central, como periféricamente, tal y como demuestran estudios en roedores [44,45]. El GLP-1, mediante la regulación de la motilidad gástrica, también mantiene la homeostasis energética. En particular, retrasa el vaciamiento gástrico lo que ralentiza la absorción de nutrientes en el intestino reduciendo la glucemia postprandial [46,47].

Sujetos obesos con diabetes tipo 2 muestran niveles basales de GLP-1 reducidos, así como una secreción deficiente de esta hormona en respuesta a glucosa o a la ingesta de nutrientes [48,49]. Además, estudios en roedores demuestran que la obesidad y la ingesta de dietas hipercalórica conllevan una reducción de la señalización de GLP-1 en las aferencias vagales [50] interfiriendo en los efectos mediados por dichas aferencias por esta hormona, como por ejemplo en el control de ingesta [51], la producción hepática de glucosa [52,53] o el vaciamiento gástrico [54,55].

1.3 Tratamientos

Un estilo de vida saludable (dieta y ejercicio físico) es clave para el manejo de la mayoría de los trastornos metabólicos; sin embargo, estas estrategias dan lugar a reducciones de peso limitadas y temporales [56,57]. El uso de estrategias quirúrgicas, como la cirugía bariátrica, son muy efectivas en la obesidad severa, pero se contempla como la última opción terapéutica por el alto coste y los riesgos quirúrgicos asociados

[58]. A pesar de la implicación de la inflamación crónica en la patogénesis de la obesidad, las terapias anti-inflamatorias evaluadas para tratar la obesidad, principalmente glucocorticoides, presentan efectos secundarios metabólicos perjudiciales y una limitada efectividad [59,60]. También se han desarrollado estrategias terapéuticas basadas en análogos de la incretina GLP-1, especialmente para el tratamiento de diabetes tipo 2 [61]. Exenatida y Liraglitina son dos análogos aprobados por la FDA (*Food and Drug Administration*) para el tratamiento de la diabetes tipo 2 [62,63]. Además, sus efectos a nivel hipotalámico conducen a una reducción del apetito [64] y una pérdida de peso de entre el 5 y el 10% en pacientes obesos [65]. En los últimos años, se han desarrollado estrategias combinadas utilizando análogos de GLP-1 como lanzadera para transportar moléculas antiinflamatorias, concretamente dexametasona, hacia las células que expresan el receptor de GLP-1 (GLP-1R). El tratamiento con el co-agonista GLP1-Dexametasona en ratones DIO revierte la disfunción inmunometabólica asociada a la obesidad, reduciendo el peso corporal, la adiposidad, la inflamación sistémica, la ingesta de alimentos y mejorando la homeostasis de glucosa [66]. Sin embargo, la dificultad para que las estrategias farmacológicas den el salto a ensayos clínicos y los efectos adversos que frecuentemente se han asociado a su administración [67] hace necesaria la búsqueda de estrategias alternativas no farmacológicas para combatir las enfermedades metabólicas como la obesidad de forma eficaz y con mínimos riesgos.

En este sentido, el descubrimiento de que la microbiota intestinal y sus metabolitos pueden desempeñar una función importante en el control del sistema inmune y la homeostasis energética ha permitido dar un nuevo enfoque al desarrollo de estrategias para combatir la obesidad y alteraciones metabólicas asociadas, basadas en la manipulación de la microbiota, que se describen con más detalle en las siguientes secciones.

2. Microbiota intestinal

Los factores relacionados con el estilo de vida, fundamentalmente la dieta, ejercen un importante impacto sobre la composición y funciones de la microbiota intestinal [68]. En las últimas décadas se ha demostrado que la microbiota, mediante la comunicación con el hospedador, ejerce un papel relevante en el mantenimiento del balance energético y salud

metabólica [69]. Estudios en humanos han revelado que el aumento en el consumo de dietas ricas en grasas y azucares está relacionado con una microbiota intestinal alterada (disbiosis), que contribuye a la fisiopatología de trastornos metabólicos como la obesidad [70]. En particular, diversos estudios revelan que la disbiosis, causada en parte por las dietas hipercalóricas y de forma sinérgica a los efectos que éstas ocasionan, contribuye a la inflamación crónica de bajo grado característica de la obesidad [71] y alteran la señales neurales y endocrinas que regulan la transmisión de la información de los nutrientes desde el intestino al cerebro [72].

La microbiota intestinal es el conjunto de microorganismos (bacterias, virus, arqueas, hongos y levaduras) que viven en el tracto gastrointestinal en relación de mutualismo con el huésped. El genoma microbiano (metagenoma) tiene una capacidad codificante 150 veces superior a la del genoma humano aportando funciones metabólicas, inmunológicas y endocrinas que influyen en la salud humana [73,74].

Es un ecosistema complejo y dinámico formado por 5-7 filos bacterianos de los 52 reconocidos actualmente. Aproximadamente el 90% de la población total de bacterias pertenecen a los filos Firmicutes y Bacteroidetes, seguidos por las Actinobacterias y Proteobacteria que representan menos del 1-5% en población adulta. El filo Bacteroidetes está formado principalmente por los géneros *Bacteroides* y *Prevotella*, que son probablemente los más estudiados. El filo Firmicutes es el más grande, formado por más de 200 géneros diferentes. Las Actinobacterias incluye el género *Bifidobacterium* cuya abundancia depende de la edad del individuo. El filo Proteobacterias son bacterias anaerobias facultativas, que incluyen a la familia *Enterobacteriaceae* [75].

La colonización microbiana del intestino comienza a producirse inmediatamente después del nacimiento. Aproximadamente a los 3 años alcanza una diversidad y composición similar a la de los adultos y, después, durante la vejez (aproximadamente es a partir de los 65 años) comienza nuevamente a alterarse [76].

La fisiología del huésped y la microbiota intestinal están íntimamente relacionadas. Cada región del tracto gastrointestinal se caracteriza por unas condiciones fisicoquímicas determinadas (oxígeno, péptidos antimicrobianos, pH, enzimas, disponibilidad de nutrientes, ácidos biliares

etc.) [77] las cuales ejercen una presión selectiva sobre la microbiota, aumentando en diversidad de forma gradual a lo largo del tracto intestinal [78].

La microbiota intestinal está implicada en diversos procesos biológicos que influyen en funciones fisiológicas esenciales para el hospedador. Entre las que se encuentran (i) funciones nutricionales y metabólicas, ya que la microbiota participa en la fermentación de componentes dietéticos no digeribles y que a su vez tienen efecto directo sobre el metabolismo energético [79] y sintetizan nutrientes esenciales, como algunas vitaminas; (ii) funciones neuroendocrinas, modulando señales endocrinas y neurales en el intestino implicadas en el metabolismo energético y el apetito [80] y (iii) funciones inmunológicas, promoviendo la maduración del sistema inmune intestinal, protegiendo frente a patógenos externos y reforzando la integridad de la barrera intestinal [81] (ver **Figura 1**).

2.1 Función nutricional y metabólica

Los componentes dietéticos no digeribles, principalmente fibra dietética incluyendo oligo y polisacáridos, son fermentados por la microbiota a lo largo del tracto gastrointestinal, sobre todo en el colon. Este proceso de fermentación da lugar a la producción principamente de ácidos grasos de cadena corta o SCFA (*short chain fatty acids*) como acetato, propionato y butirato [82], que son los metabolitos microbianos más abundantes en adultos sanos. Además, la microbiota fermenta aminoácidos derivados de las proteínas de la dieta y sintetiza nutrientes esenciales, como las vitaminas K y B12, el ácido fólico, diversos aminoácidos, etc [83].

Los metabolitos más estudiados son los SCFAs, que están implicados en diversas funciones fisilógicas, incluyendo la función barrera intetinal, la inmunidad y el metabolismo. Los SCFAs intervienen en procesos de regulación epigenética, como la inhibición de la histona deacetilasa (HDAC), que afecta a genes implicados en el ciclo celular, la apoptosis y la inflamación, en células del epitelio intestinal [84]. Mediante la activación de los receptores GPR41 y 43, el butirato desempeña un papel fundamental en la regulación de la proliferación, diferenciación y respuesta inflamatoria de los colonocitos [85]. Además, es esencial en el mantenimiento del estado de hipoxia del intestino al estimular el consumo de oxígeno por las células epiteliales a través de la β-oxidación [86].

Por otra parte, GPR41 y 43 se expresan en una amplia variedad de células relacionadas con el metabolismo energético, incluyendo las CEEs que secretan hormonas gastrointestinales, las células epiteliales, las neuronas y las células inmunes, tanto en el intestino como en tejidos asociados al metabolismo energético, como el hígado o el tejido adiposo.

A parte de proporcionar energía y mantener el epitelio intestinal, los SCFAs, a través de la activación de GPR41 y/o GPR43, modulan el metabolismo energético por mecanismos, tanto independientes, como dependientes de la secreción de hormonas gastrointestinales [87]. Independientemente de las hormonas gastrointestinales, los SCFAs actúan como mediadores entre el intestino y el metabolismo energético, tanto lipídico [88,89], como glucídico [90]. Así, se ha demostrado que la administración oral de butirato en ratones alimentados con dieta rica en grasa estimula la termogénesis y la β-oxidación de los ácidos grasos en el tejido adiposo marrón, mejorando el metabolismo energético [91]. El acetato, también mejora el metabolismo lipídico en ratones obesos, en particular restaura la función hepática al reducir la acumulación de lípidos y mejorar la actividad mitocondrial, mientras que en el tejido adiposo inhibe la lipólisis y estimula el "browning", es decir, el cambio fenotípico de los adipocitos que almacenan triglicéridos a adipocitos capaces de realizar termogénesis, reduciendo así la adiposidad corporal [92].

La homeostasis de glucosa también es influenciada por los SCFAs. En particular, se ha identificado que los SCFAs modulan la gluconeogénesis en el intestino actuando como sensor nutricional para mejorar la tolerancia a glucosa y la sensibilidad a insulina [93]. Mientras que el butirato directamente modula la actividad y expresión génica de enzimas limitantes de la gluconeogénesis, mediante un mecanismo dependiente de AMPc, el propionato modula esta ruta metabólica mediante la activación del eje intestino-cerebro a través del nervio vago [93,94].

2.2 Función neuroendocrina

La regulación de la homeostasis energética por la microbiota intestinal también puede ocurrir gracias a su capacidad para modular señales neurales y endocrinas en el intestino. Además de los SCFAs [95], otros metabolitos bacterianos, como indoles [96], ácidos biliares secundarios

[97] o neurotransmisores de origen bacteriano [72] y componentes celulares bacterianos, como el exopolisacárido capsular conocido como polisacárido A (PSA), el lipopolisacárido (LPS) [98] y el muramil dipéptido (MDP) [99,100] pueden estimular, tanto neuronas localizadas en la lámina propia del intestino, como la secreción de hormonas gastrointestinales por las CEEs.

Los SCFAs se han descrito como moléculas de señalización clave en este proceso. A través de la activación de los receptores GPR41 y 43 modulan la secreción de GLP-1 [101]. Otros secretagogos naturales de GLP-1 son los ácidos biliares secundarios, sintetizados por la microbiota a partir de los ácidos biliares primarios [102]. La activación del receptor de ácidos biliares secundarios, TGR5, incrementa el número de células L, los niveles de GLP-1 y mejora la tolerancia a glucosa [97]. Los indoles incrementan la sensibilidad de las neuronas aferentes en el colon al GLP-1, lo que puede estar implicado en la regulación central de la motilidad intestinal y en la homeostasis energética [103].

Además, se ha demostrado que varias cepas bacterianas pueden modificar los niveles de precursores de neurotransmisores en la luz intestinal e incluso sintetizarlos, entre los que están el ácido γ-aminobutírico (GABA) [104,105], la dopamina (DA) [106] y la noradrenalina (NA) [106]. En concreto, se ha demostrado que *Lactobacillus spp.* y *Bifidobacterium spp* sintetizan GABA [104,107] mientras que *Streptococcus spp*., *Enterococcus spp* y *Escherichia spp.* sintetizan DA y NA [106,108].

Por otra parte, las bacterias intestinales indirectamente modulan los niveles de neurotransmisores en el hospedador mediante la regulación de los niveles de expresión de enzimas involucradas en la biosíntesis de serotonina (5HT), DA, NA y adrenalina [109–111]. En el caso de 5HT, a través de los SCFAs, las bacterias intestinales pueden modular la expresión de la triptófano hidroxilasa 1 (Tph1) en el colon, enzima que limita la producción de serotonina [109,110]. El acetato, al atrevesar la barrera hematoencefálica, regula la producción de glutamato, glutamina y GABA en el hipotálamo resultando en un aumento de la expresión de neuropéptidos anorexigénicos y supresión de la ingesta [112].

Por tanto, el efecto de la microbiota sobre los niveles de neurotransmisores resulta clave en el mantenimiento de la homeostasis enegética considerando el papel relevante que ejercen éstos en el metabolismo y el comportamiento alimentario [112–115].

Recientes investigaciones han evidenciado que ciertos componentes estructurales de las bacterias intestinales tienen propiedades neuromoduladoras. Por ejemplo, *Bacteroides fragilis* estimula las neuronas vagales a través del PSA [116], mientras que, tanto el LPS como el MDP son capaces de incrementar la sensibilidad de neuronas intestinales productoras de óxido nítrico (NO) facilitando la regulación central de la secreción de insulina y vaciamiento gástrico mediado por GLP-1 [100]. Además, los ratones libres de gérmenes presentan un número reducido de neuronas entéricas y con ello una disminución de la motilidad intestinal [117], lo que sugiere que la microbiota desempeña un papel en el desarrollo del sistema nervioso entérico.

Por tanto, la microbiota intestinal regula la homeostasis energética a través de diversos mecanismos mediados por las hormonas gastrointestinales; los cuales pueden ser independientes del eje intestino-cerebro, modulando la función del tejido periférico diana (páncreas, hígado y tejido adiposo) al activar sus receptores de membrana por vía endocrina, o bien dependientes del eje intestino-cerebro; regulando la función del circuito hipotalámico y, por tanto, el control de ingesta o metabolismo energético en los tejidos periféricos por vía endocrina y/o paracrina [42].

2.3 Función inmunológica

La microbiota ejerce un papel fundamental en el desarrollo, maduración y función del sistema inmunitario del hospedador. Por otra parte, el sistema inmune ha evolucionado de tal manera que establece una relación simbiótica con las bacterias intestinales comensales. Este diálogo entre la microbiota y el sistema inmune intestinal permite la inducción de respuestas tolerogénicas frente a antígenos inocuos y protectoras frente a patógenos [81].

Numerosas evidencias respaldan la importancia de la colonización temprana de la microbiota en neonatos para el correcto desarrollo del

sistema inmune y así evitar, a largo plazo, la aparición de enfermedades inflamatorias crónicas [118,119].

La mucosa intestinal permite, tanto minimizar el contacto entre el epitelio y los patógenos de la luz intestinal, como mantener una interacción estable entre la microbiota comensal y el sistema inmune del hospedador [120]. Las bacterias comensales y sus metabolitos refuerzan la integridad intestinal al influir en la composición y grosor de la mucina, regulando la expresión de los genes productores de moco o aumentando la diferenciación de las células productoras, las células Goblet [121]. También modulan la secreción de péptidos antimicrobianos (AMP), producidos por las células epiteliales, los cuales ejercen un papel fundamental en procesos de quimiotaxis de células inmunes [122] y de Inmunoglobulina A (IgA) producida por los linfocitos B, que al unirse a las bacterias favorece su compartimentación y contribuye a la formación de biopelículas que sirven como barrera para la adherencia de patógenos [123].

A pesar de que la mucosa limita el contacto entre las bacterias comensales y el hospedador, éstas son detectadas a través de sus patrones moleculares (PMAM, patrones moleculares asociados a microorganismos) por el sistema inmune. Los receptores de reconocimiento de patrón molecular (PRR o RRP), principalmente de tipo Toll (TLR, *Toll like receptor*) y Nod (NLR, *Nod like receptor*), se expresan fundamentalmente en células presentadoras de antígenos (células dendríticas y macrófagos), aunque también se encuentran en algunas células epiteliales. Estas señales están involucradas en el mantenimiento de la homeostasis inmunológica y tisular [124].

La microbiota y sus metabolitos también pueden influir en la hematopoyesis y la programación de las células hematopoyéticas [26,125]. Por ejemplo, el propionato promueve la activación de precursores de células dendríticas y macrófagos en la médula ósea para su liberación al torrente sanguíneo [126] y a través de la señalización por Nod1 la microbiota activa las células mesenquimales (MSC) para producir factores de crecimiento hematopoyético [127].

Por otra parte, el establecimiento de la tolerancia oral, lo que se entiende por supresión de respuestas inflamatorias a antígenos ingeridos de forma oral y a la microbiota, no podría producirse en ausencia de las señales de la microbiota intestinal dirigidas a la activación de respuestas

reguladoras [128,129]. El control de la tolerancia inmunológica se lleva a cabo mediante la activación de diversas respuestas reguladoras [130]. Por ejemplo, *Bacteroides fragilis* estimula la producción de IL-10 por las células T reguladoras (Treg) a través del PSA de su cápsula, lo que favorece a su colonización [131]. Estas células contribuyen a la diversificación de la microbiota intestinal a través de la supresión de la respuesta inflamatoria y la regulación de la secreción de IgA [132]. Por otra parte, *Bifidobacterium breve* promueve tolerancia al disminuir la producción de citocinas proinflamatorias y prevenir la respuesta por linfocitos B [133,134], mientras que las bacterias filamentosas segmentadas (SFB) desencadenan la diferenciación de las células Th17 y, por tanto, la síntesis y liberación de IL-17, lo que resulta clave en la defensa contra patógenos [135,136]. *Bifidobacterium adolescentis* también puede promover la acumulación de células Th17 en el intestino de ratones activando un programa transcripcional distinto al promovido por las SFB [137]. *Akkermansia muciniphila* contribuye a mantener la integridad de la barrera intestinal al regular la expresión de las proteínas de unión (adherentes y estrechas) [138]. La microbiota intestinal también afecta al desarrollo de los linfocitos B residentes en la lámina propia y, por lo tanto, la producción de IgA, que, a su vez, regula la composición de la microbiota como se ha indicado anteriormente [139,140]. Algunos SCFAs promueven tolerancia hacia los microorganismos beneficiosos al estimular el desarrollo de células Treg [141,142], aumentar la expresión de AMPs y modular la producción de mediadores inmunes como la IL-18 [143]. Además, metabolitos derivados del triptófano se unen al receptor de hidrocarburos de arilo (AHR, *aryl hydrocarbon receptor*) y activan el desarrollo de células linfoides innatas de tipo 3 (ILC3, *innate lymphoid cells type 3*), que a través de la producción de IL-22, proporcionan resistencia a la colonización y protección contra la inflamación de la mucosa [144]. Además, las ILC3 expresan el complejo mayor de histocompatibilidad clase II (MHCII) e inducen la muerte celular de las células T efectoras frente a bacterias comensales [145]. La microbiota intestinal también tiene un papel relevante en el desarrollo y activación de los linfocitos intraepiteliales intestinales (IELs) [146]. Estas células participan en la defensa contra patógenos, reparación del tejido e interacciones homeostáticas con el epitelio, la microbiota y los nutrientes [147]. Los metabolitos indólicos producidos por *Lactobacillus reuteri* pueden modular la conversión de Treg de la lámina propia en IELs a través de la activación del receptor AHR [148]. Las IELs TCRγδ, la principal población de IEL, precisan de las bacterias comensales para la

liberación de efectores antibacterianos innatos, RegIIIγ (*Regenerating islet-derived protein III-gamma*), a través de la señalización Myd88 en las células epiteliales [149,150].

Las bacterias comensales residentes en el intestino pueden modular, tanto la inmunidad local, como sistémica. De hecho, los ratones libres de gérmenes muestran proporciones alteradas de la microglia, macrófagos residentes en el cerebro, así como un fenotipo inmaduro, lo que sugiere que la microbiota intestinal también tiene un papel importante en la regulación y desarrollo del sistema inmune en tejidos no intestinales, en este caso del sistema nervioso central [151].

La adquisición de un sistema inmune tan complejo y su dependencia con la microbiota intestinal tiene ciertos inconvenientes. Entre ellos, las alteraciones en la composición y función de la microbiota como resultado del mal uso de los antibióticos o cambios en la dieta pueden tener como consecuencia la falta de control de las respuestas inmunes contra autoantígenos, antígenos ambientales y/o de la propia microbiota, que pueden dar lugar a patologías de tipo autoinmune, alérgicas y/o inflamatorias [152].

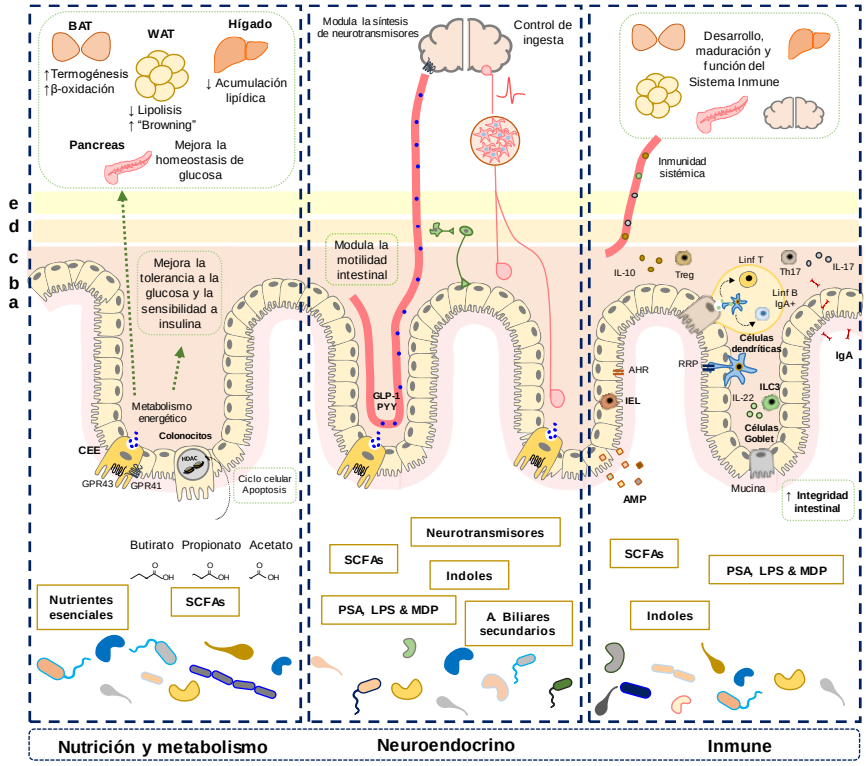

Figura 1: Esquema de los procesos biológicos a nivel intestinal en los que está implicada la microbiota intestinal. (a) mucosa, (b) células epiteliales intestinales, (c) lámina propia, (d) plexo submucoso y (e) plexo mientérico.

3. Microbiota intestinal y obesidad

La necesidad de un mayor aporte calórico en ratones GF para mantener el mismo peso corporal que ratones convencionales, fue la primera evidencia científica demostrando la relación entre la microbiota intestinal y la obesidad [153]. Más recientemente, Backhed y colaboradores demostraron que la ausencia de microbiota de ratones GF proporciona resistencia a la obesidad inducida por una dieta hipercalórica, lo cual es revertido tras la colonización de los ratones GF con la microbiota de ratones convencionales, demostrando que la microbiota intestinal es necesaria para mantener los depósitos de grasa,

probablemente mediando la absorción intestinal de lípidos entre otros procesos [154].

Además, otros estudios han mostrado que el trasplante de la microbiota procedente de animales o humanos obesos a animales GF es suficiente para desarrollar el fenotipo obeso, indicando que la microbiota intestinal puede ser un agente causal de la obesidad [155,156]. Ridaura y colaboradores también identificaron la dieta como un factor relevante en la transmisión de la microbiota y el fenotipo obeso.

Ensayos preclínicos en modelos animales de obesidad, como ratones deficientes en leptina (ob/ob) y ratones alimentados con dieta rica en grasa (HFD, *high fat diet*), revelaron una asociación entre la obesidad y la diversidad microbiana. En particular, la obesidad se asoció con una reducción del 50% en la abundancia de Bacteroidetes y un aumento proporcional de Firmicutes [157,158], aunque no todos los estudios posteriores han corroborado esta hipótesis. Estudios similares en humanos también han evidenciado reducciones en la diversidad microbiana asociadas a la obesidad [159] lo que se ha confirmado en un meta-análisis [160].

Investigaciones más recientes han encontrado niveles altos de *Lactubacillus* en pacientes obesos respecto a los controles [161] como en el caso de *Lactobacillus reuteri* y *Lactobacillus sakei* que se correlacionaron positivamente con el índice de masa corporal en estudios observacionales en adultos [162]. En cambio, algunas especies de este género, *L. casei* y *L. plantarum*, se han asociado con la pérdida de peso en animales y humanos [163], mientras que *Akkermansia muciniphila* se ha correlacionado con una atenuación de las comorbilidades asociadas al fenotipo obeso [164]. No obstante, a pesar de la gran cantidad de estudios, todavía no existe un consenso completo sobre qué características de la microbiota y que componentes pueden determinar el fenotipo metabólico del sujeto.

Las investigaciones preclínicas y clínicas sugieren que la microbiota intestinal, mediante su interacción con la dieta, puede estar involucrada en el desarrollo de la obesidad a través de diferentes mecanismos como (1) modulando la capacidad para obtener energía de la dieta, (2) controlando la transmisión de señales nutricionales mediante mecanismos neurales y endocrinos desde el intestino y (3) regulando la inmunidad intestinal [165].

(1) La microbiota de animales obesos parece tener mayor capacidad para obtener energía de la dieta y para almacenarla en tejidos periféricos. Este efecto se relaciona con la capacidad de la microbiota para digerir polisacáridos complejos, no digeribles por el hospedador, y de modular la expresión de genes del hospedador responsables de su absorción y acumulación [165,166]. Estudios posteriores también implican a la microbiota del intestino delgado en la absorción y acumulación del lípidos [42,167,168]

(2) Los metabolitos bacterianos, especialmente los SCFAs, se han visto alterados en sujetos obesos [169]. Tal y como se describe en apartados anteriores, estos metabolitos modulan la secreción de diferentes hormonas que controlan el apetito y la ingesta [165].

(3) La microbiota intestinal se considera uno de los factores clave en el desarrollo de la inflamación asociada a la obesidad [27]. Los cambios en la composición de la microbiota asociados a la dieta (disbiosis) contribuyen a un aumento de la permeabilidad intestinal y una mayor translocación de productos inmunogénicos que contribuyen al aumento de la inflamación intestinal y periférica. Este estado inflamatorio de bajo grado se considera una causa importante de la disfunción metabólica (resistencia a insulina y las rutas metabólicas que regula) y del desarrollo de enfermedades crónicas asociadas a la obesidad, como la diabetes tipo 2, enfermedad del hígado graso y enfermedades cardiovasculares [170].

3.1 Microbiota, inflamación y obesidad

La microbiota intestinal y su interacción con los componentes de la dieta median el proceso inflamatorio asociado a la obesidad, principalmente a través de los componentes del sistema inmune innato que residen en el intestino. Los desequilibrios en la microbiota inducidos por la dieta rica en grasa aumenta la permeabilidad intestinal a través de la producción de citocinas proinflamatorias y alterando las uniones estrechas entre los enterocitos [170]. El reconocimiento de componentes microbianos, como LPS y/o moléculas de DNA bacteriano por los TLRs y NLRs, activa la secreción de citocinas proinflamatorias, como TNFα, IL-1β y MCP1, y la expresión de receptores y moléculas de adhesión en el

intestino a través de diferentes vías de señalización mediadas por NF-κB o MAPKs/JNK, entre otros.

Estas señales inducen el reclutamiento de células inmunes, como linfocitos T, macrófagos, basófilos, neutrófilos y células dendríticas, desencadenando respuestas proinflamatorias [171]. A su vez, el ambiente inflamatorio afecta la barrera epitelial al alterar la estructura y función de las uniones estrechas entre los enterocitos y/o células del sistema inmune [170].

Este aumento de la permeabilidad intestinal permite la translocación de productos antigénicos como el LPS, un componente proinflamatorio de las bacterias Gram-negativas [172]. El aumento de LPS en la circulación sistémica, denominado endotoxemia metabólica, desencadena cascadas de señalización proinflamatoria mediadas por la activación de TLR4. La supresión génica de los TLRs, ha permitido demostrar la relación entre la microbiota y la desregulación inmunitaria que ocurre en obesidad. La eliminación del TLR4 en ratones protege contra la inflamación del tejido adiposo y la resistencia a insulina [173]. Del mismo modo, la ausencia de TLR2 previene los efectos de la dieta obesogénica al mejorar la tolerancia a la glucosa, la sensibilidad a la insulina y la inflamación del tejido adiposo [174]. Por el contrario, la ausencia de TLR5 se ha asociado con una microbiota alterada y el desarrollo de síndrome metabólico [175]. Además, los ratones deficientes en TLR9 alimentados con dieta rica en grasa ganan más peso y grasa corporal que los ratones de tipo salvaje y muestran una intolerancia a la glucosa y resistencia a la insulina más severas al mismo tiempo que desarrollan una mayor respuesta inflamatoria [176].Todo esto pone en evidencia la implicación de los TLRs en la homeostasis del sistema inmune intestinal y su relación con el metabolismo energético.

La inflamación sistémica, parcialmente mediada por la microbiota asociada a la obesidad y sus componentes estructurales (por ejemplo, el LPS), puede inducir inflamación central, mediante la activación de la sínteis de citocinas inflamatorias y su paso posterior a través de la barrera hematoencefálica [177] y la estimulación de la microglía [178], así como mediante la activación de las aferencias vagales [179]. La inflamación hipotalámica altera la expresión de péptidos hipotalámicos [180] y la homeostasis energética [181]. Por ejemplo, se ha demostrado que la administración intraperitoneal de LPS en ratas causa hiperfagia al inhibir la acción de las hormonas gastrointestinales sobre la ingesta de alimentos

y reducir la señalización de leptina por las aferencias vagales [182]. Estos datos sugieren que componentes derivados de las bacterias como el LPS pueden influir en la función de las neuronas aferentes vagales que conducen a alteraciones en la señalización de saciedad desde el intestino hasta el cerebro.

4. Estrategias dirigidas a modular la función de la microbiota intestinal para combatir la obesidad

Actualmente, las estrategias preventivas y terapéuticas frente a la obesidad presentan importantes limitaciones. Las basadas en cambios en el estilo de vida (dieta hipocalórica y ejercicio físico) son poco efectivas, especialmente a largo plazo, y las farmacológicas conllevan efectos secundarios. Esto se debe a que los cambios metabólicos, hormonales y neuroquímicos asociados a la obesidad suelen incluir mecanismos de resistencia a señales clave para mantener el balance energético, dificultando la pérdida de peso [183].

Las evidencias que vinculan la microbiota intestinal con el metabolismo energético del huésped también ponen de manifiesto la posibilidad de modificar su composición y funciones para influir de manera beneficiosa en el balance energético y así proporcionar protección frente al desarrollo de obesidad y sus complicaciones [184]. Existen diversas estrategias, entre las que se encuentran el uso de prebióticos, probióticos o la combinación de ambos, lo que se conoce como simbióticos.

4.1 Prebióticos

La definición más citada de prebiótico es "*ingrediente alimentario no digerible que afecta beneficiosamente al huésped estimulando el crecimiento y/o actividad de una o un número limitado de bacterias residentes en el colon*" [185]. La fibra dietética se define generalmente como carbohidratos no digeribles en la parte alta del tracto intestinal y, entre estos, se incluyen compuestos considerados como prebióticos [186]. En base a los avances en el estudio de la microbiota y sus mecanismos de acción la Asociación Internacional de Probióticos y Prebióticos (ISAPP) modificó recientemente la definición de prebiótico como "*sustrato utilizado*

selectivamente por los microorganismos del huésped confiriéndole beneficios para la salud" [187], sin restringir la definición al tracto intestinal.

Gracias a los avances en las técnicas de secuenciación masiva se han podido identificar nuevas especies bacterianas, residentes en el intestino, (más allá de lactobacilos y bifidobacterias) capaces de utilizar la fibra y los prebióticos de la dieta como fuente de energía y conocer cómo influyen en sus funciones y composición [186,188].

La mayoría de los prebióticos identificados son carbohidratos con diversas estructuras moleculares presentes en la dieta, fundamentalmente en verduras, frutas y cereales [189]. Entre ellos cabe destacar fructanos tipo inulina, los galactooligosacáridos y arabinoloxilanos, entre otros.

Los prebióticos cuyos efectos sobre el metabolismo energético se han estudiado en mayor profundidad hasta la fecha, son los oligosacáridos no digeribles de tipo galactano (GOS), trans-galactano (TOS) y fructano (FOS), preferentemente fermentados por las bifidobacterias [190].

Los estudios clínicos más recientes sobre prebióticos han tenido como objetivo evaluar sus efectos metabólicos, en concreto en la regulación de la homeostasis de glucosa y la pérdida de peso [187,191] y cardiovasculares en la mejora de la resistencia a la insulina y la reducción de los niveles de lípidos [191], así como sus efectos inmunomoduladores [191,192] y sobre el estado de ánimo y la cognición [193].

Aunque existe una fuerte evidencia epidemiológica de que la ingesta de fibra dietética, tanto de alimentos ricos en fibra como suplementados con fibra, protege contra el sobrepeso y la obesidad, existen escasas investigaciones especialmente dirigidas al estudio de los beneficios de la fibra dietética a través de su interacción con la microbiota intestinal [186,194]. Entre ellos, cabe destacar estudios de intervención en humanos donde se demuestra que fructanos como la inulina estimulan el crecimiento de *Bifidobacterium* spp. y *Faecalibacterium prausnitzii*, y que su aumento se correlaciona negativamente con los niveles de LPS en sangre en mujeres obesas [195]. Otro estudio en niños con sobrepeso y obesidad demuestra que este prebiótico reduce el peso corporal, el porcentaje de grasa y los niveles séricos de IL-6 al tiempo que aumenta las concentraciones de *Bifidobacterium* spp. [196].

La suplementación con GOS en humanos sanos de edad avanzada disminuye los marcadores proinflamatorios sistémicos asociados con un aumento de *Bifidobacterium* spp., *Lactobacillus-Enterococcus* spp*.,* y *C.coccoides-E.rectale*, junto con una reducción de *Bacteroides* spp*., E. coli y Desulfovibrio* spp. Un estudio en personas con sobrepeso tratados con GOS muestra una reducción en los niveles de insulina, de la inflamación sistémica y una mejora de la homeostasis de lípidos [197], aunque en otros estudios similares no vieron estos efectos [198]. Otro estudio ha demostrado que la dextrina resistente de trigo aumenta las proporciones de *Bifidobacterium* spp. y *Lactobacillus* spp. y reduce *Clostridium perfringens* en individuos sanos [199]. Además, la suplementación con dextrina resistente en mujeres con diabetes tipo 2 modula la inflamación y mejora la resistencia a insulina [200]. Dentro del consorcio del proyecto europeo MyNewGut se evaluó la capacidad de los arabinoxilanos (AX), la fibra dietética más abundante del salvado de trigo, así como del producto de su hidrólisis, los arabinoxilo-oligosacaridos (AXOS), de modular la microbiota intestinal e inducir beneficios metabólicos [201]. Concretamente, la ingesta de AXOS induce el aumento de *Bifidobacterium* spp. y especies productoras de butirato.

4.2 Probióticos

Los probióticos se definen como microorganismos vivos que al ser administrados en cantidades adecuadas confieren efectos beneficiosos para la salud del huésped [202].

Los probióticos tradicionales o comúnmente llamados “probióticos clásicos” son principalmente bacterias ácido-lácticas y bifidobacterias. Su larga historia de uso y su seguridad demostrada como GRAS (*Generally Recognized As Safe* según la FDA) y QPS (*Qualified Presuption as Safe* según la EFSA) ha permitido su uso regulado como alimento o suplemento alimenticio [203]. Algunos de los llamados probióticos clásicos, se han evaluado por su posible efecto frente a la obesidad. Por ejemplo, *Lactobacilus gasseri* SBT2055 ha mostrado disminuir la adiposidad abdominal y el peso corporal de adultos obesos [204]. Por otro lado, una cepa de *Lactobacillus plantarum*, ha demostrado reducir el IMC y los valores de presión arterial, síntomas del síndrome metabólico en un

estudio piloto de pacientes obesos hipertensos con una dieta hipocalórica, [205,206].

Las evidencias de la eficacia de estos probióticos para combatir la obesidad y sus comorbilidades, así como para otras aplicaciones en humanos son a menudo limitadas. Esto es, en parte, debido, a que las cepas eran tradicionalmente seleccionadas en base a criterios de seguridad y aptitud tecnológica, para facilitar su comercialización, pero no estaban basadas en un proceso de selección racional para una finalidad funcional concreta [207]. Esto ha generado la necesidad de mejorar las estrategias de la selección de nuevas cepas potencialmente probióticas, basadas en el efecto de éstas sobre dianas específicas, para situaciones fisiológicas o patologías concretas y así, aumentar su eficacia.

Gracias a las tecnologías de secuenciación masiva y a estudios epidemiológicos basados en la caracterización de perfiles de microbiota de individuos metabólicamente sanos frente a sujetos afectados por obesidad y patologías metabólicas asociadas se han establecido asociaciones entre determinados componentes de la microbiota intestinal y la salud del huésped. Estas asociaciones junto a posteriores estudios preclínicos de intervención que permiten establecer relaciones causales, constituyen una buena base para la selección de bacterias propias de la microbiota intestinal humana como potenciales probióticos de nueva generación, con una mayor eficacia potencial que los estudiados hasta el momento.

En los últimos años han salido a la luz probióticos emergentes como herramientas preventivas y terapéuticas frente a la obesidad. Entre ellos se incluyen cepas de las especies *Faecalibacterium prausnitzii*, *Akkermansia muciniphila* y *Bacteroides uniformis* y cuyas funciones se han revisado extensamente [208] y se describen brevemente a continuación.

Faecalibacterium prausnitzii

Faecalibacterium prausnitzii pertenece al filo *Firmicutes* y representa un 5% de la microbiota intestinal en humanos sanos. Es una de las principales productoras de butirato en humanos, a través del cual ejerce un papel crucial en la fisiología intestinal y la salud del huésped [209,210]. Fundamentalmente, induce efectos antiinflamatorios al inducir un perfil de citocinas tolerogénicas como TGFβ e IL-10 y una reducida secreción de

citocinas proinflamatorias como IL-12 e IFNγ [211,212]. La administración oral en ratones alimentados con HFD, reduce la inflamación en el tejido adiposo visceral y mejora la captación de glucosa y la sensibilidad a insulina en el tejido adiposo blanco subcutáneo [213]. *F. prausnitzii* o su sobrenadante libre de células, reducen la inflamación aguda [211], crónica [214] y de bajo grado inducida por sustancias químicas [215]. Los metabolitos liberados por esta bacteria atenúan la gravedad de la inflamación, reforzando la barrera intestinal, al inducir la expresión de algunas proteínas de las uniones estrechas de los enterocitos, producir moco y mantener las proporciones adecuadas de diferentes células epiteliales [216,217].

Akkermansia muciniphila

Akkermansia muciniphila es uno de los probióticos de nueva generación más estudiados en el contexto de obesidad y diabetes. Es una bacteria Gram-negativa que pertenece al filo de *Verrucomicrobia* y representa un 3-5% del total de la microbiota intestinal en individuos sanos. Coloniza la mucosa del colon donde degrada el complejo glicoproteico y participa en el intercambio de nutrientes [218–220]. Los niveles de *A.muciniphila* están inversamente relacionados con la obesidad, diabetes y síndrome metabólico [221], además, personas con sobrepeso y alta abundancia de la bacteria responden mejor a intervenciones con dietas hipocalóricas [164]. La función de *A. muciniphila* en la obesidad y los posibles mecanismos de acción han sido evaluados en diferentes modelos animales.

La administración de la cepa bacteriana de *A. muciniphila*, MucT ATTC BAA-835 en modelos de obesidad, reduce la endotoxemia metabólica, la inflamación del tejido adiposo y la resistencia a insulina inducidas por la dieta rica en grasa. Los posibles mecanismos de acción por los cuales esta cepa promueve un fenotipo metabólico saludable son el aumento del grosor del moco y de endocanabinoides intestinales. Estos efectos podrían contribuir a controlar la inflamación, fortalecer la barrera intestinal y estimular la producción de GLP-1, involucrado en la reducción de la ingesta calórica y la homeostasis energética, así como de GLP-2, esencial para la preservación de la función barrera del intestino [222]. Estudios más recientes revelan que *A. muciniphila* pasteurizada conserva su capacidad para reducir el desarrollo de masa grasa, resistencia a insulina y dislipemia en ratones, efectos que se atribuyen a la proteína Amuc_1100, proteína de la membrana externa de la bacteria estable a las

temperaturas de pasteurización. A través del TLR2, Amuc_1100 induce los efectos beneficiosos de la bacteria, al reducir la absorción de energía en el intestino, la endotoxemia y la trigliceridemia [223]. En un estudio piloto, se ha evaluado el efecto de la administración de *A. muciniphila* pasterurizada a humanos voluntarios con sobrepeso u obesidad con resistencia a insulina durante tres meses. En comparación con el placebo, la bacteria mejora la sensibilidad a la insulina, reduce el peso corporal y mejora la disfunción e inflamación hepática [224].

Bacteroides uniformis

Bacteroides uniformis CECT 7771 ha sido seleccionado como potencial probiótico de nueva generación para el tratamiento de la obesidad, en base a asociaciones entre una mayor abundancia de *Bacteroides* spp. y un fenotipo delgado en diversos estudios en humanos, así como de la especie *B. uniformis* con la lactancia materna, que a su vez está relacionada con un menor riesgo de desarrollar obesidad y diabetes tipo 2. [225,226]. La cepa *B. uniformis* CECT 7771, aislada a partir de heces de niños alimentados con leche materna, mejora la disfunción metabólica e inmune inducida por la dieta rica en grasa en ratones. Concretamente, esta cepa reduce la ganancia de peso corporal, la esteatosis hepática, las concentraciones de colesterol y triglicéridos en hígado y sangre, así como los niveles de glucosa, insulina y leptina [227]. Sobre el estado de seguridad de esta cepa, estudios toxicológicos indican que el consumo oral agudo y crónico de *B. uniformis* no plantea problemas de seguridad en modelos animales [228,229].

Más alla de los probióticos, ciertos compuestos generados en los procesos fermentativos de los microorganismos pueden tener efectos beneficiosos sobre la salud del huésped. En este caso, el efecto beneficioso se asocia a la administración de este compuesto bioactivo también conocido como postbiótico y no tanto a la bacteria viva o probiótico. Entre ellos se incluyen los SCFA, metabolitos, fracciones celulares, proteínas, polisacáridos extracelulares, etc [230].

4.3 Simbióticos

En 1995, Gibson y Roberfroid introdujeron el término “simbiótico” para describir una combinación de probióticos y prebióticos con actividad sinérgica [185]. La sinergia hace referencia a que el componente prebiótico favorece selectivamente el crecimiento de ciertos microorganismos probióticos, mejorando su adaptación al ecosistema intestinal y, por tanto, potenciando sus beneficios [231]. Así, la combinación de ambos componentes puede potencialmente presentar un efecto superior en comparación con su efecto individual [232–235]. Recientemente la ISAPP [236] ha definido como “simbiótico complementario” el que no ha sido diseñado para que sus componentes funcionen de manera cooperativa y como “simbiótico sinérgico” el que está diseñado para ser utilizado selectivamente por los microorganismos administrados.

Los estudios más recientes han demostrado que la administración de algunos simbióticos como tratamiento para la obesidad puede mejorar la función hepática [233] , el metabolismo lipídico, la homeostasis de glucosa [234], la inflamación sistémica [237], la integridad de la barrera intestinal [238] y mantener el peso corporal [235,239]. Todas estas evidencias sugieren que las combinaciones de probióticos y prebióticos podrían ser efectivas para combatir los trastornos metabólicos.

OBJETIVOS

Objetivos

El objetivo general de la tesis ha sido evaluar la eficacia de nuevas estrategias de intervención, basadas en la modulación de las funciones de la microbiota intestinal, contra la obesidad e identificar su modo de acción a través de interacciones con el hospedador.

Para lograr este objetivo global, se han abordado los siguientes objetivos específicos:

1. Seleccionar bacterias autóctonas del tracto intestinal humano que se consideren funcionalmente relevantes para el tratramiento de la obesidad y las comorbilidades asociadas, en base a los resultados de estudios epidemiológicos realizados en humanos, y la posterior evaluación de las propiedades inmunológicas y endocrinas de las bacterias identificadas como potenciales probióticos in vitro.

2. Evaluar la efectividad de las bacterias seleccionadas, que puedan constituir una nueva generación de probióticos, en modelos animales de obesidad inducida por la dieta.

3. Determinar el modo de acción de las bacterias seleccionadas en la regulación del balance energético, las alteraciones endocrinas y la inflamación, en modelos animales de obesidad inducida por la dieta.

RESULTADOS Y DISCUSIÓN

Resultados y discusión

CAPÍTULOS DE LA TESIS

Capítulo 1: Modo de acción de la cepa *Bacteroides uniformis* CECT 7771 sobre la inmunidad y efecto de su combinación con fibra dietética (extracto de salvado de trigo) en un modelo de obesidad.

- *Bacteroides uniformis* CECT 7771 alleviates inflammation within the gut-adipose tissue axis, involving TLR5 signaling, in diet-induced obese mice

- *Bacteroides uniformis* combined with fibre amplifies metabolic and immune benefits in obese mice

Capítulo 2: Evaluación de cepas de *Holdemanella biformis* y *Phascolarctobacterium faecium* como nuevos potenciales probióticos para combatir la obesidad y sus comorbilidades.

- *Holdemanella biformis* improves glucose tolerance in obese mice via GLP-1 signaling

- *Phascolarctobacterium faecium* confers resistance to diet-induced obesity through recuction of food intake and activation of anti-inflammatory and defensive immune mechanisms in mice

CAPÍTULO 1

Capítulo 1

Modo de acción de la cepa *Bacteroides uniformis* CECT 7771 sobre la inmunidad y efecto de su combinación con fibra dietética (extracto de salvado de trigo) en un modelo de obesidad.

- *Bacteroides uniformis* CECT 7771 alleviates inflammation within the gut-adipose tissue axis, involving TLR5 signaling, in diet-induced obese mice.

- *Bacteroides uniformis* combined with fibre amplifies metabolic and immune benefits in obese mice.

Bacteroides uniformis CECT 7771 alleviates inflammation within the gut-adipose tissue axis, involving TLR5 signaling, in diet-induced obese mice

Emanuel Fabersani, Kevin J. Portune, Isabel Campillo, Inmaculada López-Almela, Sergio Montserrat-de la Paz, Marina Romaní-Pérez, Alfonso Benítez-Páez and Yolanda Sanz

(Under review in *Scientific report*)

Microbial Ecology, Nutrition & Health Research Unit, Institute of Agrochemistry and Food Technology, National Research Council (IATA-CSIC). Valencia, Spain

Abstract

This study investigated the immune mechanisms whereby administration of *Bacteroides uniformis* CECT 7771 reduces metabolic dysfunction in obesity. C57BL/6 adult male mice were fed a standard diet or a Western diet high in fat and fructose, supplemented or not with *B. uniformis* CECT 7771 for 14 weeks. *B. uniformis* CECT 7771 reduced body weight gain, pl

asma cholesterol, triglyceride, glucose, and leptin levels; and improved oral glucose tolerance in obese mice. Moreover, *B. uniformis* CECT 7771 modulated the gut microbiota and immune alterations associated with obesity, increasing Tregs and reducing B cells, total macrophages and the M1/M2 ratio in both the gut and epididymal adipose tissue (EAT) of obese mice. *B. uniformis* CECT 7771 also increased the concentration of the anti-inflammatory cytokine IL-10 in the gut, EAT and peripheral blood, and protective cytokines TSLP and IL-33, involved in Treg induction and type 2 innate lymphoid cells activation, in the EAT. It also restored the obesity–reduced TLR5 expression in the ileum and EAT. The findings indicate that the administration of a human intestinal bacterium with immunoregulatory properties on the intestinal mucosa helps reverse the immuno-metabolic dysfunction caused by a Western diet acting over the gut-adipose tissue axis.

Keywords: obesity; metabolic syndrome; inflammation, TLR, microbiota, *Bacteroides*.

Running title: *Bacteroides uniformis* CECT 7771 reduces obesity-associated inflammation

Introduction

Obesity has become a major global health challenge due to its increasing prevalence. In 2016, more than 1.9 billion adults (39%) 18 years and older were overweight and of these over 650 million (13%) were obese, according to the WHO [1]. Obesity frequently results in a state of chronic low-grade inflammation that is considered a precipitating factor of metabolic complications, such as type 2 diabetes, cardiovascular disease and non-alcoholic fatty liver disease [2]. Inflammation of the white adipose tissue (WAT) is considered a major driver of metabolic alterations and, therefore, has been investigated in depth. WAT inflammation is mediated by an overall increase in macrophages largely due to the recruitment of M1 (or classically activated) macrophages and reduction of anti-inflammatory M2 macrophages (or alternatively activated macrophages). This leads to overproduction of pro-inflammatory cytokines (e.g. IL-1β, IL-6, and TNF-α) in relation to anti-inflammatory (IL-4 and IL-10) ones [3]. Although macrophages are considered the ultimate effector cells producing cytokines which cause metabolic dysfunction, IFN-γ–secreting Th1 cells, CD8+ T cells, and B cells are also increased in the WAT and contribute to macrophage recruitment and immune activation in this tissue [4]. The WAT has been considered the main contributor to inflammation and metabolic dysfunction during obesity, but now it is known that this phenomenon affects multiple organs, including the brain, muscle, liver and gut [5]. The most recent evidence specifically supports that the intestinal immune system and the microbes that expand under exposure to unhealthy diets are additional drivers of inflammation in obesity [6-8] and that this metabolic inflammation ("metainflammation") can be initiated in the gut [9].

The intestinal microbiota influences multiple aspects of immunity, both locally and systemically, allowing for the induction of pro-inflammatory or regulatory immune pathways that set the inflammatory tone of different tissues [10]. In experimental study models, gut microbiota alterations resulting from unhealthy diets have been causally related to immune and metabolic alterations associated with obesity presumably due to dysfunctions in the cross-talk between the gut and other peripheral organs, such as the liver and the adipose tissue [11,12]. Specific mechanisms whereby interactions between unhealthy diets and the gut microbiota contribute to metabolic inflammation include reduction in host intestinal antimicrobial peptide production, over-activation of innate immunity leading to pro-inflammatory cytokine production, and disruption of the gut barrier facilitating translocation of microbial products (e.g. LPS) [8,11,13]. In light of these findings, strategies to restore the functions of the gut microbiota to help recover the control over the immune-metabolic axis in obesity are being

investigated, including the administration of prebiotic fibers or specific bacterial strains [11,14].

Controversial evidence regarding the role of the gut microbiota's two dominant phyla, Bacteroidetes and Firmicutes, in diet-induced obesity has been documented. Numerous observational and intervention studies have correlated a lean phenotype or weight loss to increases in the phylum Bacteroidetes (including the genera *Bacteroides* and *Prevotella*), although a number of studies have, however, established inverse associations between obesity and these bacterial taxa [15,16]. Observational studies also associated increased abundances of Bacteroidetes or *Bacteroides* spp. with Western diets (high in animal fat and protein) related to obesity [17]. Nonetheless, a recent study indicates that associations established so far between the increased abundance of *Bacteroides* and consumption of Western diets rich in animal fat/proteins were oversimplifications and that sub-genus diversity also matters [18]. Different components of the genus *Bacteroides* were, in fact, associated with either plant-based or animal-based diets, the latest usually related to obesity [18]. In fact, *Bacteroides* spp. are known to be equipped with a metabolic machinery specialized in the utilization of oligo- and polysaccharides derived from plants that are part of healthy diets [19] and lead to the production of short-chain fatty acids [20], which may have beneficial effects on glucose metabolism and satiety. Moreover, strains of *Bacteroides fragilis* show immunomodulatory properties, optimizing the systemic Th1/Th2 balance, and inducing Treg cell differentiation, reducing autoimmune disorders in experimental models [21-23]. In a previous study carried out by our research group, *B. uniformis* CECT 7771 demonstrated an ability to reduce body weight gain and liver steatosis in mice fed a high-fat diet (HFD) [24]. Nevertheless, the possible role of *B. uniformis* CECT 7771 in the regulation of the inflammatory tone associated with obesity remains to be investigated.

This study aimed to progress in the understanding of the cellular and molecular mechanisms mediating the beneficial effects of *B. uniformis* CECT 7771 in the metabolic phenotype of diet-induced obese mice. To this end, we have specifically investigated the effects of the oral administration of this bacterial strain on immune cell populations and inflammatory mediators that may contribute to metabolic inflammation during obesity in the gut, peripheral blood and the adipose tissue. The possible molecular mechanisms mediating the effects related to TLR signaling and the microbiota configuration have also been investigated in depth.

Results

B. uniformis CECT 7771 improves the metabolic phenotype of obese mice

The oral administration of *B. uniformis* CECT 7771 significantly reduced body weight gain approximately by 20% ($p < 0.001$) at the end of the intervention in the HFHFD-fed mice, but did not modify body weight gain in the SD-fed mice (Fig. 1A). Consistent with these findings, visceral adipose tissue (VAT), epididymal adipose tissue (EAT) and mesenteric adipose tissue (MAT) weights were significantly lower in obese mice fed *B. uniformis* (HFHFD+B group) (40%; $p < 0.001$, 44%, $p < 0.001$, and 28%, $p = 0.005$, respectively) than in obese mice fed placebo (HFHFD group) (Figs. 1B-1D). Moreover, although the total caloric intake from both the solid and liquid parts of the diet was significantly higher in both mouse groups fed the HFHFD ($p < 0.001$) than in those fed the SD (Fig. 1E), the administration of *B. uniformis* CECT 7771 significantly reduced the total caloric intake, approximately by 11% in obese mice (HFHFD versus HFHFD+B $p = 0.019$), mainly by decreasing the caloric intake from solid food (Fig. 1E).

The plasma concentrations of cholesterol, triglycerides, glucose, insulin, and leptin are shown in Figs. 2A-2G. As expected, no changes in plasma values were observed between mice fed the SD and those fed the SD supplemented with *B. uniformis* CECT 7771. Compared to the SD group, the HFHFD group showed markedly increased ($p < 0.001$) plasma cholesterol (Fig. 2A), triglycerides (Fig. 2B) and glucose concentrations (Fig. 2C). Mice subjected to a glucose tolerance test displayed increased glucose levels in the HFHFD group compared to the other treatments for individual time points between 15 to 60 minutes, as well as overall AUC values (Figs. 2D-2E). Insulin and leptin concentrations were also significantly elevated ($p < 0.001$) in the HFHFD group compared to the SD group (Fig. 2F-2G). The administration of *B. uniformis* CECT 7771 to HFHF-fed mice (HFHFD+B group) significantly reduced plasma cholesterol (26%, $p = 0.043$), triglycerides (40%, $p < 0.001$), glucose (27%, $p = 0.026$), and leptin (48%, $p = 0.019$) concentrations compared to obese mice fed placebo (HFHFD group) (Fig 2A-2G).

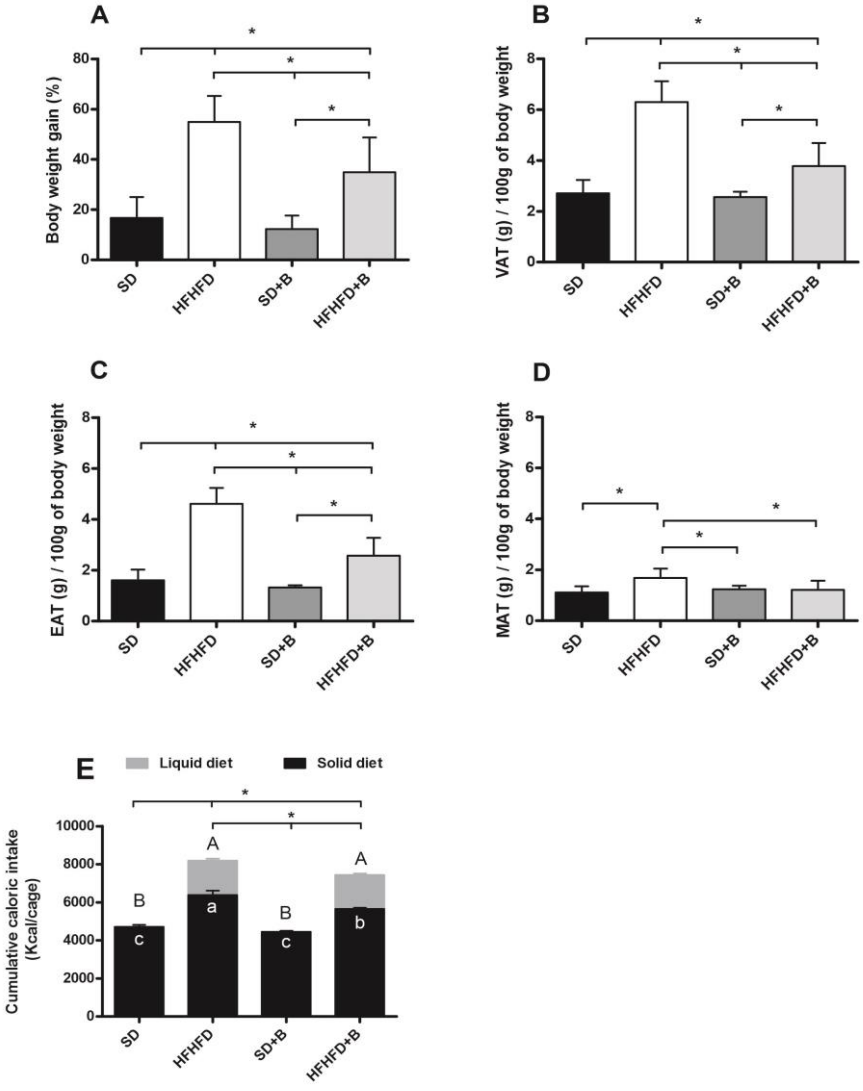

Figure 1: Anthropometric parameters and dietary intake. (A) Body weight gain, (B) Visceral adipose tissue (VAT) weight, (C) Epididymal adipose tissue (EAT) weight, (D) Mesenteric adipose tissue (MAT) weight, (E) cumulative caloric intake from liquid diet, solid food and total caloric intake. Data are expressed as mean and standard error (vertical bars). Significant differences for liquid diets, solid foods, and total caloric intake are represented by uppercase letters, lowercase letters and stars, respectively. Statistically significant differences were established by ANOVA and *post hoc* student t test ($p < 0.05$).

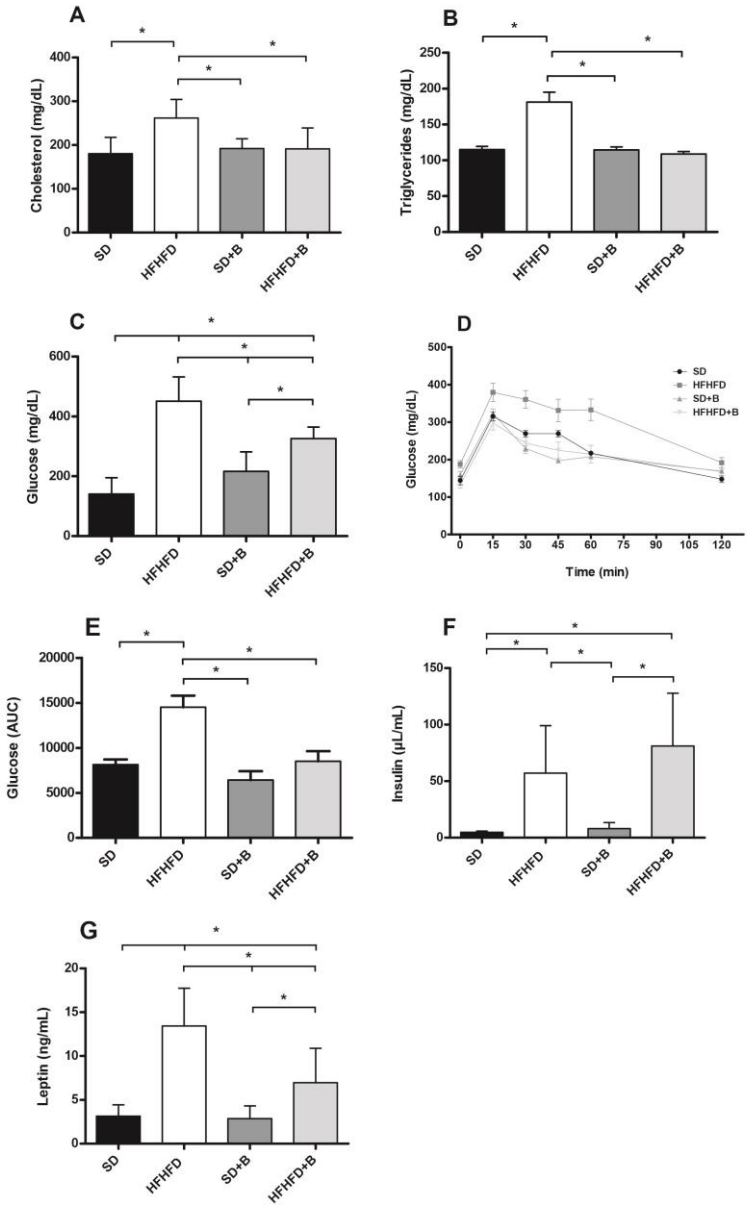

Figure 2: Plasma concentrations (mean +/- SE) of (A) cholesterol, (B) triglycerides, (C) glucose, (D) glucose levels for individual time points in a glucose tolerance, (E) AUC values for glucose in a GTT, (F) insulin and (G) leptin. Data are expressed as mean and standard error (vertical bars). Statistically significant differences were established by ANOVA and *post hoc* student t test ($p < 0.05$).

B. uniformis CECT 7771 restores the adaptive and innate immune cell imbalances of obese mice

The effects of *B. uniformis* CECT 7771 administration on lymphocyte and macrophage populations in peripheral blood, intestinal Peyer's Patches (PP), and EAT from different mouse groups are shown in Table 1. Compared to the SD group, the HFHFD group showed increased proportions of B cells and reduced Tregs in peripheral blood, intestinal PP and EAT (p = <0.001 - 0.017). The administration of *B. uniformis* in obese mice fed a HFHFD effectively reduced the proportion of B cells (p = <0.001-0.006) and increased T regs (p = 0.013- 0.041) in all tested compartments of obese mice (HFHFD+B versus HFHFD). Obese mice fed a HFHFD also showed increased proportions of total macrophages and of the M1/M2 ratio in PP and EAT compared to the SD group (p < 0.001-0.020), but these HFHFD-induced alterations were significantly reduced by the administration of *B. uniformis* CECT 7771 in both tissues (HFHFD+B versus HFHFD, p < 0.001-0.019).

B. uniformis CECT 7771 regulates the cytokine network driving obesity-associated inflammation in mice

The effects of *B. uniformis* CECT 7771 administration on cytokine concentrations in the peripheral blood, EAT and ileum (PP) from control and obese mice are shown in Table 2. The direct inflammatory effects of the HFHFD in peripheral tissues (EAT) were reflected in the reduction of the anti-inflammatory and protective cytokines IL-10, IL-33 and TSLP compared to SD mice (p = 0.009-0.022). These cytokine alterations were reversed by the administration of *B. uniformis* CECT 7771 in obese mice (HFHFD+B versus HFHFD, p = 0.011 - 0.048). The role of *B. uniformis* CECT 7771 in the promotion of intestinal immune homeostasis was also translated into systemic effects in peripheral blood and locally in the gut (Peyer's patches) of obese mice. The administration of *B. uniformis* CECT 7771 ameliorated the HFHFD-induced alterations in peripheral blood concentrations of pro-inflammatory cytokines (IL-1α, and TNF-α) and the anti-inflammatory cytokine IL-10, and also increased IL-5 (p = 0.015- 0.028), overall reducing the inflammatory tone. In PP, the HFHFD increased the concentration of IFNγ compared to the SD (p = 0.012), but *B. uniformis* CECT 7771 administration reversed this effect on IFNγ (p = 0.002) and also increased the concentrations of IL-10 (p = 0.032) in obese mice.

Cell population	Experimental Groups											
	SD		HFHFD		SD+B		HFHFD+B		p-value			
	Mean	se	Mean	se	Mean	se	Mean	se	HFHFD vs SD	SD+B vs SD	HFHFD+B vs HFHFD	HFHFD +B vs SD
Peripheral blood												
B cells (%)	22.19	3.13	60.18	10.58	28.92	6.96	18.85	5.30	0.011*	0.904	0.006*	0.986
Regulatory T cells (%)	5.69	0.73	0.75	0.20	6.75	1.76	4.99	0.40	0.017*	0.868	0.041*	0.955
Peyer's patches												
B cells (%)	2.98	0.59	6.16	0.52	2.77	0.40	3.49	0.15	0.001*	0.987	0.006*	0.847
Regulatory T cells (%)	20.50	4.09	4.00	0.57	15.75	2.13	20.50	3.20	0.013*	0.711	0.013*	0.999
Total macrophages (%)	6.15	1.17	18.37	2.80	8.23	2.01	7.73	0.70	0.002*	0.856	0.007*	0.929
M1/M2 macrophage ratio	1.09	0.42	6.29	1. 99	1.88	0.41	1.07	0.27	0.020*	0.950	0.019*	0.059
Epididymal adipose tissue												
B cells (%)	1.21	0.22	5.30	0.20	0.66	0.10	2.65	0.10	<0.001*	0.145	<0.001*	<0.001*
Regulatory T cells (%)	13.11	0.87	4.18	0.40	10.60	2.35	9.68	0.76	0.001*	0.832	0.038*	0.291
Total macrophages (%)	10.91	2.36	61.84	9.203	12.54	3.00	19.68	3.11	<0.001*	0.996	<0.001*	0.645
M1/M2 macrophage ratio	2.45	0.68	8.80	0.36	2.19	0.19	5.03	0.89	<0.001*	0.989	0.003*	0.043*

Table 1. Effects of *Bacteroides uniformis* CECT 7771 on adaptive and innate immunity from mice in all experimental groups.
SD group: control mice received a standard diet (SD) plus placebo; HFHFD group: obese mice received a high-fat high-fructose diet (HFHFD) plus placebo; SD+B group: control mice received a SD and a daily dose of 1 x 10^8 CFU *Bacteroides uniformis* CECT 7771; HFHFD+B group: obese mice received HFHFD and a daily dose of 1 x 10^8 CFU *Bacteroides uniformis* CECT 7771 by gavage during 14 weeks. Data are expressed as mean and standard error (*se*) of each mouse group (n = 10 per group). *Significant differences were established by ANOVA and *post hoc* student *t* test ($p < 0.050$).

Cell population	Experimental Groups								p-value			
	SD		HFHFD		SD+B		HFHFD+B					
	Mean	se	Mean	se	Mean	se	Mean	se	HFHFD vs SD	SD+B vs SD	HFHFD+B vs HFHFD	HFHFD+B vs SD
Peripheral blood												
IL-1α (pg/mL)	1067.96	167.88	2591.65	740.56	229.93	86.30	710.28	223.42	0.047*	0.466	0.019*	0.919
IL-5 (pg/mL)	75.34	30.97	30.54	30.54	316.07	82.82	312.36	67.19	0.945	0.041*	0.015*	0.045*
IL-10 (pg/mL)	51.18	20.84	3.00	3.00	70.62	18.17	87.29	25.59	0.038*	0.884	0.028*	0.545
IL-13 (pg/mL)	2122.85	483.78	276.66	202.83	1121.60	391.20	552.60	310.00	0.011*	0.245	0.948	0.033*
TNF-α (pg/mL)	87.26	13.36	2028.2	806.0	207.80	169.80	250.00	153.90	0.022*	0.996	0.038*	0.992
Peyer's patches												
IL-10 (pg/ g)	3846.83	683.99	2273.64	194.51	3090.06	266.77	4337.10	604.40	0.133	0.692	0.032*	0.890
IFNγ (pg/ g)	861.46	617.66	4142.19	598.51	627.70	378.15	1097.15	430.35	0.012*	0.988	0.002*	0.988
IL-33 (pg/ g)	24.10	1.10	29.73	2.55	23.92	0.53	25.82	2.11	0.142	0.999	0.420	0.899
TSLP (pg/ g)	10.76	1.67	16.80	4.67	10.75	1.89	13.52	2.72	0.504	0.999	0.862	0.912
Epididymal adipose tissue												
IL-10 (pg/ g)	52878.71	9812.70	11113.52	1555.77	57114.54	8570.28	41770.15	12392.59	0.018*	0.987	0.038*	0.819
IFNγ (pg/ g)	14383.86	5899.76	23018.19	5164.28	8224.68	2990.85	10334.88	5137.00	0.609	0.812	0.292	0.936
IL-33 (pg/ g)	8365.26	1295.68	2639.40	1234.19	4995.60	1344.29	8943.69	1228.05	0.022*	0.273	0.011*	0.988
TSLP (pg/ g)	4149.40	947.55	832.28	244.10	6917.25	842.20	3024.91	252.82	0.009*	0.034*	0.048*	0.628

Table 2. Effects of *Bacteroides uniformis* CECT 7771 on cytokine concentrations in plasma and tissues from mice in all experimental groups.
SD group: control mice received a standard diet (SD) plus placebo; HFHFD group: obese mice received a high-fat high-fructose diet (HFHFD) plus placebo; SD+B group: control mice received a SD and a daily dose of 1 x 10^8 CFU *Bacteroides uniformis* CECT 7771; HFHFD+B group: obese mice received HFHFD and a daily dose of 1 x 10^8 CFU *Bacteroides uniformis* CECT 7771 by gavage during 14 weeks. Data are expressed as mean and standard error (*se*) of each mouse group (n = 10 per group). *Significant differences were established by ANOVA and *post hoc* student *t* test ($p < 0.050$).

Induced changes in TLRs by diet and *B. uniformis* CECT 7771

To understand the molecular pathways mediating the effects of *B. uniformis* CECT 7771 in obesity, we analyzed the expression of TLRs in intestinal PP and EAT. The results show that in intestinal PP the HFHFD down-regulated the TLR2, TLR4, and TLR5 protein expression compared to SD (Figs. 3A-C), whereas *B. uniformis* CECT 7771 normalized the expression of TLR5 (Fig. 3C, $p < 0.001$) in obese mice levels compared to SD mice. Similar effects of HFHFD and *B. uniformis* CECT 7771 on TLR5 expression were detected in EAT (Fig. 3D), but with a lower magnitude than in the PP. In order to identify the possible *in vivo* activators of TLR5, *in vitro* experiments were conducted using HEK-Blue™ hTLR5 cells stimulated with fecal samples from the different experimental mouse groups and pure cultures of *B. uniformis* CECT 7771 (Figs. 3E and F). The results using HEK-Blue™ hTLR5 cells confirmed that TLR5 relative activation was significantly reduced when using fecal samples from the HFHFD-fed mice as stimulus and restored when using fecal samples from obese mice fed with *B. uniformis* CECT 7771 (Fig. 3E). Furthermore, pure cultures of *B. uniformis* CECT 7771 also significantly activated TLR5 and even more than a positive control strain of *C. butyricum* at similar cell concentrations, while bacterial cultures used as a negative control (*P. faecium*) did not activate TLR5 (Fig. 3F).

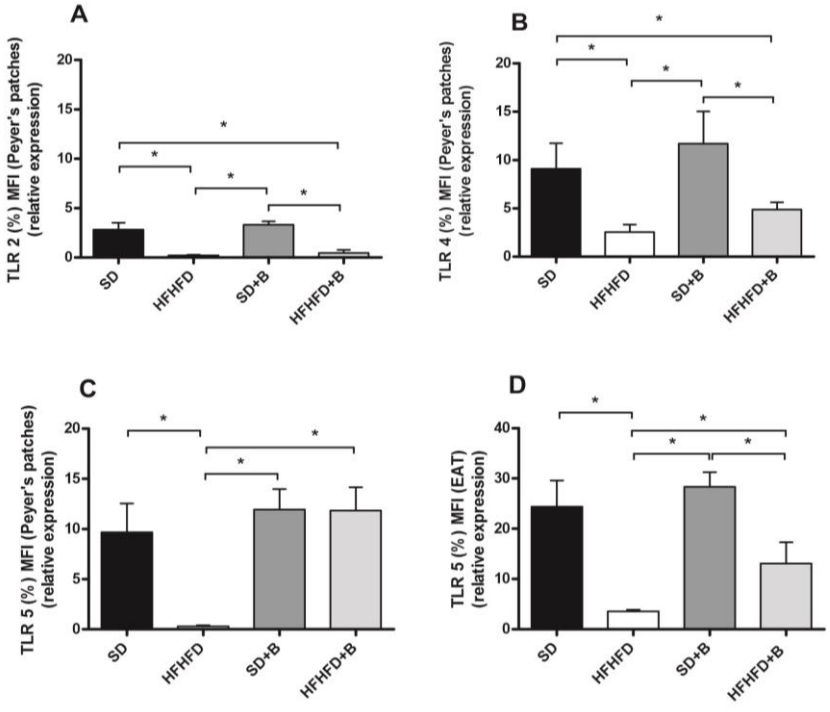

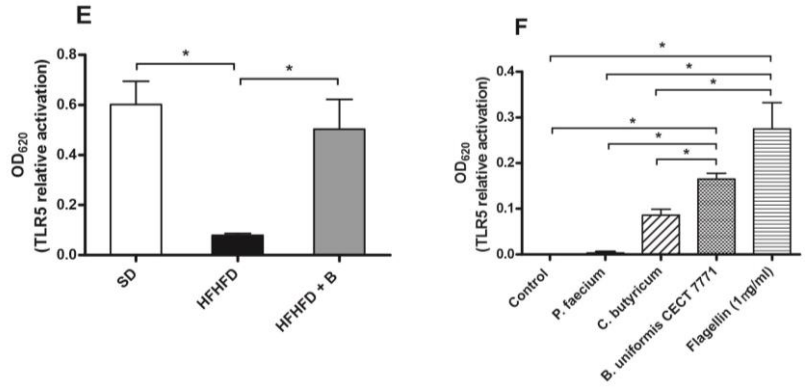

Figure 3: Relative expression of (A) TLR2, (B) TLR4 and (C) TLR5 from Peyer´s patches and (D) TLR5 from epididymal adipose tissue. Relative activation of TLR5 using HEK-Blue™ hTLR5 cells with (E) fecal samples from the SD, HFHFD and HFHFD+B experimental groups and (F) individual bacterial cultures of *Phascolarctobacterium faecium* (negative control), *Clostridium butyricum* (positive control), *B. uniformis* CECT 7771, and recombinant flagellin (RecFLA-ST, 1µg/ml) (positive control). Control samples consisting of endotoxin-free water were included as negative controls. Data are expressed as mean and standard error (vertical bars). Statistically significant differences were established by ANOVA and *post hoc* student t test ($p < 0.05$).

Gut microbiota-induced changes by the diet and *B. uniformis* CECT 7771

Alpha diversity (Simpson's diversity index) was significantly reduced ($p < 0.05$) in all treated mouse groups (HFHFD, SD+B, and HFHFD+B) compared to SD group, largely due to a significant reduction in evenness (Simpson's evenness) in these groups compared to the SD group (Fig. 4A). Significant differences in beta diversity using a global PERMANOVA test ($p = 0.001$) as well as pairwise comparisons (q = 0.0024 - 0.003) were observed between all treatments using generalized UniFrac distances (Fig. 4B) indicating distinct microbial compositions in different treatment groups by the end of the treatment period.

Individual gut microbiota taxonomic groups were affected by diet and/or the addition of *B. uniformis* CECT 7771 (Fig. 4C). As expected, substantial increases in the genus *Bacteroides* were observed in both mouse groups that were fed *B. uniformis* CECT 7771 SD+B and HFHFD+B) groups compared to their respective groups (SD and HFHFD), but differences were statistically significant only in obese mice (Fig. 4C). Interestingly, significant increases in the potentially pathogenic genus *Helicobacter* were observed in obese mice under the HFHFD, whereas abundance of this genus was reduced in the HFHFD+B

group, which were similar to the control group (SD). Further analysis via BLAST of the DNA sequence associated with the OTU classified to this genus revealed a single species identified as *Helicobacter ganmani* (100% identity). *Ruminococcaceae* UCG-014 was reduced by the HFHFD but the administration of the bacteroides strain did not restore this alteration.

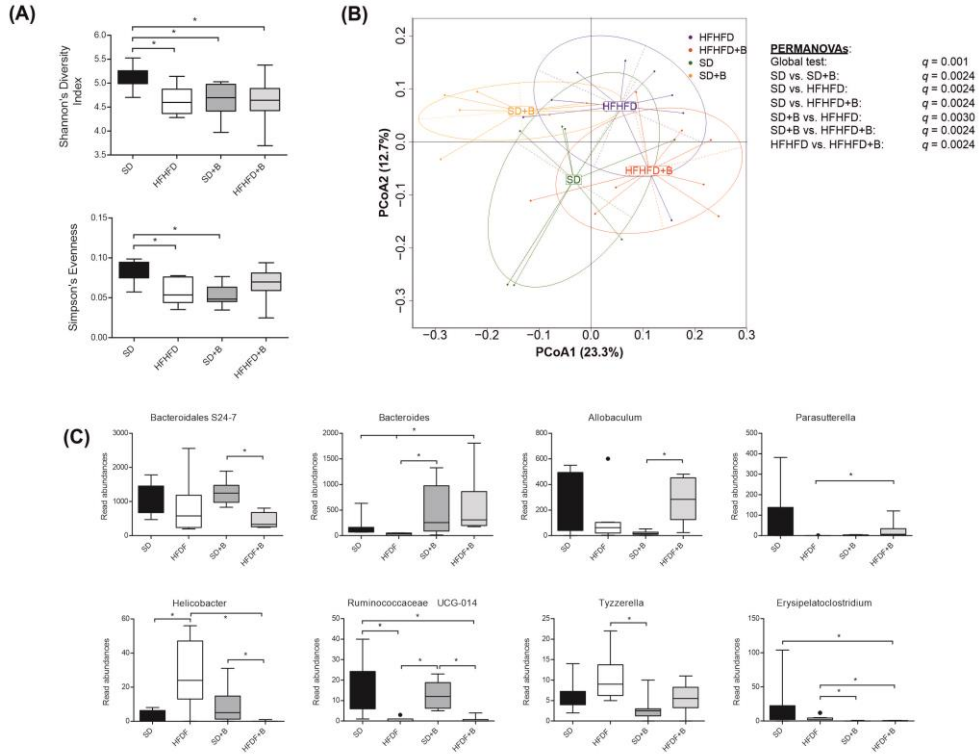

Figure 4: (A) Alpha diversity indices (Shannon's diversity index, Simpson's index, Simpson's reciprocal index and Simpson's evenness) from each treatment group. (B) Principle coordinates analysis (PCoA) plot using generalized UniFrac distances comparing microbial communities from each treatment group. Group means are indicated by the center of each ellipse. Distance-based non-parametric PERMANOVA tests were conducted at a global level as well as pairwise comparisons of treatment groups. *P* values of all pairwise comparisons were corrected for multiple comparisons (q) using false discovery rate. (C) Boxplots of gut microbiota taxonomic groups that demonstrated significant differences between treatment groups. Significant differences ($p < 0.05$) between treatment groups are represented exclusively with different letters.

Correlations between metabolic, immune and gut microbiota features

Increased weight gain was positively correlated ($q < 0.05$) with EAT weight (WAT), blood glucose, leptin, B cells (from EAT), and total macrophages and ratios of M1/M2 (from EAT) (Fig. 5). Negative correlations ($q < 0.05$) were observed between expression of TLR5 in either PP or EAT with obesity markers such as increased body weight gain, cholesterol, triglycerides, EAT weight, blood glucose and leptin as well as the blood pro-inflammatory markers IFNγ and IL-1α, while TLR5 from EAT positively correlated with anti-inflammatory makers IL-10 and TSLP from EAT (Fig. 5). Furthermore, negative correlations ($q < 0.05$) between TLR2 or TLR4 from PP were observed with weight gain, EAT weight, blood glucose and leptin, as well as with B cells and total macrophages (from EAT) and (Fig. 5).

Significant negative correlations ($q < 0.05$) were observed between the genus *Bacteroides* and body weight gain, plasma triglycerides and several blood pro-inflammatory markers (i.e. IL-1α, TNFα), while positive correlations were observed for both anti-inflammatory makers in the obesity context (e.g. IL-10 (blood and EAT), plasma IL-5, TSLP from EAT) and TLR5 expression in EAT (Fig. 5). Multiple bacterial taxonomic groups were also positively correlated ($q < 0.05$) with TLR5 from EAT (Bacteroidales *S24-7, Bacteroides* and *Ruminococcaceae* UCG-014).

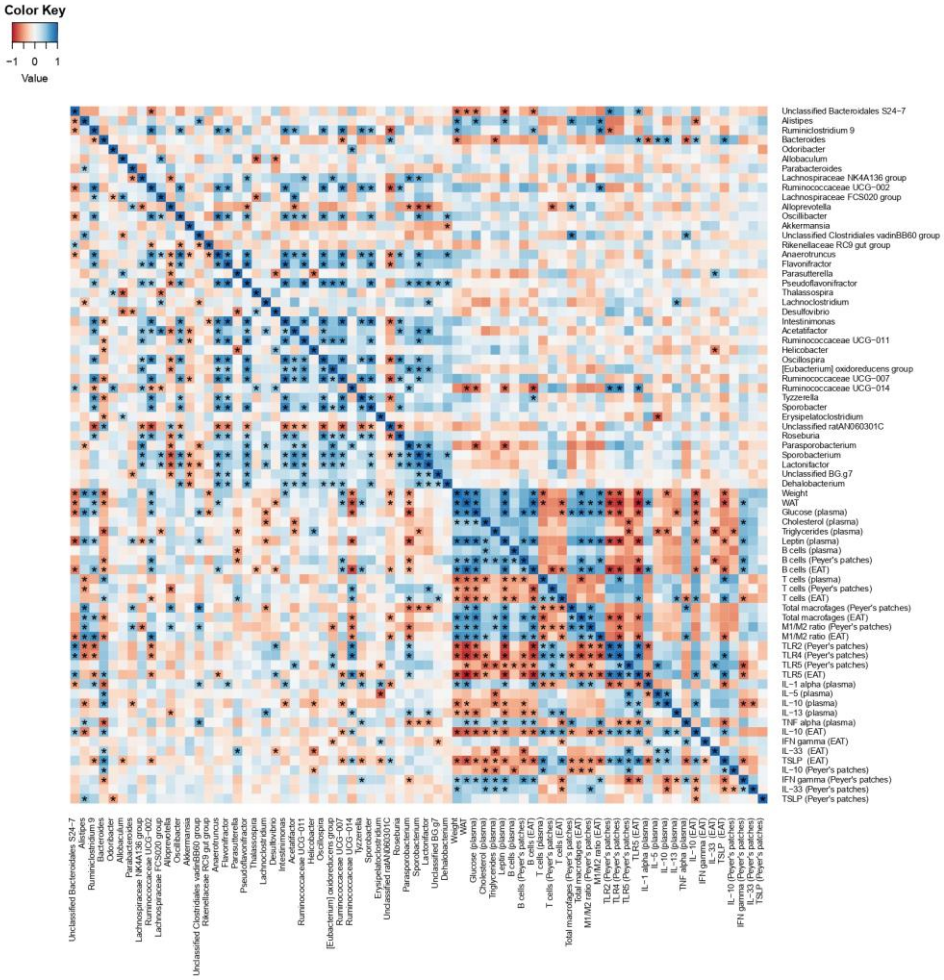

Figure 5: Heatplot of correlations between anthropometric, metabolic, and immune features with the top 50 most abundant gut microbiota taxonomic groups (classified to the highest taxonomic level). The relative key color indicates the value of Spearman's correlation coefficient rho (ρ) (blue = positive; red = negative). *P*-values were adjusted with the false discovery rate method for multiple comparisons. Variable pairs that have an "*" below the diagonal line are significantly correlated and pairs with a "*" above the diagonal line are significantly correlated after adjustment of *p*-values for multiple comparisons (q <0.05).

Discussion

This study shows that a Western-style diet locally impacts the intestine, altering the microbiome´s symbiotic configuration and enhancing the inflammatory tone, two interrelated effects linked to obesity and immune-metabolic dysfunction affecting distant organs. The present pre-clinical study also proves that interventions primarily targeting the intestine can be used to reverse the immune-metabolic deregulation caused by the diet via the cross-talk between the gut and the peripheral tissues affected in obesity, such as the adipose tissue. Specifically, the oral administration of the strain *B. uniformis* CECT 7771 partly re-establishes the state of symbiosis and resets adverse intestinal inflammation, ameliorating the systemic immune-metabolic deregulation induced by the Western diet.

Our study specifically shows that the administration of *B. uniformis* CECT 7771 restored the B and T cell deregulation that is characteristic of diet-induced obesity [25-27], reducing B cells and increasing Tregs in all body compartments studied. It also reversed the obesity-induced increase in total macrophages and the M1/M2 ratio in intestinal PP and EAT. All of these changes occurred in parallel to the restoration of the metabolic homeostasis in obese mice fed *B. uniformis* CECT 7771. In a previous study, it was specifically proven that diet-induced microbiota changes impact the intestinal adaptive immune system, leading to imbalances in effector T and regulatory cells, and that this was sufficient to trigger metabolic disease in experimental models [28]. Considering also that positive relationships have been established between increases in B cells and parallel reductions in Tregs in obesity models [29], the production of Tregs seems to be a key cellular mechanism whereby *B. uniformis* CECT 7771 restores the immune-metabolic homeostasis. This is also reflected in the shifts of the key pro-inflammatory (TNFα, IFNγ) and anti-inflammatory (IL-10) cytokines produced by macrophages (M1) and Tregs, respectively [29-31].

It is noteworthy that *B. uniformis* CECT 7771 attenuated not only intestinal inflammation but also systemic and adipose tissue inflammation, inducing changes in the same regulatory and anti-inflammatory cells (increased Tregs and decreased M1/M2 ratio) and key cytokines (TNFα and L-10). In the adipose tissue, we also observed that the intervention with this bacterium increased the concentrations of intestinal cytokines involved in the expansion of Tregs. In particular, *B. uniformis* CECT 7771 stimulates the production of TSLP, a cytokine known to be regulated by intestinal bacteria and essential for promoting the expansion of Tregs [32,33]. In addition, *B. uniformis* CECT 7771 increases intestinal IL-33 concentrations in the EAT, which is a cytokine reported to promote Treg function. IL-33 signalling in T cells stimulates Treg responses by enhancing transforming growth factor (TGF)-β1-mediated

differentiation of Treg cells and providing a necessary signal for Treg-cell accumulation and maintenance in inflamed tissues [34]. Furthermore, IL-33 contributes to orchestrating innate immune cell responses mediated by type 2 innate lymphoid cells (ILC2). In particular, IL-33-mediated ILC2 activation leads to tissue accumulation of eosinophils and M2 macrophages [35], which is consistent the reductions of the M1/M2 ratio found in the EAT of obese mice fed bacteroides. *B. uniformis* CECT 7771 may also directly stimulate Treg differentiation via similar immunomodulatory molecules such as polysaccharide A, as observed in other *Bacteroides* spp. such as *B. fragilis* [36], which was shown to depend on TLR2 signalling.

To investigate deeper into the possible molecular mechanisms that could initiate and mediate the effects of *B. uniformis* CECT 7771 on obesity-associated inflammation, we analyzed the expression of TLRs in the intestinal PP and EAT. The Western diet generally reduced expression of TLRs (TLR2, 4, 5) in the ileum PP, but the most remarkable effect was detected on TLR5, whose expression was reduced in the PP as well as in the EAT. However, the expression of TLR5 was completely normalized by the administration of *B. uniformis* CECT 7771 to obese mice in PP and partially normalized in the EAT. Previous studies in TLR5-deficient mice indicated that signaling via this innate immune receptor plays a key role in metabolism since these knock-outs develop features of metabolic syndrome such as hyperlipidemia, insulin resistance, and weight gain, which were also correlated with changes in the gut microbiota [37]. Although strains of *B. uniformis* are not described as being motile and having flagella [38], we searched for flagellin encoding genes in the whole genome of *B. uniformis* CECT 7771 [39] since TLR5 is known to be activated by bacterial flagellin. However, we could not identify any genes related to flagellin production in this species, indicating that some other ligand from this bacterium may be initiating the activation of this TLR. To confirm whether *B. uniformis per se* or the diet-induced microbiota-changes could be responsible for the effects of the interventions on TLR5 expression *in vivo*, we conducted experiments using a cell line expressing TLR5. This study showed that the Western diet-induced fecal microbiota changes and/or their metabolites were responsible for the shifts in TLR5 *in vivo* in obese mice. *Bacteroides*-induced microbiota changes could have led to the production of butyrate and this, in turn, could explain a subsequent increase of TLR5 expression as reported elsewhere [40]. The effects of *B. uniformis* CECT 7771 on TLR expression could also have been a secondary consequence of its effects on leptin levels as suggested in previous studies relating reduced concentrations of leptin with increased expression of TLRs [41]. In addition, our experiments also demonstrated that pure cultures of *B. uniformis* CECT 7771 could be directly responsible for TLR5 activation, although the responsible motif eliciting this effect remains unknown.

Experimental studies using flagellin as a ligand of TLR5 suggest that this signaling pathway can contribute to TSLP production, which plays a major role in Th2 polarization of the immune response mediated by myeloid DCs leading to IL-10 production [42]. Evidence from *in vitro* and *ex vivo* culture studies also indicate that IL-33 production can be stimulated via TLR5 signalling [43]. Therefore, the activation of TLR5 directly by cellular components of *B. uniformis* CECT 7771 and the microbiota-induced changes or their metabolites in obese mice could explain the molecular mechanism by which the administration of this strain increases both TSLP and IL-33 production with downstream effects on Tregs. The increase of Tregs in obese mice fed *B. uniformis* CECT 7771 could reduce the activation of T effector cells and, thereby, reduce the recruitment and activation of pro-inflammatory macrophages (M1) and the release of innate immune mediators that cause intestinal barrier dysfunction and subsequently enhance WAT inflammation. In our study, the Western-diet induced increases in *Helicobacter* spp., which are known to cause inflammation in murine models [44-46], could have contributed to elevating the intestinal inflammatory tone of obese mice. In fact, *Helicobacter ganmani* has been demonstrated to increase the expression of the pro-inflammatory cytokine IL12/23p40 in IL10-deficient mice [47]. The ability of *B. uniformis* CECT 7771 to partly restore the intestinal ecosystem reducing the abundance of *Helicobacter* spp., could have also contributed to limiting the expansion of the inflammatory cascade towards peripheral tissues. Consistent with this hypothesis, study models suggest that metabolic inflammation associated with Western diets originates in the intestine before affecting the WAT. The intestine is the first tissue exposed to the diet and also the first to respond by recruiting pro-inflammatory macrophages that, in turn, activate cytokine production and alter gut permeability, ultimately resulting in inflammation and insulin resistance in WAT, while inhibition of intestinal macrophage recruitment prevents insulin resistance [9]. Specifically, using a model of adipose tissue inflammation independent of the diet, it was proven that the microbiota drives metabolic inflammation, affecting ultimately the WAT [48]. Further studies using knock-outs for the monocyte chemoattractant protein CCL2 indicated that gut microbiota is responsible for induction of CCL2, which in turn enhances macrophage accumulation in WAT. The study established gut microbiota as a factor aggravating inflammation during diet-induced obesity and, therefore, as a suitable target for therapies against associated metabolic perturbations [13], as shown in our study.

All in all, this study reinforces the idea that diet-induced microbiota changes cooperate with obesogenic diets, aggravating the immune-metabolic deregulation in obesity. The findings also suggest that dietary interventions targeting intestinal inflammation can contribute to ameliorating systemic immune-metabolic dysfunction. The identification of molecular targets (TLR5)

and mediators (TSLP, IL33 and Tregs) responsible for the immune regulatory effects of *B. uniformis* CECT 7771 in diet-induced obesity also provides new insights into the mechanism whereby effector human bacterial strains can work to attenuate the adverse impact of obesity in metabolic health.

Materials and Methods

Bacterial strain and culture conditions

Bacteroides uniformis CECT 7771 was originally isolated from stools of breast-fed infants, identified by 16S rRNA gene and whole genome sequencing as described previously [39], and deposited in the Spanish Culture Collection (CECT). The bacteria were grown in Schaedler broth without hemin (Scharlau, Barcelona, Spain) at 37°C under anaerobic conditions (AnaeroGen, Oxoid, Basingstoke, UK). Cells were harvested by centrifugation (6,000 g for 15 min, at 4 ºC), washed twice in phosphate buffered saline (PBS, 130 mM sodium chloride, 10 mM sodium phosphate, pH 7.4), and then re-suspended in 10% skimmed milk. Aliquots of these suspensions were frozen in liquid nitrogen and stored at -80°C until use for animal trials. After freezing and thawing, the number of live cells was determined by colony-forming unit (CFU) counting on Schaedler agar medium after 48 h incubation. One fresh aliquot was thawed for every new experiment to avoid variability in bacterial viability.

Experimental design, animals, and diets

The experimental design and methodology was based on previous studies described in Moya-Pérez [12] and Gauffin Cano [24]. C57BL/6 adult (6–8 weeks) male mice were purchased from Charles River Laboratories (L'Arbresle Cedex, France). In the adaptation period (7 days), animals of each experimental group were housed together in a stainless-steel cage in a temperature-controlled (23°C) room with a 12-h light/dark cycle and 40–50% relative humidity and were fed a standard diet (SD) *ad libitum*. Then, mice were randomly divided into four groups (n = 10 mice per group) as follows: (1) SD group, receiving a SD plus placebo (10% skimmed milk); (2) HFHFD group, receiving a high-fat diet supplemented with fructose 20% (HFDFD) plus placebo; (3) SD+B group, receiving SD and a daily dose of 1 x 108 CFU *B. uniformis* CECT 7771 (10% skimmed milk); and (4) HFHFD+B group, receiving HFHFD and a daily dose of 1 x 108 CFU CECT 7771 by oral gavage. To induce obesity, mouse groups 2 and 4 were switched from the SD (lard/corn oil 13% Kcal) administered during the adaptation period to a HFHFD (palm oil 48% kcal) plus fructose (D (-)-Fructose ≥99%, Sigma, Saint Louis, USA) in the drinking water and this dietary regime was maintained for 14 weeks. Diet information is detailed in Supplementary Table 1. The HFHFD (S9667-E010 SSNIFF) provided 18% kcal as protein, 34% kcal as carbohydrate and 48% kcal as fat (4.7 kcal/g), whereas the SD (S9667-E020 SSNIFF) provided 23% kcal as protein, 64% kcal as carbohydrate and 13% kcal as fat (3.6 kcal/g), both diets were obtained from Ssniff (Soest, Germany). Mice had free access to water and feed. Animal experiments were carried out in strict accordance with the recommendations in

the Guide for the Care and Use of Laboratory Animals of University of Valencia (Central Service of Support to Research [SCSIE], University of Valencia, Spain) and the protocol was approved by the Local Ethical Committee of "Dirección General de Agricultura, Pesca y Ganadería de la Generalitat Valenciana" (approval ID 2017/VSC/PEA/00125). The study was also carried out in compliance with the ARRIVE guidelines. Body weight was measured once a week and stool samples were collected at the end of the experiment. After 14 weeks of dietary intervention, animals were fasted for 16 h, anaesthetized with isoflurane and sacrificed by cervical dislocation. Blood samples were collected in EDTA-containing tubes (two for each animal): one of them was centrifuged (2,000 x g for 10 min at room temperature) and the supernatant (plasma) was kept at -80°C for endocrine and metabolic marker analysis and the other tube was used for immune cell flow cytometry analysis in plasma. The EAT and the last portion of the ileum containing Peyer's patches were suspended in phosphate buffered saline solution (PBS, 130 mM sodium chloride and 10 mM sodium phosphate, pH 7.4) and kept at 4°C until further processing for flow cytometry analysis.

Quantification of endocrine and metabolic parameters

Plasma leptin concentration was determined by the Assay Max Mouse Leptin ELISA kit (ASSAYPRO, Missouri, USA) with a sensitivity threshold of 0.3 ng/mL. Insulin was measured using a Rat/Mouse ELISA kit (Sigma, Sant Louis, USA) with a sensitivity threshold of 0.3 ng/mL. Cholesterol (Cholesterol Liquid kit) and triglycerides kits (Triglyceride Liquid kit) were purchased from Química Analítica Aplicada SA (Tarragona, Spain), and measured according to the manufacturer's instructions.

Glucose tolerance test (GTT)

The GTT was performed *in vivo* after 10 weeks of dietary intervention as described in Moya-Pérez [12]. The GTT was performed after 6 h of food deprivation, after which 2.0 g/kg body weight glucose was administered by oral gavage. Blood samples were taken by saphenous vein puncture at baseline and 15, 30, 45, 60, and 120 minutes after oral glucose administration. Plasma glucose levels were analyzed with glucose test strips (Ascensia Esyfill, Bayer, NY, USA) and a glucometer (Ascensia VIGOR, Bayer, NY, USA), with a detection level ranging from 30 to 550 mg glucose/dL. The area under the glucose curve (AUC) was estimated by plotting the glucose concentration (mg/dL) versus time (min).

Cytokine quantification

Tissues (Ileum and epididymal adipose tissue [EAT]) were weighed and incubated for 10 min in RIPA buffer (1 × solution, 150 mM NaCl, 1.0% IGEPAL CA-630, 0.5% sodium deoxycholate, 0.1% SDS, and 50 mM Tris, pH 8.0) (Sigma, Madrid, Spain). Samples were then homogenised with a Tissue Ruptor (Qiagen, Madrid, Spain) at 4°C for 1 min and centrifuged at 10,000 rpm, at 4°C for 5 min. This method enables efficient cell lysis and protein solubilisation while avoiding protein degradation and interference with the proteins' immunoreactivity. Supernatants were stored at -80°C until analyzed.

For cytokine quantification, the Mouse FlowCytomix™ Multiplex Kits (eBioscience, Affymetrix Company, Vienna, Austria) were used, basically as previously described in Moya-Pérez [12]. The following cytokines were analyzed in plasma: IL-1α, IL-5, IL-10, IL-13, and TNF-α (eBioscience, Affymetrix Company, Vienna, Austria) by flow cytometry using a FACS Canto cytometer (Becton Dickinson, NJ, USA). Sensitivity thresholds for each cytokine were: IL-1α: 15.7 pg / mL, IL-5: 4.0 pg / mL, IL-10: 5.4 pg / mL, IL-13: 9.3 pg / mL and TNF-α: 2.1 pg / mL. Data are expressed as pg cytokine/mL of plasma. In addition, IL-10, IFN-γ, IL-33, and thymic stromal lymphopoietin (TSLP) were determined in ileum and epididymal WAT using ELISA kits (Biolegend, San Diego, CA and eBioscience, Affymetrix, San Diego, CA for TSLP). Sensitivity thresholds for each cytokine were: 16 pg/mL for IL-10, 4 pg/mL for IFN-γ, 25 pg/mL for IL-33 and 16 pg/mL for TSLP.

Quantification of lymphoid and myeloid cells and TLR expression by flow cytometry

The methodology was previously described in Moya-Pérez [12]. Briefly, peripheral blood, EAT, and Peyer's patches (PP) from small intestine (ileum) were used for immune-cell analysis by flow cytometry. For adipose tissue, visible vessels and connective tissue were carefully removed and the tissue was minced with fine scissors and digested with 0.15% collagenase type II from *Clostridium histolyticum* C6885 (Sigma, Saint Louis, USA) in FACS buffer (PBS with 0.5% BSA and 2 mM EDTA) at 37°C for 30 minutes. The PP were washed with FACS buffer, cut into small pieces and incubated with collagenase type I from *Clostridium histolyticum* C9891 (Sigma, Saint Louis, USA) at 37 °C for 30 minutes. Afterwards, the digested tissues were passed through 40 µm mesh filters and washed in FACS buffer, then centrifuged at 2,000 rpm for 5 min at 4ºC and the pelleted cells were stained and analyzed. To analyze immune markers in peripheral blood, 100 µL were resuspended in antibody solution for 30 min in darkness, then mixed vigorously with 2 mL FACS buffer (160 mM NH_4Cl, 0.1 mM EDTA, 12 mM $NaHCO_3$) to lyse red blood cells for 10 minutes at

room temperature. The samples were centrifuged at 2,000 rpm for 5 min, the pellet was washed twice with 2 mL FACS buffer, resuspended in 300 µL FACS buffer and analyzed by flow cytometry.

Cells were stained with the following fluorescent dye-labelled mouse monoclonal antibodies for lymphoid cell analysis: $CD3^{FITC}$, $CD4^{BV510}$, $CD8^{APC}$, $CD25^{PE}$, and $CD19^{BV421}$. The following cellular subsets were analyzed for myeloid cell analysis: total lymphocytes (CD3+), regulatory T cells (CD3+CD4+CD25+), and B cells (CD3-CD19+). The following cellular subsets were analyzed: total macrophages (F4/80+), M1 macrophages (F4/80+CD11c+CD206-) and M2 macrophages (F4/80+CD11c-CD206+). In addition, $CD282^{FITC}$ and $CD284^{PE}$ antibodies were used to determine TLR2 and TLR4, respectively, in PP. For detection of TLR5, primary (rabbit anti-mouse TLR5) and secondary (goat anti-rabbit $IgG^{PerCP\text{-}Cy5.5}$) antibodies were used in PP and EAT. All conjugated antibodies were from BD Biosciences (San Jose, CA, USA) except for CD206 and TLR5 that were from BioLegend (Fell, Germany) and from Santa Cruz (Heidelberg, Germany), respectively. All antibodies were used according to the manufacturer's instructions. After washing, cells were analyzed with BD LSRFortessa and BD FACSVerse cytometers (Becton Dickinson, NJ, USA). The data were analyzed using BD FACS DIVA Software v.7.0. and BD FACS Suite Software v.1.0.3.2942.

TLR5 activation assays in human HEK-Blue h TLR5 cell cultures

To test whether pure cultures of *B. uniformis* CECT 7771 as well as fecal samples from mice exposed to the different experimental treatment conditions stimulate TLR5, *in vitro* experiments using a HEK293 cell line were carried out. The HEK293 cell line stably transfected with human TLR5 (HEK-Blue hTLR5 cells) were obtained directly from Invivogen (CA, USA). TLR5 activity can be determined by measuring embryonic alkaline phosphatase (SEAP) in which production is induced by NF-κB and AP-1 after TLR5 activation. Levels of SEAP can be determined with HEK-Blue Detection (Invivogen), a cell culture medium that allows for real-time detection of SEAP. HEK-Blue hTLR5 cells were grown and cultured up to 70-80% confluency using as a maintenance medium Dulbecco's Modified Eagle Medium (DMEM) supplemented with 4.5g/l D-glucose, 10% fetal bovine serum (FBS), 50 U/ml penicillin, 50 µg/ml streptomycin, 100 µg/ml Normocin and 2mM L-glutamine. Cells were seeded into flat-bottom 96-well plates and resuspended in HEK-Blue Detection (25,000 cells/well). The 96-well plates were incubated for 6 h at 37ºC in a 5% CO_2 incubator. Fecal samples from the different mouse groups (SD, HFHFD and HFHFD+B) and pure cultures of *B. uniformis* CECT 7771 were used as different stimuli. Fecal samples were previously diluted in 1X PBS buffer (1:10 w/v final)

and submitted to low speed centrifugation (2,000 x g for 10 min at 4°C) to eliminate particulate material (20 µl). Cell suspensions of *B. uniformis* CECT 7771 were adjusted to final concentrations of 1:100 HEK293 cells:bacterial cells. Recombinant flagellin (RecFLA-ST, 1µg/ml) and cell suspensions of pure cultures of *Clostridium butyricum* were used as a positive control while endotoxin-free water and cell suspensions of pure cultures of a strain of *Phascolarctobacterium faecium,* a known species lacking flagellin*,* were used as negative controls. SEAP secretion was detected after 16 h of stimulation by measuring the OD_{600} in HEK-Blue h TLR5 supernatant using a Spectrophotometer (Multiskan Spectrum, Thermo Fisher Scientific).

Analysis of gut microbiota

Processing of samples for gut microbiota analysis was carried out according to the methods described in González-Ramos [49]. Fecal samples from individual mice from each experimental group were collected at the end of the intervention and were immediately frozen in liquid nitrogen and stored at -80°C until processing. DNA extraction was carried out using a Fast DNA Stool Mini Kit (Qiagen) according to the manufacturer's instructions with several modifications. First, fecal samples (up to 220 mg) were added to sterile 2 mL tubes filled with glass beads and one ml of Inhibitex buffer (Qiagen) was added to each tube. Samples were homogenized using a beadbeater for 2 successive rounds for 1 minute and then heated to 95 °C for 10 minutes. Samples were amplified in triplicate via PCR using primers (S-D-Bact-0563-a-S-15 / S-D-Bact-0907-b-A-20) that target the V4-V5 variable regions of the 16S rRNA gene [50]. Samples were tagged with barcodes to allow multiplexing during the sequencing process. Triplicate reactions consisted of final concentrations of Buffer HF (1X), dNTPs (0.11 µM) primers (0.29 µM each) and Taq Phusion High Fidelity (0.007 U/µL) in final volumes of 35 µL. Cycling conditions consisted of 98°C for 3 min, followed by 25 cycles of 95 °C for 20 seconds, 55°C for 20 seconds, and 72°C for 20 seconds, followed by a final extension step of 72°C for 5 minutes. Triplicate sample amplicons were combined and purified using the Illustra GFX PCR DNA and Gel Band Purification Kit (GE Healthcare) according to the manufacturer's instructions and combined in equimolar concentrations before carrying out sequencing on a MiSeq instrument (Illumina). All raw sequence data has been submitted to ENA-EMBL Accession #: (PRJEB22917).

Bioinformatic processing of data was carried out using the software QIIME [51], Mothur [52], and UPARSE [53]. Briefly, using QIIME, paired-end forward and reverse Illumina reads were joined into contigs, barcodes were extracted and reads were demultiplexed. Primers were then removed using the software program Mothur. Using UPARSE, chimeras were removed and reads were

clustered at 97 % identity into OTUs using default settings. An OTU abundance table was generated within the UPARSE pipeline by mapping reads to representative sequences for each OTU. Using QIIME, a biom file was created from the OTU table and reads were rarefied and singletons were removed. A phylogenetic tree was constructed from representative sequences for each OTU, and aligned using PYNAST [54] and filtered using default settings. Alpha diversity metrics (Shannon's, Simpson's, and Simpson's reciprocal diversity index, Simpson's evenness) were calculated. Beta diversity analysis was conducted using generalized UniFrac (GUniFrac) [55] and principal coordinates analyses (PCoA). Samples were classified taxonomically with Mothur using taxonomic assignments and full-length sequences from the SILVA database (release 123) [56].

Statistical analyses

Data from animal experiments were analyzed using Graph Pad Prism software (LaJolla, CA). Data distribution was assessed by the Kolmogorov-Smirnov normality test. For normally distributed data, differences were determined with one or two-way ANOVAs (as appropriate) and *post hoc* Bonferroni's tests. Non-normally distributed data were analyzed with the non-parametric Mann-Whitney U test. In every case, p values < 0.05 were considered statistically significant. Gut microbiota statistics and data visualization of sequencing data were carried out using the R statistical software and related R packages or QIIME [51,57]. Comparison between dietary groups of relative abundances of taxonomic groups was carried out using a Kruskal-Wallis test followed by a Wilcoxon rank-sum test to identify significant differences. All p values were corrected for multiple comparisons using false discovery rate where ($q < 0.05$) was a cutoff for significance. Comparisons of beta diversity between dietary groups using generalized UniFrac distances were performed by generating a principle coordinates analysis (PCoA) and conducting PERMANOVAs with adonis() within the GUniFrac package in R. Correlations between gut microbiota taxonomic groups and biochemical and immunological parameters were performed using Spearman's rank correlation coefficients (ρ) using the (cor function) and p-values were adjusted with the false discovery rate method for multiple correlations. Correlation plots were visualized using the R heatmap.2() function.

Acknowledgements

This work is supported by the European Union's Seventh Framework Program under the grant agreement no 613979 (MyNewGut) and grant AGL2017-88801-P from the Spanish Ministry of Economy and Competitiveness (MCIU, Spain). The Santiago Grisolía scholarship (GRISOLIAP/2014/110) to E.F from Generalitat Valenciana and the FPI scholarship (BES-2015-073930) of I López-Almela and the PTA contract (PTA2013-8836-I) of I. Campillo from MCIU are fully acknowledged. The authors declare that there are no competing interests in this research.

Author contributions

YS design the study; EF and IC did the animal experiments; ILA and MRP did the in vitro experiments; ABP search in the B. uniformis genome for TLR5 ligands; KJP did the microbiota analysis; SMP contributed to data analysis; KJP, EF, and YS drafted the paper, and all authors revised and agreed with the final version.

Competing interests

YS is author of a patent on *B. uniformis* CECT 7771. The rest of the authors declare no competing interests.

References

1 World Health Organization, W. H. Obesity and overweight, <http://www.who.int/news-room/fact-sheets/detail/obesity-and-overweight> (2017).

2 Kanneganti, T. D. & Dixit, V. D. Immunological complications of obesity. *Nat Immunol* **13**, 707-712, doi:10.1038/ni.2343 (2012).

3 Glass, C. K. & Olefsky, J. M. Inflammation and lipid signaling in the etiology of insulin resistance. *Cell Metab* **15**, 635-645, doi:10.1016/j.cmet.2012.04.001 (2012).

4 McNelis, J. C. & Olefsky, J. M. Macrophages, immunity, and metabolic disease. *Immunity* **41**, 36-48, doi:10.1016/j.immuni.2014.05.010 (2014).

5 Saltiel, A. R. & Olefsky, J. M. Inflammatory mechanisms linking obesity and metabolic disease. *J Clin Invest* **127**, 1-4, doi:10.1172/JCI92035 (2017).

6 Cani, P. D. *et al.* Metabolic endotoxemia initiates obesity and insulin resistance. *Diabetes* **56**, 1761-1772, doi:10.2337/db06-1491 (2007).

7 McLaughlin, T., Ackerman, S. E., Shen, L. & Engleman, E. Role of innate and adaptive immunity in obesity-associated metabolic disease. *J Clin Invest* **127**, 5-13, doi:10.1172/JCI88876 (2017).

8 Sanz, Y. & Moya-Perez, A. Microbiota, inflammation and obesity. *Adv Exp Med Biol* **817**, 291-317, doi:10.1007/978-1-4939-0897-4_14 (2014).

9 Kawano, Y. *et al.* Colonic Pro-inflammatory Macrophages Cause Insulin Resistance in an Intestinal Ccl2/Ccr2-Dependent Manner. *Cell Metab* **24**, 295-310, doi:10.1016/j.cmet.2016.07.009 (2016).

10 Belkaid, Y. & Harrison, O. J. Homeostatic Immunity and the Microbiota. *Immunity* **46**, 562-576, doi:10.1016/j.immuni.2017.04.008 (2017).

11 Cani, P. D. & Everard, A. Talking microbes: When gut bacteria interact with diet and host organs. *Mol Nutr Food Res* **60**, 58-66, doi:10.1002/mnfr.201500406 (2016).

12 Moya-Perez, A., Neef, A. & Sanz, Y. *Bifidobacterium pseudocatenulatum* CECT 7765 Reduces Obesity-Associated Inflammation by Restoring the Lymphocyte-Macrophage Balance and Gut Microbiota Structure in High-Fat Diet-Fed Mice. *PLoS One* **10**, e0126976, doi:10.1371/journal.pone.0126976 (2015).

13 Caesar, R., Tremaroli, V., Kovatcheva-Datchary, P., Cani, P. D. & Backhed, F. Crosstalk between Gut Microbiota and Dietary Lipids Aggravates WAT

Inflammation through TLR Signaling. *Cell Metab* **22**, 658-668, doi:10.1016/j.cmet.2015.07.026 (2015).

14 Romani-Perez, M., Agusti, A. & Sanz, Y. Innovation in microbiome-based strategies for promoting metabolic health. *Curr Opin Clin Nutr Metab Care* **20**, 484-491, doi:10.1097/MCO.0000000000000419 (2017).

15 Sanz, Y., Rastmanesh, R. & Agostoni, C. Understanding the role of gut microbes and probiotics in obesity: how far are we? *Pharmacol Res* **69**, 144-155, doi:10.1016/j.phrs.2012.10.021 (2013).

16 Wang, J. & Jia, H. Metagenome-wide association studies: fine-mining the microbiome. *Nat Rev Microbiol* **14**, 508-522, doi:10.1038/nrmicro.2016.83 (2016).

17 David, L. A. *et al.* Diet rapidly and reproducibly alters the human gut microbiome. *Nature* **505**, 559-563, doi:10.1038/nature12820 (2014).

18 De Filippis, F., Pellegrini, N., Laghi, L., Gobbetti, M. & Ercolini, D. Unusual sub-genus associations of faecal *Prevotella* and *Bacteroides* with specific dietary patterns. *Microbiome* **4**, 57, doi:10.1186/s40168-016-0202-1 (2016).

19 Matijasic, B. B. *et al.* Association of dietary type with fecal microbiota in vegetarians and omnivores in Slovenia. *Eur J Nutr* **53**, 1051-1064, doi:10.1007/s00394-013-0607-6 (2014).

20 Rios-Covian, D., Salazar, N., Gueimonde, M. & de Los Reyes-Gavilan, C. G. Shaping the Metabolism of Intestinal Bacteroides Population through Diet to Improve Human Health. *Front Microbiol* **8**, 376, doi:10.3389/fmicb.2017.00376 (2017).

21 Lee, N. & Kim, W. U. Microbiota in T-cell homeostasis and inflammatory diseases. *Exp Mol Med* **49**, e340, doi:10.1038/emm.2017.36 (2017).

22 Mazmanian, S. K., Liu, C. H., Tzianabos, A. O. & Kasper, D. L. An immunomodulatory molecule of symbiotic bacteria directs maturation of the host immune system. *Cell* **122**, 107-118, doi:10.1016/j.cell.2005.05.007 (2005).

23 Surana, N. K. & Kasper, D. L. The yin yang of bacterial polysaccharides: lessons learned from *B. fragilis* PSA. *Immunol Rev* **245**, 13-26, doi:10.1111/j.1600-065X.2011.01075.x (2012).

24 Gauffin Cano, P., Santacruz, A., Moya, A. & Sanz, Y. *Bacteroides uniformis* CECT 7771 ameliorates metabolic and immunological dysfunction in mice with high-fat-diet induced obesity. *PLoS One* **7**, e41079, doi:10.1371/journal.pone.0041079 (2012).

25 DeFuria, J. *et al.* B cells promote inflammation in obesity and type 2 diabetes through regulation of T-cell function and an inflammatory cytokine profile. *Proc Natl Acad Sci U S A* **110**, 5133-5138, doi:10.1073/pnas.1215840110 (2013).

26 Feuerer, M., Hill, J. A., Mathis, D. & Benoist, C. Foxp3+ regulatory T cells: differentiation, specification, subphenotypes. *Nat Immunol* **10**, 689-695, doi:10.1038/ni.1760 (2009).

27 Nishimura, S. *et al.* CD8+ effector T cells contribute to macrophage recruitment and adipose tissue inflammation in obesity. *Nat Med* **15**, 914-920, doi:10.1038/nm.1964 (2009).

28 Garidou, L. *et al.* The Gut Microbiota Regulates Intestinal CD4 T Cells Expressing RORγt and Controls Metabolic Disease. *Cell Metab* **22**, 100-112, doi:10.1016/j.cmet.2015.06.001 (2015).

29 Mraz, M. & Haluzik, M. The role of adipose tissue immune cells in obesity and low-grade inflammation. *J Endocrinol* **222**, R113-127, doi:10.1530/JOE-14-0283 (2014).

30 Laidlaw, B. J. *et al.* Production of IL-10 by CD4(+) regulatory T cells during the resolution of infection promotes the maturation of memory CD8(+) T cells. *Nat Immunol* **16**, 871-879, doi:10.1038/ni.3224 (2015).

31 Winer, D. A., Luck, H., Tsai, S. & Winer, S. The Intestinal Immune System in Obesity and Insulin Resistance. *Cell Metab* **23**, 413-426, doi:10.1016/j.cmet.2016.01.003 (2016).

32 Mosconi, I. *et al.* Intestinal bacteria induce TSLP to promote mutualistic T-cell responses. *Mucosal Immunol* **6**, 1157-1167, doi:10.1038/mi.2013.12 (2013).

33 Negishi, H. *et al.* Essential contribution of IRF3 to intestinal homeostasis and microbiota-mediated Tslp gene induction. *Proc Natl Acad Sci U S A* **109**, 21016-21021, doi:10.1073/pnas.1219482110 (2012).

34 Schiering, C. *et al.* The alarmin IL-33 promotes regulatory T-cell function in the intestine. *Nature* **513**, 564-568, doi:10.1038/nature13577 (2014).

35 Molofsky, A. B., Savage, A. K. & Locksley, R. M. Interleukin-33 in Tissue Homeostasis, Injury, and Inflammation. *Immunity* **42**, 1005-1019, doi:10.1016/j.immuni.2015.06.006 (2015).

36 Round, J. L. & Mazmanian, S. K. Inducible Foxp3+ regulatory T-cell development by a commensal bacterium of the intestinal microbiota. *PNAS* **107**, 12204-12209 (2010).

37 Vijay-Kumar, M. *et al.* Metabolic syndrome and altered gut microbiota in mice lacking Toll-like receptor 5. *Science* **328**, 228-231, doi:10.1126/science.1179721 (2010).

38 Lakhdari, O. *et al.* Identification of NF-κB modulation capabilities within human intestinal commensal bacteria. *J Biomed Biotechnol* **2011**, 282356, doi:10.1155/2011/282356 (2011).

39 Benitez-Paez, A., Gomez Del Pulgar, E. M. & Sanz, Y. The Glycolytic Versatility of *Bacteroides uniformis* CECT 7771 and Its Genome Response to Oligo and Polysaccharides. *Front Cell Infect Microbiol* **7**, 383, doi:10.3389/fcimb.2017.00383 (2017).

40 Thakur, B. K., Dasgupta, N., Ta, A. & Das, S. Physiological TLR5 expression in the intestine is regulated by differential DNA binding of Sp1/Sp3 through simultaneous Sp1 dephosphorylation and Sp3 phosphorylation by two different PKC isoforms. *Nucleic Acids Res* **44**, 5658-5672, doi:10.1093/nar/gkw189 (2016).

41 Batra, A. *et al.* Leptin-dependent toll-like receptor expression and responsiveness in preadipocytes and adipocytes. *Am J Pathol* **170**, 1931-1941, doi:10.2353/ajpath.2007.060699 (2007).

42 Lee, L. M. *et al.* Determinants of divergent adaptive immune responses after airway sensitization with ligands of toll-like receptor 5 or toll-like receptor 9. *PLoS One* **11**, e0167693, doi:10.1371/journal.pone.0167693 (2016).

43 Zhang, L., Lu, R., Zhao, G., Pflugfelder, S. C. & Li, D. Q. TLR-mediated induction of pro-allergic cytokine IL-33 in ocular mucosal epithelium. *Int J Biochem Cell Biol* **43**, 1383-1391, doi:10.1016/j.biocel.2011.06.003 (2011).

44 Fox, J. G., Ge, Z., Whary, M. T., Erdman, S. E. & Horwitz, B. H. *Helicobacter hepaticus* infection in mice: models for understanding lower bowel inflammation and cancer. *Mucosal Immunol* **4**, 22-30, doi:10.1038/mi.2010.61 (2011).

45 Kullberg, M. C. *et al. Helicobacter hepaticus* triggers colitis in specific-pathogen-free interleukin-10 (IL-10)-deficient mice through an IL-12- and gamma interferon-dependent mechanism. *Infect Immun* **66**, 5157-5166 (1998).

46 Matharu, K. S. *et al.* Toll-like receptor 4-mediated regulation of spontaneous Helicobacter-dependent colitis in IL-10-deficient mice. *Gastroenterology* **137**, 1380-1390 e1381-1383, doi:10.1053/j.gastro.2009.07.004 (2009).

47 Alvarado, C. G. *et al.* Pathogenicity of *Helicobacter ganmani* in mice susceptible and resistant to infection with *H. hepaticus. Comp Med* **65**, 15-22 (2015).

48 Caesar, R. *et al.* Gut-derived lipopolysaccharide augments adipose macrophage accumulation but is not essential for impaired glucose or insulin tolerance in mice. *Gut* **61**, 1701-1707, doi:10.1136/gutjnl-2011-301689 (2012).

49 González-Ramos, S. *et al.* NOD1 deficiency promotes an imbalance of thyroid hormones and microbiota homeostasis in mice fed high fat diet. *Scientific Reports* **10** (2020).

50 Claesson, M. J. *et al.* Comparison of two next-generation sequencing technologies for resolving highly complex microbiota composition using tandem

variable 16S rRNA gene regions. *Nucleic Acids Res* **38**, e200, doi:10.1093/nar/gkq873 (2010).

51 Caporaso, J. G. *et al.* QIIME allows analysis of high-throughput community sequencing data. *Nat Methods* **7**, 335-336, doi:10.1038/nmeth.f.303 (2010).

52 Schloss, P. D. *et al.* Introducing mothur: open-source, platform-independent, community-supported software for describing and comparing microbial communities. *Appl Environ Microbiol* **75**, 7537-7541, doi:10.1128/AEM.01541-09 (2009).

53 Edgar, R. C. UPARSE: highly accurate OTU sequences from microbial amplicon reads. *Nat Methods* **10**, 996-998, doi:10.1038/nmeth.2604 (2013).

54 Caporaso, J. G. *et al.* PyNAST: a flexible tool for aligning sequences to a template alignment. *Bioinformatics* **26**, 266-267, doi:10.1093/bioinformatics/btp636 (2010).

55 Chen, J. *et al.* Associating microbiome composition with environmental covariates using generalized UniFrac distances. *Bioinformatics* **28**, 2106-2113, doi:10.1093/bioinformatics/bts342 (2012).

56 Quast, C. *et al.* The SILVA ribosomal RNA gene database project: improved data processing and web-based tools. *Nucleic Acids Res* **41**, D590-596, doi:10.1093/nar/gks1219 (2013).

57 Team, R. C. R: *A language and environment for statistical computing,* <https://www.R-project.org/> (2017).

Bacteroides uniformis combined with fibre amplifies metabolic and immune benefits in obese mice

Inmaculada López-Almela*[1], Marina Romaní-Pérez*[1], Clara Bullich-Vilarrubias[1], Alfonso Benítez-Páez[1], Eva M. Gómez del Pulgar[1], Rubén Francés[2], Gerhard Liebisch[3], Yolanda Sanz[1]

Gut microbes. 2020 Dec 4; 13:1, 1-20,

*Both authors contributed equally to the paper

[1]Microbial Ecology, Nutrition & Health Research Unit. Institute of Agrochemistry and Food Technology, Spanish National Research Council (IATA-CSIC), Valencia, Spain.

[2]CIBERehd, Hospital General Universitario, Alicante, Spain; Dpto. Medicina Clínica, Universidad Miguel Hernández, San Juan, Spain.

[3]Institute of Clinical Chemistry and Laboratory Medicine, University Hospital Regensburg,Regensburg,Germany.

Abstract

Gut microbiota represents a therapeutic target for obesity. We hypothesize that *B. uniformis* CECT 7771 combined with wheat bran extract (WBE), its preferred carbon source, may exert superior anti-obesity effects. We performed a 17-week intervention in diet-induced obese mice receiving either *B. uniformis*, WBE, or their combination to identify interactions and independent actions on metabolism and immunity. *B. uniformis* combined with WBE was the most effective intervention, curbing weight gain and adiposity, while exerting more modest effects separately. The combination restored insulin-dependent metabolic routes in fat and liver, although the bacterium was the primary driver for improving whole-body glucose disposal. Moreover, *B. uniformis*-combined with WBE caused the highest increases in butyrate and restored the proportion of induced intraepithelial lymphocytes and type-3 innate lymphoid cells in the intestinal epithelium. Thus, strengthening the first line of immune defence against unhealthy diets and associated dybiosis in the intestine. This intervention also attenuated the altered IL22 signalling and liver inflammation. Our study shows opportunities for employing *B. uniformis*, combined with WBE, to aid in the treatment of obesity.

Key words: obesity/ dietary fibre/ microbiota/ intraepithelial lymphocytes/ innate lymphoid cells

Abbreviations

Acc, acetyl-CoA carboxylase; AXOS arabinoxylan oligosaccharides; AUC, area under the curve; BAT, brown adipose tissue; *Chrebpα*, carbohydrate responsive-element-binding protein α; *Cpt1a*, carnitine palmitoyltransferase 1a; *Fas*, fatty acid synthase; FAs, fatty acids; GLP-1, glucagon-like peptide-1; *Gck*, glucokinase; *Glut2*, glucose transporter 2; *Glut4*, glucose transporter 4; G6P, glucose-6-phosphate; HFHSD, high-fat high-sugar diet; *Hsl,* hormone sensitive lipase; ILC, innate lymphoid cells; IEL, intraepithelial lymphocytes; *Lpl*, lipoprotein lipase; *Lyz1*, lysozyme 1; MUFAs, monounsaturated FAs; OGTT, oral glucose tolerance test; PYY, peptide YY *Pla2g2a*, phospholipase A2 group IIA; PUFAs, polyunsaturated FAs; *Reg3γ*, regenerating islet-derived protein 3 gamma**;** SCFAs, short-chain fatty acids; T2D, type-2 diabetes; *Ucp-1*, uncoupling protein-1; WBE, wheat-bran extract; WAT, white adipose tissue.

Introduction

Obesity is a leading public-health problem given its high prevalence and associated complications [e.g., type 2 diabetes (T2D) and cardiovascular diseases]. A deeper understanding of the multiple factors controlling body weight is urgently needed to tackle obesity. Gut microbiota has been identified as a key factor that, through interactions with the diet and intestinal immunity, influence metabolic health [1–3]. Western diets (low-fibre, high-fat and simple sugars) induce gut-microbiota imbalances (dysbiosis) [4,5] and damage intestinal barrier integrity and immune homeostasis [6,7]. Alterations to intestinal microbiota and leakage of their components (cells, proteins, and metabolites) across the intestinal barrier, permeabilized by unhealthy diets, contributes to obesity-associated low-grade inflammation and insulin resistance in metabolic tissues [7,8].

Moreover, investigations revealing interactions between diet, gut microbiota and host metabolism [9,10] have allowed the identification of key intestinal bacteria that represent new targets to improve metabolic health [11].

For instance, *Bacteroides uniformis* CECT 7771 reduced the high-fat diet-induced metabolic alterations while improving antigen-presentation by dendritic cells, impacting on CD4+ T-cell proliferation in an obesity model [12]. On the other hand, fibre serves as fuel for commensal intestinal bacteria, promoting their growth and metabolic activity, which could also mediate some of the fibre-induced benefits on human metabolism [13,14]. Indeed, high intake of dietary fibre is known to help in weight maintenance and reduce the risk of coronary heart disease and T2D [15]. Furthermore, *Bacteroides* spp. thrive in fibre-enriched environments as they have complex enzymatic machinery to utilize oligo- and poly-saccharides as nutrients [16,17]. *B. uniformis* CECT 7771 preferred carbon source was evaluated *in vitro*, thus maximizing potential benefits of their combined administration. This could also help lower the effective bacterial dose required, overcoming the challenge of producing intestinal anaerobes at high cell densities. Compared to other carbon sources, *B. uniformis* CECT 7771 thrived on wheat-bran extract (WBE), enriched in arabinoxylan oligosaccharides (AXOS) [16]. Interventions studies in humans reveal that wheat-derived AXOS have multiples metabolic benefits [13] especially on the maintenance of glucose homeostasis [17] and also exert a bifidogenic effect and promote the abundance of butyrate-producing bacteria [18].

Here, we hypothesised that *B. uniformis* CECT 7771 combined with WBE could have an additive impact on restoring the metabolic and immune alterations of diet-induced obesity and exert greater effects than either WBE or the bacterium alone in mice. Specifically, we assessed whether combined

intervention protects against the Western diet-induced intestinal immune impairment, which is one of the causative mechanism underlying metabolic dysfunction in obesity.

Results

B. uniformis and WBE amplified the reduction of weight-gain in mice fed HFHSD

At week 8 body-weight gain induced by high-fat high-sugar diet (HFHSD) was lower when *B. uniformis* and/or WBE were administered (Figure 1A). Nonetheless, these effects diminished over time, especially in mice fed WBE alone, while the downward trend continued in those administered *B. uniformis* alone or combined with WBE until week 12, with *B. uniformis* and WBE inducing a greater impact on the prevention of weight gain comparatively until week 17 (Figure 1A and Figure S2A). Compared to controls, HFHSD-fed mice showed a slight increase in fasting triglycerides in plasma, cholesterol and glucose (Figure 1B) and impaired OGTT (Figure 1C). WBE reduced cholesterol and normalized glycaemia but did not affect triglycerides (Figure 1B). By contrast, *B. uniformis* alone significantly reduced triglycerides in HFHSD-fed mice. Alone or combined with WBE, this bacterium also diminished plasma cholesterol and glucose (Figure 1B) and ameliorated oral glucose intolerance of HFHSD-fed mice and the area under the curve (AUC) (Figure 1C). By contrast, compared to controls, AUC remained elevated in HFHSD-fed mice receiving WBE alone. This suggests that *B. uniformis* rather than WBE improved whole glucose clearance in the OGTT. Insulin plasma levels remained unaffected whatever the treatment (Figure S2B). Neither glucagon-like peptide-1 (GLP-1) nor peptide YY (PYY) in plasma were significantly affected by HFHSD, however, the bacterium-WBE combination normalized GLP-1 levels compared to untreated HFHSD-fed mice and those receiving *B. uniformis* or WBE separately, while *B. uniformis* increased PYY in mice compared to controls (Figure S2B).

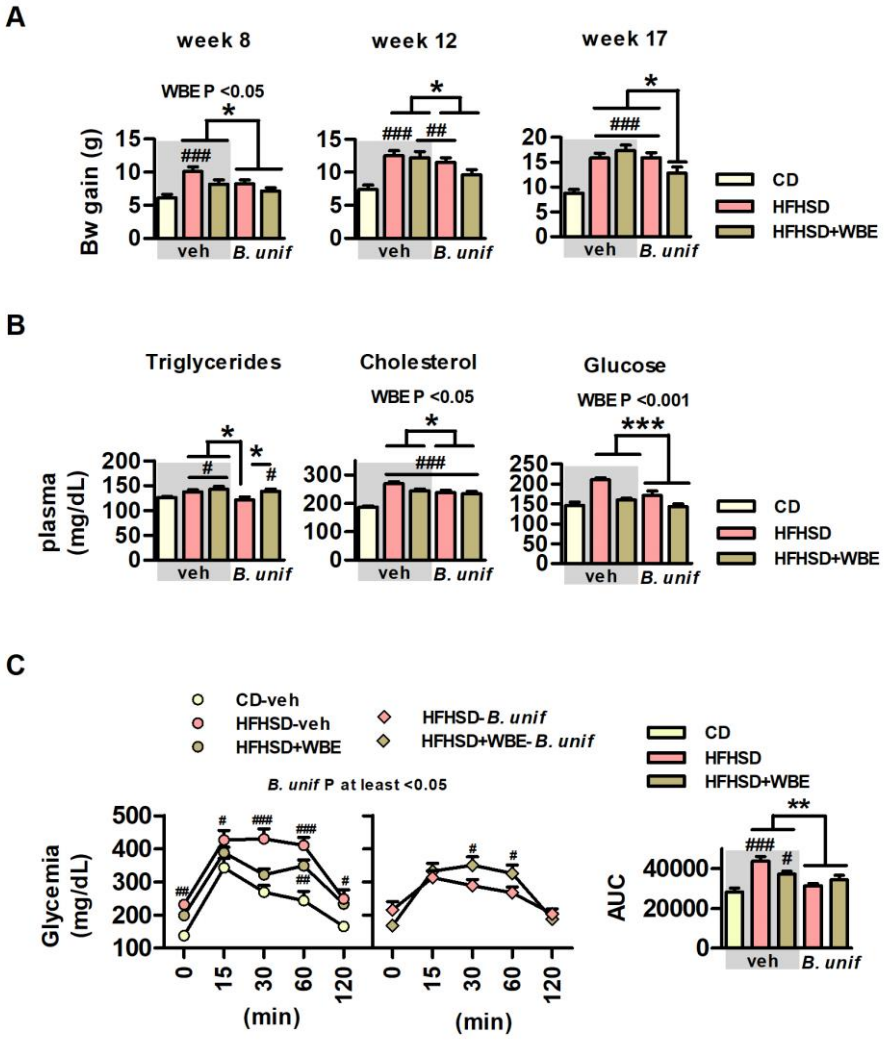

Figure 1. *B. uniformis* CECT 7771 combined with WBE reduces weight gain in mice fed HFHSD. Bw gain, triglycerides and OGTT of controls (CD fed mice receiving vehicle, CD-veh) and HFHSD fed mice receiving vehicle, WBE, *B. unif* or the combination of both: HFHSD-veh, HFHSD+WBE, HFHSD-*B. unif* or HFHSD+WBE-*B. unif. (**A**)* Bw gain at week 8 (two-way ANOVA in HFHSD-fed groups: *B. unif* effect or WBE effect P <0.05), at week 12 (two-way ANOVA in HFHSD-fed groups: *B. unif* effect P <0.05) and at week 17 (two-way ANOVA in HFHSD-fed groups: *B. unif* x WBE interaction P <0.05; *post hoc* P <0.05). N = 10 for all groups. (**B**) Triglycerides (Kruskal-Wallis: HFHSD-*B. unif* vs HFHSD-veh, HFHSD+WBE or HFHSD+WBE-*B. unif* P <0.05), cholesterol and glucose concentrations in plasma (two-way ANOVA in HFHSD-fed groups: WBE and *B.*

unif effect P <0.05 and P <0.001, respectively) after 12 weeks of HFHSD feeding. Triglycerides: CD-veh N = 8; HFHSD-veh N = 9; HFHSD+WBE and HFHSD+WBE-*B. unif* N = 10 and HFHSD-*B. unif* N = 7; cholesterol: CD-veh and HFHSD-veh N = 8; HFHSD+WBE and HFHSD+WBE-*B. unif* N = 10 and HFHSD-*B. unif* N = 7. Glucose: CD-veh and HFHSD-veh N = 9, HFHSD+WBE, HFHSD-*B. unif* and HFHSD+WBE-*B. unif* = 10. (**C**) OGTT (two-way ANOVA in HFHSD-fed groups: *B. unif* effect P at least <0.05 vs HFHSD-fed mice that did not receive the bacteria) and AUC (two-way ANOVA in HFHSD-fed groups: *B. unif* effect P <0.01) at week 14. CD-veh, HFHSD-veh, HFHSD-*B. unif* and HFHSD+WBE-*B. unif* N = 10 and HFHSD+WBE N = 8. Data were represented as the mean ± SEM. Statistical differences between HFHSD-fed groups (receiving or not the bacterium and/or WBE) and controls (CD-veh) were analysed using one-way ANOVA followed by post-hoc Tuckey. $^{\#}$P <0.05, $^{\#\#}$P <0.01, $^{\#\#\#}$P <0.001 vs control group. *P <0.05, **P <0.01 and ***P <0.001 indicate differences within HFHSD-fed groups. AUC, area under the curve; *B. unif*, *Bacteroides uniformis* CECT 7771; Bw, body weight; CD, control diet; HFHSD, high-fat high-sugar diet; WBE, wheat-bran extract.

B. uniformis CECT 7771 combined with WBE reduces epididymal fat and restores insulin-dependent metabolic routes in adipose tissue and liver in mice fed HFHSD

Compared to controls, epididymal fat was higher in untreated mice fed HFHSD and those receiving *B. uniformis* or WBE separately (Figure 2A). This increased visceral adiposity was only attenuated by the bacterium-WBE combination (Figure 2A). The expression of lipoprotein lipase (*Lpl*) or the hormone sensitive lipase (*Hsl*) remained unaffected in epididymal WAT of mice fed HFHSD whatever the treatment (Figure S3A) but the lipogenic genes, acetyl-CoA carboxylase (*Acc*) and fatty acid synthase (*Fas*) were reduced after HFHSD feeding (Figure 2B). Separately, neither the bacteria nor WBE modified *Acc* in obese mice, while only the combination of both attenuated HFHSD-induced lipogenesis inhibition, as reflected in the normalization of *Acc* mRNA expression (Figure 2B). Overall, *B. uniformis* raised *Fas* expression in epididymal WAT compared to untreated obese mice but this effect was strengthened by its combination with WBE (Figure 2B). The expression of glucose transporter 4 (*Glut4*) in epididymal WAT was unaltered in HFHSD-fed mice whatever the treatment (Figure S3B). Nevertheless, compared to controls, the carbohydrate responsive-element-binding protein α (*Chrebpα*), a transcriptional factor stimulating *Acc* and *Fas* to induce *de novo* lipogenesis using glucose-derived metabolites as precursors, were reduced by HFHSD-feeding, reaching statistical significance in WBE-treated mice fed HFHSD

(Figure 2B). The bacteria and the fibre interacted, normalizing *Chrebpα* expression compared to untreated mice fed HFHSD.

In liver, the expression of the glucose transporter 2 (*Glut2*) (Figure S3C) and glucokinase (*Gck*) (Figure 2C) were unaltered by HFHSD. However, *B. uniformis*, with or without WBE, increased *Gck* expression (Figure 2C) as well as glucose-6-phosphate (G6P) levels (Figure 2D), a product of *Gck* that stimulates glycogenogenesis, compared to HFHSD-fed groups not administered the bacteria. Liver glycogen was reduced in untreated HFHSD-fed mice (Figure 2E) and strongly increased by the *B. uniformis*-WBE combination, reaching levels close to those of controls. The increased G6P in liver, which is also a precursor for lipogenesis, did not affect this route as suggested by unchanged hepatic levels of lipogenic genes (*Acc* and *Fas*, Figure S3D), triglycerides (Figure S3E) and free fatty acids (Figure S3F).

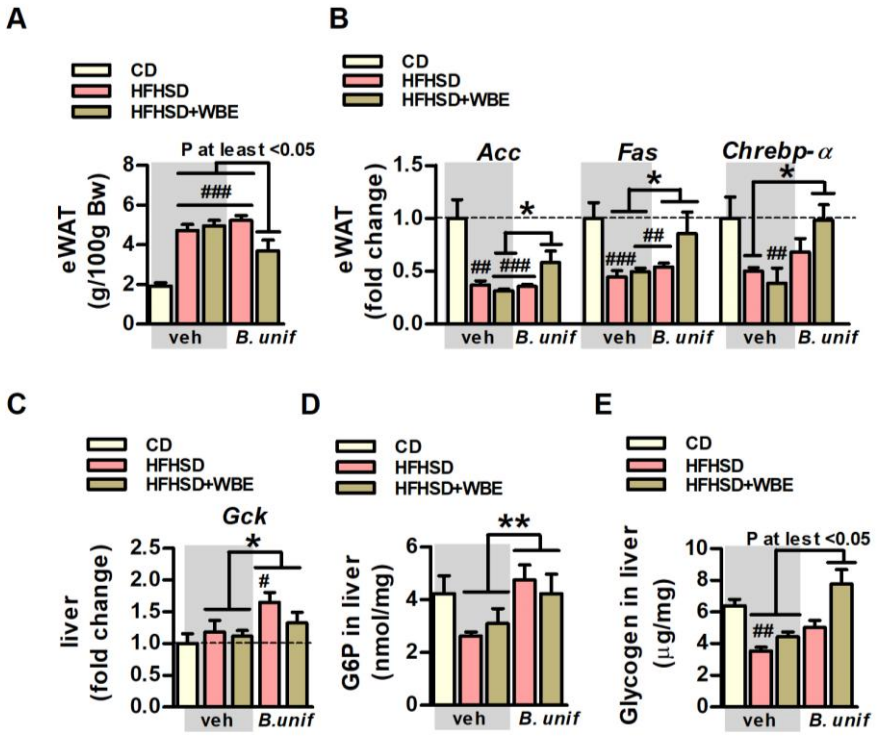

Figure 2. *B. uniformis* CECT 7771 combined with WBE curbs fat gain and normalizes insulin-dependent metabolic routes in adipose tissue and liver in HFHSD-fed mice. Weight of epididymal WAT, levels of expression of *de novo* lipogenesis-related genes in epididymal WAT, correlation between these

genes and adiposity and glucose metabolism-related markers in liver of controls (CD fed mice receiving vehicle, CD-veh) and HFHSD fed mice receiving vehicle, WBE, *B. unif* or the combination of both: HFHSD-veh, HFHSD+WBE, HFHSD-*B. unif* or HFHSD+WBE-*B. unif.* (**A**) Weight of epididymal WAT at week 17 (two-way ANOVA in HFHSD-fed groups: *B. unif* x WBE interaction P <0.01, *post hoc* P at least <0.05). N = 10 for all groups. (**B**) Gene expression of *Acc* (two-way ANOVA in HFHSD-fed groups: *B. unif* x WBE interaction P <0.05; *post hoc* P <0.05 compared to HFHSD+WBE), *Fas* (two-way ANOVA in HFHSD-fed groups: *B. unif* effect P <0.05) and *Chrebpα* (two-way ANOVA in HFHSD-fed groups: *B. unif* x WBE P <0.05; *post hoc* P <0.05 compared to HFHSD-veh) in epididymal WAT at week 17. *Acc*: CD-veh N = 6; HFHSD-veh, HFHSD+WBE and HFHSD+WBE-*B. unif* N = 7 and HFHSD-*B. unif* N = 8. *Fas*: CD-veh N = 6; HFHSD-veh, HFHSD+WBE and HFHSD-*B. unif* N = 8 and HFHSD+WBE-*B. unif* N = 7. *Chrebpα*: CD-veh and HFHSD-veh N = 5; HFHSD+WBE and HFHSD+WBE-*B. unif* N = 7 and HFHSD-*B. unif* N = 6. (**C**) Gene expression of *Gck* at week 17 in liver (two-way ANOVA in HFHSD-fed groups: *B. unif* effect P <0.05). *Gck*: CD-veh, HFHSD-veh, HFHSD-*B. unif* and HFHSD+WBE-*B. unif* N = 8 and HFHSD+WBE N = 6 (**D**) G6P concentration in liver at week 17 (two-way ANOVA in HFHSD-fed mice; *B. unif* effect P <0.01). CD-veh and HFHSD-veh N = 9, HFHSD+WBE N = 7 and HFHSD-*B. unif* and HFHSD+WBE-*B. unif* N = 9. (**E**) Glycogen concentration in liver at week 17 (Kruskal-Wallis test P at least <0.05 vs HFHSD-veh). CD-veh and HFHSD-veh N = 9; HFHSD+WBE N = 7 and HFHSD-*B. unif* and HFHSD+WBE-*B. unif* N = 8. Data were represented as the mean ± SEM. Statistical differences between HFHSD-fed groups (receiving or not the bacterium and/or WBE) and controls (CD-veh) were analysed using one-way ANOVA followed by post-hoc Tuckey. $^{\#}$P <0.05, $^{\#\#}$P <0.01, $^{\#\#\#}$P <0.001 vs control group. *P <0.05 and **P <0.01 indicate differences within HFHSD-fed groups. *Acc*, acetyl-CoA carboxylase; *B. unif*, *Bacteroides uniformis* CECT 7771; Bw, body weight; *Chrebpα*, Carbohydrate-responsive element-binding protein-alpha; CD, control diet; eWAT, epididymal white adipose tissue; *Fas*, fatty acid synthase G6P, glucose-6-phosphate; *Gck*, glucokinase; *Glut2*, glucose transporter 2; HFHSD, high-fat high-sugar diet; *Hsl*, hormone sensitive lipase; *Lpl*, lipoprotein lipase; veh, vehicle; WBE, wheat bran extract.

Visceral fat thermogenesis normalized by bacteria-WBE combination in mice fed HFHSD

Thermogenesis in the brown adipose tissue (BAT) was enhanced in HFHSD-fed mice as suggested by the increased expression of the uncoupling protein-1 (*Ucp-1*) after HFHSD-feeding (Figure 3A). WBE, but not *B. uniformis*, normalized the expression of *Ucp1* in HFHSD-fed mice. Food efficiency, an indirect measure of energy expenditure, was reduced by week-6 of HFHSD-

feeding (Figure 3B) which was normalized by WBE, combined or not with *B. uniformis*. Although *Ucp-1* abundance was much lower in epididymal fat compared to BAT, its expression also showed a 3-fold increase in untreated mice fed HFHSD (Figure 3C). While *Ucp-1* remained high in mice fed HFHSD receiving either *B. uniformis* or WBE, their combination interacts to normalize *Ucp-1* (Figure 3C). The mRNA levels of carnitine palmitoyltransferase 1a (*Cpt1-a*), the rate-limiting enzyme of fatty acid oxidation and normally coupled with thermogenesis in the adipose tissue, was also increased in untreated mice fed HFHSD and remained high in either *B. uniformis* or WBE-treated mice and, to a lesser extent, in those receiving the combination of both (Figure 3C). Positive correlations between *Ucp-1* or *Cpt1a* to epididymal WAT or weight gain were identified (Figure 3D).

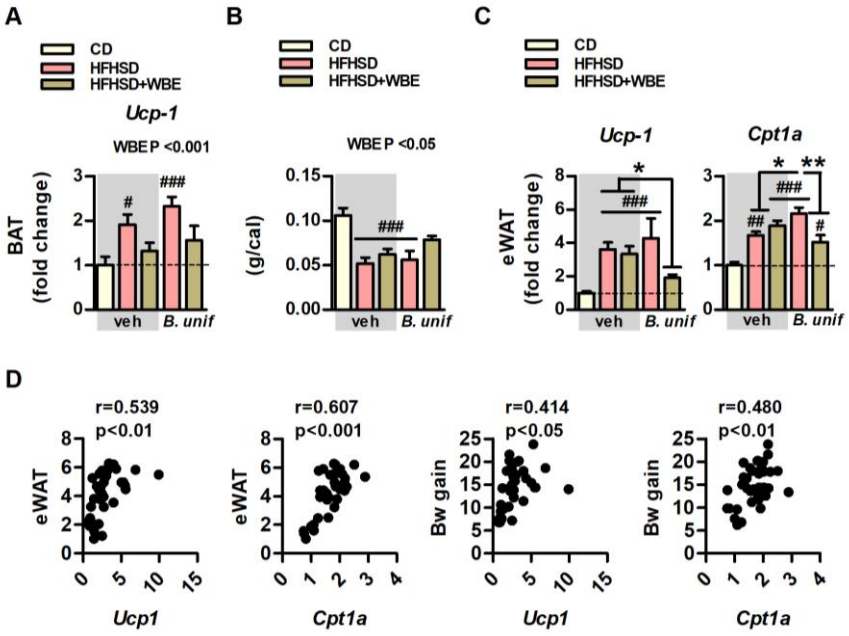

Figure 3. *B. uniformis* CECT 7771 combined with WBE restores the obesity-associated increased expression of *Ucp-1* in epididymal fat which correlates with a healthier metabolic phenotype. *Ucp-1 gene* expression in BAT, food efficiency, *ucp-1* and c*pt1a* gene expression in epididymal WAT, correlation between *ucp-1* and *cpt1a* in epididymal WAT to adiposity or to Bw gain of controls (CD fed mice receiving vehicle, CD-veh) and HFHSD fed mice receiving vehicle, WBE, *B. unif* or the combination of both: HFHSD-veh, HFHSD+WBE, HFHSD-*B. unif* or HFHSD+WBE-*B. unif.* (**A**) *Ucp-1 gene* expression pattern in BAT (two-way ANOVA in HFHSD-fed groups: WBE effect

P <0.001) at week 17. N = 10 for all groups. (**B**) Food efficiency at week 6 (two-way ANOVA in HFHSD-fed groups: WBE effect P <0.05). N = 10 for all groups. (**C**) *Ucp-1* (Kruskal-Wallis test HFHSD+WBE-*B*. *unif* vs HFHSD+WBE and HFHSD-veh P <0.001) and *Cpt1-a* (two-way ANOVA in HFHSD-fed groups: *B. unif* x WBE interaction P <0.01, *post hoc* P at least <0.05) gene expression of in epididymal WAT at week 17. *Ucp-1*: CD-veh N = 6; HFHSD-veh, HFHSD+WBE and HFHSD+WBE-*B. unif* N = 8 and HFHSD-*B. unif* N = 7. *Cpt1-a*: CD-veh and HFHSD+WBE-*B. unif* N = 7 and HFHSD-veh, HFHSD+WBE and HFHSD-*B. unif* N = 8. (**D**) Bravais-Pearson´s correlation between *Ucp-1* or *Cpt1-a* expression in epididymal WAT to epididymal WAT weight or to Bw gain, N = 38. Data were represented as the mean ± SEM. Statistical differences between HFHSD-fed groups (receiving or not the bacterium and/or WBE) and controls (CD-veh) were analysed using one-way ANOVA followed by post-hoc Tukey $^{\#}$P <0.05, $^{\#\#}$P <0.01, $^{\#\#\#}$P <0.001 vs control group. *P <0.05 and **P <0.01 indicate differences within HFHSD-fed groups. *B. unif*, *Bacteroides uniformis* CECT 7771*;* BAT, brown adipose tissue*;* Bw, body weight*;* CD, control diet*; Cpt1-a*, carnitine palmitoyltransferase 1a*;* eWAT, epididymal white adipose tissue*;* HFHSD, high-fat high-sugar diet*; Ucp-1*, uncoupled protein-1*;* veh, vehicle*;* WBE, wheat bran extract.

B. uniformis CECT 7771 and WBE administration modifies gut microbiota, while caecal abundance of fatty acids is mainly affected by *B. uniformis* CECT 7771 in mice fed HFHSD

Alpha diversity descriptor analysis did not show a major effect of HFHSD on the cecal microbiota structure compared to controls. However, the WBE reduced diversity while *B. uniformis* increased diversity, and their combination restored diversity metrics to control levels (Figure S4A). The multivariate dbRDA analysis showed how treatments affected the microbial community structure at OTUs level. The dbRDA1 dimension better discriminated WBE-treated groups, whereas dbRDA2 showed the HFHSD shifted microbiota structure and this change was partially restored by *B. uniformis* administration (Figure S4B). The interventions also influenced OTUs abundance (potential bacterial species) identified among groups (p < 0.001). Specifically, the HFHSD caused a depletion of *Alistipes* spp. (OTU117), *Odoribacter* spp. (OTU124), *Roseburia* spp. (OTU87) and *Christensenella* spp. (OTU114), which was restored efficiently only by *B. uniformis* (Figure S4C). WBE increased *Bifidobacterium* species abundance (OTU102) and, particularly, Lachnospiraceae species including those belonging to Lachnospiraceae NK4A136 and the genus *Blautia* (OTU273). Concomitantly, WBE reduced the proportion of certain Ruminococcaceae and Oscillospiraceae species together with *Bilophila* spp (OTU22) (Figure S4C). WBE and *B. uniformis* combined

administration increased several Lachnospiraceae (OTU30, OTU180, OTU415, OTU76, OTU59, OTU155) and Muribaculaceae (OTU214) species, compared to the other groups (corrected $p < 0.05$).

In accordance with WBE increasing SCFAs-producing species (Lachnospiraceae NK4A136 group and *Blautia* genus), the actual concentration of acetate, propionate and butyrate were increased while that of iso-butyrate was reduced in the cecal content of mice fed HFHSD receiving the WBE (Figure 4A). Nevertheless, the butyrate increase was higher in HFHSD-fed mice receiving the combination of WBE and *B. unformis*, suggesting an additive effect in the production of this key metabolite (Figure 4A).

Caecal concentrations of either palmitic (16:0) or stearic (18:0) acid, the most abundant dietary saturated fatty acids (FAs) (Table S1), were unchanged or increased, respectively, in HFHSD-fed mice untreated or treated (with *B. uniformis* or WBE) compared to controls (Figure 4B). Under HFHSD, *B. uniformis* and WBE, in combination, interacted increasing stearic (18:0) (Figure 4b) and arachidic acid (20:0) (Figure S5A). Similarly, concentrations of total monounsaturated FAs (MUFAs) [mainly 10-heptadecenoic acid (17:1, n-7), oleic acid (18:1, n-9) and vaccenic acid (17:1, n-7), Figure S5B] and polyunsaturated FAs (PUFAs) [mostly dihomo-ϒ-linolenic (20:3, n-6), arachidonic (20:4, n-6), eicosapentaenoic (20:5, n-3), adrenic (22:4, n-6), docosapentaenoic (22:5, n-3) and docosahexaenoic (22:6, n-3) acid, Figure S5D] were higher in the cecal content after HFHSD-feeding compared to controls (Figure 4C). Independently of WBE, *B. uniformis* reduced cecal MUFAs (Figure 4C and online Figure S5B), diunsaturated FAs (Figure 4C and Figure S5C) and PUFAs (Figure 4C and Figure S5D) compared to mice not administered the bacteria (untreated and WBE-treated mice fed HFHSD).

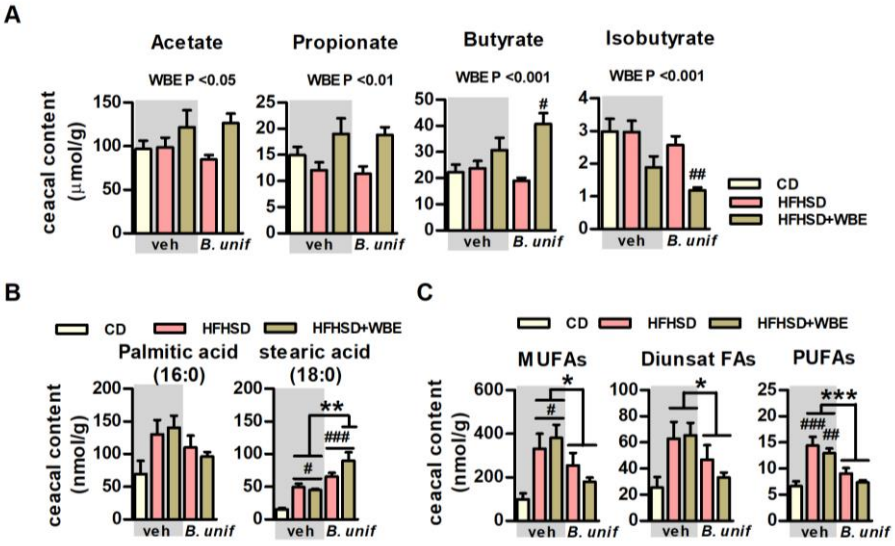

Figure 4. *B. uniformis* CECT 7771, combined or not with WBE, differently influences caecal concentrations short and long chain fatty acids. Levels of SCFAs, saturated and unsaturated long chain FAs in the ceacal content of controls (CD fed mice receiving vehicle, CD-veh) and HFHSD fed mice receiving vehicle, WBE, *B. unif* or the combination of both: HFHSD-veh, HFHSD+WBE, HFHSD-*B. unif* or HFHSD+WBE-*B. unif.* (**A**) Concentrations of short chain fatty acids (SCFAs, acetate, propionate, butyrate and isobutyrate) in the cecum (nmol/g of dry weight of caecal content) at week 17 (two-way ANOVA in HFHSD-fed groups: WBE effect P at least <0.05). CD-veh N = 8 and HFHSD-veh, HFHSD+WBE, HFHSD-*B. unif* and HFHSD+WBE-*B. unif* N = 10. (**B**) Caecal levels of saturated fatty acids (palmitic and stearic acids, 16:0 and 18:0, respectively; nmol/g of dry weight of caecal content) (for stearic acid, two-way ANOVA in HFHSD-fed groups: *B. unif* x WBE interaction P <0.05; *post hoc* P <0.01 vs HFHSD-veh or HFHSD+WBE) at week 17. FA 16:0: CD-veh N = 8 and HFHSD-veh, HFHSD+WBE, HFHSD-*B. unif* and HFHSD+WBE-*B. unif* N = 10. FA 18:0 CD-veh N = 8; HFHSD-veh and HFHSD-*B. unif* N =10; HFHSD+WBE N = 7 and HFHSD+WBE-*B. unif* N = 9. (**C**) Concentrations of unsaturated fatty acids (total MUFAs, diunsaturated FAs and PUFAs) in cecum (nmol/g of dry weight of caecal content) at week 17 (two-way ANOVA in HFHSD-fed groups: *B. unif* effect P at least <0.05) MUFAs: CD-veh N = 8; HFHSD-veh, HFHSD-*B. unif* and HFHSD+WBE-*B. unif* N = 10 and HFHSD+WBE N = 9. Diunsaturated FAs and PUFAs: CD-veh N = 7 and HFHSD-veh, HFHSD+WBE, HFHSD-*B. unif* and HFHSD+WBE-*B. unif* N = 10**.** Data were represented as the mean ± SEM. Statistical differences between HFHSD-fed groups (receiving or not the bacterium and/or WBE) and controls

(CD-veh) were analysed using one-way ANOVA followed by post-hoc Tuckey $^{\#}P < 0.05$, $^{\#\#}P < 0.01$, $^{\#\#\#}P < 0.001$ vs control group. *P <0.05, **P <0.01 and ***P <0.001 indicate differences within HFHSD-fed groups. *B. unif*, *Bacteroides uniformis* CECT 7771*;* CD, control diet*;* Diunsat FAs, diunsaturated fatty acids; HFHSD, high-fat high-sugar diet*;* MUFAs, monounsaturated fatty acids; PUFAs, polyunsaturated fatty acids; veh, vehicle and WBE, wheat bran extract.

B. uniformis CECT 7771 combined with WBE prevents the HFHSD-associated pro-inflammatory shift in the gut

To unravel mechanisms through which *B. uniformis* combined with WBE improved the metabolic phenotype of HFHSD-fed mice, we examined intestinal barrier integrity-related mediators. In colon, the expression of antimicrobial peptides, i.e. lysozyme 1 (*Lyz1*), regenerating islet-derived protein 3 gamma (*Reg3γ*) and phospholipase A2 group IIA (*Pla2g2a*) or the proliferator marker *Ki67* remained unchanged regardless of treatment (Figure S6A). In ileum, the analysis of tight junction protein expression showed reduced *occludin* in HFHSD-fed mice (Figure S6B). Separately, neither *B. uniformis* nor WBE reversed this reduction but their combination increased *occludin* expression in HFHSD-fed mice. *Occludin* in ileum negatively correlated to weight gain and adiposity and positively to hepatic glycogen (Figure S6C). As we demonstrated that the combination of *B. uniformis* and WBE has an additive effect preventing body weight gain and visceral adiposity, we further analysed key intestinal immune cell populations in this intervention group, and compared it to controls and untreated mice fed HFHSD.

Untreated obese mice showed increased intracellular levels of IFNγ in the epithelium of small intestine (Figure 5A) indicating that HFHSD-feeding induced a pro-inflammatory shift in the gut. The analysis of INFγ-producing cells revealed that, compared to controls, HFHSD also led to a higher abundance of macrophages in lamina propria, with similar levels of type 1 and type 2 macrophages (Figure S6D). In the intestinal epithelium, HFHSD-feeding did not impact on innate lymphoid cells (ILC) type 1 (Figure 5C). Nevertheless, intraepithelial lymphocytes (IEL) were altered, showing reduced levels of natural IEL but higher induced IEL (Figure 5D) which highlights a primary role of induced IEL on IFNγ production as a consequence of HFHSD-feeding. *B. uniformis* combined with WBE seemed to alleviate the intestinal proinflammatory state since this intervention restored the levels of IFNγ in the epithelium (Figure 5A) and normalized macrophages in the lamina propria (Figure 5B) and the levels of induced IEL in the epithelium of the small intestine (Figure 5D).

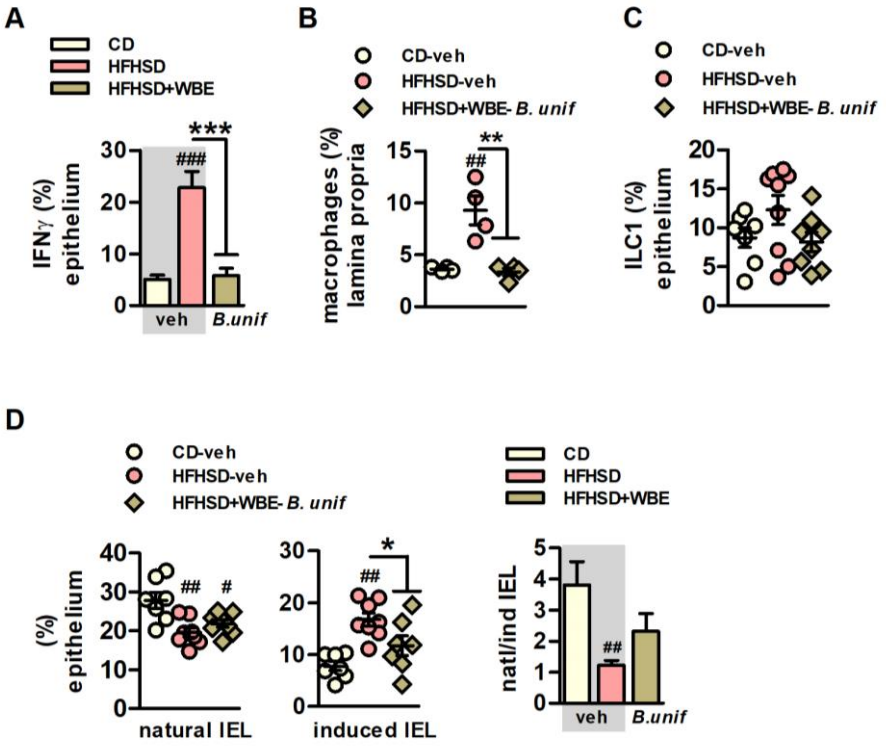

Figure 5. *B. uniformis* CECT 7771 combined with WBE protects against the intestinal immune imbalance of HFHSD-fed mice, curbing induced IEL and increasing ILC3 in the intestinal epithelium. (**A**) IFNϒ+ intestinal epithelial cells of the total intestinal epithelial cells (percentage) at week 17 in controls (CD-fed mice receiving vehicle, CD-veh) and HFHSD fed mice receiving vehicle or the combination of *B. uniformis* and WBE: HFHSD-veh and HFHSD+WBE-*B. unif*. N = 8 for all groups. (**B**) Macrophages in lamina propria (percentage) at week 17 in controls (CD-fed mice receiving vehicle, CD-veh N = 7) and HFHSD fed mice receiving vehicle or the combination of *B. uniformis* and WBE. N = 4. (**C**) ILC1 of the total intestinal epithelial cells (percentage) week 17 in controls (CD-fed mice receiving vehicle, CD-veh) and HFHSD fed mice receiving vehicle or the combination of *B. uniformis* and WBE: HFHSD-veh and HFHSD+WBE-*B. unif*. ILC1: CD-veh N = 7; HFHSD-veh N = 9 and HFHSD+WBE N = 8. (**D**) Natural and induced IEL (percentage of total intestinal epithelial cells and ratio) in the intestinal epithelium at week 17 in controls (CD-fed mice receiving vehicle, CD-veh N = 7) and HFHSD fed mice receiving vehicle or the combination of *B. uniformis* and WBE: HFHSD-veh N = 8 and HFHSD+WBE-*B. unif* N = 8. Data were represented as the mean ± SEM. one-way ANOVA followed by *post hoc* Tuckey was conducted for panels C-E. #P

<0.05, ##P <0.01, ###P <0.001 vs control group. *P <0.05, **P <0.01 and ***P <0.001 indicate differences within HFHSD-fed groups (fed or not WBE). *B. unif*, *Bacteroides uniformis;* Bw, body weight; CD, control diet; epididymal WAT, epididymal white adipose tissue; HFHSD, high-fat high-sugar diet; IEL, intraepithelial lymphocytes; ILC, innate lymphoid cells; WBE, wheat bran extract.

B. uniformis CECT 7771 combined with WBE ameliorates HFHSD-associated systemic inflammation through IL22 signalling

The expression of *Il22* in ileum was increased by combination of *B. uniformis* and WBE compared to untreated mice fed CD and HFHSD (Figure 6A). In the small intestine, the abundance of ILC3, a major source of IL22 once activated, was lower in untreated mice fed HFHSD compared to controls and augmented in HFHSD-fed mice receiving *B. uniformis* combined with WBE (Figure 6B). Compared to controls, the detrimental effects of HFHSD on intestinal immunity were related to plasma IL22 reductions (Figure 6C), but not coupled to other changes in plasma pro-inflammatory (IFNɣ and IL12) and anti-inflammatory cytokines (IL10 and IL4) (Figure 6C and Figure S7A). The serum concentration of IFNɣ was lower in HFHSD-fed mice receiving *B. uniformis* combined with WBE and IL22 reduction was attenuated (Figure 6C) compared to untreated mice fed HFHSD, while IL12, IL10 and IL4 remained unchanged (Figure S7A). Expression of *Il22r1* and *Il10r2*, the membrane receptor complex triggering IL22-mediated intracellular cascade, was unaffected in epididymal fat (Figure S7B) while, in liver, *Il10r2* was slightly higher in HFHSD-fed mice receiving *B. uniformis* combined with WBE compared to untreated mice fed HFHSD (Figure 6D), while no changes were observed in *Il22r1* expression. Hepatic IL22 signal transduction tended to be attenuated in untreated mice fed HFHSD as shown by reduced pSTAT3/STAT3 ratio compared to controls (Figure 6E). This ratio was increased by the administration of *B. uniformis* combined with WBE to mice fed HFHSD. HFHSD-feeding altered hepatic inflammation, showing higher levels of IFNɣ and IL10 compared to controls (Figure 6F). Again, *B. uniformis* combined with WBE normalised the increase in both cytokines in liver (Figure 6F), helping to maintain hepatic immune homeostasis in diet-induced obesity. Hepatic levels of IFNɣ or IL10 levels negatively correlated to glycogen levels (Figure 6G).

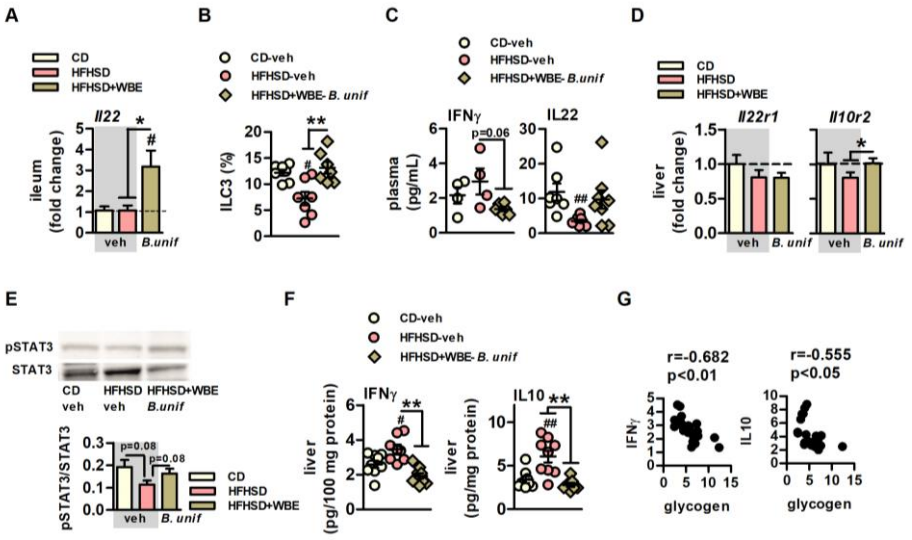

Figure 6. *B. uniformis* CECT 7771 combined with WBE ameliorates obesity-associated systemic inflammation in HFHSD-fed mice. Plasma and hepatic levels of inflammatory markers of controls (CD-fed mice receiving vehicle, CD-veh) and HFHSD fed mice receiving vehicle or the combination of *B. uniformis* and WBE: HFHSD-veh and HFHSD+WBE-*B. unif.* (**A**) *Il22* gene expression in ileum. CD-veh and HFHSD-veh N = 6 and HFHSD+WBE-*B. unif* N = 7. (**B**) ILC3 of the total intestinal epithelial cells (percentage) week 17 in controls (CD-fed mice receiving vehicle, CD-veh) and HFHSD fed mice receiving vehicle or the combination of *B. uniformis* and WBE. N = 7. (**C**) IFNɣ and IL22 plasma concentrations (pg/mL) at week 17. IFNɣ: CD-veh and HFHSD-veh N = 4 and HFHSD+WBE-*B. unif* N = 6. IL22: CD-veh N = 7; HFHSD-veh N = 9 and HFHSD+WBE-*B. unif* N = 8. (**D**) *Il22r1* and *Il10r* gene expression in liver. CD-veh N = 6 and HFHSD-veh and HFHSD+WBE-*B. unif* N = 8. (**E**) IL22 intracellular signalling (pSTAT3/STAT3 ratio) at week 17. CD-veh and HFHSD-veh N = 8 and HFHSD+WBE-*B. unif* N = 9. (**F**) IFNɣ and IL10 concentrations (pg/100mg protein) in liver at week 17. IFNɣ: CD-veh N = 8; HFHSD-veh N = 9 and HFHSD+WBE-*B. unif* N =7. IL10 CD-veh and HFHSD+WBE-*B. unif* N = 9 and HFHSD-veh N = 8. (**G**) Bravais-Pearson´s correlation between between IL10 or IFNɣ and glycogen hepatic depots. N = 22**.** Data were represented as the mean ± SEM. Panels A, C and D were assessed by one-way ANOVA followed by *post hoc* Tuckey, while Kruskal-Wallis test was used to analyse panel B. $^{\#}$P <0.05 and $^{\#\#}$P <0.01 vs control group. *P <0.05 and **P <0.01 indicate differences within HFHSD-fed groups (fed or not WBE). *B. unif*, *Bacteroides uniformis* CECT 7771*;* Bw, body weight; CD, control diet; HFHSD, high-fat high-sugar diet; WBE, wheat bran extract.

Discussion

This study provides a rationale to select dietary fibres that amplifies the benefits of specific intestinal bacteria to tackle obesity, enhancing our knowledge on the underlying mechanisms of action of both the bacterium and the fibre over the immune-metabolic axis. In particular, we demonstrate that body weight and adiposity reduction in diet-induced obesity is greater when *B. uniformis* CECT 7771 and WBE are administered in combination than separately. Furthermore, our study disentangles the respective contribution of *B. uniformis* and WBE to the benefits reported, indicating a key role of the bacterium in regulating oral glucose tolerance, promoting hepatic glucose storage and influencing selective intestinal lipid absorption and serum triglyceride levels. The study also shows how *B. uniformis* combined with WBE contributes to maintain the intestinal immune homeostasis in obesity, partly by increasing butyrate production, which translates to reduced markers of systemic inflammation and may account for restoration of the metabolic phenotype in diet-induced obesity.

Herein, *B. uniformis* was administered at a lower dose than in previous pre-clinical trials [12] since we hypothesized its effects would be boosted *in vivo* by its combination with a fibre previously selected as its best carbon source in vitro [16]. Our results confirmed that while this bacterial dose or WBE administered separately failed to induce anti-obesity effects, their combination reduced body weight gain and adiposity. This was accompanied by improvements in energy metabolic routes and restoration of intestinal immune homeostasis. Nevertheless, each intervention separately ameliorated some metabolic alterations in obesity, independently of weight loss; i.e. reduced cholesterolemia and glycaemia and improved glucose intolerance, although *B. uniformis* plays a greater role than WBE in restoring metabolic alterations.

The effects of the *B. uniformis*–WBE combination on adiposity were parallel to improvements of some insulin-regulated metabolic routes in adipose tissue and liver. Notably, HFHSD reduced lipogenesis in epididymal fat and hepatic glycogenesis, while both routes were normalized by the *B. uniformis*–WBE combination. In visceral fat, this intervention restored lipogenic markers (*Acc* and *Fas*) and the transcriptional factor regulating their expression *Chrebpα* [19]. The expression of lipogenic enzymes and *Chrebpα* in WAT positively correlates to insulin sensitivity in obesity. In fact, the reactivation of *de novo* lipogenesis in the adipose tissue, which mainly uses glycolysis-derived metabolites as precursors of fatty acids, acts as an insulin sensitizer mechanism improving whole-body metabolism in obese subjects [20–22]. We also showed hepatic glycogen depots were restored by the *B. uniformis*–WBE combination, which

were reduced by HFHSD, supporting a cross-talk between the visceral fat and liver. Furthermore, the combined intervention enhanced both, *Gck* expression, which is insulin-dependent [23] and its enzymatic product G6P, diminished in mice fed HFHSD. However, this effect was primarily driven by *B. uniformis* as it was also identified in group receiving bacteria alone supporting a major contribution of the bacterium restoring hepatic glycogenesis.

Overall, we identified specific metabolic routes through which the combination of *B. unformis* and WBE favours glucose disposal and improves whole-body insulin sensitivity; i.e. enhancing glucose utilization in the adipocyte of visceral fat to synthesize fatty acids without increasing adiposity and facilitating hepatic glucose storage via stimulation of diverse routes like glucose phosphorylation, which limits glucose output, and glycogenesis [24]. Targeting these metabolic routes, the *B. uniformis*–WBE combination would maintain physiological lipid storage in adipose tissue to limit ectopic fat accumulation in other organs under a Western diet.

Thermogenesis, mainly fuelled by fatty acids [25], was increased in HFHSD-fed mice, as indicated by overexpression of *Ucp-1* in BAT and in epididymal fat, whose thermogenic potential may increase under β3 adrenergic stimulation [26]. Although increased adrenergic-induced thermogenesis associated to diet-induced obesity remains controversial [27], it may be a mechanism to increase metabolic rate under a Western diet in order to maintain energy balance [28]. The overexpression of *Ucp-1* in epididymal fat, coupled with increased *Cpt1-α* expression of mice fed HFHSD and their positive correlation to fat mass and weight gain, suggests excess energy from the obesogenic diet was partially counteracted by triggering fatty acid degradation by thermogenesis and fatty acid oxidation, albeit insufficient to prevent obesity. Also, the activation of this mechanism was unnecessary in mice receiving *B. uniformis* and WBE. Therefore, the beneficial effect of *B. uniformis* and WBE on adiposity was not mediated by the activation of energy dissipating metabolic routes using lipids as fuel, which suggests that the improved whole-energy disposal was through a mechanism independent of adipose tissue.

Alternatively, we hypothesized that the *B. uniformis*-WBE combination modifies the metabolites resulting for diet-microbiota interactions, leading to the production of those beneficial for the host metabolism. Notably, WBE increased the concentration of acetate, propionate and butyrate and the abundance of SCFAs-producing species (i.e. Lachnospiraceae species), which are intestinal bacteria associated with anti-inflammatory properties [29]. Moreover, the intervention with *B. uniformis* and WBE also led to a gain in several species belonging to the Lachnospiraceae family, which are enriched in oligo- and poly-

saccharide degrading genes and SCFA metabolic pathways [30]. In fact, the B. uniformis-WBE combination caused the highest increase in butyrate, one of the key metabolites for improving both metabolism and immunity that could account for the amplified benefits in obesity.

Furthermore, the combined treatment may modify microbial metabolic pathways that, in turn, would modify the nutrients available in the intestinal lumen and thus their accessibility to the host.

Accordingly, and based on the hypothesis that *B. uniformis* combined with WBE would limit the access to HFHSD-associated excess energy by reducing intestinal lipid absorption, we analysed the impact of each intervention on long chain FAs, the most abundant dietary component of HFHSD in the cecum, which may indirectly reflect their intestinal uptake. *B. uniformis* combined with WBE increased saturated FAs abundance (stearic and arachidic acids) in the cecum, reflecting their reduced absorption. By contrast, *B. uniformis*, with or without WBE, reduced cecal unsaturated fatty acids (MUFAs, diunsaturated FAs and PUFAs) concentration, which may indicate increased absorption in HFHSD-fed mice. This suggests that B. uniformis combined with WBE would attenuate the damaging effects of saturated lipids on the host (i.e. impairment of intestinal integrity, insulin resistance and systemic inflammation). Previous studies support this, demonstrating the metabolic benefits of *B. uniformis* CECT 7771 were associated with reduced fat depots in the enterocytes in diet-induced obese mice [12]. Moreover, the bacterium with or without WBE would strengthen the metabolic and anti-inflammatory benefits associated with unsaturated FAs. In particular, increased intestinal uptake of oleic acid may improve glucose homeostasis by preventing the impaired β cell function and the inflammatory associated insulin resistance in liver and adipose tissue induced by palmitic acid [31,32]. In addition, higher absorption of ω3 fatty acids, such as α-linolenic acid, may prevent the disruption of the inflammatory cascade and reverse insulin resistance of diet induced obese mice [33].

As the maintenance of the immune homeostasis in the gut protects against systemic inflammation and contributes to preventing onset of obesity and T2D [34], we investigated whether this could be a mechanism whereby interventions improved the metabolic phenotype in HFHSD-fed mice. *B. uniformis* and WBE together restored *occludin* expression, a marker of gut integrity, strongly diminished by HFHSD-feeding. *Occludin* expression inversely correlated to weight gain, adiposity and liver glycogen, supporting a relationship between gut integrity and a healthier metabolic state. Furthermore, HFHSD-feeding induced a pro-inflammatory state in the gut showing higher levels of IFNɣ and increased macrophages infiltration into the small intestine. Additionally, we have described

for the first time that HFHSD-feeding increased induced IEL and its effector cytokine IFNɤ, while decreasing natural IEL. Each IEL subset mainly diverges in its differentiation process; while naïve T cells differentiate into natural IEL in thymus to directly seed the intestine early in life, induced IEL differentiation occurs in lymphoid intestinal organs in response to local tissue damage [35,36]. The increased abundance of induced IEL of mice fed HFHSD could result from a response to enhanced bacterial antigen exposure and/or signals of epithelial cell damage under HFHS-feeding, potentially associated with HFHSD-induced deficits in specific microbial species (*Alistipes* spp., *Odoribacter* spp., *Roseburia* spp. and *Christensenella* spp). This, in turn, lowers natural IEL, mainly associated with surveillance and maintenance of intestinal homeostasis [37,38]. HFHSD also reduced ILC3, which play a critical role in containing commensal bacteria in the luminal side and replenishing epithelial cells in response to a damage [39,40]. Diminished Th17 cells in the lamina propria, the adaptive counterpart of ILC3, accounts for obesity onset by impairing intestinal surveillance which aggravates dysbiosis-mediated inflammation [41]. Similarly, we also found reduced ILC3 in the intraepithelial layer, the main cells producing IL22 in the intestine [42]. This suggests that the Western diet diminished the IL22-mediated defence and mucosal reparation mechanisms accounting for the inflammatory state in obesity [43]. In parallel with the metabolic benefits, the *B. uniformis*–WBE combination completely normalized the abundance of induced IEL and ILC3, both immune cell populations are regulated by the intestinal microbiota and their dietary metabolic products and provide the first line of immune defence against microbes in the gut and their dysregulation causes loss of gut barrier integrity and inflammation [42,44,45]. Considering gut microbiota analysis, we could postulate that the intervention-mediated restoration of IEL and ILC3 was partly due to the associated changes in gut microbiota composition and derived metabolites like SCFAs which are also present in the small intestine [46]. SCFAs enhance ILC proliferation [47] and, in particular, butyrate increases the production of IL22 by RORγt+ ILC3 and CD4+ T cells 48. Here we showed that *B. uniformis* combined with WBE restored diversity and enrichment of Lachnospiraceae species that are butyrate producers and induced the higher increase of butyrate in the cecum, mechanisms through which this intervention may promote ILC3 proliferation.

Plasma IL22 was reduced similarly to the intestinal ILC3 in HFHSD-fed mice, suggesting a link between intestinal and systemic immune alterations. We also showed that hepatic IL22 signal transduction cascade was reduced in mice fed HFHSD along with increased IFNɤ and IL10 concentrations, while *B. uniformis* and WBE partially restored IL22 in plasma and IL22 signalling in liver. These findings suggest the combined intervention may attenuate the HFHSD-associated increase in pro-inflammatory IFNɤ-producing cells in liver, causing

insulin resistance, through improved IL22 signalling. Supporting our findings, IL22 displays protective functions in response to hepatic tissue damage [49,50] reducing inflammation in an animal model of alcoholic liver [51] and improving hepatic insulin sensitivity in obesity [43,50].

In conclusion, we reveal the mode of action of *B. uniformis* CECT 7771 combined with WBE on the metabolic-immune axis in obesity. Limiting intestinal lipid absorption, lipogenesis-related glucose consumption in the adipose tissue and glycogenesis in liver seemed to be the metabolic routes through which *B. uniformis* combined with WBE attenuated obesity progression in mice. Furthermore, ILC3 and IEL appeared to be critical intestinal immune mediators of the metabolic benefits of the combined intervention, whose regulation may provide protection against Western diet-induced intestinal immune dysregulation and systemic inflammation.

Material and methods

Bacterial growth conditions

B. uniformis CECT 7777, a bacterial strain originally isolated from healthy breast-fed infants and deposited in the Spanish Culture Collection (CECT) [53], was grown in Schaeldler broth at 37°C under anaerobiosis (AnaeroGen, ThermoFisher UK) as previously described [12,52]. The bacteria were harvested by centrifugation (6000g, 10 min), washed twice with phosphate buffer saline (PBS) solution and finally re-suspended in PBS containing cysteine (0.05%) and glycerol (10%). Aliquots were immediately frozen in liquid nitrogen and stored at -80°C until use. After freezing and thawing, the number of viable bacteria per milliliter was calculated by counting the colony forming units (CFU) in Schaeldler agar medium after incubation for 48h, at 37°C under anaerobic conditions. The bacterial identity was routinely confirmed during production and storage by partial 16S rRNA gene sequencing as described previously [12].

Mice and diets

The murine model comprised 6-8 week-old C57BL/6J male mice (Charles Rivers, France), with *ad-libitum* access to water and food except for oral glucose tolerance test (OGTT), housed in collective cages (5 mice per cage) under 12h of light/dark cycle (lights on at 8:00) in a temperature-controlled room (23±2°C). Mice were randomly allocated into 5 experimental groups by the animal health care technicians. For 17 weeks, mice were fed either control diet (CD; D12450K Research Diet NJ, USA; 10% of energy from fat and without sucrose; N = 10), high-fat high-sugar diet (HFHSD, D12451 Research Diet NJ, USA; 45% of energy from fat and 35% from sucrose; N = 20) or HFHSD supplemented with 5% of wheat-bran extract (WBE, provided by Cargill, Belgium) (HFHSD-WBE; N = 20) (dietary FAs composition is detailed in Table S1). Both mice fed HFHSD alone or HFHSD+WBE were subdivided into two experimental groups. One of these groups received an oral dose of vehicle (PBS with 0.05% cysteine and 10% glycerol, N = 10) and the other an oral dose *B. uniformis* CECT 7771 ($5x10^7$ CFU per mouse, N = 10) daily. CD-fed mice received only vehicle (N = 10).

Body weight was determined weekly. Glucose, triglycerides and cholesterol in plasma were measured at week 12 and an oral glucose tolerance test (OGTT) was conducted at week 14. At week 17, cardiac puncture was performed in isoflurane anesthetized mice for blood collection. Animals were then sacrificed by cervical dislocation and liver, epididymal white adipose tissue

(WAT), ileum and colon (2 cm pieces both) tissues and cecal content were isolated, snap-frozen in liquid nitrogen and stored at -80ºC until use. Whole small intestine (except the 2 cm-long distal part) was embedded in cold PBS and immediately processed for the analysis intraepithelial mononuclear cells by flow cytometry. Another batch of animals were used to estimate food efficiency at week 6 of HFHSD intervention by calculating the ratio between the weight gain and the amount of energy consumed *ad libitum* during 24h after 18h of fasting (refeeding period) (experimental procedure detailed in Figure S1). All experimental procedures were performed in accordance with European Union 2010/63/UE and Spanish RD53/201 guidelines and approved by the ethics committee of the University of Valencia (Animal Production Section, Central Service of Support to Research [SCSIE], University of Valencia, Spain) and authorized by Dirección General de Agricultura, Ganadería y Pesca (Generalidad Valenciana" (approval ID 2018/VSC/PEA/0090).

Oral glucose tolerance test (OGTT)

At week 14, an OGTT was conducted in 4-hour fasted mice. Blood from the saphenous vein was collected at 0, 15, 30, 60 and 120 minutes of being administered an oral glucose load (2g/Kg). Glucose was measured through glucose test strips using a glucometer (CONTOUR®-NEXT meter, Bayer, Leverkusen, Germany).

Blood metabolic parameters

Blood from the mandibular vein of 4-hour fasted mice was collected at week 12 in microtubes with K3 EDTA (Sarstedt, Nümbrecht Germany) to determine glycemia, measured as conducted in the OGTT, and triglycerides and cholesterol in plasma (blood centrifugation at 400g for 15 minutes at 4°C) using a colorimetric kit assay according to manufacturer´s instructions (Química Clínica Aplicada, Tarragona, Spain). Plasma from blood collected by cardiac puncture in 4-hour fasted mice at week 17, was used to measure insulin, glucagon-like peptide 1 (GLP-1), peptide YY (PYY) and the cytokine tumor necrosis factor α (TNFα), interleukins IL12, IL10, IL4 and IL22 and interferon ϒ (IFNϒ) using Multiplex Assays Using Luminex® (Milliplex, Merck group, Darmstadt, Germany) according to manufacturer´s instructions.

Isolation of intraepithelial mononuclear cells and flow cytometry analysis

Isolation of intraepithelial cells was conducted as previously described [54,55]. In brief, small intestine was washed with cold PBS and longitudinally opened and cut into small pieces. For the isolation of the epithelium, tissue was incubated twice in Hansk´s balanced salt solution with calcium and magnesium (HBSS; ThermoFisher Scientific, Massachusetts, USA) containing 5mM EDTA (Scharlab), 1mM DTT, 100 µg/ml streptomycin and 100 U/ml penicillin (Merck, Darmstadt, Germany) for 30 minutes at 37°C with orbital shaking. After each incubation, supernatant fractions were filtrated using 100µm nylon cell strainers (Biologix, Shandong, China) and centrifuged to harvest cell suspensions. Remaining tissue was washed with PBS for being incubated twice with HBSS containing 0.5 mg/mL collagenase D (Roche Diagnostics GmbH, Mannheim, Germany), 3 mg/mL dispase II (Sigma-Aldrich), 1 mg/mL DNase I (Roche Diagnostics GmbH), and streptomycin 100 µg/ml and penicillin 100 U/ml with orbital agitation for 30 minutes at 37°C. Cells from the lamina propria were collected by filtrating supernatant fractions with 70µm nylon cell strainers that were then centrifuged to harvest cell suspensions. Isolated cells in FACS buffer (PBS with BSA 0.5%) were then incubated with different immune markers during 30 min at 4ºC in darkness to measure lymphocyte subpopulations (natural and induced) in the epithelium as follows. Natural (CD45+ CD2+ CD5+) and induced (CD45+ CD2- CD5-) intraepithelial lymphocytes (IEL) were determined by phycoerithrin (PE)-conjugated anti-CD45, allophycocyanin (APC)-conjugated anti-CD2 and PE-Vio770-conjugated anti-CD5 (Miltenyi Biotec, Bergisch Gladbach, Germany) antibodies. Innate lymphoid cells (ILC) type 1 (ILC1: CD90+ CD127+ LIN- Tbet+ IFNɣ+) and type 3 (ILC3: CD90+ CD127+ LIN- RORɣt+ IL22+) were labeled by PerCP-Cy™5.5-conjugated anti-Lineage antibody cocktail (LIN) (BD-Bioscience, USA), phycoerithrin (PE)-conjugated anti-Tbet, allophycocyanin (APC)-conjugated anti-IFNɣ, phycoerithrin (PE)-conjugated anti- RORɣt (Miltenyi Biotec, Bergisch Gladbach, Germany) and allophycocyanin (APC)-conjugated anti-IL22 (Biolegend, San Diego, California, USA) antibodies. Pro-inflammatory (M1: F4/80+ CD80+ iNOS+) and anti-inflammatory (M2: F4/80+ CD206+ Arg1+) macrophages from lamina propria were determined using FITC-conjugated antiF4/80+, Pe-Vio770-conjugated anti-CD80 (Miltenyi, Biotec, Bergisch Gladbach, Germany), APC-conjugated anti-iNOS (Thermo Fisher Scientific, MA, USA), PerCPCy5.5-conjugated anti-CD206 (Biolegend, San Diego, California, USA) and PE-conjugated anti-Arg1 (R&D Systems, Minneapolis, USA) antibodies. Additionally, for intracellular markers staining (Tbet, IFNɣ, RORɣt, IL22, iNOS and Arg1) cells were permeabilized and fixed (fixation/permeabilization solution kit, BD Bioscience, USA). Data acquisition and analysis were performed using a

BD LSRFortessa (Becton Dickinson, USA) flow cytometer operated by FACS Diva software v.7.0 (BD Biosciences, USA).

Gene expression by RT-qPCR

Total RNA was isolated with TRIsure™ reagent (Bioline, London, UK) according to manufacturer´s instructions. For reverse transcription to cDNA, 2-1.5µg of RNA were incubated with reverse transcription buffer, dNTPs (4mM), random primers and 50 units of MultiScribe™ Reverse Transcriptase at 25°C for 10 minutes followed by 120 minutes at 37°C and 5 minutes at 85°C. The qPCR was performed on a LightCycler® 480 Instrument (Roche, Boulogne-Billancourt, France). The reaction consisted of LightCycler 480 SYBR Green I Master mix (Roche, Branchburg, USA) and 300 nM of gene-specific primer pairs. The primer sequences of each gene are detailed in Appendix Table S2. Ribosomal protein L19 (Rpl19) was used as housekeeping gene. The qPCR program included the following steps: a denaturation step at 95°C for 10 minutes; followed by 45 amplification cycles (95°C for 10 seconds, 60°C for 30 seconds and 72°C for 5 seconds) and a final melting stage at 95°C for 5 seconds and at 65°C for 1 minute. Variation of cDNA abundance was calculated according to the $2^{-(\Delta\Delta Ct)}$ method and represented as fold change expression relative to the control group.

Western blot

One hundred micrograms of denatured total proteins from liver, extracted using RIPA buffer (Merck, Germany) were separated by SDS-PAGE electrophoresis and transferred onto polyvinylidene difluoride (PVDF) membranes (Thermo Fisher Scientific, MA, USA). Membranes were overnight incubated at 4°C with 1:1000 dilution of phospho-STAT3 (Tyr705, #9138 Cell Signaling, Beverly, MA, USA), STAT3 (#4904 Cell Signaling, Beverly, MA, USA) and β-actin (#4967 Cell Signaling, Beverly, MA, USA) primary antibodies followed by 1 h incubation at RT with horse anti-mouse IgG-HRP at 1:5000 (#7076 Cell Signaling, Beverly, MA, USA) for phospho-STAT3 antibody binding and goat anti-rabbit IgG-HRP at 1:5000 (#7074 Cell Signaling, Beverly, MA, USA) for STAT3 and β-actin antibodies binding. Chemiluminescence signal was enhanced by adding ECL (SuperSignalTM West Dura Extended Duration Substrate, Thermo Fisher Scientific, MA, USA) and quantified using ImageJ 1.8 software.

Metabolites and cytokines in liver

Lipids from liver were extracted as previously described [56,57]. In brief, a solution of chloroform/methanol (2:1) was used for tissue homogenization. After 3h of shaking, milliQ water was added and the organic layer was separated by centrifugation (16000g, 20 minutes), collected and dried overnight. Then, triglycerides and free fatty acids were measured in the isolated organic layer using the Triglyceride colorimetric Assay Kit (Elabscience, USA) and the Free Fatty Acid Quantitation Kit (Sigma, Missouri, USA), respectively. Hepatic glycogen and glucose-6-phosphate (G6P) were quantified in the total homogenized tissue through the Glycogen Assay Kit (Sigma-Aldrich, Missouri, USA) and the Glucose-6-Phosphate Colorimetric Assay Kit, (BioVision, California, USA), respectively. Cytokines (TNFα, IL10, IL6 and IFNɤ) were measured using ProcartaPlex multiplex immunoassays according to manufacturer´s instructions (Thermo Fisher Scientific, MA, USA).

Fatty acid analysis

Cecal content was homogenized by bead beating in 70%-isopropanol [58]. SCFA were quantified by liquid chromatography coupled to tandem mass spectrometry (LC-MS/MS) upon derivatization to 3-nitrophenylhydrazones [58]. Concentrations of total fatty acids were determined by gas chromatography coupled to mass spectrometry (GC-MS) after derivatization to fatty acid methyl esters (FAMEs) [59].

Microbiota analysis

DNA of the caecal content was isolated using the QIAamp PowerFecal DNA kit (Qiagen, Hilden, Germany) following the manufacturer's instructions. The DNA concentration was measured by UV methods (Nanodrop, Thermo Scientific, Wilmington, USA) and an aliquot of every sample was prepared at ~20 ng/µL with nuclease-free water for polymerase chain reaction (PCR). The V3-V4 hypervariable regions of the 16S ribosomal ribonucleic acid (rRNA) gene were amplified using 1 µL aliquot DNA and 25 PCR cycles consisting of the following steps: 95 ºC for 20 sec., 55 ºC for 20 sec. and 72 ºC for 20 sec. Phusion High-Fidelity Taq Polymerase (Thermo Scientific, Wilmington, USA) and the 6-mer barcoded primers, S-D-Bact-0341-b-S-17 (TAGCCTACGGGNGGCWGCAG) and S-D-Bact-0785-a-A-21 (ACTGACTACHVGGGTATCTAATCC), which target a wide repertoire of bacterial 16S rRNA genes [60], were used for PCR. Dual barcoded PCR products, consisting of ~500 bp, were purified from triplicate reactions with the Illustra GFX PCR DNA and Gel Band Purification Kit (GE Healthcare, UK) and

quantified through Qubit 3.0 and the Qubit dsDNA HS Assay Kit (Thermo Fisher Scientific, Waltham, MA, USA). The samples were multiplexed in one sequencing run by combining equimolar quantities of amplicon DNA (~50 ng per sample) and sequenced in one lane of the Illumina MiSeq platform with 2x300 PE conFigureuration (Eurofins Genomics GmbH, Germany). Raw data was delivered in fastq files and pair ends with quality filtering were assembled using Flash software [61]. Sample de-multiplexing was carried out using sequence information from forward/reverse primers, the respective DNA barcodes, and the SeqKit suite of analysis [62]. After demultiplexing, the barcodes/primers were removed and sequences were processed for chimera removal using UCHIME algorithm [63] and the SILVA reference set of 16S sequences (Release 128) [64]. Operational Taxonomic Unit (OTU) information was retrieved by using a rarefied subset of 17,000 sequences per sample, randomly selected after multiple shuffling (10,000X) from of the original dataset, and the UCLUST algorithm implemented in USEARCH v8.0.1623 [65]. Common alpha diversity descriptors including the Observed OTUs, Reciprocal Simpson's index, dominance, and phylogenetic distance (PD) were computed using QIIME v1.9.1 [66]. For phylogenetic-based metrics the OTUs sequences were aligned using the PyNAST algorithm implemented in QIIME and the SILVA aligned reference database, whereas the tree topology reconstruction was completed with the FastTree algorithm [67] using the generalized time-reversible (GTR) model and gamma-based likelihood. The evaluation of the community structure across the sample groups was performed with the *Vegan* R package through interpretative multivariate and constrained appraisal based on the distance-based redundancy analysis (dbRDA) (*vegan::dbrda* function and "bray" method). Taxonomic identification of differentially abundant OTUs was achieved by submitting respective sequences to the SINA aligner web server (https://www.arb-silva.de/aligner/) and using the SILVA database for classification.

Statistical analysis

G*Power 3.1.9.2 was used to calculate sample size and SPSS (IBM SPSS Statistics 24) to conduct statistics. Shapiro-Wilk test was employed to assess normality. Statistics of normal distributed data were performed using different parametric tests, including repeated measures two-way ANOVA for the analysis of multiple measures of the same variable taken on the same subjects over the time (body weight gain and OGTT); one-way ANOVA followed by post-hoc Tuckey test to compare controls (CD-fed mice orally administered the vehicle) vs HFHSD-fed mice, receiving or not the bacterium and/or WBE and two-way ANOVA restricted to HFHSD-fed mice to examine both, the main effect of each independent variable (*B. uniformis* or the WBE) and the interactions between

them. For the analysis showing interactions between variables a post-hoc Tukey test was conducted. Kruskal-Wallis test followed by pairwise multiple comparisons was used to analyse non-normally distributed data. Bravais-Pearson´s correlation coefficient was used to test correlations between two variables. Only set of data with not significantly different slopes and intercepts, analysed using linear regression, were combined to calculate a global correlation coefficient between variables.

Statistical analyses on microbiota data were done applying non-parametric methods such as Kruskal-Wallis and pairwise Wilcoxon Rank Sum tests (for unpaired samples) with Benjamini-Hochberg *post hoc* correction for multiple group comparison across the alpha diversity descriptors. Statistical differences in the microbial community structure were assessed by the permutation-based *vegan::adonis* function. Differential abundance of OTUs across groups was assisted by applying the Kruskal-Wallis test with Benjamini-Hochberg *post hoc* correction. Highly divergent OTUs in terms of abundance were selected when Kruskal-Wallis chi-squared test was ≥ 30 and corrected $P \leq 0.001$. Additionally, pairwise Wilxocon Rank Sum test with Benjamini-Hochberg correction was applied to identify precise sample groups showing up- or down-representation of different OTUs. Graphs and plots were drawn using *ggplot2* and *grid* R v3.6 packages, Heatmap hierarchical clustering of OTUs (scaled read counts) was obtained using *"correlation"* as a distance and "*complete"* as clustering method. Results were not assessed by blinded investigators.

Availability of data

The caecal content microbiota data generated in this study is publicly available in the European Nucleotide Archive (ENA), and the raw fastq files associated can be accessed through the bioproject accession number PRJEB37867 (https://www.ebi.ac.uk/ena/data/search?query=PRJEB37867).

Acknowledgements

The authors thank Isabel Campillo Nuevo and Inmaculada Noguera for technical assistance. This study was funded by the European Commission 7th Framework Programme through the MyNewGut project (Grant agreement No. 613979). The FPI scholarship from MCIU (Spain) to IL-A and the Erasmus+ (European commission) to CB-V are fully acknowledged.

Author contribution

Conceptualization, IL-A, MR-P, AB-P and YS; Investigation, IL-A, MR-P, CB-V, AB-P, EGP and GL; Writing—Original Draft, IL-A, MR-P and YS; Writing—Reviewing & Editing, all authors;

Funding Acquisition YS; Supervision MR-P and YS.

Disclosure of potential conflicts of interest

YS is author of a patent related to *B. uniformis* CECT7771 (PCT/ES2013/070309). The other authors declare that they have no conflict of interest

References

1. Cani PD. Human gut microbiome: hopes, threats and promises. Gut 2018; 67:1716–25.

2. Rooks MG, Garrett WS. Gut microbiota, metabolites and host immunity. Nature Reviews Immunology 2016; 16:341–52.

3. Hooper LV, Littman DR, Macpherson AJ. Interactions between the microbiota and the immune system. Science 2012; 336:1268–73.

4. Sonnenburg ED, Smits SA, Tikhonov M, Higginbottom SK, Wingreen NS, Sonnenburg JL. Diet-induced extinctions in the gut microbiota compound over generations. Nature 2016; 529:212–5.

5. Wan Y, Wang F, Yuan J, Li J, Jiang D, Zhang J, Li H, Wang R, Tang J, Huang T, et al. Effects of dietary fat on gut microbiota and faecal metabolites, and their relationship with cardiometabolic risk factors: a 6-month randomised controlled-feeding trial. Gut 2019; 68:1417–29.

6. Levy M, Thaiss CA, Zeevi D, Dohnalová L, Zilberman-Schapira G, Mahdi JA, David E, Savidor A, Korem T, Herzig Y, et al. Microbiota-Modulated Metabolites Shape the Intestinal Microenvironment by Regulating NLRP6 Inflammasome Signaling. Cell 2015; 163:1428–43.

7. Caesar R, Tremaroli V, Kovatcheva-Datchary P, Cani PD, Bäckhed F. Crosstalk between Gut Microbiota and Dietary Lipids Aggravates WAT Inflammation through TLR Signaling. Cell Metab 2015; 22:658–68.

8. Tilg H, Zmora N, Adolph TE, Elinav E. The intestinal microbiota fuelling metabolic inflammation. Nat Rev Immunol 2020; 20:40–54.

9. Rodriguez J, Hiel S, Neyrinck AM, Roy TL, Pötgens SA, Leyrolle Q, Pachikian BD, Gianfrancesco MA, Cani PD, Paquot N, et al. Discovery of the gut microbial signature driving the efficacy of prebiotic intervention in obese patients. Gut 2020; Available from: https://gut.bmj.com/content/early/2020/02/10/gutjnl-2019-319726

10. Adeshirlarijaney A, Gewirtz AT. Considering gut microbiota in treatment of type 2 diabetes mellitus. Gut Microbes 2020; 11:253–64.

11. Romaní-Pérez M, Agusti A, Sanz Y. Innovation in microbiome-based strategies for promoting metabolic health. Curr Opin Clin Nutr Metab Care 2017; 20:484–91.

12. Gauffin Cano P, Santacruz A, Moya Á, Sanz Y. Bacteroides uniformis CECT 7771 Ameliorates Metabolic and Immunological Dysfunction in Mice with High-Fat-Diet Induced Obesity. PLoS ONE 2012; 7:e41079.

13. Delzenne NM, Olivares M, Neyrinck AM, Beaumont M, Kjølbæk L, Larsen TM, Benítez-Páez A, Romaní-Pérez M, Garcia-Campayo V, Bosscher D, et al. Nutritional interest of dietary fiber and prebiotics in obesity: Lessons from the MyNewGut consortium. Clin Nutr 2019;

14. Portune KJ, Benítez-Páez A, Del Pulgar EMG, Cerrudo V, Sanz Y. Gut microbiota, diet, and obesity-related disorders-The good, the bad, and the future challenges. Mol Nutr Food Res 2017; 61.

15. EFSA Panel on Dietetic Products, Nutrition, and Allergies (NDA). Scientific Opinion on Dietary Reference Values for carbohydrates and dietary fibre. 3 2010; 8:1462.

16. Benítez-Páez A, Gómez Del Pulgar EM, Sanz Y. The Glycolytic Versatility of *Bacteroides uniformis* CECT 7771 and Its Genome Response to Oligo and Polysaccharides. Front Cell Infect Microbiol 2017; 7:383.

17. Boll EVJ, Ekström LMNK, Courtin CM, Delcour JA, Nilsson AC, Björck IME, Östman EM. Effects of wheat bran extract rich in arabinoxylan oligosaccharides and resistant starch on overnight glucose tolerance and markers of gut fermentation in healthy young adults. Eur J Nutr 2016; 55:1661–70.

18. Kjølbæk L, Benítez-Páez A, Gómez Del Pulgar EM, Brahe LK, Liebisch G, Matysik S, Rampelli S, Vermeiren J, Brigidi P, Larsen LH, et al. Arabinoxylan oligosaccharides and polyunsaturated fatty acid effects on gut microbiota and metabolic markers in overweight individuals with signs of metabolic syndrome: A randomized cross-over trial. Clin Nutr 2020; 39:67–79.

19. Iizuka K, Bruick RK, Liang G, Horton JD, Uyeda K. Deficiency of carbohydrate response element-binding protein (ChREBP) reduces lipogenesis as well as glycolysis. Proc Natl Acad Sci USA 2004; 101:7281–6.

20. Herman MA, Peroni OD, Villoria J, Schön MR, Abumrad NA, Blüher M, Klein S, Kahn BB. A novel ChREBP isoform in adipose tissue regulates systemic glucose metabolism. Nature 2012; 484:333–8.

21. Eissing L, Scherer T, Tödter K, Knippschild U, Greve JW, Buurman WA, Pinnschmidt HO, Rensen SS, Wolf AM, Bartelt A, et al. De novo lipogenesis in human fat and liver is linked to ChREBP-β and metabolic health. Nat Commun 2013; 4:1528.

22. Solinas G, Borén J, Dulloo AG. De novo lipogenesis in metabolic homeostasis: More friend than foe? Mol Metab 2015; 4:367–77.

23. Petersen MC, Vatner DF, Shulman GI. Regulation of hepatic glucose metabolism in health and disease. Nat Rev Endocrinol 2017; 13:572–87.

24. Rui L. Energy metabolism in the liver. Compr Physiol 2014; 4:177–97.

25. Chouchani ET, Kazak L, Spiegelman BM. New Advances in Adaptive Thermogenesis: UCP1 and Beyond. Cell Metab 2019; 29:27–37.

26. Zhang F, Hao G, Shao M, Nham K, An Y, Wang Q, Zhu Y, Kusminski CM, Hassan G, Gupta RK, et al. An Adipose Tissue Atlas: An Image-Guided Identification of Human-like BAT and Beige Depots in Rodents. Cell Metab 2018; 27:252-262.e3.

27. Kozak LP. Brown fat and the myth of diet-induced thermogenesis. Cell Metab 2010; 11:263–7.

28. Feldmann HM, Golozoubova V, Cannon B, Nedergaard J. UCP1 ablation induces obesity and abolishes diet-induced thermogenesis in mice exempt from thermal stress by living at thermoneutrality. Cell Metab 2009; 9:203–9.

29. Hu S, Wang J, Xu Y, Yang H, Wang J, Xue C, Yan X, Su L. Anti-inflammation effects of fucosylated chondroitin sulphate from Acaudina molpadioides by altering gut microbiota in obese mice. Food Funct 2019; 10:1736–46.

30. Vacca M, Celano G, Calabrese FM, Portincasa P, Gobbetti M, De Angelis M. The Controversial Role of Human Gut Lachnospiraceae. Microorganisms 2020; 8.

31. Maedler K, Oberholzer J, Bucher P, Spinas GA, Donath MY. Monounsaturated fatty acids prevent the deleterious effects of palmitate and high glucose on human pancreatic beta-cell turnover and function. Diabetes 2003; 52:726–33.

32. Palomer X, Pizarro-Delgado J, Barroso E, Vázquez-Carrera M. Palmitic and Oleic Acid: The Yin and Yang of Fatty Acids in Type 2 Diabetes Mellitus. Trends Endocrinol Metab 2018; 29:178–90.

33. Oliveira V, Marinho R, Vitorino D, Santos GA, Moraes JC, Dragano N, Sartori-Cintra A, Pereira L, Catharino RR, da Silva ASR, et al. Diets Containing α-Linolenic (ω3) or Oleic (ω9) Fatty Acids Rescues Obese Mice From Insulin Resistance. Endocrinology 2015; 156:4033–46.

34. Winer DA, Luck H, Tsai S, Winer S. The Intestinal Immune System in Obesity and Insulin Resistance. Cell Metab 2016; 23:413–26.

35. Mayassi T, Jabri B. Human intraepithelial lymphocytes. Mucosal Immunol 2018; 11:1281–9.

36. Cheroutre H, Lambolez F, Mucida D. The light and dark sides of intestinal intraepithelial lymphocytes. Nat Rev Immunol 2011; 11:445–56.

37. Boismenu R, Havran WL. Modulation of epithelial cell growth by intraepithelial gamma delta T cells. Science 1994; 266:1253–5.

38. Roberts SJ, Smith AL, West AB, Wen L, Findly RC, Owen MJ, Hayday AC. T-cell alpha beta + and gamma delta + deficient mice display abnormal but distinct phenotypes toward a natural, widespread infection of the intestinal epithelium. Proc Natl Acad Sci USA 1996; 93:11774–9.

39. Ebbo M, Crinier A, Vély F, Vivier E. Innate lymphoid cells: major players in inflammatory diseases. Nat Rev Immunol 2017; 17:665–78.

40. Omenetti S, Bussi C, Metidji A, Iseppon A, Lee S, Tolaini M, Li Y, Kelly G, Chakravarty P, Shoaie S, et al. The Intestine Harbors Functionally Distinct Homeostatic Tissue-Resident and Inflammatory Th17 Cells. Immunity 2019; 51:77-89.e6.

41. Garidou L, Pomié C, Klopp P, Waget A, Charpentier J, Aloulou M, Giry A, Serino M, Stenman L, Lahtinen S, et al. The Gut Microbiota Regulates Intestinal CD4 T Cells Expressing RORγt and Controls Metabolic Disease. Cell Metab 2015; 22:100–12.

42. Sawa S, Lochner M, Satoh-Takayama N, Dulauroy S, Bérard M, Kleinschek M, Cua D, Di Santo JP, Eberl G. RORγt+ innate lymphoid cells regulate intestinal homeostasis by integrating negative signals from the symbiotic microbiota. Nat Immunol 2011; 12:320–6.

43. Wang X, Ota N, Manzanillo P, Kates L, Zavala-Solorio J, Eidenschenk C, Zhang J, Lesch J, Lee WP, Ross J, et al. Interleukin-22 alleviates metabolic disorders and restores mucosal immunity in diabetes. Nature 2014; 514:237–41.

44. Ismail AS, Severson KM, Vaishnava S, Behrendt CL, Yu X, Benjamin JL, Ruhn KA, Hou B, DeFranco AL, Yarovinsky F, et al. Gammadelta intraepithelial lymphocytes are essential mediators of host-microbial homeostasis at the intestinal mucosal surface. Proc Natl Acad Sci USA 2011; 108:8743–8.

45. McDonald BD, Jabri B, Bendelac A. Diverse developmental pathways of intestinal intraepithelial lymphocytes. Nat Rev Immunol 2018; 18:514–25.

46. Cummings JH, Pomare EW, Branch WJ, Naylor CP, Macfarlane GT. Short chain fatty acids in human large intestine, portal, hepatic and venous blood. Gut 1987; 28:1221–7.

47. Sepahi A, Liu Q, Friesen L, Kim CH. Dietary fiber metabolites regulate innate lymphoid cell responses. Mucosal Immunol 2020;

48. Yang W, Yu T, Huang X, Bilotta AJ, Xu L, Lu Y, Sun J, Pan F, Zhou J, Zhang W, et al. Intestinal microbiota-derived short-chain fatty acids regulation of immune cell IL-22 production and gut immunity. Nat Commun 2020; 11:4457.

49. Zenewicz LA, Yancopoulos GD, Valenzuela DM, Murphy AJ, Karow M, Flavell RA. Interleukin-22 but not interleukin-17 provides protection to hepatocytes during acute liver inflammation. Immunity 2007; 27:647–59.

50. Sabat R, Wolk K. Deciphering the role of interleukin-22 in metabolic alterations. Cell Biosci 2015; 5:68.

51. Hendrikx T, Duan Y, Wang Y, Oh J-H, Alexander LM, Huang W, Stärkel P, Ho SB, Gao B, Fiehn O, et al. Bacteria engineered to produce IL-22 in intestine induce expression of REG3G to reduce ethanol-induced liver disease in mice. Gut 2019; 68:1504–15.

52. Sánchez E, De Palma G, Capilla A, Nova E, Pozo T, Castillejo G, Varea V, Marcos A, Garrote JA, Polanco I, et al. Influence of environmental and genetic factors linked to celiac disease risk on infant gut colonization by Bacteroides species. Appl Environ Microbiol 2011; 77:5316–23.

53. Gómez Del Pulgar EM, Benítez-Páez A, Sanz Y. Safety Assessment of Bacteroides Uniformis CECT 7771, a Symbiont of the Gut Microbiota in Infants. Nutrients 2020; 12.

54. Juanola O, Piñero P, Gómez-Hurtado I, Caparrós E, García-Villalba R, Marín A, Zapater P, Tarín F, González-Navajas JM, Tomás-Barberán FA, et al. Regulatory T Cells Restrict Permeability to Bacterial Antigen Translocation and Preserve Short-Chain Fatty Acids in Experimental Cirrhosis. Hepatol Commun 2018; 2:1610–23.

55. Moratalla A, Gómez-Hurtado I, Moya-Pérez Á, Zapater P, Peiró G, González-Navajas JM, Gómez Del Pulgar EM, Such J, Sanz Y, Francés R. Bifidobacterium pseudocatenulatum CECT7765 promotes a TLR2-dependent anti-inflammatory response in intestinal lymphocytes from mice with cirrhosis. Eur J Nutr 2016; 55:197–206.

56. Storlien LH, Jenkins AB, Chisholm DJ, Pascoe WS, Khouri S, Kraegen EW. Influence of dietary fat composition on development of insulin resistance in rats. Relationship to muscle triglyceride and omega-3 fatty acids in muscle phospholipid. Diabetes 1991; 40:280–9.

57. Frayn KN, Maycock PF. Skeletal muscle triacylglycerol in the rat: methods for sampling and measurement, and studies of biological variability. J Lipid Res 1980; 21:139–44.

58. Liebisch G, Ecker J, Roth S, Schweizer S, Öttl V, Schött H-F, Yoon H, Haller D, Holler E, Burkhardt R, et al. Quantification of Fecal Short Chain Fatty Acids by Liquid Chromatography Tandem Mass Spectrometry-Investigation of Pre-Analytic Stability. Biomolecules 2019; 9.

59. Ecker J, Scherer M, Schmitz G, Liebisch G. A rapid GC-MS method for quantification of positional and geometric isomers of fatty acid methyl esters. J Chromatogr B Analyt Technol Biomed Life Sci 2012; 897:98–104.

60. Klindworth A, Pruesse E, Schweer T, Peplies J, Quast C, Horn M, Glöckner FO. Evaluation of general 16S ribosomal RNA gene PCR primers for classical and next-generation sequencing-based diversity studies. Nucleic Acids Res 2013; 41:e1.

61. Magoč T, Salzberg SL. FLASH: fast length adjustment of short reads to improve genome assemblies. Bioinformatics 2011; 27:2957–63.

62. Shen W, Le S, Li Y, Hu F. SeqKit: A Cross-Platform and Ultrafast Toolkit for FASTA/Q File Manipulation. PLoS ONE 2016; 11:e0163962.

63. Edgar RC, Haas BJ, Clemente JC, Quince C, Knight R. UCHIME improves sensitivity and speed of chimera detection. Bioinformatics 2011; 27:2194–200.

64. Quast C, Pruesse E, Yilmaz P, Gerken J, Schweer T, Yarza P, Peplies J, Glöckner FO. The SILVA ribosomal RNA gene database project: improved data processing and web-based tools. Nucleic Acids Res 2013; 41:D590-596.

65. Edgar RC. Search and clustering orders of magnitude faster than BLAST. Bioinformatics 2010; 26:2460–1.

66. Caporaso JG, Kuczynski J, Stombaugh J, Bittinger K, Bushman FD, Costello EK, Fierer N, Peña AG, Goodrich JK, Gordon JI, et al. QIIME allows analysis of high-throughput community sequencing data. Nat Methods 2010; 7:335–6.

67. Price MN, Dehal PS, Arkin AP. FastTree: computing large minimum evolution trees with profiles instead of a distance matrix. Mol Biol Evol 2009; 26:1641–50.

Supplemental figures

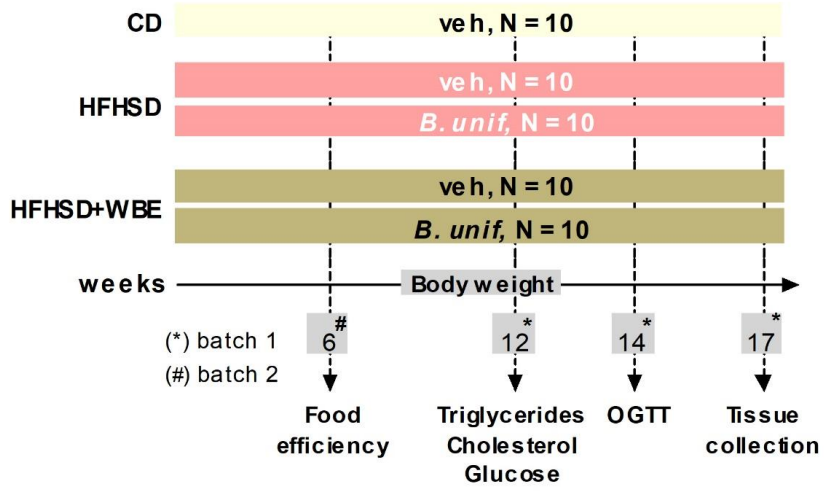

Figure S1. Schematic representation of the experimental procedure. Mice were fed either control diet (CD: 10% of energy from fat and without sucrose; N = 10), high-fat high-sugar diet (HFHSD: 45% of energy from fat and 35% from sucrose; N = 20) or HFHSD supplemented with 5% of wheat-bran extract (WBE) (HFHSD+WBE; N = 20) for 17 weeks. Both mice fed the HFHSD or HFHSD+WBE were subdivided into two experimental groups. One of these groups received an oral dose of vehicle (veh, N = 10) and the other an oral dose *B. uniformis* CECT 7771 ($5x10^7$ CFU per mouse, N = 10) daily. CD-fed mice received only vehicle (N = 10). Body weight was determined weekly. At week 12, glucose, triglycerides and cholesterol were determined in plasma and OGTT was conducted at week 14. Mice were sacrificed at week 17 for blood collection and isolation of tissues (small and large intestine, liver, epididymal WAT, and caecal content). Food efficiency was estimated at week 6 of HFHSD in another batch of animals. CD, control diet; *B. unif*, *Bacteroides uniformis* CECT 7771; HFHSD, high-fat high-sugar diet; OGTT, oral glucose tolerance; WBE, wheat bran extract.

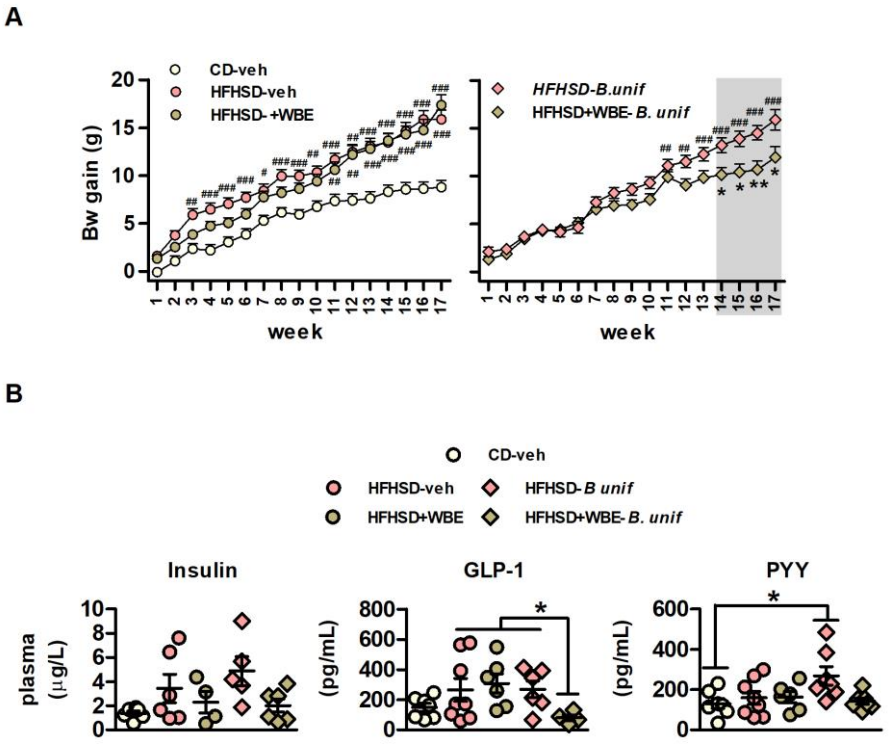

Figure S2 related to Figure 1. Effects *B. uniformis* CECT 7771 and WBE, separately or combined, on body weight evolution and key hormones controlling energy metabolism. Body weight evolution and plasma levels of insulin, GLP-1 and PYY of controls (CD-fed mice receiving vehicle, CD-veh) and HFHSD fed mice receiving vehicle, WBE, *B. uniformis*, or the combination of both: HFHSD-veh, HFHSD+WBE, HFHSD-*B. unif* or HFHSD+WBE-*B. unif*). (**A**) Body weight evolution from week 1 to 17 (two-way ANOVA HFHSD-fed groups; *B. unif* x WBE interaction P <0.05 at week 14 to 17; *post hoc* P <0.05. N = 10 for all groups. (**B**) Insulin, GLP-1 (Kruskal-Wallis test: HFHSD+WBE-*B. unif* vs HFHSD-veh, HFHSD-*B. unif* or HFHSD+WBE P <0.05) and PYY concentrations in plasma at week 17 (Kruskal-Wallis test: HFHSD+WBE-*B. unif* vs CD-veh P <0.05). Insulin: CD-veh, HFHSD-veh and HFHSD+WBE-*B. unif* N = 6; HFHSD+WBE N = 4 and HFHSD-*B. unif* N = 5. PYY: CD-veh, HFHSD-B. unif and HFHSD+WBE-B. unif N = 7; HFHSD-veh N =8 and HFHSD+WBE N = 6. GLP-1: CD-veh N = 7; HFHSD-veh N = 8; HFHSD+WBE and HFHSD-*B. unif* N = 6 and HFHSD+WBE-*B. unif* N = 4. Data were represented as the mean ± SEM. $^{\#}$P <0.05, $^{\#\#}$P <0.01, $^{\#\#\#}$P <0.001 vs control group. *P <0.05 indicates

differences within HFHSD-fed groups. *B. unif*, *Bacteroides uniformis* CECT 7771, CD, control diet; GLP-1, glucagon-like peptide 1; HFHSD, high-fat high-sugar diet; PYY, peptide YY; veh, vehicle and WBE, wheat bran extract.

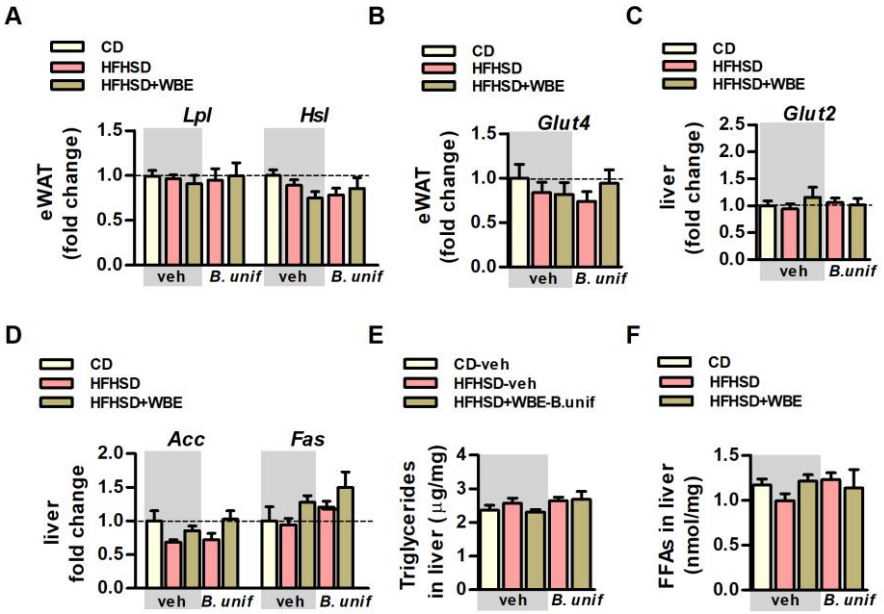

Figure S3. Related to Figure 2. Characterization of markers of lipid metabolism in fat and liver of controls (CD-fed mice receiving vehicle, CD-veh) and HFHSD-fed mice receiving vehicle, WBE, *B. uniformis* or the combination of both (WBE+*B. unif*): HFHSD-veh, HFHSD+WBE, HFHSD-*B. unif* or HFHSD+WBE-*B. unif*). (**A**) *Lpl* and *Hsl* gene expression in epididymal WAT at week 17. *LpL*: CD-veh, HFHSD-veh and HFHSD+WBE-*B.unif* N = 7; HFHSD+WBE N = 8 and HFHSD-*B.unif* N = 9. *Hsl*: CD-veh, HFHSD-veh and HFHSD+WBE-*B.unif* N = 7 and HFHSD+WBE and HFHSD-B.unif N = 8. (**B**) Gene expression of *Glut4* in epididymal WAT at week 17. *Glut4*: CD-veh and HFHSD-*B. unif* N = 6 and HFHSD-veh, HFHSD+WBE and HFHSD+WBE-*B. unif* N = 7. (**C**) Gene expression of *Glut2* in liver at week 17. *Gltu2*: CD-veh and HFHSD+WBE N = 6; HFHSD-veh N =6 and HFHSD-*B. unif* and HFHSD+WBE-*B. unif* N = 8. (**D**) *Acc* and *Fas* gene expression in liver at week 17. CD-veh, HFHSD-veh and HFHSD+WBE-B.unif N = 8; HFHSD+WBE N = 6 and HFHSD+WBE-B.unif N = 7. (**E**) Triglycerides levels in liver at week 17. CD-veh, HFHSD-veh and HFHSD+WBE-*B.unif* N = 10 and HFHSD+WBE and HFHSD-*B.unif* N = 9. (**F**) Free fatty acids (FFAs) levels in liver at week 17. CD-veh N =

8; HFHSD-veh and HFHSD-*B.unif* N = 9 and HFHSD+WBE and HFHSD-*B.unif* N = 7. Data were represented as the mean ± SEM. Parametric tests (one-way ANOVA to compare controls vs HFHSD-fed mice and two-way ANOVA restricted to HFHSD-fed mice) were conducted to analyse data of panels A and C while Kruskal-Wallis test was used to assessed data of panel B. *Acc*, acetyl-CoA carboxylase; *B. unif*, *B. uniformis* CECT 7771; eWAT, epididymal white adipose tissue; CD, control diet; *Fas*, fatty acid synthase; FFAs, free fatty acids; HFHSD, high-fat high-sugar diet; *Hsl*, hormone sensitive lipase; *Lpl*, lipoprotein lipase; veh, vehicle; WBE, wheat bran extract.

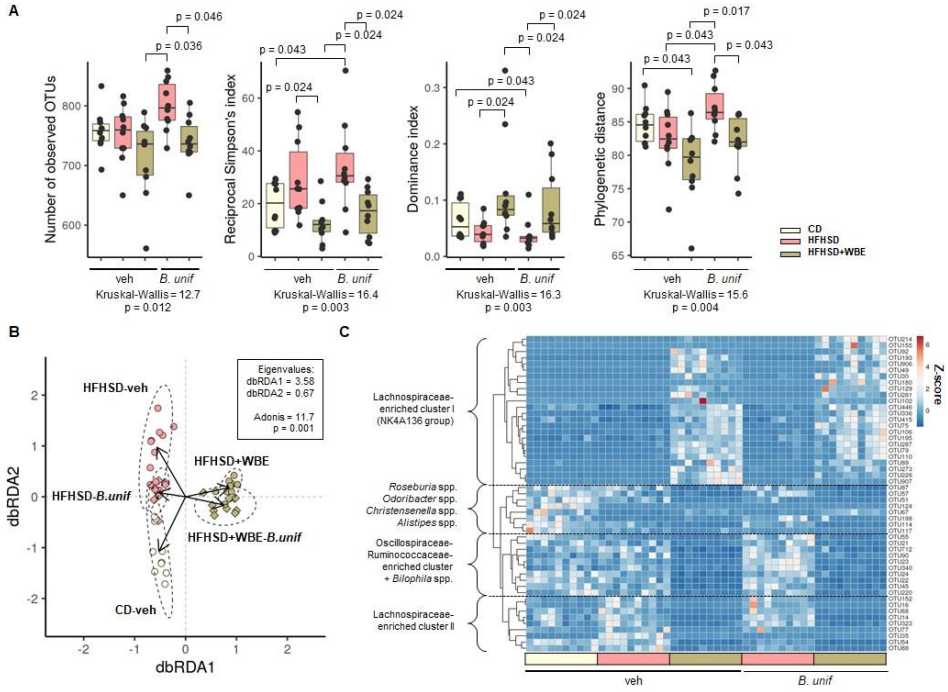

Figure S4. **Related to Figure 4. Effects of *B. uniformis* CECT 7771 and WBE, separately or in combination, on gut microbiota of control and diet-induced obese mice.** Microbiota analysis of the caecal content at week 17 of controls (CD-fed mice receiving vehicle, CD-veh) and HFHSD fed mice receiving vehicle, WBE, *B. uniformis*, or the combination of both: HFHSD-veh, HFHSD+WBE, HFHSD-*B. unif* or HFHSD+WBE-*B. unif*). (**A**) The alpha diversity, including study of the observed OTUs, Simpson's reciprocal index, dominance index, and phylogenetic distance descriptors, was assessed and compared among experimental groups. Alpha diversity data is presented in a boxplot and results of the statistical analysis are shown at the bottom of

boxplots, respectively. Pairwise differences between groups are stated at top by showing respective corrected p-values. (**B**) A beta diversity evaluation of the caecal microbial community structure is provided using distance-based redundancy analysis (dbRDA). The two gradients of dataset dispersion in ordination space with more strength (eigenvalues) of this constrained approach are shown in a scatter-plot. Dashed lines circumscribe the confidence interval (95%) for distribution of respective grouped samples. The eigen values, as well as the result of the adonis test, are depicted in the text box embedded. Arrows' heads point out the respective centroids of data dispersion. N = 10 for all groups. (**C**) Scaled read counts for top differentially abundant OTUs (Kruskal-Wallis chi-squared test ≥ 30, corrected P ≤ 0.001) across groups are shown as a heatmap. Clustering of OTUs was carried out by using "correlation" as distance metrics and "complete" as clustering method. The OTUs from major clusters were identified using SINA aligner and taxonomy is presented accordingly. Heat scale is based on Z-scores resulting from rarefied read counts per OTU (raw scaling). N = 10 for all groups. *B. unif*, *Bacteroides uniformis* CECT 7771; CD, control diet; HFHSD, high fat high sugar diet; veh, vehicle; WBE, wheat bran extract. N = 10 for all groups.

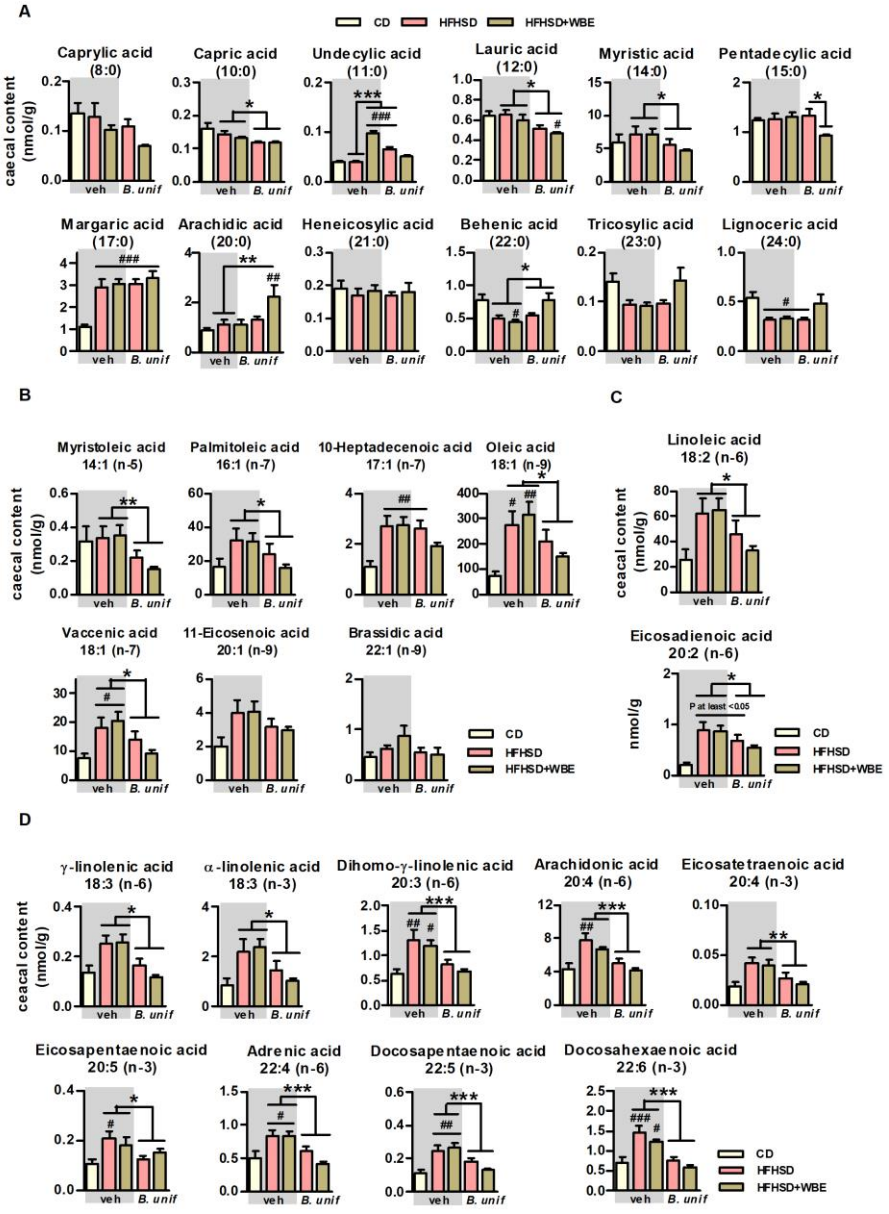

Figure S5. Related to Figure 4. Effects of *B. uniformis* CECT 7771 and WBE, separately or in combination, on caecal long chain fatty acids. (**A-D**) Saturated FAs, MUFAs, diunsaturated FAs and PUFAs concentrations (nmol/ g of dry weight of caecal content) in controls (CD-fed mice receiving vehicle, CD-veh) and HFHSD-fed mice receiving vehicle, WBE, *B. uniformis* or the combination of both (WBE+*B. unif*): HFHSD-veh, HFHSD+WBE, HFHSD-*B. unif*

or HFHSD+WBE-*B. unif*) at week 17. CD-veh N = 8; HFHSD-veh, HFHSD-B-unif, HFHSD+WBE-B. unif N = 10 and HFHSD+WBE N = 9**.** Data were represented as the mean ± SEM. Parametric tests (one-way ANOVA to compare controls vs HFHSD-fed mice and two-way ANOVA restricted to HFHSD-fed mice) were conducted to analyse all panels. $^{\#}P < 0.05$, $^{\#\#}P < 0.01$ and $^{\#\#\#}P < 0.01$ vs control group. *P <0.05, **P <0.01 and ***P <0.001 indicate differences within HFHSD-fed groups. CD, control diet; *B. unif*, *Bacteroides uniformis* CECT 7771; FAs, fatty acids; HFHSD, high-fat high-sugar diet; MUFAs, monounsaturated FAs; PUFAs, polyunsaturated FAs; veh, vehicle and WBE, wheat bran extract.

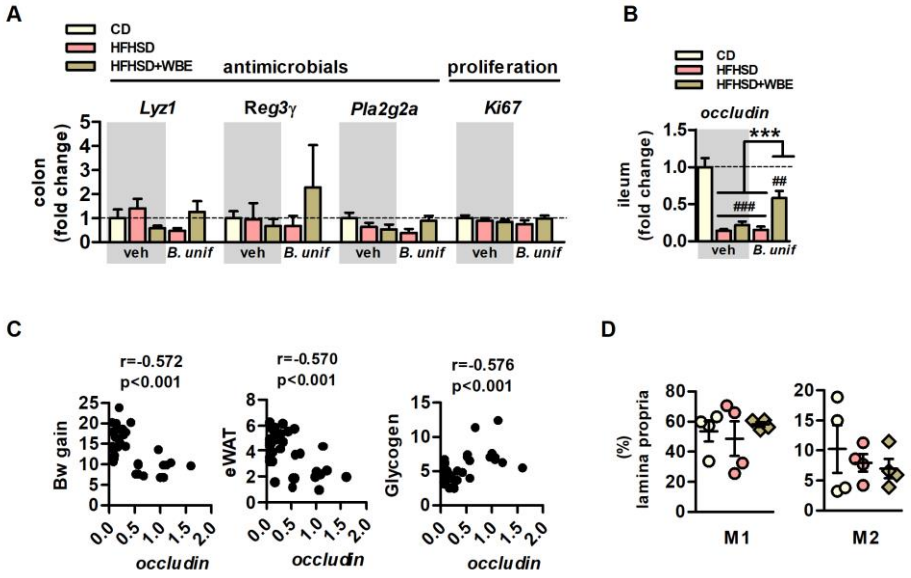

Figure S6. Related to Figure 5. Markers of: defence barrier in colon, intestinal integrity and type 1 and type 2 macrophages in small intestine. (**A**) Gene expression of *Lyz1*, R*eg3ϒ*, *Pla2g2a* and *Ki67* in colon of controls (CD-fed mice receiving vehicle, CD-veh) and HFHSD-fed mice receiving vehicle, WBE, *B. uniformis* or the combination of both: HFHSD-veh, HFHSD+WBE, HFHSD-*B. unif* or HFHSD+WBE-*B. unif*) at week 17. *Lyz1*: CD-veh, HFHSD+WBE, HFHSD-*B.unif* and HFHSD+WBE-*B.unif* N = 10 and HFHSD-veh N = 9. R*eg3ϒ*: CD-veh and HFHSD-*B.unif* N = 9; HFHSD-veh and HFHSD+WBE-*B.unif* N = 10 and HFHSD+WBE N = 8. *Pla2g2a*: CD-veh, HFHSD-veh and HFHSD+WBE-*B.unif* N = 10; HFHSD+WBE N =8 and HFHSD-*B.unif* N = 9. *Ki67*: CD-veh and HFHSD+WBE-*B.unif* N = 10 and HFHSD-veh, HFHSD+WBE and HFHSD-*B.unif* N = 8. (**B**) *Occludin* gene expression in ileum

of controls (mice fed CD and receiving vehicle, CD-veh N = 7) and HFHSD fed mice receiving or not WBE, *B. uniformis*, or the combination of both: HFHSD-veh, HFHSD+WBE, HFHSD-*B. unif*, or HFHSD+WBE-*B. unif*) (two-way ANOVA in HFHSD-fed groups: *B. unif* x WBE interaction P <0.01; *post-hoc* P <0.001 vs HFHSD-veh, HFHSD+WBE or HFHSD-*B. unif*) at week 17. CD-veh, HFHSD+WBE and HFHSD-*B. unif* N = 7; HFHSD-veh N =8 and HFHSD+WBE-*B. unif* N = 9. (**C**) Bravais-Pearson´s correlation between *occludin* expression in ileum and Bw gain, epididymal fat or hepatic glycogen depots at week 17. N = 38. (**D**) Type 1 and type 2 macrophages in lamina propria (percentage) at week 17 in controls (CD-fed mice receiving vehicle, CD-veh N = 7) and HFHSD fed mice receiving vehicle or the combination of *B. uniformis* and WBE. N = 4. Data were represented as the mean ± SEM. Parametric tests (one-way ANOVA to compare controls vs HFHSD-fed mice and two-way ANOVA restricted to HFHSD-fed mice) were used to analyse *Ki67*, *Tcf4* and occludin and Kruskal-Wallis test to analyse *Lyz1*, R*eg3ɣ* and *Pla2g2a*. *B. unif*, *B. uniformis* CECT 7771; CD, control diet; HFHSD, high-fat high-sugar diet; L*yz1*, lisozyme 1; M1, type 1 macrophages; M2, type 2 macrophages; *Pla2g2a*, phospholipase A2 group IIA; R*eg3ɣ*, regenerating islet-derived protein 3 gamma; veh, vehicle; WBE, wheat bran extract.

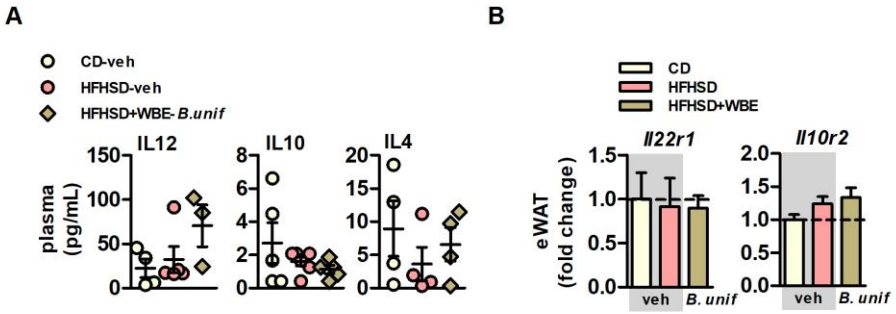

Figure S7. Related to Figure 6. Inflammation markers in plasma and fat. (**A**) IL12, IL10 and IL4 in plasma of controls (CD-fed mice receiving vehicle, CD-veh) and HFHSD-fed mice receiving vehicle or *B. uniformis* combined with WBE: HFHSD-veh or HFHSD+WBE-*B. unif*) at week 17. IL12: CD-veh N = 4; HFHSD-veh N = 5 and HFHSD+WBE-*B.unif* N = 3. IL10: N = 5 for all groups. IL4: N = 4 for all groups. (**B**) *Il22r1* and *Il10r2* expression in epididymal WAT at week 17. N = 8 for all groups. Data were represented as the mean ± SEM. IL10 and panel B were assessed by one-way ANOVA followed by *post hoc* Tuckey, while Kruskal was used to analyse data of panel *B. unif*, *Bacteroides uniformis* CECT 7771; eWAT,

epididymal white adipose tissue; CD, control diet; HFHSD, high-fat high-sugar diet; veh, vehicle; WBE, wheat bran extract.

Table S1. Dietary fatty acid composition.

Fatty acids (FAs)	D12450K [%]	D12451 [%]
C 12:0	0.01	0.05
C 14:0	0.04	0.29
C 16:0	0.69	5.33
C 18:0	0.31	2.92
C 20:0	0.02	0.07
C 16:1	0.05	0.62
C 18:1	1.3	9.42
C 18:2	1.43	3.46
C 18:3	0.15	0.37

Table S2. Gene names, abbreviations and primer sequences.

Gene name	Abbreviation	Sequence 5´- 3´	Supplier
Acetyl-CoA carboxylase	***Acc***	Forward: TAATGGGCTGCTTCTGTGACTC Reverse: CTCAATATCGCCATCAGTCTTG	Isogen Science
Carbohydrate response element-binding protein alpha	***ChREBPα***	Forward: CGACACTCACCCACC Reverse: TTGTTCAGCCGGATC	Isogen Science
Carnitine plamitoyltransferase 1a	***Cpt1a***	Forward: TTTGAATCGGCTCCTAATGG Reverse: CCCAAGTATCCACAGGGTCA	Isogen Science
Fatty acid synthase	***Fas***	Forward: GGAGGTGGTGATAGCCGGTAT Reverse: TGGGTAATCCATAGAGCCCAG	Isogen Science
Glucokinase	***Gck***	Forward: ATGTGAGGTCGGCATGATTGT Reverse: CCTTCCACCAGCTCCACATT	Isogen Science
Glucose transporter 2	***Glut2***	Forward: TTGTGCTGCTGGATAAATTC Reverse: AAATTCAGCAACCATGAACC	Sigma-Aldrich
Glucose transporter 4	***Glut4***	Forward: CAATGGTTGGGAAGGAAAAG Reverse: AATGAGTATTCTCATAGGAGGC	Sigma-Aldrich
Hormone sensitive lipase	***Hsl***	Forward: ATGCCACTCACCTCTGATCC Reverse: CTGTCCTGTCCTTCCCGTAG	Isogen Science
Interleukin 22	***Il22***	Forward: GACATAAACAGCAGGTCCAGTT Reverse: AGAAGGCTGAAGGAGACAGT	Isogen Science
Interleukin 10 receptor type 2	***Il10r2***	Forward: GGACGTCTCTTCCACAGCAC Reverse: CTGCTTGCTGCCTTCAGACT	Isogen Science
Interleukin 22 receptor type 1	***Il22r1***	Forward: GCTCGCTGCAGCACACTACCAT Reverse: TGAGTGTGGGGTGGACCAGCAT	Isogen Science
Ki67	***Ki67***	Forward: CAGACTTGCTCTGGCCTACC Reverse: GGTTGGCGTTTCTCCTCTTT	Isogen Science

Lipoprotein lipase	***Lpl***	Forward: TGAAAGCCGGAGAGACTCAG Reverse: AGTGTCAGCCAGACTTCTTCAG	Isogen Science
Lisozyme 1	***Lyz1***	Forward: GCCAAGGTCTACAATCGTTGTGAGTT Reverse: CAGTCAGCCAGCTTGACACCACG	Isogen Science
Occludin	***occludin***	Forward: ATGTCCGGCCGATGCTCTC Reverse: TTTGGCTGCTCTTGGGTCTGTAT	Isogen Science
Phospholipase A2 group IIA	***Pla2g2a***	Forward: AAGGATCCCCCAAGGATGCCAC Reverse: CAGCCGTTTCTGACAGTTCTGG	Isogen Science
Regenerating islet-derived protein 3 gamma	***Reg3γ***	Forward: TTCCTGTCCTCCATGATCAAA Reverse: CATCCACCTCTGTTGGGTTC	Isogen Science
Ribosomal protein L19	***Rpl19***	Forward: CCTTGTCTGCCTTCAGCTTGT Reverse: GAAGGTCAAAGGGAATGTGTTCA	Isogen Science
Uncoupling protein 1	***Ucp-1***	Forward: ACTGCCACACCTCCAGTCATT Reverse: CTTTGCCTCACTCAGGATTGG	Isogen Science

CAPÍTULO 2

Capítulo 2

Evaluación de cepas de *Holdemanella biformis* y *Phascolarctobacterium faecium* como nuevos potenciales probióticos para combatir la obesidad y sus comorbilidades.

- *Holdemanella biformis* improves glucose tolerance in obese mice via GLP-1 signaling.

- *Phascolarctobacterium faecium* confers resistance to diet-induced obesity trough recuction of food intake and activation of anti-inflammatory and defensive immune mechanisms in mice.

Holdemanella biformis improves glucose tolerance in obese mice via GLP-1 signaling

Marina Romaní-Pérez[1,*], Inmaculada López-Almela[1, *], Clara Bullich-Vilarrubias[1], Lola Rueda-Ruzafa[2], Eva M. Gómez Del Pulgar[1], Alfonso Benítez-Páez[1], Gerhard Liebischb[3], José Antonio Lamas[2], Yolanda Sanz[1]

(Under review in The FASEB J)

*Both authors contributed equally to the paper

[1]Microbial Ecology, Nutrition & Health Research Unit. Institute of Agrochemistry and Food Technology, National Research Council (IATA-CSIC), 46980 Valencia, Spain.

[2]Laboratory of Neuroscience, Biomedical Research Center (CINBIO), University of Vigo, 36310 Vigo, Spain.

[3]Institute of Clinical Chemistry and Laboratory Medicine, University of Regensburg, 93053 Regensburg, Germany.

Running title: *Holdemanella biformis* has glucoregulatory properties

Nonstandard abbreviations

*Acc***,** Acetyl-CoA carboxylase; AP, action potential; *ARα1b,* α 1b adrenergic receptor; CD, control diet; *Cldn3,* Claudin 3; *Cpt1a,* Carnitine plamitoyltransferase 1ª; DIO, diet-induced obesity; DPP-4, Dipeptidyl peptidase-4; *Fas,* Fatty acid synthase; FFA, free fatty acids; G6P, glucose 6 phosphate; *G6pase,* Glucose-6-phosphatase; *GcK,* Glucokinase; GLP-1, glucagon like peptide-1; *Glp-1r,* GLP-1 receptor; *Glut2,* Glucose transporter 2; *Glut4,* Glucose transporter 4; HFHSD, high fat high sugar diet; *Hsl,* Hormone sensitive lipase; *Ki67,* Proliferation marker Ki67; LCFA, long chain fatty acids; LC-MS/MS, Liquid chromatography–mass spectrometry; *Lpl,* Lipoprotein lipase; *Lyz1,* Lisozyme 1; *M_3R***,** Muscarinic acetylcholine receptor M3; MS (GC-MS), Gas chromatography–mass spectrometry; MUFAs, monounsaturated fatty acids; NG, nodose ganglion; *Ocln,* Occludin; OGTT, oral glucose tolerance test; *Pck1,* Phosphoenolpyruvate carboxykinase 1; *Pla2g2a,* Phospholipase A2 group IIA; PUFAs, polyunsaturated fatty acids; PYY, peptide tyrosine tyrosine; *Pyy***,** Peptide tyrosine tyrosin**e**; *Reg3g***,** Regenerating islet-derived protein 3 gamma; RMP, resting membrane potential; *RpL19,* Ribosomal protein 19; SCFAs, short chain fatty acids; T2D, type 2 diabetes; *Tfc4,* Transcription factor 4; WAT, white adipose tissue

Abstract

Impaired glucose homeostasis in obesity is mitigated by enhancing the glucoregulatory actions of glucagon-like peptide 1 (GLP-1), and thus strategies that improve GLP-1 sensitivity and secretion have therapeutic potential for the treatment of type 2 diabetes. This study shows that *Holdemanella biformis*, isolated from the feces of a metabolically healthy volunteer, ameliorates hyperglycemia, improves oral glucose tolerance and restores gluconeogenesis and insulin signaling in the liver of obese mice. These effects appear to be mediated through the ability of *H. biformis* to restore GLP-1 levels, enhancing GLP-1 neural signaling in the ileum and GLP-1 sensitivity of vagal sensory neurons, and to modify the cecal abundance of monounsaturated fatty acids and the bacterial species associated with metabolic health. Our findings overall suggest the potential use of *H. biformis* in the management of type 2 diabetes in obesity through direct and indirect mechanisms that optimize the sensitivity and function of the GLP-1 system

Keywords

Obesity, type 2 diabetes, glucagon-like peptide 1, gut microbiota, *Holdemanella biformis*, vagal afferent neurons

Introduction

The increasing worldwide prevalence of obesity and its associated disorders are a major global health challenge. Growing evidence supports a role for the gut microbiota in insulin resistance and in the onset of type 2 diabetes (T2D) in obesity. For example, human observational studies have shown that specific changes in the structure and/or function of gut microbiota (dysbiosis) correlate with impaired metabolic health [1,2]. Additionally, transplantation of gut microbiota from twins discordant for obesity to mice replicates the donor metabolic phenotype, demonstrating its causality in metabolic diseases [3]. Western diets (high in fats and simple sugars) can trigger gut microbiota dysbiosis [4, 5], which might disturb the interactions between microbiota-derived metabolites and/or subcellular bacterial components and the immune, endocrine and/or neural pathways that control host metabolism [6,7]. Indeed, it has been shown that Western diet-associated microbiota has a negative impact on intestinal immunity [8,9] and impairs the functionality of gut-derived hormones such as glucagon-like peptide-1 (GLP-1) [10,11], ultimately affecting energy homeostasis. This evidence also supports the notion that gut microbiota can be manipulated to restore the misconfigured signaling pathways between the gut and distant organs and systems and, thus, beneficially influence metabolic phenotypes.

Given the known benefits of GLP-1, including its insulinotropic effects in the pancreas and improving peripheral insulin sensitivity, several GLP-1-based therapies have been developed to counteract the development of obesity-induced glucose intolerance [12]. GLP-1 and its mimetics modulate insulin and glucagon secretion in distal β and α pancreatic cells, respectively, via endocrine routes, and can stimulate intestinal vagal afferents in a paracrine manner, thereby indirectly controlling glucose tolerance through central nervous system-mediated metabolic circuits [13,14]. By-products of microbiota metabolism or bacterial structural components might affect the function of GLP-1-secreting enteroendocrine L cells [15–17], and thus influence both endocrine- and neuroparacrine-mediated GLP-1 actions. Indeed, a recent study suggests that the commensal gut microbiota is necessary to adequately maintain the sensitivity of GLP-1-mediated paracrine signaling through the activation of vagal afferent fibers in the intestine [10]. Accordingly, there is growing interest in the development of microbiota-based therapies to potentiate the activity of antidiabetic drugs targeting GLP-1 signaling [18]. In this line, several studies have attempted to identify specific gut bacteria of lean subjects that might contribute to restore the metabolic signaling that often goes awry in obesity [19–21]. Some of the bacteria investigated so far, such as Akkermansia muciniphila or Bacteroides spp., have demonstrated beneficial effects on glucose homeostasis in preclinical studies of obesity [22–24]. Mechanistic studies have established that

these effects can be partly attributed to the ability of the bacteria to reduce intestinal inflammation and protect against the gut barrier disruption associated with obesity [22,24,25]. Nonetheless, the contribution of intestinal bacteria to regulate the neuroendocrine mechanisms involved in obesity remains poorly understood.

Holdemanella biformis, previously misclassified as *Eubacterium biformis*, is a human gut bacterium [26] that, through the release of short chain fatty acids (SCFAs) and the long chain fatty acid (LCFAs) 3-hydroxyoctadecaenoic is reported to induce anti- tumourigenesis and anti-inflammatory effects [27, 28]. In addition, this bacterial species strain might potentially modulate the enteroendocrine cells since SCFAs as well as certain LCFAs act as a GLP-1 secretagogues [29,30]. Here, we postulate that the intestinal bacterium *Holdemanella biformis*, through the modulation of immune and/or neuroendocrine routes of communications with the host, has a beneficial impact on obesity. To test this hypothesis, we used a diet-induced obese (DIO) mouse model to explore (1) the effects of a strain of *H. biformis*, isolated from a metabolically healthy human subject, on energy homeostasis; (2) whether the benefits on glucose metabolism are mediated through immune-regulatory mechanisms or by stimulating the secretion of gastrointestinal hormones (PYY and GLP-1) and/or signaling via endocrine or paracrine routes through vagal afferent neurons ; and (3) whether the metabolic effects are related to gut microbiota changes, analyzed by 16S rRNA gene sequencing and fecal metabolomics using liquid chromatography–tandem mass spectrometry (LC-MS/MS) and gas chromatography–MS (GC-MS).

Results

Holdemanella biformis improves glucose homeostasis and restores the plasma levels of PYY and GLP-1 in diet-induced obese mice independent of obesity

We tested whether or not *H. biformis* DSM 3989, isolated from a metabolically healthy human subject, was capable of improving metabolic health in a rodent model of diet-induced obesity (DIO) receiving or not a daily oral dose of the bacteria for 13 weeks.

Compared with mice fed a control diet (CD), both body weight gain throughout the 13-week experimental period (**Figure 1A**) and end of study plasma cholesterol (**Figure 1B**) levels were markedly increased in untreated and *H. biformis*-treated mice on a high-fat/high-sugar diet (HFHSD) to induce DIO, whereas triglycerides levels and caloric intake were unaffected (**Figure 1C** and **1D**, respectively). Basal glycemia was increased after 10 weeks of HFHSD (**Figure 1E**) Additionally, untreated DIO mice showed impaired oral glucose tolerance as revealed by higher blood glucose levels at 15, 30 and 60 minutes after an oral glucose challenge and a significant increase of the area under the curve (AUC) of the OGTT (**Figure 1F**). DIO mice administered *H. biformis* showed similar basal glycemia to CD mice but improved glucose clearance in response to an oral glucose load, as revealed by a partial restoration of glucose clearance over time and a reduction of the AUC compared with untreated DIO mice (**Figure 1F**), independent of obesity.

Immune-related markers in the lamina propria of the small intestine, such as type 1 (M1), type 2 macrophages (M2), the M1/M2 ratio or eosinophils remained unaffected after 13 weeks of HFHSD-feeding (**Figure S1A-D**). The levels of cytotoxic T cells in the lamina propria and in the blood were increased in untreated DIO mice but *H. biformis* administration to DIO did not seem to reverse this increase (**Figure S1E and S1F**).

The increased body weight and the impaired glucose homeostasis in untreated DIO mice was accompanied by higher levels of insulin in plasma compared with CD controls (**Figure 1G**). Whereas glucagon levels remained unchanged in untreated DIO mice (**Figure 1H**), the levels of the gastrointestinal hormones PYY and GLP-1 were reduced (**Figure 1I** and **1J**). Of note, 13 weeks of *H. biformis* administration under an obesogenic diet failed to normalize the HFHSD-induced hyperinsulinemia (**Figure 1G**) or the level of glucagon in

plasma (**Figure 1H**), but increased both PYY and GLP-1 levels to CD values (**Figure 1I** and **1J**). Thus, excluding the weight loss confounding effects and immune-associated mechanisms, these data indicate that *H. biformis* improves systemic glucose homeostasis in obesity and that restoration of PYY and GLP-1 levels might contribute to the metabolic benefits of *H. biformis.*

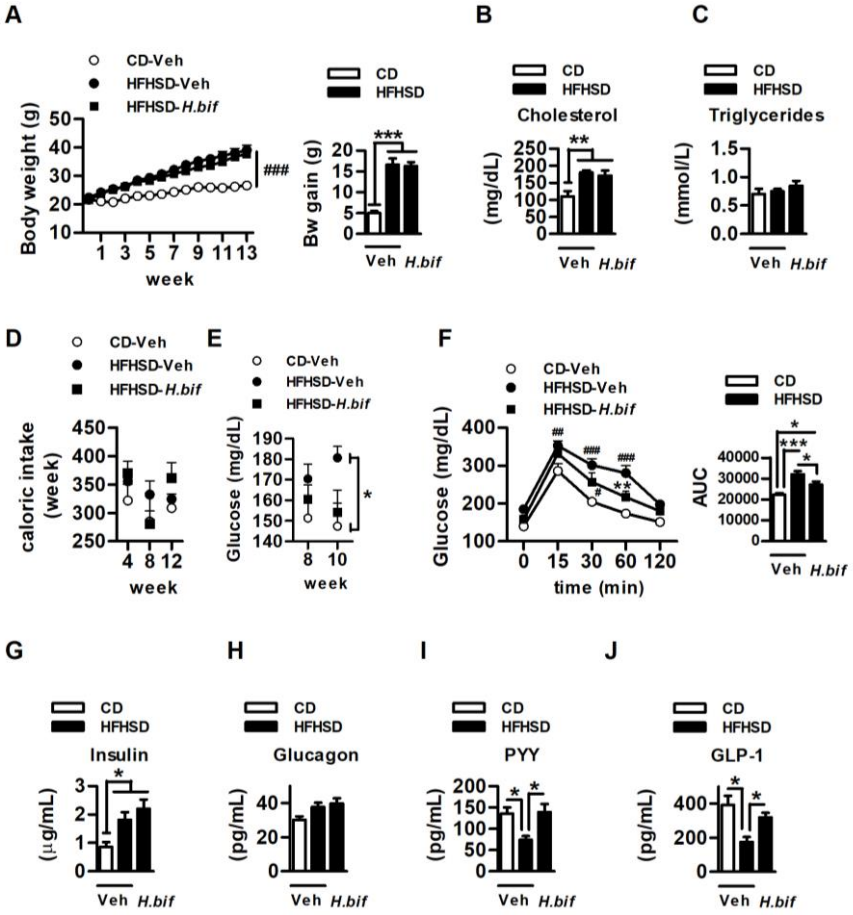

Figure 1. *Holdemanella biformis* improves glucose homeostasis and restores the plasma levels of PYY and GLP-1 in diet-induced obese mice independent of body weight. (**A-J**) Mice were fed CD or HFHSD for 13 weeks. *H. biformis* or its vehicle (10% skimmed milk) was daily administered by oral gavage. (**A**) Body weight evolution over time and body weight gain at the end of the tudy (n=9-10). (**B**) Cholesterol measured in plasma at the end of the study (n=9-10). (**C**) Triglycerides measured in plasma at the end of the study (n=9-10). (**D**) Caloric intake of collectively housed mice (4-5 mice per cage) measured weekly (n=2 cages). (**E**) Glucose levels in plasma at week 8 and 10 of the study. (**F**) Blood glucose levels after 0, 15, 30, 60 and 120 min of an oral

load of glucose (2 g/kg) to 4 h-fasted mice (OGTT) and area under the curve (AUC) (at week 10 of intervention, n=9). (**G-J**) Plasma levels of insulin (G, n=9-10), glucagon (H, n=9-10), PYY (I, n=8-9) and GLP-1 (J, n=5-6) at the end of the study. Data represent the mean ± SEM. Significant differences were assessed by two-way ANOVA followed by Bonferroni *post hoc* test (body weight and OGTT) or one-way ANOVA followed by Tukey *post hoc* test. There were insufficient data in (D) to conduct the statistical analysis. $^{\#}p<0.05$ and $^{\#\#\#}p<0.001$ vs controls; *p<0.05, **p<0.01 and ***p<0.001.

Holdemanella biformis **improves insulin sensitivity and gluconeogenesis in the liver of diet-induced obese mice**

Our findings suggest that *H. biformis* mitigates the onset of HFHSD-induced diabetes rather than obesity *per se*. We thus explored the metabolic pathways mediating glucose homeostasis in adipose tissue and liver. The observed hyperinsulinemia in DIO mice was accompanied by a decrease in the expression of glucose transporter 4 (*Glut4*) in epididymal white adipose tissue (WAT) in both untreated and *H. biformis*-treated mice as compared with CD mice (**Figure S2A**), suggesting disrupted insulin-dependent glucose uptake in WAT. Likewise, the expression levels of acetyl-CoA carboxylase (*Acc*) and fatty acid synthase (*Fas*) were lower in DIO mice, irrespective of *H. biformis* administration, than in CD mice (**Figure S2A**), suggesting a decrease in "de novo" lipogenesis, an insulin-stimulated pathway for glucose utilization. Since visceral adipose tissue seemed not be involved in the antihyperglycemic effect of *H. biformis*, we studied glucose metabolism in the liver, a critical organ for the maintenance of normal blood glucose. The evident hyperglycemia induced by HFHSD-feeding seemed to enhance hepatic glucose uptake through Glut2-mediated facilitated glucose diffusion, as suggested by the increased gene expression of this transporter in liver (**Figure 2A**). Likewise, *Glut2* expression remained elevated after *H. biformis* administration. *H. biformis* administration restored the expression of the insulin-dependent glucose transporter *Glut4* in the liver, which was reduced by HFHSD-feeding (**Figure 2A**). We then investigated whether the *H. biformis*-associated improvement in hyperglycemia in DIO mice impacted on hepatic insulin signaling, and thus on the glucose metabolic pathways under its control (i.e., *de novo* lipogenesis, glycogen stores and gluconeogenesis). Analysis of basal insulin signaling in liver revealed that DIO mice had a significantly lower level of AKT phosphorylation than CD mice, and this was restored by *H. biformis* administration (**Figure 2B**). In line with a deficient insulin cascade, untreated DIO mice showed reduced *Acc* and *Fas* expression in liver (**Figure S2B**) although glycogen levels were normal (**Figure S2C**). The restoration of liver AKT phosphorylation by *H. biformis* was not

accompanied by increase in lipogenic gene expression or glycogen content (**Figure S2B** and **S2C**, respectively).

Further gene expression analysis in liver showed that the expression of glucokinase (*Gck*), which provides glucose-6-phosphate (G6P) for glycolysis or glycogenogenesis, and phosphoenolpyruvate carboxykinase 1 (*Pck1*) (**Figure S2D**) and glucose-6-phosphatase (*G6Pase*) (**Figure 2C**), rate-limiting enzymes of gluconeogenesis, were unaffected by HFHSD. By contrast, the administration of *H. biformis* in DIO mice led to a decrease in liver *G6pase* levels (**Figure 2C**) but *Gck* and *Pck1* were unaffected (**Figure S2D**). Despite the unaffected *G6pase* gene expression, DIO enhanced hepatic G6Pase activity, which was normalized by *H. biformis* (**Figure 2D**). Also, lipoprotein lipase (*Lpl*) expression was lower in untreated and *H. biformis*-treated DIO mice than in CD mice, whereas hormone sensitive lipase (*Hsl*) remained unchanged (**Figure S2E**). HFHSD-feeding increased expression of carnitine plamitoyltransferase 1a (*Cpt1a*), an enzyme that initiates the mitochondrial oxidation of long chain fatty acids, and, again, this was normalized in *H. biformis*-administered mice (**Figure 2E**). Hepatic levels of acetyl-CoA, a byproduct of fatty acid oxidation which promotes gluconeogenesis [48], were lower in *H. biformis*-treated DIO mice than in untreated DIO mice or controls (**Figure 2F**). Variations in hepatic *Cpt1a* expression did not influence on triglycerides levels in liver since no differences were observed between untreated and *H. biformis*-treated DIO mice (**Figure S2F**), although free fatty acid (FFA) levels were increased in the latter (**Figure S2G**). Overall, our data support the notion that H. biformis reduces gluconeogenesis in the liver through the improvement of insulin sensitivity or by reducing acetyl-CoA levels, which might contribute to improving whole-body glucose excursion.

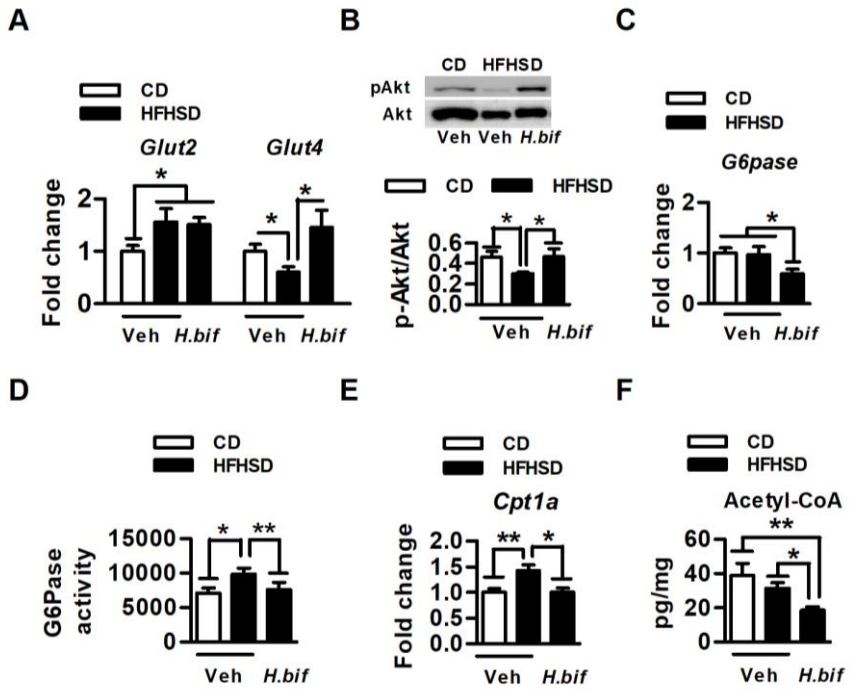

Figure 2. *Holdemanella biformis* normalizes insulin sensitivity and gluconeogenesis in the liver of diet-induced obese mice. (**A-F**) Analysis of energy-related metabolic circuits in liver of control (CD-fed mice receiving vehicle) and DIO mice (HFHSD-fed mice receiving either vehicle or *H. biformis*) at the end of the study. (**A**) mRNA levels of *Glut2* and *Glut4* (n=7-8). (**B**) Representative western blot and p-Akt quantification relative to total Akt (n=8-10). (**C**) mRNA levels of *G6pase* (n=7-8). (**D**) G6Pase activity (nmol/min/g) (n=9-10). (**E**) mRNA levels of *Cpt1a* (n=7-8). (**F**) Acetyl-CoA concentration (n=9-10). Value were represented as the mean ± SEM. Statistical significance was assessed by one-way ANOVA followed by Tukey *post hoc* test. *p<0.05 and **p<0.01. (See also Figure S2)

Holdemanella biformis enhances pyy and proglucagon expression in the colon and monounsaturated fatty acid abundance in the cecum of diet-induced obese mice

The mRNA levels of pyy and proglucagon, the precursor of GLP-1, were increased by H. biformis administration in the colon but not in the ileum of DIO mice (**Figure 3A and 3B**), pointing to a major contribution of colonic L cells in the elevated circulating levels of PYY and GLP-1 (**Figure 1I and 1J**). No

significant changes in the expression of these genes in the colon or ileum were observed as a consequence of HFHSD-feeding (**Figure 3A and 3B**).

Examination of cecal short chain fatty acids (SCFAs), GLP-1- and PYY-stimulating metabolites, in HFHSD-fed mice revealed an increase in the levels of acetate and isobutyrate but a decrease in the levels of propionate (**Figure 3C**), despite the reduced levels of PYY and GLP-1 in the plasma of these mice. Acetate and isobutyrate levels were normalized by *H. biformis* administration, but this was significant only for acetate, and propionate levels were lower than in untreated DIO mice (**Figure 3C**). The colonic expression of the SCFA receptor gene *Gpr41*, but not *Grp43*, mirrored the changes in acetate levels, with enhanced expression in untreated DIO mice compared with CD mice and normalized levels in *H. biformis*-treated mice (**Figure 3D**).

The abundance of cecal saturated long chain fatty acids (LCFAs) longer than C12 (**Figure 3E**) and total monounsaturated and polyunsaturated fatty acids (MUFAs and PUFAs, respectively) was significantly higher in untreated DIO mice than in CD mice (**Figure 3F**), and the administration of *H. biformis* enhanced the abundance of MUFAs (**Figure 3F**), particularly oleic acid [(FA 18:1 (n-9)] (**Figure S3B**). Likewise, administration of *H. biformis* increased the abundance of other PUFAs over CD and untreated DIO mice, especially α-linolenic acid [(FA 18:3 (n-3)] (**Figure S2D**). Only total MUFAs in the cecum of *H. biformis*-treated mice showed a positive correlation with circulating GLP-1, but not PYY (**Figure 3G**), suggesting that *H. biformis*-associated MUFAs enhancement favors GLP-1 secretion in mice receiving the bacterium. Further exploration of potential intestinal mediators of the *H. biformis*-related benefits on glucose homeostasis was restricted to GLP-1 because of the primary role of this peptide in glucose metabolism and, accordingly, its therapeutic potential to treat T2D.

H. biformis administration failed to modulate *proglucagon* expression and GLP-1 secretory capacity in a human L cell line (HuTu-80) *in vitro* (**Figure S4**), suggesting that restoration of the circulating levels of GLP-1 under HFHSD was not due to a direct effect of *H. biformis* on L cells *per se*. Nonetheless, the possibility that metabolites directly or indirectly produced by *H. biformis* could influence GLP-1 secretion cannot be disregarded.

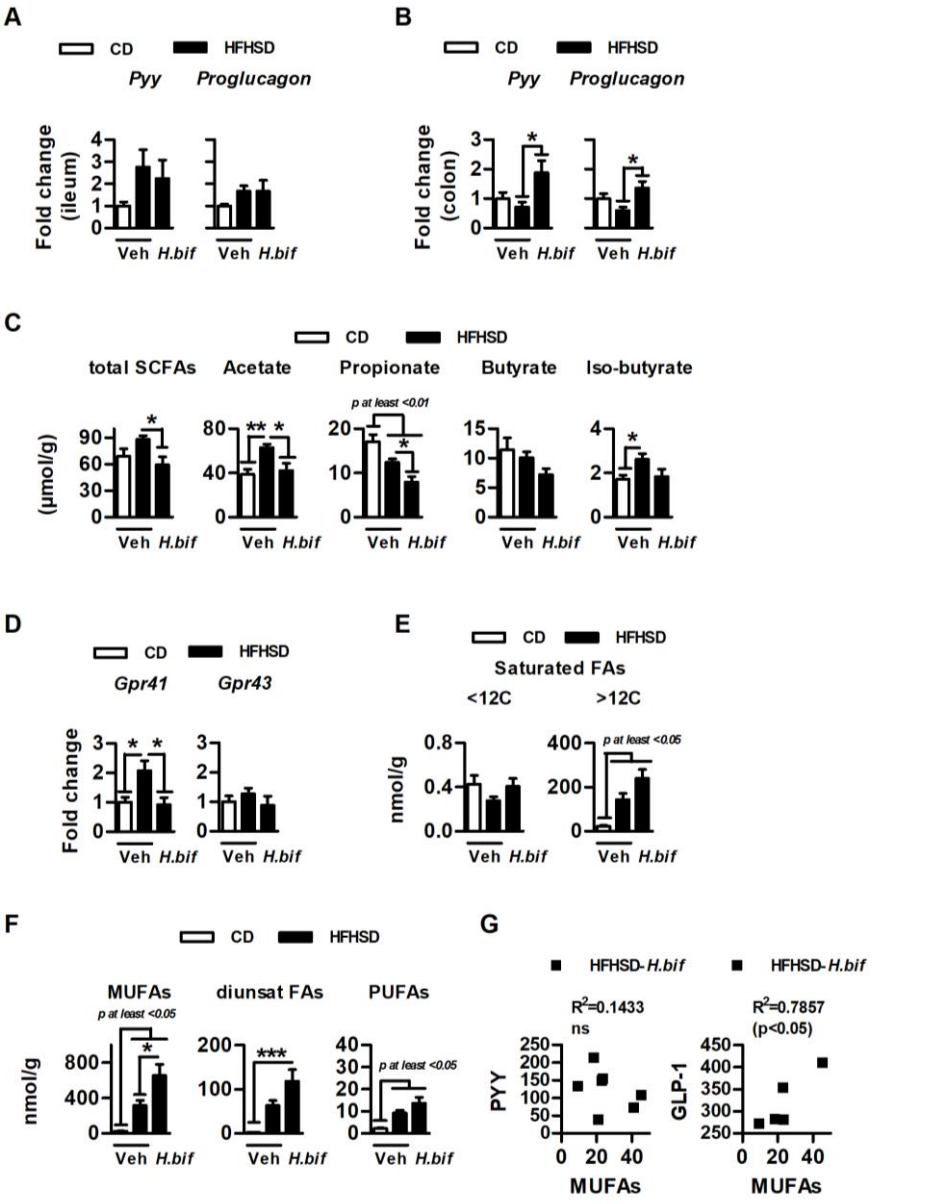

Figure 3. *Holdemanella biformis* enhances pyy and proglucagon expression in the colon and monounsaturated fatty acids concentration in the cecum of diet-induced obese mice. (**A-G**) Mice were fed CD or HFHSD for 14 weeks. *H. biformis* or its vehicle (10% skimmed milk) was daily administered by oral gavage. The following parameters were analyzed: (**A**) mRNA levels of of *proglucagon* and *pyy* in ileum (n=8-10). (**B**) mRNA levels of

of *proglucagon* and *pyy* in colon (n=8). (**C**) Total SCFAs, acetate, propionate, butyrate and isobutyrate concentration (µmol/g of dry weight of cecal content; n=9). (**D**) mRNA levels of *Gpr41* and *Gpr43* in colon (n=8). (**E**) Saturated FAs with less or more than 12C (nmol/g of dry weight of cecal content; n=9). (**F**) Total MUFAs, diunsaturated FAs and PUFAs (nmol/g of dry weight of cecal content; n=9). (**G**) Correlation between plasma levels in *H. biformis*-treated mice of PYY (n=8-9) or GLP-1 (pg/mL) and MUFAs (nmol/g of dry weight of cecal content). Data represent the mean ± SEM. Statistical significance was assessed by one-way ANOVA followed by Tukey post hoc test. *p<0.05. (See also Figure S3 and S4)

Holdemanella biformis enhances GLP-1 signaling in the distal small intestine and GLP-1 responsiveness in vagal afferent neurons

In addition to serving as an endocrine signal, GLP-1 might act on gut afferent neurons in a paracrine manner to transmit intestinal sensory information to the brain. Both endocrine- and neural afferent-mediated central mechanisms ultimately control whole-body energy homeostasis through efferent sympathetic and parasympathetic outflows. We thus surveyed the expression of the GLP-1 receptor (*Glp-1r*), mainly found in afferent endings, and *peripherin*, a peripheral nervous system marker, in ileum and colon samples. *Glp-1r* and *peripherin* expression in the ileum of untreated DIO mice was similar to that of CD mice, whereas the expression of both genes was increased in *H. biformis*-administered mice (**Figure 4A**). Also, *Glp-1r* and *peripherin* expression positively correlated in CD and *H. biformis*-treated DIO mice, but not in in untreated DIO mice (**Figure 4B**). In contrast to our observations in the ileum, HFHSD feeding increased both Glp-1r and peripherin expression in the colon, but the increased expression was normalized by *H. biformis* administration (**Figure 4C**). Additionally, the expression of both Glp-1r and peripherin positively correlated in all groups (**Figure 4D**), suggesting that GLP-1 signaling in colon is mainly mediated through neural endings.

Our findings suggest that *H. biformis* might influence both endocrine and neural GLP-1-mediated pathways. We thus investigated the upstream brain structures potentially mediating the effect of *H. biformis* on glucose homeostasis, finding no major changes in the expression of *Glp-1r* in the nucleus of the solitary tract (NTS) or the hypothalamus (**Figure S5A**), and also no changes in the expression of neuropeptides in the hypothalamus (**Figure S5B**). Given that *H. biformis* administration did not seem to impact on the transcription of signals involved in the central regulation of glucose homeostasis, we further explored its potential neuromodulatory properties on

GLP-1-sensitive neurons involved in the gut-to-brain sensory transmission, to question whether this it has the capacity to functionally modulate the central control of meal-related glycemic excursion. We tested this in nodose ganglion (NG) neurons (cell bodies of the visceral afferents) to discriminate the effects of *H. biformis* on the extrinsic intestinal nervous system (vagus nerve) from those induced on the intrinsic nervous system (enteric nervous system).

Despite the lack of action on GLP-1 secretion, *H. biformis* exhibited neuroactive properties on GLP-1-responsive primary cultures of NG neurons, as indicated by the increased neural activity measured as enhanced intracellular Ca2+ levels in Fluo4-loaded cells in response to the bacterium (**Figure 4E**), and the depolarization of resting membrane potential (RMP) (5.69 ± 1.7 mV) in current-clamp recordings, similar to that triggered by GLP-1 (4.30 ± 0.4mV) (**Figure 4F**). Additionally, prestimulation of NG neurons with *H. biformis* had an additive effect on GLP-1-induced depolarization of the RMP (7.11 ± 0.9mV) (**Figure 4F**). GLP-1, but not *H. biformis*, enhanced action potential (AP) firing in response to current pulses in NG neurons prestimulated or not with *H. biformis* (**Figure 4G**). When compared with GLP-1-stimulated cells, no major changes were observed in the GLP-1-related AP firing pattern in *H. biformis* prestimulated neurons, although there was a tendency for an increased number of APs in response to 175 pA (p=0.09, **Figure 4H**). Likewise, no major changes were observed in the gene expression of receptors involved in the sympathetic or parasympathetic-mediated regulation of gluconeogenesis in liver, alpha 1b adrenergic (*ARα1b*) and M3 muscarinic acetylcholine receptor (M_3R), respectively (**Figure S5C**), likely excluding the involvement of these receptors in the *H. biformis*-mediated effects *in vivo*. Altogether, our findings suggest that *H. biformis* administration enhances GLP-1-mediated neural signaling in the small intestine of DIO mice. Also, we demonstrate *in vitro* that *H. biformis* stimulates sensory neurons involved in gut-to-brain nutrient signal transmission, which might enhance their sensitivity to GLP-1.

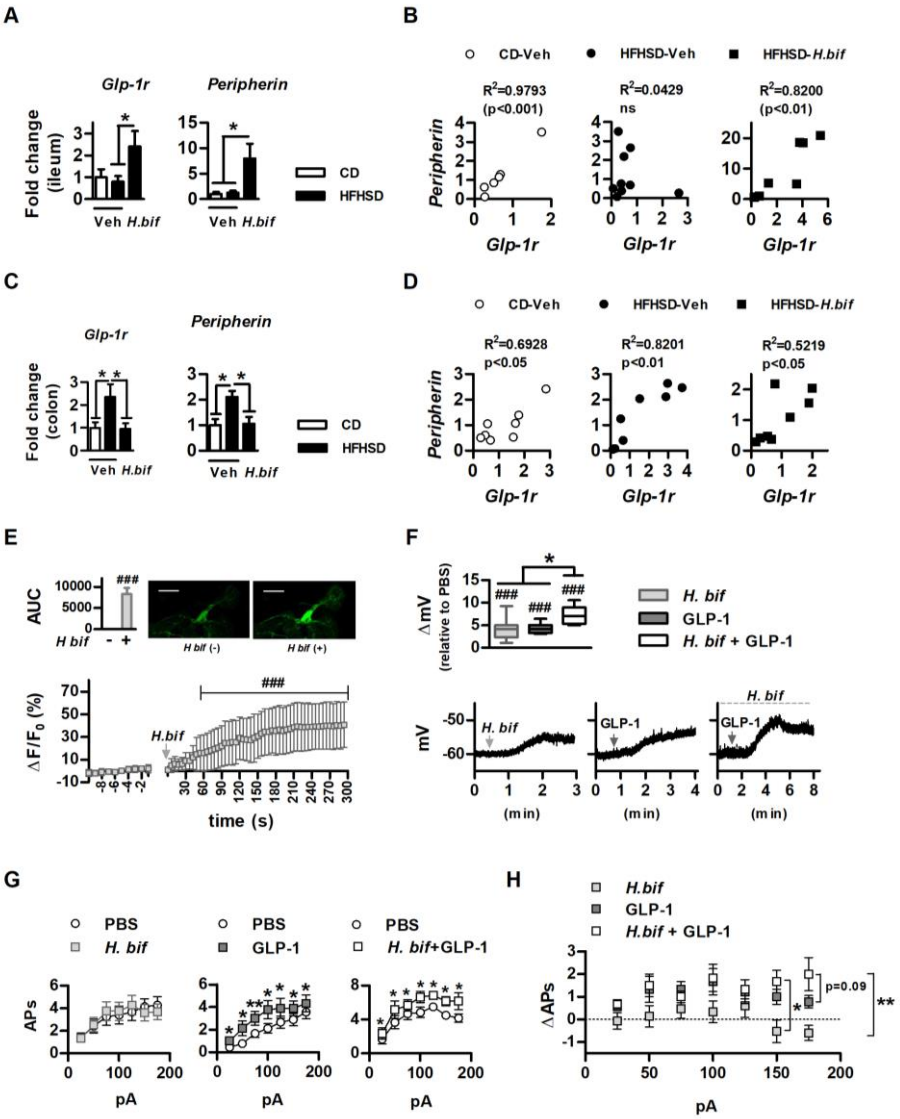

Figure 4. *Holdemanella biformis* promotes GLP-1 signaling in distal small intestine and GLP-1 responsiveness in vagal afferent neurons. (**A-D**) Analysis of markers of GLP-1-mediated signaling in ileum and colon of control (CD-fed mice receiving vehicle) and DIO mice (HFHSD-fed mice receiving either vehicle or *H. biformis*) at the end of the study. (**A**) mRNA levels of *Glp-1r* and *peripherin* in ileum (n=8-10). (**B**) Correlation between *Glp-1r* and *peripherin* in ileum (n=8-10). (**C**) mRNA levels of of *Glp-1r* and *peripherin* in colon (n=8). (**D**) Correlation between *Glp-1r* and *peripherin* in colon (n=8). (**E**) Relative fluorescence intensity ($\Delta F/F_0$) of Fluo-4-preloaded nodose ganglion cells in

response to *H. biformis* (n=10 cells). (**F-H**) Perforated whole-cell patch-clamp recordings in nodose ganglion neurons. (**F**) RMP changes in nodose ganglion neurons after stimulation with *H. biformis* (n=20 cells), GLP-1 (n=8 cells) or with GLP-1 in *H. biformis*-prestimulated cells (n=5 cells) relative to their respective RMP in response to PBS and representative voltage recording of the RMP changes in response to each treatment. (**G**) Number of APs fired by nodose ganglion neurons at different current pulses in presence of *H. biformis* (n=15), GLP-1 (n=9) or GLP-1 after prestimulation with *H. biformis* (n=6). (**H**) Difference in the number of fired APs of each treatment relative to PBS. Data represent the mean ± SEM. Statistical significance was assessed by two-way ANOVA followed by Bonferroni post hoc test (A: stimuli × time interaction and G: stimuli × current pulses interaction); one-way ANOVA followed by Tukey post hoc test (B, E), Pearson correlation coefficient (C), repeated measures ANOVA followed by Tukey post hoc test (D), paired Student's t test (F, G) and unpaired Student's t test (H). $^{\#\#}p<0.01$ and $^{\#\#\#}p<0.001$ vs basal condition; $^{*}p<0.05$ and $^{**}p<0.01$. Only GLP-1-responding nodose ganglion cells (9 out of 14) were considered for the perforated whole-cell patch-clamp recordings.

***Holdemanella biformis* increases the abundance of intestinal bacteria associated with metabolic health and restores the expression of gut barrier integrity-related markers**

We first examined the impact of HFHSD on the gut microbiota by assessing differences in alpha and beta diversity (**Figure 5A and 5B**). Regarding alpha diversity, we observed an increase in richness in untreated DIO mice ($p<0.018$), supported by the differential distribution of the Chao index and observed operation taxonomic units (OTUs), suggesting the acquisition of new bacterial species (**Figure 5A**). *H. biformis* administration attenuated the increases in species richness, with values similar to those in CD-fed mice ($p > 0.110$). The microbial community structure as a whole clearly shifted as a consequence of the HFHSD according to multivariate analysis based on the Bray-Curtis dissimilarity index (PERMANOVA = 10.8, $p = 0.001$) (**Figure 5B**). This pattern was not reversed by *H. biformis* administration. Also, HFHSD caused a depletion of several OTUs belonging to the family Muribaculaceae (linear discriminant analysis [LDA] score=3.10, $p<0.021$), species being predominant in murids (**Figure 5C**). Conversely, HFHSD increased the abundance of some OTUs belonging to the genera *Bacteroides* (LDA = 3.46, $p = 0.049$) and *Alistipes* (LDA = 3.47, $p = 0.008$) and of some species from the families Lachnospiraceae and Ruminococcacea (LDA>3.04, $p<0.011$) (**Figure 5C**), and this was attenuated in DIO mice administered *H. biformis*. We also found that *H. biformis* intake increased *Lactobacillus* (LDA=3.73, p=0.001) and *Akkermansia* (LDA=4.88, p=0.045) species in mice despite their exposure to HFHSD.

Additionally, *H. biformis* promoted the growth of butyrate-producing bacterial species of the genera *Oscillibacter* (Clostridium cluster IV) (LDA=3.48, p=0.002) and *Blautia* (Clostridium cluster XIVa) (LDA=4.01, p=0.029). Given these evident changes in the microbiota, we next analyzed gut barrier integrity-related markers that might be linked to ecological changes and contribute to the metabolic benefits of the intervention in DIO.

Gene expression of the tight junction proteins occludin (*Ocln*) and claudin 3 (C*ldn3*), as well as the proliferation marker *Ki67,* was reduced in the colon of HFHSD-fed mice, but was partially restored by administartion of *H. biformis* (**Figure 5D**), suggesting that it exerted a protective effect in gut barrier integrity. Analysis of colon samples showed that expression of T cell-specific transcription factor 4 (*Tcf4*), involved in Paneth cell differentiation (**Figure 5D**), was higher in DIO mice than in CD mice Accordingly, lysozyme 1 *(Lyz1*) expression was also increased, although other antimicrobial peptides such as phospholipase A2 group IIA (*Pla2g2a)* or regenerating islet-derived protein 3 gamma (*Reg3g*) tended to be reduced or remained unchanged, respectively (**Figure 5D**). *Tcf4* mRNA levels remained elevated in the colon of *H. biformis*-treated DIO mice, whereas *Lyz1* or *Pla2g2a* levels tended to be normalized after the intervention.

Thus, these results suggest that *H. biformis* intervention confers protection against HFHSD by promoting the abundance of intestinal bacterial species of genera related to a healthy metabolic phenotype that might contribute to maintain intestinal integrity and thus glucose homeostasis.

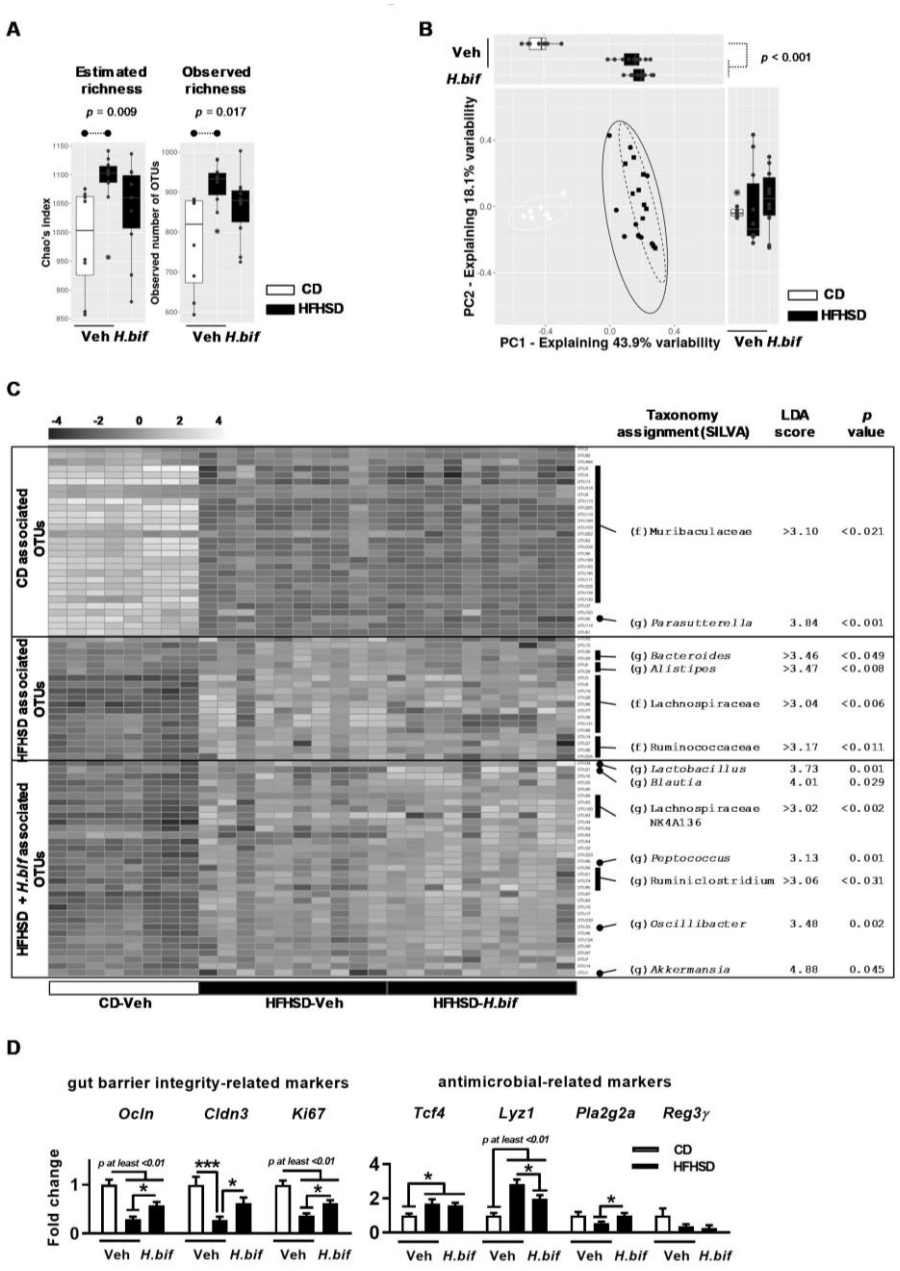

Figure 5. *Holdemanella biformis* increases the abundance of bacterial genera associated with metabolic health and restores the expression of gut barrier integrity-related markers. (**A**) Richness-based alpha diversity analysis of OTUs in feces of mice receiving CD or HFHSD with or without *H. biformis*. P-values obtained after pairwise Wilcoxon Rank Sum test (unpaired)

with Benjamini-Hochberg post hoc correction are shown on top boxplots when equal or less than 0.05 (n=9-10)**.** (**B**) Exploratory analysis based on principal coordinate analysis (PCoA) using Bray-Curtis dissimilarity index. Two main principal coordinates (PC) explaining more than 60% variability are shown in a scatter plot. Marginal boxplots disclose individual distribution of PC values. Differences in PC distribution across group samples were assessed using pairwise Wilcoxon Rank Sum test (unpaired) with Benjamini-Hochberg post hoc correction (n=9-10). (**C**) Heatmap compiling profiles for more than 80 OTUs detected to have differential abundance across sample groups (columns). Gray-scale represents values after raw-scaling of normalized DNA read counts. The most accurate taxonomy identification, linear discriminant analysis (LDA) score and p-value resulting from LDA are shown for all OTUs accordingly. Taxonomy for OTUs with uncertain classification at the family, genus or species level was omitted (n=9-10). (**D**) mRNA levels of tight junction protein genes (*Ocln* and *Cldn3*); a proliferation marker (*Ki67*) a Paneth cell differentiation marker (*Tcf4*) and antimicrobial peptide genes (*Lyz1*, *Pla2g2a* and *Reg3g*) in colon (n=8). Data represent the mean ± SEM. Significant differences were assessed by one-way ANOVA and Tukey *post hoc* test *p<0.05.

Discussion

Herein, we show that *H. biformis* DSM 3989, an intestinal bacterium isolated from a metabolically healthy human subject, has antidiabetic effects in a rodent model of DIO. Mechanistically, we demonstrate that the glucoregulatory effects of *H. biformis* are mediated through improvements in GLP-1 production and signaling by both endocrine and neural pathways, but not by influencing intestinal immunity. Our findings thus support a direct role for *H. biformis* in neural GLP-1 signaling by stimulating GLP-1-responsive neurons and increasing GLP-1-sensitivity, mediating microbiota-driven gut-to-brain cross-talk for glucose homeostasis. We also found that *H. biformis* triggers increases in lipid metabolites, which are known to act as GLP-1 secretagogues, and modifications to the gut microbiota, which likely contribute to maintain gut barrier integrity, and secondarily accounting for its antidiabetic effects.

H. biformis administration reduced fasting glucose levels and improved oral glucose tolerance in DIO mice, but it failed to alleviate body weight gain and plasma markers of lipid metabolism such as cholesterol. These data indicate that *H. biformis* specifically regulates glucose homeostasis and that this is not a consequence of the common weight loss-associated metabolic benefits. Independent of the administration of *H. biformis* in DIO, however, plasma insulin levels remained elevated, at least in the fasting nutritional state, suggesting that the diminution of fasting glycemia induced by *H. biformis* was insufficient to

normalize the circulating levels of insulin. Nonetheless, *H. biformis* reduced blood glucose in response to an oral glucose challenge, which is evidence of improved glucose control in obesity. In addition to insulin and glucagon, meal-related glycemic excursions are controlled by gut hormones such as PYY and GLP-1, which are secreted by enteroendocrine L cells in response to nutrients. The secretion of gut hormones in a glucose intolerance state is reduced, enhanced or unaffected depending on the experimental setting [49,50]. We found reduced circulating levels of PYY and GLP-1 after HFHSD-feeding, which might account for the impaired glucose homeostasis in obesity. Administration of *H. biformis* restored the levels of these hormones in DIO, as has been reported for other microbiota-based intervention strategies in obesity models [51,52]. Both hormones can improve oral glucose tolerance through insulin-independent and dependent mechanisms. Independent of insulin, PYY and GLP-1 contribute to attenuate hyperglycemia by slowing gastric emptying, which in turn reduces glucose delivery into the small intestine and thus its absorption [53,54]. Additionally, GLP-1 has been extensively demonstrated to enhance the insulin action on glucose disposal [12], and a similar effect has been shown for PYY in recent studies [55–57].

Although we did not explore pancreatic insulin secretion capacity, the restoration of circulating levels of PYY and GLP-1 in DIO mice by *H. biformis* administration might account for the improved insulin sensitivity in peripheral tissues and, by extension, glucose disposal. Indeed, our study also reveals that hepatic insulin signaling is improved in *H. biformis*-treated DIO mice despite a background of hyperinsulinemia. By exploring insulin-dependent circuits such as gluconeogenesis in liver, the main contributor to endogenous glucose production and crucial for systemic glucose homeostasis, we found that while HFHSD-feeding increased the hepatic activity of G6Pase, a rate-limiting enzyme of glucose synthesis, administration of *H. biformis* reduced both its expression and activity; these findings might account for the effects on glucose balance. The restoration of insulin signaling in *H. biformis*-treated DIO mice, the main suppressor route of gluconeogenic gene transcription [58], might contribute to reduce the hepatic G6Pase expression in DIO mice. However, the downregulation of the hepatic insulin cascade by HFHSD did not seem to affect the expression of G6Pase in untreated DIO mice, which was similar to that in controls, suggesting the modulation of other pathways as compensatory mechanisms to regulate the transcriptional balance. While no effects of HFHSD were observed on G6Pase at the transcriptional level in liver, its activity was augmented and normalized by *H. biformis*, suggesting that HFHSD alters the hepatic provision of its substrate (G6P) and/or of allosteric metabolites, the main regulators of enzymatic activity. Along this line, we found that the levels of acetyl-CoA, a fatty acid oxidation product and an allosteric metabolite that

enhances gluconeogenesis, were reduced in *H. biformis*-administered DIO mice, although they were unaffected in untreated DIO mice. Given the role of hepatic acetyl-CoA as a regulator of hepatic glucose production by enhancing gluconeogenesis via the allosteric activation of pyruvate carboxylase [48,59], our findings suggest that the lower acetyl-CoA levels lessen the activity of G6Pase in *H. biformis*-treated DIO mice. In line with the decreased hepatic content of acetyl-CoA, we also found that *H. biformis* attenuated the expression of Cpt1a in liver, in accordance with other investigations revealing antihyperglycemic effects of a downregulated fatty acid oxidation [60,61].

With regards to how the bacterial intervention impacted on glucose homeostasis, our data indicate that the attenuation of gluconeogenic markers and the amelioration of insulin signaling in the hyperglycemic state were not due to a restoration of circulating insulin levels. In this line, it has been demonstrated that GLP-1 can reduce endogenous glucose production independently of variations of insulin and glucagon levels in plasma [62,63] and improve insulin sensitivity [64]. Consistent with this, we found that *H. biformis* selectively enhanced pyy and proglugagon gene expression in colonic rather than in ileal L cells, indicating a higher contribution of distal gut to the increased plasma PYY and GLP-1 levels in DIO mice receiving the bacterium. Cecal acetate, the most abundant SCFA, as well as the colonic expression of its receptor Gpr41, were enhanced in mice fed HFHSD and were normalized by *H. biformis*. This metabolite might contribute to metabolic syndrome when produced by a Western diet-associated microbiota, as previously reported [65]. By contrast, *H. biformis* reduced the levels of acetate increased by HFHSD feeding, which might reflect its ability to mitigate adverse metabolic effects secondarily to obesity-associated microbiota alterations.

As anticipated, HFHSD-fed mice showed elevated concentrations of cecal LCFAs, reflecting the higher intake of these dietary lipids. However, the profile of unsaturated LCFAs differed between untreated and *H. biformis*-treated DIO mice, likely as a consequence of variations in intestinal lipid digestion and/or absorption, which are dependent on gut microbiota [66,67]. Notably, *H.biformis* enhanced the cecal abundance of oleic and α-linolenic acid, which act as GLP-1 secretagogues [30,68,69]. Indeed, we found a positive correlation between total cecal MUFAs and plasma GLP-1 in *H. biformis*-treated DIO mice, suggesting that the intraluminal MUFAs enhancement induces GLP-1 colonic secretion to ultimately improve glucose tolerance via the endocrine system.

There is growing evidence that circulating GLP-1 influences hepatic glucose metabolism through central signaling, independently of the incretin effect, rather than through a direct effect on liver, as there is no robust evidence for Glp1-r

expression in hepatocytes [70]. Thus, we further explored how *H. biformis* mediates the gut-to-brain communication through GLP-1 as a potential mechanism of glucose tolerance and hepatic glucose metabolism, independently of pancreatic insulin secretion. Endocrine effects of GLP-1 on the brain are limited due to its rapid degradation in circulation after meal-induced secretion. We therefore explored paracrine GLP-1 signaling in the distal small intestine and colon, which is mediated by Glp-1r in vagal afferents, near to the sites of hormone release that rapidly transmit intestinal sensory information to the brain [71]. The modulation of Glp-1r signaling by *H. biformis* was different in the ileum than in the colon, indicating a differential response to the variations in the nutrient and microbial microenvironment along the intestine [72]. *H. biformis* enhanced Glp-1r signaling in the ileum and normalized it in the colon in DIO mice. Additionally, we established neuroactive properties of *H. biformis* since it directly depolarized NG neurons, which receive sensory information from the extrinsic primary neurons of the gut to be transmitted to the brain, and increased their GLP-1 responsiveness. The improvement of vagal afferent GLP-1 signaling by *H. biformis* in the gut might have an impact on hepatic glucose production and insulin sensitivity, as previously demonstrated by others [13,73, 74]. Also, it has been shown that intestinal dysbiosis impairs enteric GLP-1 neural communication to the brain, which in turn impacts metabolic health [10]. Here, we extend these findings and identify a specific intestinal bacterial strain that, likely through a neuroactive cell wall component, enhances GLP-1-mediated neural signaling in the small intestine. This might facilitate signal transmission from the gut to the brain to more effectively control glucose homeostasis. Further studies are needed to identify the hypothalamic nuclei involved in the integration of the *H. biformis*-mediated intestinal GLP-1 signaling to ultimately control glucose homeostasis through efferent outputs. This could be highly relevant for addressing GLP-1 resistance in T2D [75,76].

To evaluate whether changes in the gut microbial community could mediate the effects of *H. biformis* in DIO mice, we compared the microbiota composition of the different experimental groups. Interestingly, *H. biformis* increased the abundance of species of the genera *Akkermansia* and *Blautia*, related to a healthy metabolic phenotype in previous studies in rodents and humans [22,25,77–79]. This was accompanied by the normalization of the colonic expression of tight junction proteins and also a proliferation marker, which could contribute to bolster the gut barrier integrity altered in DIO and also explain improvements in glucose metabolism. Indeed, *Akkermansia muciniphila* has been demonstrated to repair gut barrier function in rodents through restoration of the mucus layer and the intestinal endocannabinoid content that, in turn, could stimulate the production of enteroendocrine peptides such as GLP-1 [23]. Accordingly, a role

for *H. biformis* in glucose metabolism as a secondary consequence of changes in both metabolites and gut microbiota composition cannot be disregarded.

Taken together, our study shows that *H. biformis* DSM 3989 improves glucose tolerance independent of obesity, impacting mainly on different aspects of the GLP-1 signaling pathway. First, *H. biformis* increases the expression of the GLP-1 precursor (proglucagon) in the colon and the hormone concentration in circulation, likely as a result of secondary changes in intestinal metabolites and bacteria. Second, *H. biformis* administration enhances GLP-1 sensitivity and signaling through endocrine and neural circuits, at least partly through direct host-microbe interactions in the ileum. Third, the effects of *H. biformis* administration on glucose homeostasis are not limited to the GLP-1 system, but might also be a consequence of increases in other endocrine peptides (PYY) as well as of secondary effects on the gut barrier integrity. Of special interest are, however, the effects of this bacterial strain on GLP-1 sensitivity, which could help to boost the efficacy of GLP-1-based therapies in patients with T2D.

Herein, we establish that *H. biformis* DSM 3989 exerts benefits on glucose tolerance and hepatic glucose metabolism in DIO mice independent of obesity. We also show that the beneficial glucoregulatory effects of *H. biformis* are chiefly mediated through increases in GLP-1 secretion, which are related to changes in specific bacterial species and metabolites that are GLP-1 secretagogues in the colon, and through improvements in neural GLP-1 signaling in the ileum. Overall, our data provide support for the use of *H. biformis* DSM 3989 as a therapeutic option to target T2D.

Material and methods

Isolation and cultivation of *Holdemanella biformis*

Feces from healthy volunteers were homogenized in PBS containing cysteine (0.05%) and NaCl (130 mM) (stomacher Lab-Blender 400, Seward Medical, London, UK), inoculated at 1:5 proportion in intestinal bacterial medium (composition detailed by Gibson et al. 1988; Lesmes et al., 2008 with some modifications [0.5% starch; 0.4% mucin; 0.3% casein; 0.2% peptone, NaHCO3, pectin, xylan and wheat bran extract; 0.1% arabinogalactans, arabic gum and inulin; 0.05% cysteine; 0.01% NaCl; 0.005% hemin; 0.004% K2HPO4; 0.001% CaCl2 and MgSO4; and 0.0001% menadione]) and fermented for 24 h in an anerobic chamber (Whitley DG250 Workstation, Don Whitley Scientific Ltd., Shipley, UK) with stirring and pH control (6.9–7.0).

Serial dilutions of fermented feces were plated in fastidious anaerobe agar media plates containing 0.5% defibrinated sheep blood and filtered (0.22 µm) and fermented intestinal bacteria medium, used as a nutritional supplement (0.1 mL of medium per agar plate). Dilutions were then incubated at 37°C for 72 hours in an anaerobic chamber. Bacterial DNA of each isolate (more than 200 colonies) was obtained by incubating pure colonies suspended in sterile PBS treated at 100°C for 10 minutes. The identification of each isolate was performed by PCR amplification of the16S rRNA gene using the primers 27f (5'–AGAGTTTGATCCTGGCTCAG-3') and 1401r (5'-CGGTGTGTACAAGACCC-3'). PCR products were cleaned with the Illustra GFX PCR DNA and Gel Band Purification Kits (GE Healthcare, Madison, WI) and sequenced by Sanger technology in an ABI 3730XL sequencer (Stabvida, Portugal). Using the BLASTn algorithm and the NCBI database we identified one of the colonies as *Holdemanella biformis,* with an identity of 98%, with others belonging to this species. The strain was deposited in the German Collection of Microorganisms and Cell Cultures (DSMZ), with the reference number DSM 3989. The strain was further grown in chopped meat medium supplemented with 0.1% Tween80 (according to DSMZ culture collection recommendations). For *in vivo* experiments, bacterial cells were harvested by centrifugation (6000 × *g* for 10 min) from broth cultures and washed in PBS (130 mM sodium chloride, 10 mM sodium phosphate, pH 7.4). Bacterial cells were then resuspended in 10% sterile skimmed milk for animal trials (Scharlau, Spain). Aliquots were immediately frozen in liquid nitrogen and stored at -80 °C until use. After freezing and thawing, live cell numbers were measured using BD Trucount™ Tubes (BD) in a BD LSRFortessa (Becton Dickinson, Franklin Lakes, NJ) flow cytometer running FACS Diva software v.7.0.

Mice and diets

Adult C57BL/6 mice (6–8 weeks old, Charles River, Saint Germain, Nuelles, France) were housed under controlled conditions of temperature (23ºC), light/dark cycle of 12 hours and relative humidity (40–50%). Mice were fed for 14 weeks with a high-fat/high-sugar diet (HFHSD, D12451) containing 45% of kcal from fat and 17% of kcal from sucrose, or with a control diet (CD, D12450K), without sucrose and with 10% kcal from fat (Research Diets, Inc., Brogaarden, Denmark). HFHSD-fed mice received a daily oral dose of *H biformis* (5×10^8 cells in 10% skimmed milk, n=10) or vehicle (10% skimmed milk, n=10), while CD-fed mice received only vehicle (n=10). Fourteen weeks after the intervention, blood from obtained by cardiac puncture from isofluorane-anesthetized mice, and was collected into microfuge tubes containing K3 EDTA (Sarstedt, Nümbrecht Germany) and immediately centrifuged to obtain plasma and stored at -80°C until use. Mice were then sacrificed by cervical dislocation for sampling collection, including ileum and colon (2 cm), liver, epididymal white adipose tissue (WAT), brain, intestinal content and feces, which were all immediately frozen until use. All experimental procedures were performed in accordance with European Union 2010/63/UE and Spanish RD53/2013 guidelines and approved by the local ethics committee (Animal Production Section, Central Service of Support to Research [SCSIE], University of Valencia, Spain) and authorized by Dirección General de Agricultura, Ganadería y Pesca (Generalitad Valenciana; approval ID 2017/VSC/PEA/00015)

HuTu-80 cell culture

HuTu-80 cells (ATCC® HTB-40, Manassas, VA) were cultured in Dulbecco's modified Eagle's medium (DMEM; Gibco-Invitrogen, Carlsbad, CA), supplemented with 10% fetal bovine serum (FBS, Capricorn Sicentific, Germany) and streptomycin (100 µg/mL), penicillin (100 IU/mL) (Sigma-Aldrich, Madrid, Spain) in a 5% CO_2 atmosphere at 37°C.

Primary culture of nodose ganglion neurons

Swiss CD-1 mice were anesthetized by CO2 inhalation and sacrificed by decapitation. The NG was isolated and cultured as described [33]. Briefly, the NG was bilaterally isolated from the ventral neck and incubated with collagenase (2.5 mg/mL) in Hank's Balanced Salt Solution (HBSS) with 1% HEPES (Sigma-Aldrich) for 15 min, followed by 30-min incubation with trypsin (1 mg/mL, Sigma-Aldrich) in HBSS-1% HEPES. The NG was then mechanically disaggregated,

centrifuged (500 × g, 3 min at 22°C) and seeded onto laminin-precoated culture dishes containing L15 medium with sodium bicarbonate (24 mM), FBS (10%), glucose (38 mM), streptomycin (100 µg/mL), penicillin (100 IU/mL) and nerve growth factor (50 ng/mL) (Sigma-Aldrich). Neurons were maintained at 37°C/5% CO2/95% O2 for 24 h before electrophysiological recordings or Ca2+ imaging.

Flow Cytometry

Small intestine was cleaned with cold PBS, opened longitudinally and cut into small pieces. Tissue were incubated twice in Hansk´s balanced salt solution (HBSS) with calcium and magnesium (ThermoFisher Scientific, Massachusetts, USA) containing 5mM EDTA (Scharlab), 1mM DTT, 100 µg/mL streptomycin and 100 U/mL penicillin (Merck, Darmstadt, Germany) in orbital shaker for 30 minutes at 37°C. Thereafter, remaining tissue was washed with PBS and incubated twice in HBSS supplemented with 0.5 mg/mL collagenase D (Roche Diagnostics GmbH, Mannheim, Germany), 3 mg/mL dispase II (Sigma-Aldrich), 1 mg/mL DNase I (Roche Diagnostics GmbH), and streptomycin 100 µg/ml and penicillin 100 U/ml with orbital agitation for 30 minutes at 37°C. Cells from the lamina propria were collected by filtrating supernatant fractions with 70µm nylon cell strainers that were then centrifuged to harvest cell suspensions. Peripheral blood was collected into microfuge tubes with K3 EDTA (Sarstedt, Nümbrecht Germany) and samples were subject to red blood cell lysis (BD Biosciences, USA). Lamina propia and blood isolated cells in FACS buffer (PBS with BSA 0.5%) were incubated with different immune markers during 30 min at 4ºC in darkness. Different types of macrophages, pro-inflammatory (M1: F4/80+ CD80+ iNOS+) and anti-inflammatory (M2: F4/80+ CD206+ Arg1+) from lamina propria were determined using FITC-conjugated anti-F4/80, Pe-Vio770-conjugated anti-CD80 (Miltenyi, Biotec, Bergisch Gladbach, Germany), APC-conjugated anti-iNOS (Thermo Fisher Scientific, MA, USA), PerCPCy5.5-conjugated anti-CD206 (Biolegend, San Diego, California, USA) and PE-conjugated anti-Arg1 (R&D Systems, Minneapolis, USA) antibodies. Eosinophils (CD11b+ Singlec-F+) from lamina propria were detected using PE-conjugated anti-CD11and Pe-Vio770-conjugated anti-Singlec-F (Miltenyi, Biotec, Bergisch Gladbach, Germany). Cytotoxic T cells (CD3+ CD4- CD8+) from lamina propria and blood were detected using FITC-conjugated anti-CD3, Vioblue-conjugated anti-CD4 and Pe-Vio770-conjugated anti-CD8 (Miltenyi, Biotec, Bergisch Gladbach, Germany). Additionally, staining cells were permeabilized and fixed (fixation/permeabilization solution kit, BD Bioscience, USA) when intracellular markers were required. Data acquisition and analysis were performed using a BD LSRFortessa (Becton Dickinson, USA) flow cytometer operated by FACS Diva software v.7.0 (BD Biosciences, USA).

Oral glucose tolerance test and blood metabolic parameters

After 10 weeks of HFHSD feeding, blood from the saphenous vein was used to measure baseline fasting blood glucose in 4-h food-deprived mice using the Contour® XT glucometer (Bayer, Germany) and oral glucose tolerance was determined by conducting an oral glucose tolerance test (OGTT) 15, 30, 60 and 120 minutes after administering an oral glucose load (2 g/kg). At week 14, metabolic parameters including triglycerides, cholesterol and hormones such as glucagon, insulin, the active isoform of glucagon-like peptide-1 (GLP-1) and peptide YY (PYY) were analyzed in plasma obtained by blood centrifugation at 2500 rpm for 15 min at 4°C. Dipeptidyl-peptidase (DPP)-4 inhibitor (Merck, Germany) was added into blood collecting tubes to prevent GLP-1 degradation. Triglyceride Colorimetric Assay Kit (Elabscience, Houston, TX) and the Cholesterol Liquid Kit (Química Clínica Aplicada SA, Spain) were employed to measure triglycerides and cholesterol, respectively. Insulin, PYY and GLP-1 were quantified using the multiplex assay Milliplex MAP Mouse Metabolic Hormone Magnetic Bead Panel kit (Merck, Darmstadt, Germany) on a Luminex 200 platform (Luminex, Austin, TX), and glucagon was quantified using the Glucagon EIA Kit (Sigma-Aldrich). Colorimetric signals from triglycerides, cholesterol and glucagon analysis were measured in a Thermo Scientific MultiSkan 1500 Reader (Thermo Fisher Scientific, Rockford, IL).

Metabolites in liver

Lipids were extracted from liver using a previously described adapted method [34,35]. In brief, tissue was homogenized in a mixture of chloroform/methanol (2:1), shaken for 3 h at room temperature (RT) and centrifuged at 13000 rpm at RT for 20 minutes after MilliQ water addition for the isolation of the organic layer, which was dried overnight. Triglycerides, cholesterol and free fatty acids were measured in the isolated organic layer using a Triglyceride Kit (Elabscience), Cholesterol Liquid kit (Química Clínica Aplicada SA, Spain) and a Free Fatty Acid Quantitation Kit (Sigma-Aldrich), respectively. Hepatic glycogen, acetyl-CoA and glucose-6-phosphatase activity were quantified in the total homogenized tissue using a Glycogen Assay Kit, Acetyl-Coenzyme A Assay Kit (Sigma-Aldrich) and Glucose-6-phosphatase (G6P) Assay kit (Elabscience), respectively.

RT-qPCR

Total RNA from colon, ileum, liver, epididymal WAT, hypothalamus and nucleus of the solitary tract was isolated using TRIsure™ lysis reagent (Bioline,

London, UK). Nucleus of the solitary tract was isolated by micropunches of 1 mm diameter (from -6.24 to -8.24mm; AP, antero-posterior from bregma) in 100-µm brain slices [36]. A total of 2 µg of RNA, quantified using a NanoDrop ND-1000 spectrophotometer (Thermo Fisher Scientific), was reverse transcribed using a High-Capacity cDNA Reverse Transcription Kit (Thermo Fisher Scientific) and incubated for 10 min at 25°C, 120 min at 37°C and 5 min at 85°C, with a final cooling step at 4°C. cDNA amplification was conducted with the LightCycler 480 SYBR Green I Master Mix (Roche, Basel, Switzerland) containing an appropriate primer pair of each gene [*Acc, ARα1b, Cldn3, Cpt1a, Fas, G6pase, GcK, Hsl,Ki67, Lpl, Lyz1, M3R, Ocln, Pck1, Peripherin Pla2g2a, Proglucagon, Pyy, Reg3g* and *Tcfc4,* (Isogen Life Science, Utrecht, The Netherlands), *Glp-1r*, *Glut2*, *Glut4* (Sigma-Aldrich)]. Ribosomal protein L19 (*Rpl19*) was used as housekeeping gene (primer pair sequences are detailed in **Table S1**). qPCR reactions were performed using a LightCycler® 480 Instrument (Roche) and variation of cDNA abundance was calculated according to the $2^{-(\Delta\Delta Ct)}$ method and represented as fold change expression relative to the control group.

Western blotting

Total proteins from liver were extracted from the organic phase obtained using the TRIsure™ RNA Isolation Reagent (Bioline). In total, 5 µg of denatured proteins, quantified using Bradford's method, were separated by SDS-PAGE electrophoresis and transferred onto polyvinylidene difluoride (PVDF) membranes (Thermo Fisher Scientific). Membranes were incubated overnight at 4°C with 1:1000 dilution of phospho-Akt (Ser473), Akt and β-actin primary antibodies (Cell Signaling Technology, Beverly, MA) followed by a 1-h incubation at RT with anti-rabbit IgG, HRP-linked antibody at 1:5000 (Cell Signalling Technology). Chemiluminescence signals were enhanced by adding the ECL reagent (SuperSignal™ West Dura Extended Duration Substrate, Thermo Fisher Scientific) and quantified using ImageJ 1.8 software.

Proglucagon expression and GLP-1 secretion in human HuTu-80 cells

HuTu-80 cells were seeded into 24-well plates (1×10^5 cells per well) 24 h prior to the experiment. On the day of the experiment, cells were washed twice with 500 µL of glucose-free Krebs–Ringer buffer containing 120 mM NaCl, 5 mM KCl, 2 mM $CaCl_2$, 1 mM $MgCl_2$, 22 mM $NaHCO_3$, and 0.1 mM DiprotinA (Merck) for 10 min at 37°C in a 5% CO_2 incubator. Cells were then incubated for 3 or 6 h either with *H. biformis* (1:100 cell/bacteria proportion) or with GLP-1 secretion

enhancers [i.e. forskolin, 10 μM or phorbol 12-myristate 13-acetate (PMA), 200nM; Sigma-Aldrich] used as positive controls or PBS used as negative control. Cells and supernatants were separated by centrifugation and then collected and frozen until used. Total RNA, isolated using the NucleoSpin RNA Kit (MACHEREY-NAGEL, Düren, Germany) was retrotranscribed to measure *proglucagon* gene expression by qPCR. Total GLP-1 protein levels in supernatants were quantified using Milliplex MAP Human Metabolic Magnetic Bead Panel (Merck) on a Luminex 200 platform (Luminex).

Electrophysiological recordings in primary cultures of nodose ganglion neurons

Resting membrane potential (RMP) and action potential (AP) firing were measured in NG neurons using perforated whole-cell patch-clamp recordings. Cells were maintained in a continuous perfusion (10 mL/min) of extracellular solution containing: 140 mM NaCl, KCl 3 mM, $MgCl_2$ 1 mM, $CaCl_2$ 2 mM, D-glucose 10 mM, HEPES 10 mM, gassed with O_2; pH was adjusted to 7.2 with Tris. The pippete solution contained: K-acetate 90 mM, KCl 20 mM, $MgCl_2$ 3 mM, $CaCl_2$ 1 mM, EGTA 3 mM, HEPES 40 mM, with pH adjusted to 7.2 using NaOH. Pipette solution also contained amphoterincin-B (75 μg/mL) and tips were fire-polished to give a resistance of 4–6 MΩ. Experiments were performed in current clamp mode (holding at -60 mV) using an Axopatch 200B (Axon Instruments Inc., Burlingame, CA) amplifier. To study AP firing, currents from 25 to 175 pA with increases of 25 pA were sequentially injected. First, the effect of *H. biformis* on RMP and firing was studied in extracellular solution containing PBS or 2×10^6 cells/mL *H. biformis*. Similarly, the potential GLP-1 effect was studied comparing solutions containing PBS or 100 mM GLP-1. Finally, NG neurons were perfused with PBS or with 2×10^6 cells/mL of *H. biformis* followed by 100 nM GLP-1. In all cases, neurons were manually clamped at -60 mV and the depolarizing effect of *H. biformis* corrected before adding GLP-1. For the study of APs only adapting neurons were considered.

Fluorescent Ca2+ imaging

NG neurons were seeded onto μ-slide chamber slides (ibiTreat; Sanilabo SL, Valencia, Spain) and loaded for 45 min at 37°C with Fluo-4 AM loading solution (Thermo Fisher Scientific). Fluo-4 AM loading solution was removed and medium was added again after one wash with HBSS-1% HEPES. Ca2+ responses were assessed by monitoring Fluo-4 dye fluorescence (excitation: 494 nm, emission: 506 nm) using a 40× magnification oil objective in an Olympus FV1000 confocal laser scanning microscope (*Central Service for Experimental Research of University of Valencia*) equipped with a heated stage

maintained at 37°C/ 5% CO_2. Time-lapse images were captured every second for 300 seconds after addition of *H. biformis* (2×10^6 cells/mL) or every second for 30 seconds after addition of PBS. Ca2+-mediated fluorescence intensities of cells were determined as mean grey values using ImageJ1.8.0 (www.imagej.nih.gov). For each timepoint, the relative fluorescence intensity ($\Delta F/F_0$) was calculated as fluorescence intensity after bacteria stimulation minus fluorescence intensity at baseline (ΔF) divided by the fluorescence intensity at baseline (F_0), and expressed as percentage. All fluorescence intensity values had been previously corrected by subtracting the background fluorescence intensity from the cell fluorescence intensity.

Fecal metabolomics

Cecal content was homogenized by bead beating in 70% isopropanol [37]. Short chain fatty acids (SCFAs) were quantified by liquid chromatography coupled to tandem mass spectrometry (LC-MS/MS) upon derivatization to 3-nitrophenylhydrazones [37]. Concentrations of total fatty acids (LCFA) were determined by gas chromatography coupled to mass spectrometry (GC-MS) after derivatization to fatty acid methyl esters (FAMEs) [38].

Fecal microbiota analysis

Fecal DNA was extracted using the QIAamp® PowerFecal® DNA Kit (Qiagen, Hilden, Germany). Bead beating was carried out in a Mini-Bead Beater apparatus (BioSpec Products, Bartlesville, OK) with two cycles of shaking during 1 min and incubation on ice between cycles. The fecal DNA concentration was measured using a Nanodrop spectrophotometer and an aliquot of every sample was prepared at 10 ng/µL with nuclease-free water for PCR. The V3-V4 hypervariable regions of the 16S ribosomal ribonucleic acid (rRNA) gene were amplified using 10 ng DNA (1 µL diluted aliquot) and 25 PCR cycles consisting of the following steps: 95ºC for 20 sec., 55ºC for 20 sec. and 72ºC for 20 sec. Phusion High-Fidelity Taq Polymerase (Thermo Fisher Scientific) and 6-mer barcoded primers, S-D-Bact-0341-b-S-17 (TAGCCTACGGGNGGCWGCAG) and S-D-Bact-0785-a-A-21 (ACTGACTACHVGGGTATCTAATCC) that target a wide repertoire of bacterial 16S rRNA genes [39] were used for PCR. Dual barcoded PCR products of ~500 bp were purified from triplicate reactions with the Illustra GFX PCR DNA and Gel Band Purification Kit (GE Healthcare, Bucks, UK) and quantified using the Qubit 3.0 and the Qubit dsDNA HS Assay Kit (Thermo Fisher Scientific). The samples were multiplexed in one sequencing run by combining equimolar

quantities of amplicon DNA (~50 ng per sample) and sequenced in one lane of the Illumina MiSeq platform with 2×300 PE configuration (Eurofins Genomics GmbH, Ebersberg, Germany). Raw data was delivered in fastq files and pair ends with quality filtering were assembled using Flash software [40]. Sample de-multiplexing was carried out using sequence information from the respective DNA barcodes and Mothur v1.39.5 suite of analysis [41,42] After assembly and barcodes/primers removal, the sequences were processed for chimera removal using the Uchime algorithm [43] and the SILVA reference set of 16S sequences (Release 128) [44]. Alpha diversity descriptors (Chao's richness, Simpson's evenness and Simpson's reciprocal index) were computed using QIIME v1.9.1 [41] and a rarefied subset of 35,000 sequences per sample, randomly selected after multiple shuffling (10,000×) from of the original dataset. The information derived from the Operational Taxonomic Unit (OTU)-picking approach by using the rarefied set of sequences and the uclust algorithm, implemented in USEARCH v8.0.1623 [45], was also used to evaluate the beta-diversity with the respective algorithms implemented in QIIME v1.9.1. The evaluation of the community structure across the sample groups was assisted by Principal Coordinate Analysis (PCoA) from Bray-Curtis dissimilarity indexes retrieved from sample pairwise comparisons. The taxonomy identification of OTUs were based on SILVA database and retrieved from SINA aligner [46].

Quantification and statistical analysis

Statistics of Figures 1–4 and Figure 5D and supplemental figures were performed using GraphPad Prism 5. Data were analyzed through one-way ANOVA followed by the Tukey post hoc test to compare the three experimental groups (CD-Veh, HFHSD-Veh and HFHSD-*H. bif*). Two-way ANOVA followed by the Bonferroni post hoc test was used to examine the interaction between two independent variables. The differences between two matched groups were analyzed with paired samples. Correlations were calculated using Pearson's test. Differences were considered significant at $p<0.05$. All data are shown as mean ± standard error of the mean (SEM). Statistical assessment of microbiota data (Figure 5A-C) was performed in R v3.5 and supported by application of non-parametric methods such as Kruskal-Wallis and pairwise Wilcoxon Rank Sum test with the Benjamini-Hochberg post hoc correction followed by linear discriminant analysis (LDA) [47]. The relationships between microbiota changes and the different experimental mouse groups were established for those OTUs exhibiting an LDA score ≥ 3.0. A permutation-based analysis (Permanova) was applied to evaluate changes in the microbial structure.

Acnowledgements

The authors thank Isabel Campillo Nuevo and Inmaculada Noguera for technical assistance.

This study received funding from the European Union Horizon 2020 research and innovation program under the Marie Sklodowska-Curie grant agreement No. 797297 (M.R-P) and from the European Union 7th Framework Program through the *MyNewGut* project (Grant agreement No. 613979). The FPI grant of I.L.-A. from the Ministry of Science, Innovation and Universities (MCIU; Spain) and the contract of C. B-V for promotion of youth employment in R+D+I from MCIU (Spain) are fully acknowledged.

Conflict of interest

The authors declare no competing interests.

Author's contributions

Conceptualization: M.R-P, I.L-A, AJ.L and Y.S; Methodology: M.R-P, I.L-A, C.B-V, L.R-R, EM.G, A.B-P, G.L; Investigation: M.R-P, I.L-A, C.B-V, L.R-R, EM-G, A.B-P and G.L; Writing – Original Draft: I.L-A, M.R-P; Writing – Review & Editing: AJ.L and Y.S; Funding Acquisition: Y.S; Resources: AJ.L and Y.S; Supervision: Y.S

Availability of data and materials

The files containing fastq raw data can be publicly accessed at the European Nucleotide Archive (ENA) via bioproject number PRJEB38356.

References

1. Ley, R. E., Turnbaugh, P. J., Klein, S., and Gordon, J. I. (2006) Microbial ecology: human gut microbes associated with obesity. Nature 444, 1022–1023
2. Turnbaugh, P. J., Hamady, M., Yatsunenko, T., Cantarel, B. L., Duncan, A., Ley, R. E., Sogin, M. L., Jones, W. J., Roe, B. A., Affourtit, J. P., Egholm, M., Henrissat, B., Heath, A. C., Knight, R., and Gordon, J. I. (2009) A core gut microbiome in obese and lean twins. Nature 457, 480–484
3. Ridaura, V. K., Faith, J. J., Rey, F. E., Cheng, J., Duncan, A. E., Kau, A. L., Griffin, N. W., Lombard, V., Henrissat, B., Bain, J. R., Muehlbauer, M. J., Ilkayeva, O., Semenkovich, C. F., Funai, K., Hayashi, D. K., Lyle, B. J., Martini, M. C., Ursell, L. K., Clemente, J. C., Van Treuren, W., Walters, W. A., Knight, R., Newgard, C. B., Heath, A. C., and Gordon, J. I. (2013) Gut microbiota from twins discordant for obesity modulate metabolism in mice. Science 341, 1241214
4. Carmody, R. N., Gerber, G. K., Luevano, J. M., Gatti, D. M., Somes, L., Svenson, K. L., and Turnbaugh, P. J. (2015) Diet dominates host genotype in shaping the murine gut microbiota. Cell Host Microbe 17, 72–84
5. David, L. A., Maurice, C. F., Carmody, R. N., Gootenberg, D. B., Button, J. E., Wolfe, B. E., Ling, A. V., Devlin, A. S., Varma, Y., Fischbach, M. A., Biddinger, S. B., Dutton, R. J., and Turnbaugh, P. J. (2014) Diet rapidly and reproducibly alters the human gut microbiome. Nature 505, 559–563
6. Fung, T. C., Olson, C. A., and Hsiao, E. Y. (2017) Interactions between the microbiota, immune and nervous systems in health and disease. Nat. Neurosci. 20, 145–155
7. Martin, C. R., Osadchiy, V., Kalani, A., and Mayer, E. A. (2018) The Brain-Gut-Microbiome Axis. Cell. Mol. Gastroenterol. Hepatol. 6, 133–148
8. Christ, A., Lauterbach, M., and Latz, E. (2019) Western Diet and the Immune System: An Inflammatory Connection. Immunity 51, 794–811
9. Garidou, L., Pomié, C., Klopp, P., Waget, A., Charpentier, J., Aloulou, M., Giry, A., Serino, M., Stenman, L., Lahtinen, S., Dray, C., Iacovoni, J. S., Courtney, M., Collet, X., Amar, J., Servant, F., Lelouvier, B., Valet, P., Eberl, G., Fazilleau, N., Douin-Echinard, V., Heymes, C., and Burcelin, R. (2015) The Gut Microbiota Regulates Intestinal CD4 T Cells Expressing RORγt and Controls Metabolic Disease. Cell Metab. 22, 100–112
10. Grasset, E., Puel, A., Charpentier, J., Collet, X., Christensen, J. E., Tercé, F., and Burcelin, R. (2017) A Specific Gut Microbiota Dysbiosis of Type 2 Diabetic Mice Induces GLP-1 Resistance through an Enteric NO-Dependent and Gut-Brain Axis Mechanism. Cell Metab. 25, 1075-1090.e5
11. Wollam, J., Riopel, M., Xu, Y.-J., Johnson, A. M. F., Ofrecio, J. M., Ying, W., El Ouarrat, D., Chan, L. S., Han, A. W., Mahmood, N. A., Ryan, C. N., Lee, Y. S., Watrous, J. D., Chordia, M. D., Pan, D., Jain, M., and Olefsky, J. M. (2019) Microbiota-Produced N-Formyl Peptide fMLF Promotes Obesity-Induced Glucose Intolerance. Diabetes 68, 1415–1426
12. Drucker, D. J. (2018) Mechanisms of Action and Therapeutic Application of Glucagon-like Peptide-1. Cell Metab. 27, 740–756

13. Krieger, J.-P., Arnold, M., Pettersen, K. G., Lossel, P., Langhans, W., and Lee, S. J. (2016) Knockdown of GLP-1 Receptors in Vagal Afferents Affects Normal Food Intake and Glycemia. Diabetes 65, 34–43
14. Sandoval, D. A., Bagnol, D., Woods, S. C., D'Alessio, D. A., and Seeley, R. J. (2008) Arcuate glucagon-like peptide 1 receptors regulate glucose homeostasis but not food intake. Diabetes 57, 2046–2054
15. Breton, J., Tennoune, N., Lucas, N., Francois, M., Legrand, R., Jacquemot, J., Goichon, A., Guérin, C., Peltier, J., Pestel-Caron, M., Chan, P., Vaudry, D., do Rego, J.-C., Liénard, F., Pénicaud, L., Fioramonti, X., Ebenezer, I. S., Hökfelt, T., Déchelotte, P., and Fetissov, S. O. (2016) Gut Commensal E. coli Proteins Activate Host Satiety Pathways following Nutrient-Induced Bacterial Growth. Cell Metab. 23, 324–334
16. Chimerel, C., Emery, E., Summers, D. K., Keyser, U., Gribble, F. M., and Reimann, F. (2014) Bacterial metabolite indole modulates incretin secretion from intestinal enteroendocrine L cells. Cell Rep. 9, 1202–1208
17. Natividad, J. M., Agus, A., Planchais, J., Lamas, B., Jarry, A. C., Martin, R., Michel, M.-L., Chong-Nguyen, C., Roussel, R., Straube, M., Jegou, S., McQuitty, C., Le Gall, M., da Costa, G., Lecornet, E., Michaudel, C., Modoux, M., Glodt, J., Bridonneau, C., Sovran, B., Dupraz, L., Bado, A., Richard, M. L., Langella, P., Hansel, B., Launay, J.-M., Xavier, R. J., Duboc, H., and Sokol, H. (2018) Impaired Aryl Hydrocarbon Receptor Ligand Production by the Gut Microbiota Is a Key Factor in Metabolic Syndrome. Cell Metab. 28, 737-749.e4
18. Claus, S. P. (2017) Will Gut Microbiota Help Design the Next Generation of GLP-1-Based Therapies for Type 2 Diabetes? Cell Metab. 26, 6–7
19. O'Toole, P. W. and Paoli, M. (2017) The contribution of microbial biotechnology to sustainable development goals: microbiome therapies. Microb. Biotechnol. 10, 1066–1069
20. Romaní-Pérez, M., Agusti, A., and Sanz, Y. (2017) Innovation in microbiome-based strategies for promoting metabolic health. Curr. Opin. Clin. Nutr. Metab. Care 20, 484–491
21. Tsai, Y.-L., Lin, T.-L., Chang, C.-J., Wu, T.-R., Lai, W.-F., Lu, C.-C., and Lai, H.-C. (2019) Probiotics, prebiotics and amelioration of diseases. J. Biomed. Sci. 26, 3
22. Depommier, C., Everard, A., Druart, C., Plovier, H., Van Hul, M., Vieira-Silva, S., Falony, G., Raes, J., Maiter, D., Delzenne, N. M., de Barsy, M., Loumaye, A., Hermans, M. P., Thissen, J.-P., de Vos, W. M., and Cani, P. D. (2019) Supplementation with Akkermansia muciniphila in overweight and obese human volunteers: a proof-of-concept exploratory study. Nat. Med. 25, 1096–1103
23. Everard, A., Belzer, C., Geurts, L., Ouwerkerk, J. P., Druart, C., Bindels, L. B., Guiot, Y., Derrien, M., Muccioli, G. G., Delzenne, N. M., de Vos, W. M., and Cani, P. D. (2013) Cross-talk between Akkermansia muciniphila and intestinal epithelium controls diet-induced obesity. Proc. Natl. Acad. Sci. U. S. A. 110, 9066–9071
24. Gauffin Cano, P., Santacruz, A., Moya, Á., and Sanz, Y. (2012) Bacteroides uniformis CECT 7771 ameliorates metabolic and immunological dysfunction in mice with high-fat-diet induced obesity. PloS One 7, e41079

25. Plovier, H., Everard, A., Druart, C., Depommier, C., Van Hul, M., Geurts, L., Chilloux, J., Ottman, N., Duparc, T., Lichtenstein, L., Myridakis, A., Delzenne, N. M., Klievink, J., Bhattacharjee, A., van der Ark, K. C. H., Aalvink, S., Martinez, L. O., Dumas, M.-E., Maiter, D., Loumaye, A., Hermans, M. P., Thissen, J.-P., Belzer, C., de Vos, W. M., and Cani, P. D. (2017) A purified membrane protein from Akkermansia muciniphila or the pasteurized bacterium improves metabolism in obese and diabetic mice. Nat. Med. 23, 107–113
26. Schwiertz, A., Le Blay, G., and Blaut, M. (2000) Quantification of different Eubacterium spp. in human fecal samples with species-specific 16S rRNA-targeted oligonucleotide probes. Appl. Environ. Microbiol. 66, 375–382
27. Zagato, E., Pozzi, C., Bertocchi, A., Schioppa, T., Saccheri, F., Guglietta, S., Fosso, B., Melocchi, L., Nizzoli, G., Troisi, J., Marzano, M., Oresta, B., Spadoni, I., Atarashi, K., Carloni, S., Arioli, S., Fornasa, G., Asnicar, F., Segata, N., Guglielmetti, S., Honda, K., Pesole, G., Vermi, W., Penna, G., and Rescigno, M. (2020) Endogenous murine microbiota member Faecalibaculum rodentium and its human homologue protect from intestinal tumour growth. Nat. Microbiol. 5, 511–524
28. Pujo, J., Petitfils, C., Faouder, P. L., Eeckhaut, V., Payros, G., Maurel, S., Perez-Berezo, T., Hul, M. V., Barreau, F., Blanpied, C., Chavanas, S., Immerseel, F. V., Bertrand-Michel, J., Oswald, E., Knauf, C., Dietrich, G., Cani, P. D., and Cenac, N. (2020) Bacteria-derived long chain fatty acid exhibits anti-inflammatory properties in colitis. Gut
29. Tolhurst, G., Heffron, H., Lam, Y. S., Parker, H. E., Habib, A. M., Diakogiannaki, E., Cameron, J., Grosse, J., Reimann, F., and Gribble, F. M. (2012) Short-chain fatty acids stimulate glucagon-like peptide-1 secretion via the G-protein-coupled receptor FFAR2. Diabetes 61, 364–371
30. Hirasawa, A., Tsumaya, K., Awaji, T., Katsuma, S., Adachi, T., Yamada, M., Sugimoto, Y., Miyazaki, S., and Tsujimoto, G. (2005) Free fatty acids regulate gut incretin glucagon-like peptide-1 secretion through GPR120. Nat. Med. 11, 90–94
31.Gibson, G. R., Cummings, J. H., and Macfarlane, G. T. (1988) Use of a three-stage continuous culture system to study the effect of mucin on dissimilatory sulfate reduction and methanogenesis by mixed populations of human gut bacteria. Appl. Environ. Microbiol. 54, 2750–2755
32. Lesmes, U., Beards, E. J., Gibson, G. R., Tuohy, K. M., and Shimoni, E. (2008) Effects of Resistant Starch Type III Polymorphs on Human Colon Microbiota and Short Chain Fatty Acids in Human Gut Models. J. Agric. Food Chem. 56, 5415–5421
33. Cadaveira-Mosquera, A., Pérez, M., Reboreda, A., Rivas-Ramírez, P., Fernández-Fernández, D., and Lamas, J. A. (2012) Expression of K2P channels in sensory and motor neurons of the autonomic nervous system. J. Mol. Neurosci. MN 48, 86–96
34. Frayn, K. N. and Maycock, P. F. (1980) Skeletal muscle triacylglycerol in the rat: methods for sampling and measurement, and studies of biological variability. J. Lipid Res. 21, 139–144
35. Storlien, L. H., Jenkins, A. B., Chisholm, D. J., Pascoe, W. S., Khouri, S., and Kraegen, E. W. (1991) Influence of dietary fat composition on development

of insulin resistance in rats. Relationship to muscle triglyceride and omega-3 fatty acids in muscle phospholipid. Diabetes 40, 280–289
36. Franklin, K. and Paxinos, G. (2008) The Mouse Brain in Stereotaxic Coordinates. ELSEVIER
37. Liebisch, G., Ecker, J., Roth, S., Schweizer, S., Öttl, V., Schött, H.-F., Yoon, H., Haller, D., Holler, E., Burkhardt, R., and Matysik, S. (2019) Quantification of Fecal Short Chain Fatty Acids by Liquid Chromatography Tandem Mass Spectrometry-Investigation of Pre-Analytic Stability. Biomolecules 9
38. Ecker, J., Scherer, M., Schmitz, G., and Liebisch, G. (2012) A rapid GC-MS method for quantification of positional and geometric isomers of fatty acid methyl esters. J. Chromatogr. B Analyt. Technol. Biomed. Life. Sci. 897, 98–104
39. Klindworth, A., Pruesse, E., Schweer, T., Peplies, J., Quast, C., Horn, M., and Glöckner, F. O. (2013) Evaluation of general 16S ribosomal RNA gene PCR primers for classical and next-generation sequencing-based diversity studies. Nucleic Acids Res. 41, e1
40. Magoč, T. and Salzberg, S. L. (2011) FLASH: fast length adjustment of short reads to improve genome assemblies. Bioinforma. Oxf. Engl. 27, 2957–2963
41. Caporaso, J. G., Kuczynski, J., Stombaugh, J., Bittinger, K., Bushman, F. D., Costello, E. K., Fierer, N., Peña, A. G., Goodrich, J. K., Gordon, J. I., Huttley, G. A., Kelley, S. T., Knights, D., Koenig, J. E., Ley, R. E., Lozupone, C. A., McDonald, D., Muegge, B. D., Pirrung, M., Reeder, J., Sevinsky, J. R., Turnbaugh, P. J., Walters, W. A., Widmann, J., Yatsunenko, T., Zaneveld, J., and Knight, R. (2010) QIIME allows analysis of high-throughput community sequencing data. Nat. Methods 7, 335–336
42. Schloss, P. D., Westcott, S. L., Ryabin, T., Hall, J. R., Hartmann, M., Hollister, E. B., Lesniewski, R. A., Oakley, B. B., Parks, D. H., Robinson, C. J., Sahl, J. W., Stres, B., Thallinger, G. G., Van Horn, D. J., and Weber, C. F. (2009) Introducing mothur: open-source, platform-independent, community-supported software for describing and comparing microbial communities. Appl. Environ. Microbiol. 75, 7537–7541
43. Edgar, R. C., Haas, B. J., Clemente, J. C., Quince, C., and Knight, R. (2011) UCHIME improves sensitivity and speed of chimera detection. Bioinforma. Oxf. Engl. 27, 2194–2200
44. Quast, C., Pruesse, E., Yilmaz, P., Gerken, J., Schweer, T., Yarza, P., Peplies, J., and Glöckner, F. O. (2013) The SILVA ribosomal RNA gene database project: improved data processing and web-based tools. Nucleic Acids Res. 41, D590-596
45. Edgar, R. C. (2010) Search and clustering orders of magnitude faster than BLAST. Bioinforma. Oxf. Engl. 26, 2460–2461
46. Pruesse, E., Peplies, J., and Glöckner, F. O. (2012) SINA: accurate high-throughput multiple sequence alignment of ribosomal RNA genes. Bioinforma. Oxf. Engl. 28, 1823–1829
47. Segata, N., Izard, J., Waldron, L., Gevers, D., Miropolsky, L., Garrett, W. S., and Huttenhower, C. (2011) Metagenomic biomarker discovery and explanation. Genome Biol. 12, R60

48. Petersen, M. C., Vatner, D. F., and Shulman, G. I. (2017) Regulation of hepatic glucose metabolism in health and disease. Nat. Rev. Endocrinol. 13, 572–587
49. Duca, F. A., Sakar, Y., and Covasa, M. (2013) The modulatory role of high fat feeding on gastrointestinal signals in obesity. J. Nutr. Biochem. 24, 1663–1677
50. Hira, T., Pinyo, J., and Hara, H. (2020) What Is GLP-1 Really Doing in Obesity? Trends Endocrinol. Metab. TEM 31, 71–80
51. Covasa, M., Stephens, R. W., Toderean, R., and Cobuz, C. (2019) Intestinal Sensing by Gut Microbiota: Targeting Gut Peptides. Front. Endocrinol. 10, 82
52. Everard, A. and Cani, P. D. (2014) Gut microbiota and GLP-1. Rev. Endocr. Metab. Disord. 15, 189–196
53. Marathe, C. S., Rayner, C. K., Jones, K. L., and Horowitz, M. (2013) Relationships between gastric emptying, postprandial glycemia, and incretin hormones. Diabetes Care 36, 1396–1405
54. Steinert, R. E., Feinle-Bisset, C., Asarian, L., Horowitz, M., Beglinger, C., and Geary, N. (2017) Ghrelin, CCK, GLP-1, and PYY(3-36): Secretory Controls and Physiological Roles in Eating and Glycemia in Health, Obesity, and After RYGB. Physiol. Rev. 97, 411–463
55. Guida, C., Stephen, S., Guitton, R., and Ramracheya, R. D. (2017) The Role of PYY in Pancreatic Islet Physiology and Surgical Control of Diabetes. Trends Endocrinol. Metab. TEM 28, 626–636
56. Guida, C., Stephen, S. D., Watson, M., Dempster, N., Larraufie, P., Marjot, T., Cargill, T., Rickers, L., Pavlides, M., Tomlinson, J., Cobbold, J. F. L., Zhao, C.-M., Chen, D., Gribble, F., Reimann, F., Gillies, R., Sgromo, B., Rorsman, P., Ryan, J. D., and Ramracheya, R. D. (2019) PYY plays a key role in the resolution of diabetes following bariatric surgery in humans. EBioMedicine 40, 67–76
57. van den Hoek, A. M., Heijboer, A. C., Corssmit, E. P. M., Voshol, P. J., Romijn, J. A., Havekes, L. M., and Pijl, H. (2004) PYY3-36 reinforces insulin action on glucose disposal in mice fed a high-fat diet. Diabetes 53, 1949–1952
58. Hatting, M., Tavares, C. D. J., Sharabi, K., Rines, A. K., and Puigserver, P. (2018) Insulin regulation of gluconeogenesis. Ann. N. Y. Acad. Sci. 1411, 21–35
59. Perry, R. J., Camporez, J.-P. G., Kursawe, R., Titchenell, P. M., Zhang, D., Perry, C. J., Jurczak, M. J., Abudukadier, A., Han, M. S., Zhang, X.-M., Ruan, H.-B., Yang, X., Caprio, S., Kaech, S. M., Sul, H. S., Birnbaum, M. J., Davis, R. J., Cline, G. W., Petersen, K. F., and Shulman, G. I. (2015) Hepatic acetyl CoA links adipose tissue inflammation to hepatic insulin resistance and type 2 diabetes. Cell 160, 745–758
60. Conti, R., Mannucci, E., Pessotto, P., Tassoni, E., Carminati, P., Giannessi, F., and Arduini, A. (2011) Selective reversible inhibition of liver carnitine palmitoyl-transferase 1 by teglicar reduces gluconeogenesis and improves glucose homeostasis. Diabetes 60, 644–651
61. Lee, J., Choi, J., Selen Alpergin, E. S., Zhao, L., Hartung, T., Scafidi, S., Riddle, R. C., and Wolfgang, M. J. (2017) Loss of Hepatic Mitochondrial Long-Chain Fatty Acid Oxidation Confers Resistance to Diet-Induced Obesity and Glucose Intolerance. Cell Rep. 20, 655–667

62. Sandhu, H., Wiesenthal, S. R., MacDonald, P. E., McCall, R. H., Tchipashvili, V., Rashid, S., Satkunarajah, M., Irwin, D. M., Shi, Z. Q., Brubaker, P. L., Wheeler, M. B., Vranic, M., Efendic, S., and Giacca, A. (1999) Glucagon-like peptide 1 increases insulin sensitivity in depancreatized dogs. Diabetes 48, 1045–1053
63. Seghieri, M., Rebelos, E., Gastaldelli, A., Astiarraga, B. D., Casolaro, A., Barsotti, E., Pocai, A., Nauck, M., Muscelli, E., and Ferrannini, E. (2013) Direct effect of GLP-1 infusion on endogenous glucose production in humans. Diabetologia 56, 156–161
64. Ayala, J. E., Bracy, D. P., James, F. D., Julien, B. M., Wasserman, D. H., and Drucker, D. J. (2009) The glucagon-like peptide-1 receptor regulates endogenous glucose production and muscle glucose uptake independent of its incretin action. Endocrinology 150, 1155–1164
65. Perry, R. J., Peng, L., Barry, N. A., Cline, G. W., Zhang, D., Cardone, R. L., Petersen, K. F., Kibbey, R. G., Goodman, A. L., and Shulman, G. I. (2016) Acetate mediates a microbiome-brain-β-cell axis to promote metabolic syndrome. Nature 534, 213–217
66. Araújo, J. R., Tazi, A., Burlen-Defranoux, O., Vichier-Guerre, S., Nigro, G., Licandro, H., Demignot, S., and Sansonetti, P. J. (2020) Fermentation Products of Commensal Bacteria Alter Enterocyte Lipid Metabolism. Cell Host Microbe 27, 358-375.e7
67. Martinez-Guryn, K., Hubert, N., Frazier, K., Urlass, S., Musch, M. W., Ojeda, P., Pierre, J. F., Miyoshi, J., Sontag, T. J., Cham, C. M., Reardon, C. A., Leone, V., and Chang, E. B. (2018) Small Intestine Microbiota Regulate Host Digestive and Absorptive Adaptive Responses to Dietary Lipids. Cell Host Microbe 23, 458-469.e5
68. Iakoubov, R., Ahmed, A., Lauffer, L. M., Bazinet, R. P., and Brubaker, P. L. (2011) Essential role for protein kinase Cζ in oleic acid-induced glucagon-like peptide-1 secretion in vivo in the rat. Endocrinology 152, 1244–1252
69. Rocca, A. S., LaGreca, J., Kalitsky, J., and Brubaker, P. L. (2001) Monounsaturated fatty acid diets improve glycemic tolerance through increased secretion of glucagon-like peptide-1. Endocrinology 142, 1148–1155
70. Sandoval, D. and Sisley, S. R. (2015) Brain GLP-1 and insulin sensitivity. Mol. Cell. Endocrinol. 418 Pt 1, 27–32
71. Krieger, J.-P., Langhans, W., and Lee, S. J. (2015) Vagal mediation of GLP-1's effects on food intake and glycemia. Physiol. Behav. 152, 372–380
72. Habib, A. M., Richards, P., Cairns, L. S., Rogers, G. J., Bannon, C. A. M., Parker, H. E., Morley, T. C. E., Yeo, G. S. H., Reimann, F., and Gribble, F. M. (2012) Overlap of endocrine hormone expression in the mouse intestine revealed by transcriptional profiling and flow cytometry. Endocrinology 153, 3054–3065
73. Gaykema, R. P., Newmyer, B. A., Ottolini, M., Raje, V., Warthen, D. M., Lambeth, P. S., Niccum, M., Yao, T., Huang, Y., Schulman, I. G., Harris, T. E., Patel, M. K., Williams, K. W., and Scott, M. M. (2017) Activation of murine pre-proglucagon-producing neurons reduces food intake and body weight. J. Clin. Invest. 127, 1031–1045
74. Yang, M., Wang, J., Wu, S., Yuan, L., Zhao, X., Liu, C., Xie, J., Jia, Y., Lai, Y., Zhao, A. Z., Boden, G., Li, L., and Yang, G. (2017) Duodenal GLP-1

signaling regulates hepatic glucose production through a PKC-δ-dependent neurocircuitry. Cell Death Dis. 8, e2609
75. Knop, F. K., Aaboe, K., Vilsbøll, T., Vølund, A., Holst, J. J., Krarup, T., and Madsbad, S. (2012) Impaired incretin effect and fasting hyperglucagonaemia characterizing type 2 diabetic subjects are early signs of dysmetabolism in obesity. Diabetes Obes. Metab. 14, 500–510
76. Muscelli, E., Mari, A., Casolaro, A., Camastra, S., Seghieri, G., Gastaldelli, A., Holst, J. J., and Ferrannini, E. (2008) Separate impact of obesity and glucose tolerance on the incretin effect in normal subjects and type 2 diabetic patients. Diabetes 57, 1340–1348
77. Benítez-Páez, A., Gómez Del Pugar, E. M., López-Almela, I., Moya-Pérez, Á., Codoñer-Franch, P., and Sanz, Y. (2020) Depletion of Blautia Species in the Microbiota of Obese Children Relates to Intestinal Inflammation and Metabolic Phenotype Worsening. mSystems 5
78. Dao, M. C., Everard, A., Aron-Wisnewsky, J., Sokolovska, N., Prifti, E., Verger, E. O., Kayser, B. D., Levenez, F., Chilloux, J., Hoyles, L., MICRO-Obes Consortium, Dumas, M.-E., Rizkalla, S. W., Doré, J., Cani, P. D., and Clément, K. (2016) Akkermansia muciniphila and improved metabolic health during a dietary intervention in obesity: relationship with gut microbiome richness and ecology. Gut 65, 426–436
79. Depommier, C., Van Hul, M., Everard, A., Delzenne, N. M., De Vos, W. M., and Cani, P. D. (2020) Pasteurized Akkermansia muciniphila increases whole-body energy expenditure and fecal energy excretion in diet-induced obese mice. Gut Microbes 11, 1231–1245

Supplemental figures

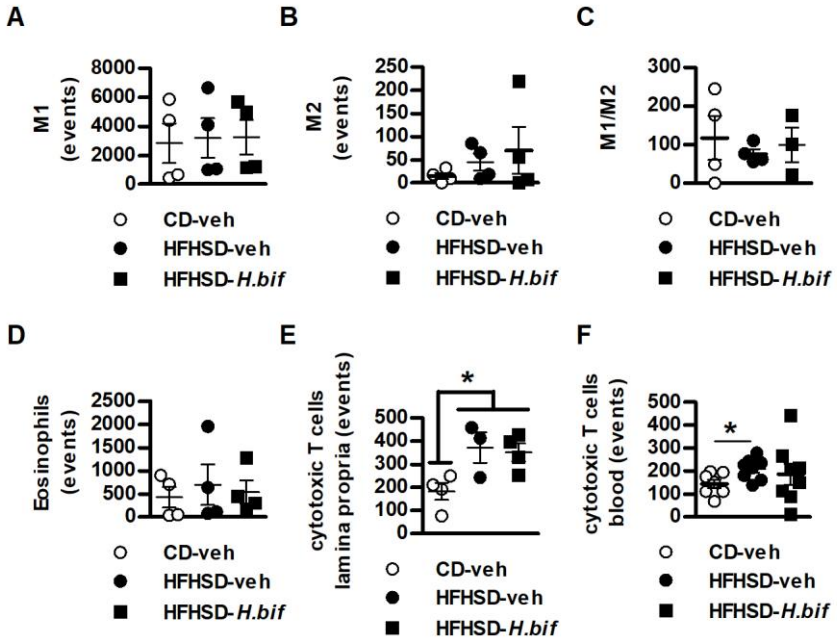

Figure S1 (related to Figure 1). Intestinal or systemic immune-related markers. (**A**) Type 1 macrophages (M1) in the lamina propria (n=4). (**B**) Type 2 macrophages (M1) in the lamina propria (n=4). (**C**) M1/M2 ratio in the lamina propria (n=4). (**D**) Eosinophils in the lamina propria (n=4). (**E**) Cytotoxic T cells in the lamina propria (n=4)**.** (**F**) Cytotoxic T cells in blood (n=7)**.** Data represent the mean ± SEM. Significant differences were established by one-way ANOVA and Tukey post hoc test. *p<0.05

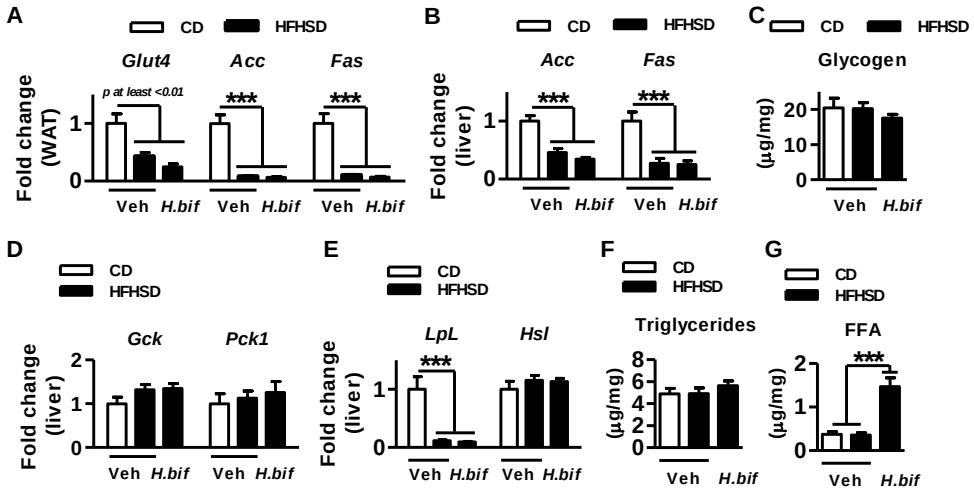

Figure S2 (related to Figure 2). Analysis of energy-related metabolic routes in epididymal WAT and liver. (**A**) mRNA levels of *Glut4* and lipogenic genes (*Acc* and *Fas*) in epididymal WAT (n=8). (**B**) mRNA levels of lipogenic genes (*Acc* and *Fas*) in liver (n=8). (**C**) Hepatic glycogen concentration (µg/mg; n=9-10). (**D**) mRNA levels of *GcK* and *Pck1* in liver (n=8). (**E**) mRNA levels of *LpL* and *HSL* in liver (n=8). (**F**) Triglyceride concentrations (µg/mg) in liver (n=9-10). (**G**) FFA concentration (µg/mg) in liver (n=9-10). Data represent the mean ± SEM. Significant differences were established by one-way ANOVA and Tukey post hoc test. ***p<0.001.

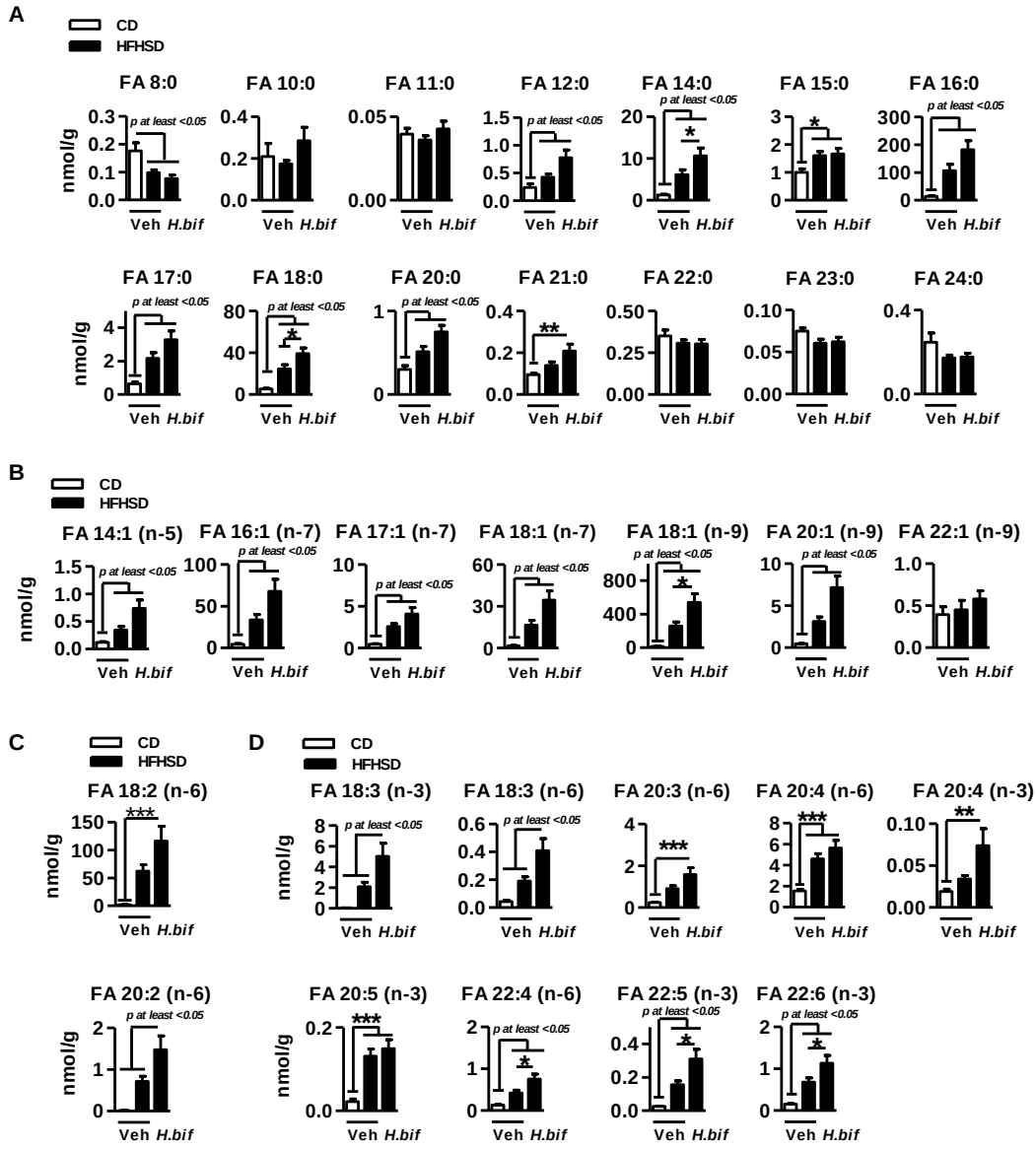

Figure S3 (related to Figure 3). LCFAs cecal abundance in mice fed CD or HFHSD orally receiving vehicle or *H.biformis* for 14 weeks. (**A**) Saturated FAs concentration (nmol/g of dry weight of ceacal content; n=9-10). (**B**) MUFAs concentration (nmol/g of dry weight of ceacal content; n=9-10). (**C**) Diunsaturated FAs concentration (nmol/g of dry weight of ceacal content; n=9-10). (**D**) PUFAs concentration (nmol/g of ceacal content; n=9-10). Data represent the mean ± SEM. Significant differences were determined using one-

way ANOVA followed by Tukey post hoc test. *p<0.05, **p<0.01 and ***p<0.001.

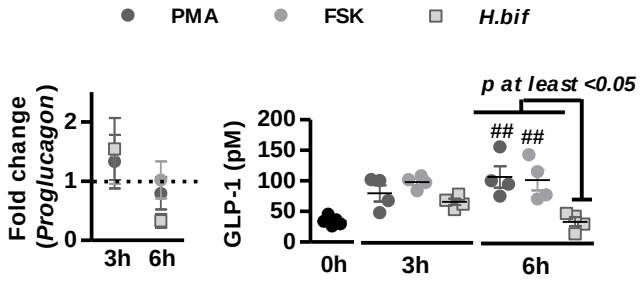

Figure S4 (related to Figure 3). *Proglucagon* expression and GLP-1 secretion by human L cells incubated with *H. biformis*. mRNA levels of *proglucagon* of cultured HuTu-80 cells and total GLP-1 concentration (pM) released into the culture medium measured after stimulation with either PBS, PMA, forskolin or *H.biformis* (n=3-4 trials) (relative expression was calculated respect to expression at time 0).

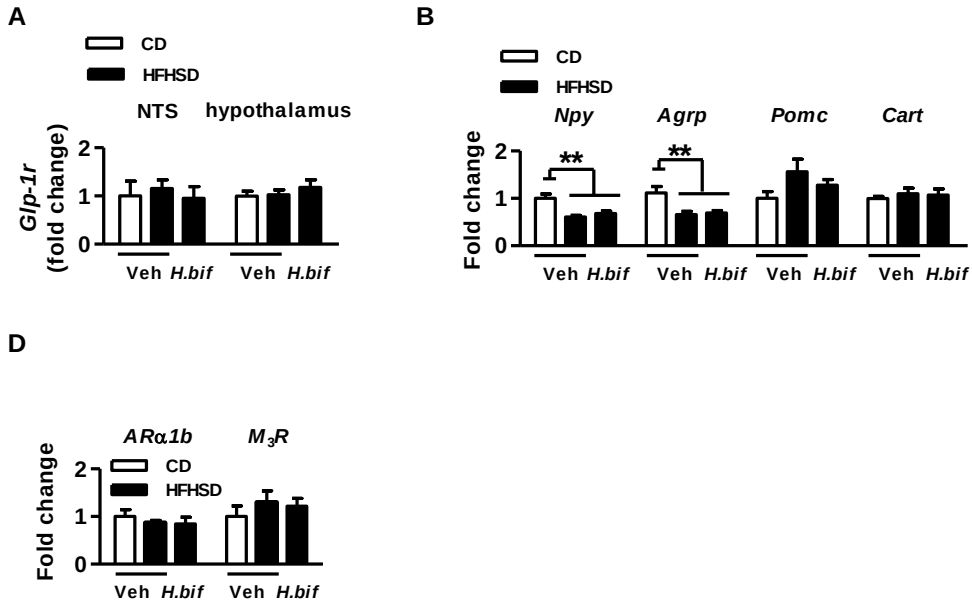

Figure S5 (related to Figure 4). Relative gene expression of energy metabolism-related genes involved in the gut-brain-liver axis. Mice were fed CD or HFHSD for 14 weeks. *H.biformis* or its vehicle (10% skimmed milk) was daily administered by oral gavage. (**A**) mRNA levels of *Glp-1r* in the NTS

(n=6-10) and mRNA levels of *Glp-1r* in the hypothalamus (n=8-10). (**B**) mRNA levels of hypothalamic neuropeptides (*Npy*, *Agrp*, *Pomc* and *Cart*) (n=8-10). (**C**) mRNA levels of *ARα1b* and M_3R in liver (n=7-8). Data represent the mean ± SEM. Significant differences were determined using one-way ANOVA followed by Tukey *post hoc* test **p<0.01.

Phascolarctobacterium faecium confers resistance to diet-induced obesity through reduction of food intake and activation of anti-inflammatory and defensive immune mechanisms in mice

López-Almela Inmaculada*, Romaní-Pérez Marina*, Bullich-Vilarrubias Clara, Cenit María Carmen, Benítez-Páez A, Sanz Y

*Both authors contributed equally to the paper

Microbial Ecology, Nutrition & Health Research Unit. Institute of Agrochemistry and Food Technology, Spanish National Research Council (IATA-CSIC), Valencia, Spain.

Abstract

The prevalence of obesity continues to grow worldwide, as do the associated comorbidities and economic burden, reflecting the lack of effective therapies to tackle this problem. Gut microbiota is considered an additional player in host metabolism regulation and represents a therapeutic target. Nevertheless, further research is called for if we are to progress in the clinical applicability of antiobesity microbiome-based strategies. Here, we have evaluated the effects and mode of action of *Phascolarctobacterium faecium* DSM 32890, isolated from the feces of a metabolically healthy volunteer, on diet-induced obese mice. This study demonstrated that *P. faecium* improved glucose tolerance and reduced food intake, curbing body-weight gain. These effects were mirrored by increases in the anorexigenic gut hormone PYY in plasma and reductions in the high-fat high-sugar diet (HFHSD)-induced GIP hypersecretion. Additionally, *P. faecium* normalized the augmented abundance of pro-inflammatory type 1 innate lymphoid cells (ILC1) and TCRαβ intraepithelial lymphocytes in obese mice. The bacterium also increased the abundance of intestinal anti-inflammatory macrophages (M2) and Treg cells and strengthened primary defense mechanisms, including antimicrobial peptide expression and IgA concentrations, which could protect against diet-induced intestinal immune dysregulation. The administration of *P. faecium* also led to changes in the microbiota structure and increased other bacterial species linked to a healthy metabolic phenotype, possibly exerting direct and indirect effects on the obese phenotype. Overall, our findings indicate that the oral administration of *P. faecium* could help to mitigate obesity and its metabolic complications through both enteroendocrine and immune mechanisms.

Abbreviations

AMP, Antimicrobial peptides; AUC, area under the curve; BSA, bovine serum albumin; Bw, Body weight; CD, control diet; *Cldn3,* claudin 3; *DefA,* defensin alpha 1; DTT, dithiothereitol; EDTA, Ethylenediamine tetraacetic acid; FACS, fluorescence-activated cell sorter; GIP, gastric inhibitory peptide; GLP-1, glucagon-like peptide-1; *GrB,* granzime B; HBSS, Hansk´s balanced salt solution; HFHSD, high-fat-high- sugar diet; IEL, intraepithelial lymphocytes; IL, Interleukin; ILC, innate lymphoid cells; *Lyz1,* lysozyme 1; M1, Pro-inflammatory macrophage; M2, anti-inflammatory macrophage; *Ocln,* occluding; OGTT, oral glucose tolerance test; PBS, phosphate buffer saline; *Pla2g2a*, phospholipase A2 group IIA; PYY, peptide YY *Reg3g*, regenerating islet-derived protein 3 gamma; *Rpl19,* ribosomal protein L19; T2D, type-2 diabetes; TCR, T cell receptor; TG, Triglycerides; Th17, T helper 17 cells; TLR, Toll-like receptor; Treg, regulatory T cells; WAT, white adipose tissue; αEβ7, integrin αEβ7.

Introduction

Obesity has already reached epidemic proportions, mainly due to the sedentary lifestyle and unhealthy dietary habits of Western societies. High consumption of dietary fats and simple sugars contributes to impairing the hypothalamic circuits involved in the homeostatic control of food intake, leading to an excessive caloric intake (hyperphagia), which contributes to obesity onset [1]. The failure to control food intake may be driven by a defective hypothalamic responsiveness to short- as well as long-term peripheral signals that control appetite [2]. Short-term signals; i.e. gut hormones that induce postprandial meal termination, show defective secretion and/or signaling, principally due to impaired nutrient sensing in entero-endocrine cells and/or vagal afferents [3-6]. Furthermore, inadequate hormone function (insulin and leptin), essential for the long-term maintenance of energy homeostasis, is associated with chronic low-grade inflammation in obesity [7]. Impaired intestinal immunity due to the continuous exposure to inflammatory dietary insults (mainly saturated fat) and associated intestinal microbiota changes are considered to play a role in systemic inflammation in obesity [8-10].

Causal associations between gut microbiota alterations and obesity have been demonstrated by fecal microbiota transfer studies, showing the subsequent replication of the metabolic phenotype in the recipient host [11-13]. Studies in rodents have also revealed that obesity-associated dysbiosis triggers defective gut hormone secretion and signaling [14] or intestinal inflammation [15]. This has led to explore different strategies to modulate the gut microbiota to restore energy metabolism in obese subjects [16,17]. Nevertheless, the clinical applicability of the microbiome-based strategies calls for further investigation in order to identify key intestinal bacteria involved in obesity and their modes of action.

In a previous observational study, we showed that the genus *Phascolarctobacterium* was more abundant in children who retained normal weight than in children who became overweight or obese in a four-year follow-up study [18]. In addition, an increase in the abundance of this genus as a consequence of metformin or berberine ingestion is associated with the antidiabetic effects of both drugs in obese rats [19]. Furthermore, other association studies point out its beneficial effects on inflammatory and metabolic diseases such as inflammatory bowel disease in humans and nonalcoholic fatty liver in rats [20-22]. In particular, the species *P. faecium* is a succinate-consumer that produces propionate [23], which could exert beneficial metabolic effects by reducing appetite [24,25] and obesity-associated inflammation [26].

Based on the aforementioned evidence, here we evaluate the effects and mode of action of *Phascolarctobacterium faecium* DSM 32890, isolated from a

metabolically healthy volunteer, in a diet-induced obesity murine model and explore the entero-endocrine and immune mechanisms that could account for the improvements in metabolic health.

Results

P. faecium curbs body weight gain and reduces adiposity, normalizes food intake and increases plasma levels of PYY in obese mice

As expected, HFHSD feeding induced a more rapid increase in body weight gain than CD feeding throughout the study time (**Figure 1A**). Nevertheless, mice administered *P. faecium* gained less weight than untreated mice after 4 and 12 weeks of HFHSD-feeding, proving more effective in curbing weight gain over time (**Figure 1A**). The administration of *P. faecium* to HFHSD-fed mice reduced the subcutaneous fat mass (inguinal) at 4 and 12 weeks as well as epididymal fat at 12 weeks of intervention, compared to untreated obese mice (**Figure 1B**). In addition, the bacterium reduced the HFHSD-induced increase of plasma triglycerides reaching levels of CD-mice after 12 weeks of intervention (**Figure 1C**).

Four weeks of HFHSD-feeding induced resistance to lose weight after 12h of dark-phase fasting compared with CD mice, which curbed weight gain after 2h of *ad-libitum* refeeding in the light-phase (**Figure 1D**). By that time (4 weeks of intervention) *P. faecium* began to curb body weight gain in HFHSD-fed mice (**Figure 1A**). Accordingly, *P. faecium* administration contributed to normalizing body-weight changes after either fasting or refeeding, showing similar trends to those observed in CD mice after 4 weeks of intervention (**Figure 1D**). In addition, body weight after a fasting-refeeding cycle compared to body weight under *ad libitum* conditions was lower only in mice receiving *P. faecium* (**Figure 1E**), suggesting that the bacterium made mice more prone to losing weight under an intermittent feeding pattern. Notably, body weight variations in response to fasting and refeeding were not associated with significant changes in caloric intake during the 2h of refeeding (**Figure S2A**). Nevertheless, 4 weeks of *ad-libitum* intake of HFHSD induced hyperphagia in mice, which was fully prevented by *P. faecium* intervention (**Figure 1F**). The analysis of food intake every 12h after 4 weeks of HFHSD-feeding revealed that suppression of the *P. faecium*-induced food intake only occurred during the dark phase and not during the light phase (**Figure 1F**). Importantly, after 12 weeks of HFHSD-feeding, mice still showed hyperphagia and *P. faecium* continued to reduce caloric intake (**Figure 1F**). In line with the food intake suppression induced by *P. faecium*, the plasma levels of the anorexigenic hormone PYY were increased in mice receiving the bacteria compared with HFHSD-fed mice at week 12 but also compared with CD-mice at 4 and 12 weeks of the intervention (**Figure 1G**). GLP-1 remained unaffected (**Figure S2B**).

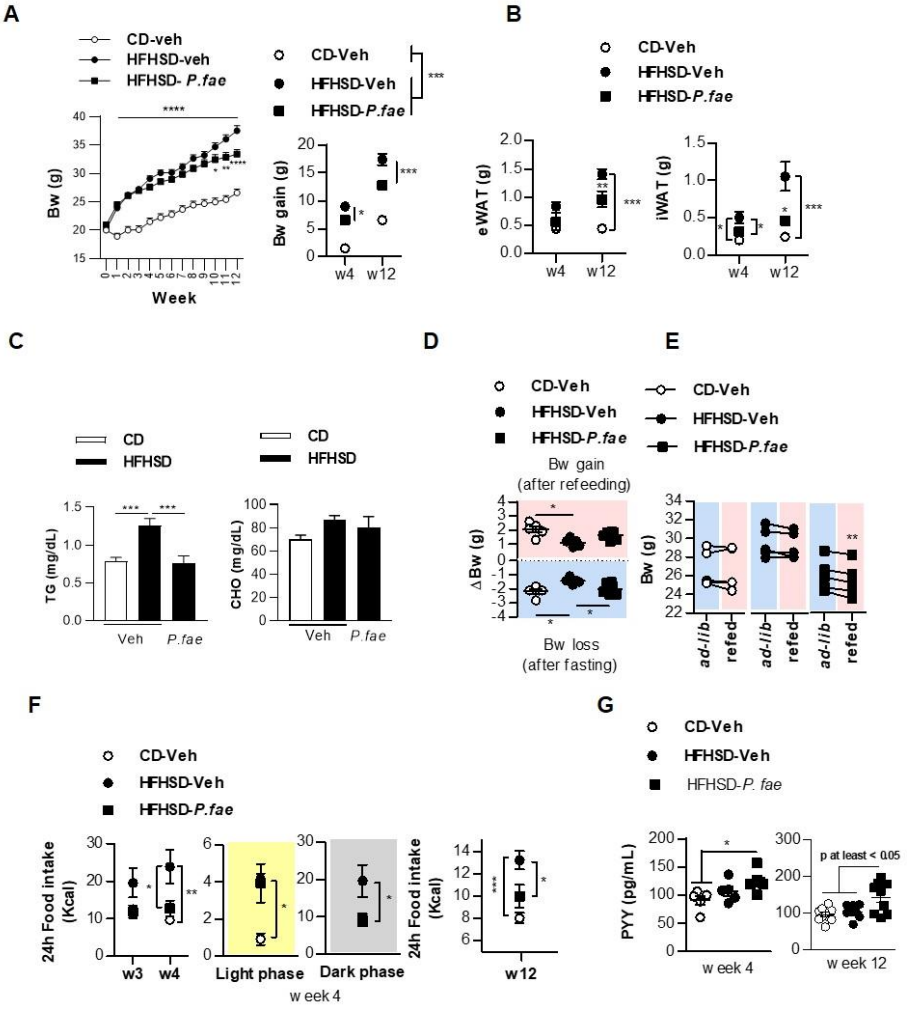

Figure 1. *P. faecium* reduces body weight gain and adiposity, normalizes food intake and increases plasma levels of PYY in obese mice. (**A**) Body weight (Bw) evolution over time and Bw gain (g) at week 4 (n=5-6) and 12 (n=9-10). (**B**) Weight (g) of epididymal and inguinal white adipose tissue (eWAT and iWAT) at week 4 (n=5-6) and 12 (n=9-10). (**C**) Triglycerides and cholesterol concentration in plasma (mg/dL) at week 12 (n=9-10). (**D**) Body weight (Bw) loss (g) after fasting and Bw gain (g) after refeeding at week 4 (n=5-6). (**E**) Body weight (g) *ad-libitum* and after refeeding at week 4 (n=5-6). (**F**) Food intake (Kcal) at week 3 and food intake during light (8-20h) and dark (20-8h) phase at week 4 (n=5-6). Food intake (Kcal) for 24h at week 12 (n=9-10). (**G**) Plasma levels (pg/mL) of PYY at week 4 and 12. Experimental groups abbreviations: CD-Veh, mice fed control diet and vehicle; HFHSD-Veh, obese mice fed the

high-fat-high sucrose diet (HFHSD) and receiving vehicle; HFHSD-*P. fae*, mice receiving (HFHSD) and 1-5x10^8 live cells of *P. faecium*. Data represent the mean ± SEM. Significant differences were assessed by two-way ANOVA followed by Tukey *post hoc* test (body weight and OGTT) or one-way ANOVA followed by Tukey *post hoc* test. *p<0.05, **p<0.01, ***p<0.001 and ****p<0.0001. (See also Figure S2).

P. faecium improves fasting glucose and oral glucose tolerance in obese mice

The bacterium reduced fasting glycaemia after 10 weeks of HFHSD-feeding compared to untreated HFHSD-fed mice (**Figure 2A**). *P. faecium* also facilitated whole-body glucose clearance in response to an oral glucose load, which was impaired by 10 weeks of HFHSD-feeding, as shown by a partial restoration of glycaemia over time, resulting in a reduced AUC (**Figure 2B**). HFHSD intake also induced hyperinsulinemia which was not restored in mice receiving *P. faecium* for 12 weeks (**Figure 2C**). HFHSD strongly increased the incretin hormone GIP in plasma at week 12, which was completely normalized by *P. faecium* (**Figure 2C**), while GLP-1 remained unaffected, as previously stated (**Figure S2B**). Also at week 12, GIP plasma levels of untreated mice fed HFHSD tended to positively correlate to epididymal fat depots, while this trend was not observed in either CD-mice or HFHSD-fed mice receiving *P. faecium* (**Figure 2D**).

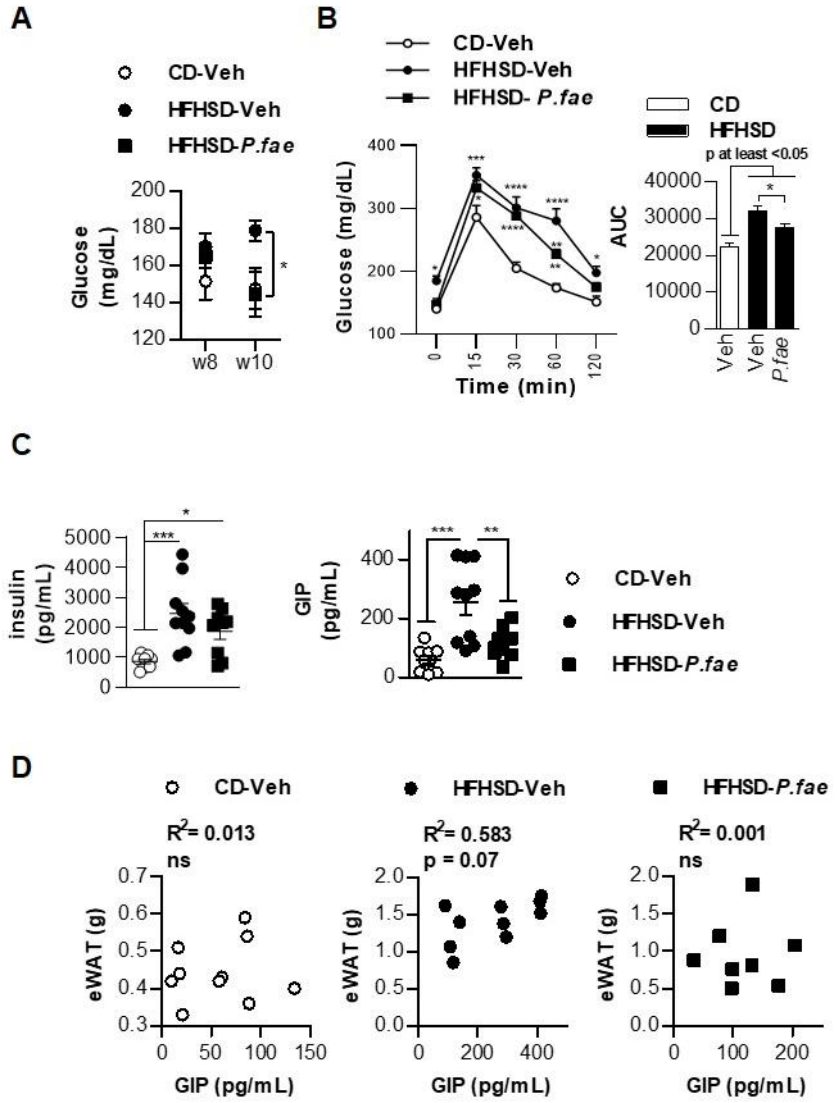

Figure 2. *P. faecium* improves fasting glucose and oral glucose tolerance in obese mice. (**A**) Glucose levels in plasma (mg/dL) at week 8 and 10 (n=9-10). (**B**) Blood glucose levels at 0, 15, 30, 60 and 120 min after an oral load of glucose (2 g/kg) to 4 h-fasted mice (OGTT) and area under the curve (AUC) at week 10 of intervention (n=9-10). (**C**) Plasma levels of insulin and GIP at week 12 (pg/mL) (n=9-10). (**D**) Correlations between plasma levels of GIP and epididymal fat depots (eWAT) (n=9-10)**.** Experimental groups abbreviations: CD-Veh, mice fed control diet and vehicle; HFHSD-Veh, obese mice fed the high-fat-high sucrose diet (HFHSD) and receiving vehicle; HFHSD-*P. fae*, mice

receiving (HFHSD) and 1-5x10^8 live cells of *P. faecium*. Data represent the mean ± SEM. Significant differences were assessed by two-way ANOVA followed by Tukey *post hoc* test (body weight and OGTT) or one-way ANOVA followed by Tukey *post hoc* test. *p<0.05, **p<0.01, ***p<0.001 and ****p<0.0001.

P. faecium counteracts the HFHSD-induced increase of intraepithelial ILC1 and TCRαβ lymphocytes and strengthens primary intestinal defense mechanisms

We explored whether or not the metabolic *P. faecium*-induced benefits were coupled with immune regulatory effects in the intestine. Thus we analyzed innate lymphoid cells group 1 (ILC1) and their adaptive counterpart intraepithelial lymphocytes (IEL) that are in direct contact with luminal dietary and/or bacterial components for the surveillance, defense and repair of the gut epithelium in response to damage.

Compared with CD-mice, HFHSD-feeding increased ILC1abundance (**Figure 3A**) and induced TCRαβ IELs (**Figure 3B**). However, HFHSD-fed mice receiving *P. faecium* showed similar levels of ILC1 (**Figure 3A**) and TCRαβ IELs (**Figure 3B**) as those of CD-fed mice. As increased food intake might also be linked to changes in intestinal immunity, we investigated potential associations between ILC1 or TCRαβ IELs and food intake. A positive correlation between ILC1 and food intake was identified in untreated HFHSD-fed mice but not in either CD-fed or *P. faecium*-treated mice (**Figure S3A**). No significant correlations were detected between food intake and TCRαβ IELs in any of the experimental mouse groups (**Figure S3B**). The abundance of TCRγδ IELs (or unconventional IELs), which is the major T cell population in the epithelium, programmed by self-ligands recognition, was enhanced by *P. faecium* compared with CD or HFHSD-fed mice (**Figure 3C**). Accordingly, *P. faecium* normalized the ratio of TCRαβ to TCRγδ IEL, which was altered by prolonged exposure to HFHSD in mice (**Figure 3D**).

In addition, compared with CD- and HFHSD-fed mice, those administered *P. faecium* experimented an increase in the ileal expression of antimicrobial peptides (AMPs) *Reg3γ* (**Figure 3E**) and *Pla2g2a* (**Figure 3F**), which are produced by TCRγδ IELs to maintain intestinal immune homeostasis. By contrast, *DefA* and *Lyz1* remained unchanged in all experimental groups (**Figure S3C and S3D**). Cecal levels of IgA, whose secretion is partially dependent on TCRγδ IELs, remained unaffected by HFHSD-feeding but it was enhanced by *P. faecium* intervention compared with CD- and HFHSD-fed mice (**Figure 3G**). *P. faecium* also increased the abundance of CD3+CD5+ (**Figure**

3H) while reducing CD3+CD2+ (**Figure 3I**) in the intestinal epithelium, although their levels were not affected by HFHSD, suggesting that the bacteria were able to beneficially modulate the expression of the lymphocyte surface receptors CD5 and CD2, involved in immune tolerance. Compared with CD and HFHSD-mice, *P. faecium* also enhanced the expression of *αEβ7* integrin (**Figure 3K**) and *GrB* (**Figure 3L**), proteins involved in IEL epithelial anchoring and on the cytolytic activity of lymphocytes, respectively. The analysis of tight protein expression, which could indicate changes in intestinal epithelium integrity, revealed that *P. faecium* slightly increased ileal expression of *cldn3* compared with CD-mice (**Figure 3J**), but had no impact on occludin (**Figure S3E**).

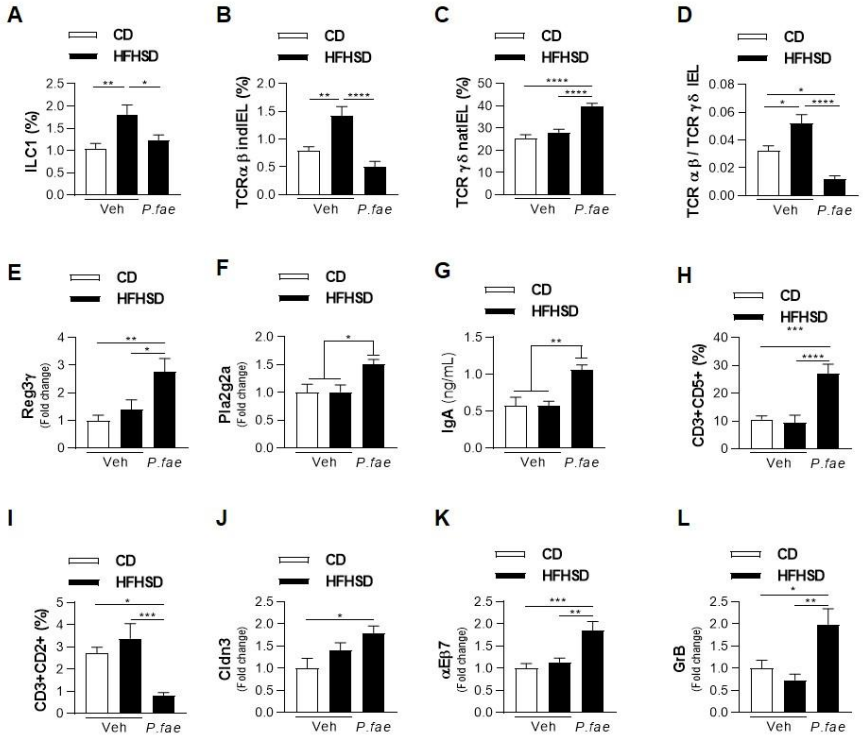

Figure 3. *P. faecium* counteracts the HFHSD-induced increase of intraepithelial ILC1 and TCRαβ lymphocytes and strengthens primary intestinal defense mechanisms. (**A**) ILC1 (percentage of LIN- cells of total intestinal epithelial cells) in the small intestine (n=9-10). (**B**) TCRαβ induced intraepithelial lymphocytes (IEL) (percentage of CD45+ cells of the total intestinal epithelial cells) in the small intestine (n=9-10). (**C**) TCRγδ natural IEL (percentage of CD45+ cells of the total intestinal epithelial cells) in the small intestine (n=9-10). (**D**) TCRαβ induced and TCRγδ natural IEL ratio in the small intestine (n=9-10). (**E-F**) mRNA levels of *Reg3γ* and *Pla2g2a* in ileum (n=9-10).

(**G**) IgA cecal concentration (ng/mL) (n=9-10). (**H**) CD3+ CD5+ cells (percentage of the total intestinal epithelial cells) in the small intestine (n=9-10). (**I**) CD3+ CD2+ cells (percentage of total intestinal epithelial cells) in the small intestine (n=9-10). (**J-L**) mRNA levels of claudin in ileum, *αEβ7* integrin and *granzyme B* in the small intestinal epithelium (n=9-10). Data represent the mean ± SEM. Statistical significance was assessed by one-way ANOVA followed by Tukey *post hoc* test. *p<0.05, **p<0.01 and ***p<0.001. (See also Figure S3).

P. faecium increases the abundance of intestinal anti-inflammatory and immune regulatory cells in obese mice

We assessed whether the immune alterations identified in the intestinal epithelium were coupled with changes in the lamina propria as a consequence of HFHSD feeding and *P. faecium* administration. Contrary to ILC1 in the intestinal epithelium, neither ILC2 nor ILC3 were significantly affected by the diet or the bacterium (**Figure S4A and S4B**). Nevertheless, HFHSD-feeding increased the abundance of type-1 macrophages (M1) compared to type-2 macrophages (M2) (**Figure 4A**), mainly due to a reduction in M2 rather than an increase in M1 (**Figure 4B**). Oral administration of *P. faecium* markedly reduced M1 levels relative to M2 in lamina propia (**Figure 4A**) as compared with CD and HFHSD-fed mice since it significantly reduced M1 abundance and enhanced that of M2 (**Figure 4B**).

Adaptive immune cells were differently affected by the diet and the bacterium. HFHSD-feeding induced an increase in Th17 cells (**Figure 4C**) while neither naïve CD4+ T cells (**Figure 4D**) nor Treg (**Figure 4E**) were affected. Th17 cells remained high in HFHSD-fed mice after *P. faecium* intervention (**Figure 4C**), but the bacterium reduced *naïve* CD4+ T cells (**Figure 4D**) and increased the Treg cells (**Figure 4E**). In line with these findings, the intracellular levels of the transcription factor Gata-3 (**Figure 4F**) and TLR5 expression (**Figure 4G**), which are both involved in the development and physiology of Treg during inflammation, remained unaffected by HFHSD-feeding but were increased by the *P. faecium* intervention. Thus, our results suggest that *P. faecium* specifically induces polarization of macrophages toward the anti-inflammatory M2 phenotype and Treg to restore intestinal inflammation induced by HFHSD in obese mice.

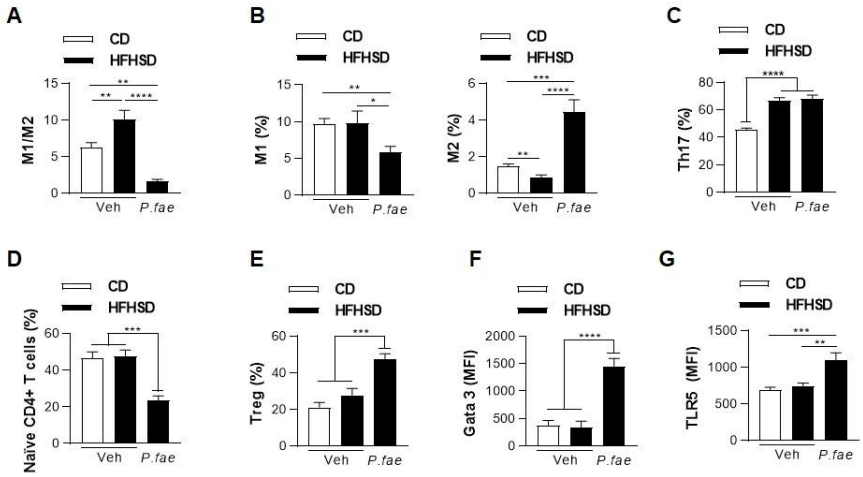

Figure 4. *P. faecium* increases the proportion of intestinal anti-inflammatory and immune regulatory cells in obese mice. (**A-B**) Pro-inflammatory (M1) and anti-inflammatory (M2) macrophages (percentage of F4/80+ cells of the total lamina propria cells) and ratio of M1 to M2 (n=9-10). (**C**) Th17 (percentage of CD4+ cells of the total lamina propria cells) (n=9-10). (**D-E**) Naïve CD4+ T cells and Regulatory T cells (Treg) (percentage of CD4+ cell of the total lamina propria cells) (n=9-10). (**F-G**) Mean fluorescence intensity (MFI) of transcription factor Gata-3 and TLR5 in the total cells of lamina propria (n=9-10). Experimental groups abbreviations: CD-Veh, mice fed control diet and vehicle; HFHSD-Veh, obese mice fed the high-fat-high sucrose diet (HFHSD) and receiving vehicle; HFHSD-*P. fae*, mice receiving (HFHSD) and 1-5x10^8 live cells of *P. faecium*. Data represent the mean ± SEM. Statistical significance was assessed by one-way ANOVA followed by Tukey *post hoc* test. *p<0.05, **p<0.01 and ***p<0.001. (See also Figure S4).

P. faecium modifies HFHSD-induced microbiota alterations and enhances the abundance of *Lactobacillus* spp. and *Akkermansia muciniphila*

The impact of the HFHSD and *P. faecium* on alpha and beta diversity of gut microbiota was determined considering the presence and abundance of the 692 OTUs identified (**Figure 5A and 5B**). We detected drastic differences in richness, supported by the differential distribution of the observed OTUs in HFHSD mice ($p < 0.019$), which exhibited the lower values, suggesting that the HFHSD induced losses in species (**Figure 5A**). *P. faecium* administration did not attenuate the loss of microbial species in HFHSD-fed mice. However, other alpha diversity descriptors like the reciprocal Simpson's index, evenness and

dominance were strongly influenced by *P. faecium* administration, reversing the HFHSD-induced changes beyond the values shown by CD-fed mice. The study of the microbial community structure as a whole (beta diversity) by multivariate analysis, based on Bray-Curtis dissimilarity index among samples and redundancy analysis (RDA), showed that HFHSD induced a marked shift (Adonis = 9.66, $p < 0.001$) (**Figure 5B**). This alteration was not normalized by *P. faecium,* but the administration of the bacterium generated a distinctive microbiota structure from that of HFHSD- and CD-fed mice. We also found that approximately one third of the OTUs identified showed differential abundance across the experimental groups (N = 209). HFHSD induced a depletion of several OTUs belonging to the Muribaculaceae bacterial family, bacterial species being predominant in murids. This loss of commensal bacteria in mice was not restored by *P. faecium* administration (**Figure 5C**). Nevertheless, *P. faecium* exerted a protective role given that the profile for the cluster of Lachnospiraceae-enriched OTUs was restored to CD levels (including a few species of the Ruminococcaceae, Oscillospiraceae, Eggerthellaceae, and Erysipelotrichaceae families), which was augmented in HFHSD-fed mice. Finally, *P. faecium* administration also increased *Lactobacillus* species (OTU43, OTU104 OTU517, $p = 0.031$) and *Akkermansia muciniphila* (OTU197, $p = 0.017$) in HFHSD-fed mice, which was also a distinctive feature when compared to CD-fed mice (**Figure 5D**).

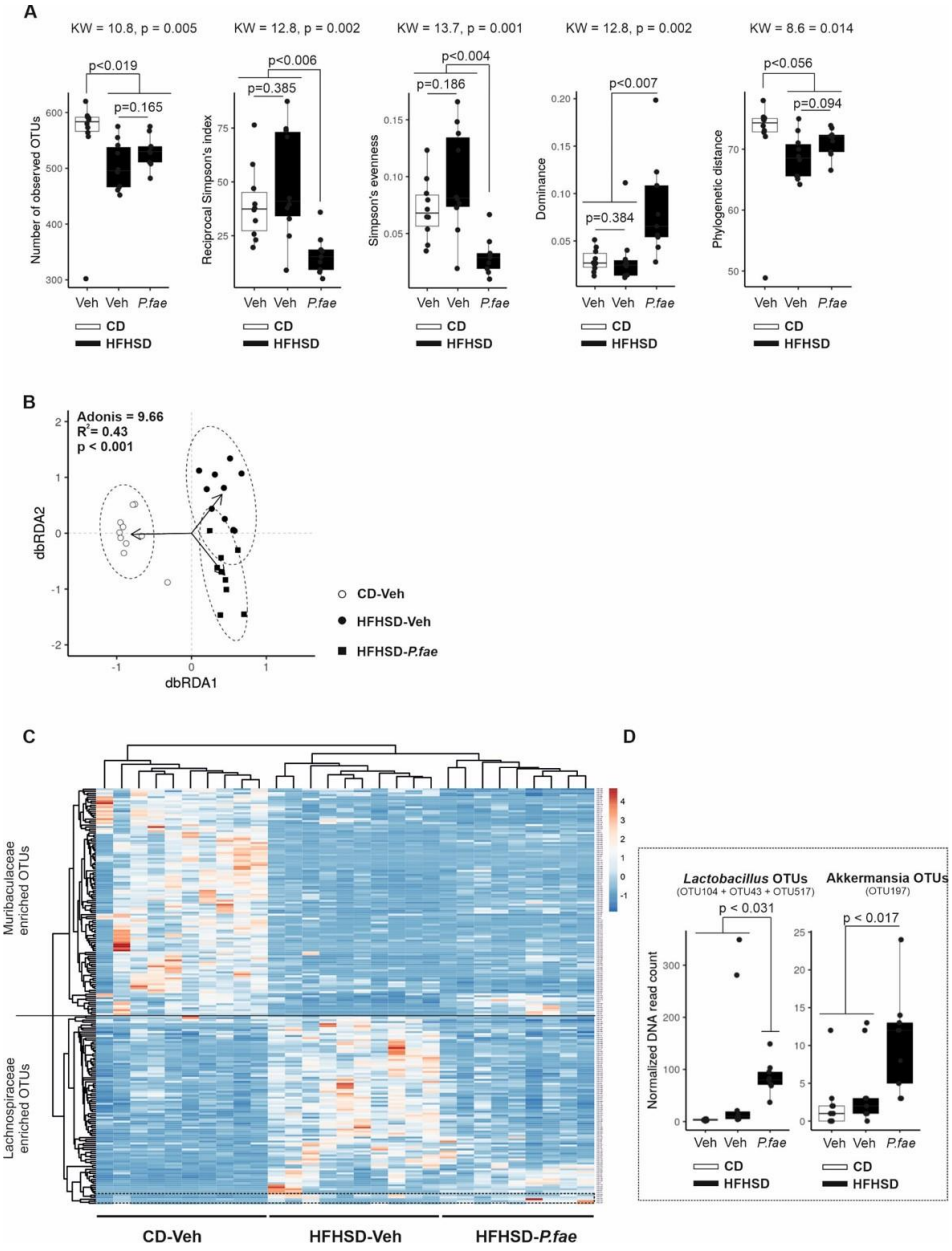

Figure 5. *P. faecium* modifies the HFHSD-induced microbiota alterations and enhances the abundance of *Lactobacillus* species and *Akkermansia muciniphila*. (**A**) The alpha diversity of the cecal microbiota including the observed OTUs, Simpson's reciprocal index, Simpson's evenness index, dominance index, and phylogenetic distance descriptors were assessed and compared among experimental groups. Color legend and group labeling is

maintained as in previous artwork. Alpha diversity data is presented in a boxplot (N = 29 samples) and results of the Kruskal-Wallis (KW) statistical appraisal is shown at the bottom of the boxplots. Corrected *p*-values resulting from pairwise comparisons between groups are shown at the top. (**B**) Analysis of beta diversity of the cecal microbiota is provided using distance-based redundancy analysis (dbRDA). The two gradients of dataset dispersion in ordination space explaining greatest variation are shown in scatter-plot fashion. Color, symbols, and labels assigned to experimental groups are those used in previous figures. Dashed lines circumscribe the confidence interval (95%) of the distribution of the different sample groups. Arrows' heads point out the respective centroids of data dispersion. The result of the Adonis test is shown at the top. (**C**) Scaled read counts for the most differentially abundant OTUs (N = 209, chi-squared test ≥ 11.5, corrected p ≤ 0.01) across groups are shown as a heatmap. Color legend and labeling assigned to experimental groups are those used in previous figures as shown at the bottom. Clustering of OTUs was carried out by using euclidean distance and "complete" clustering method. The OTUs from major clusters were identified using SINA aligner and taxonomy is presented accordingly. Heat scale is based on Z-scores resulting from rarefied read counts per OTU (raw scaling). (D) Distribution of normalized DNA read counts for OTUs identified as *Lactobacillus* (OTU104, OTU43, OTU517) and *Akkermanisa muciniphila* (OTU197). Corrected p-values resulting from pairwise comparisons between groups are shown at the top. Abbreviations: CD, control diet; HFHSD, high-fat-high-sugar diet; *P.*fae, *Phascolarctobacterium faecium*; veh, vehicle.

Discussion

Our study provides primary evidence of the role of P. *faecium* DSM 32890 in intercepting the development of obesity and its metabolic complications in rodents. In particular, our findings demonstrate that oral administration of *P. faecium* to diet-induced obese mice curbs weight gain and reduces adiposity, as well as restoring glucose homeostasis. These effects may result from the primary role played by the bacteria in reducing food intake, and in activating anti-inflammatory mechanisms that counteract the HFHSD-induced immune dysregulation in the intestine.

P. faecium helped to maintained energy homeostasis after 4 and 12 weeks of HFHSD, whereas untreated mice showed positive energy balance as indicated by increased weight gain, adiposity and caloric intake. Theoretically, this effect could be due to the influence of *P. faecium* on hormonal signals controlling short and long-term energy homeostasis. On the one hand, since increased fat depots positively correlate to leptin [36], the main peripheral signal controlling long-term energy homeostasis [37], *P. faecium* could improve the impaired leptin sensitivity induced by HFHSD-feeding after prolonged administration to obese mice. In this regard, previous studies have demonstrated that leptin signaling evolves during the course of exposure to hypercaloric diets [38,39], showing normal hypothalamic sensitivity after 4 weeks of HFHSD-feeding when peripherally administered, but impaired after 14 weeks. On the other hand, *P. faecium* could have limited the progression of obesity at early stages of intervention (week 4) through its impact on short-term signals controlling food intake, independently of the hypothalamic leptin signaling. In fact, *P. faecium* completely normalized the feeding behavior of mice at week 4 of the intervention, specifically reducing hyperphagia in the dark phase. This suggests that *P. faecium* probably requires an active feeding phase, which supplies dietary nutrients, in order to suppress the HFHSD-induced increase in appetite. To date, very few studies have addressed the mechanisms through which the gut microbiota regulates feeding behavior. Noteworthy research has demonstrated the role of the caseinolytic protease (Clp) B, an antigen-mimetic of αMSH, produced by nutrient-induced growth of *Escherichia coli*. This stimulates the response of hypothalamic POMC, thus suppressing appetite directly or indirectly through GLP-1 or PYY secretion [40,41]. Although our study did not investigate either microbial-derived metabolite production or the secretion of food intake-related gastrointestinal hormones postprandrially, we did observe that *P. faecium* administration led to an increase in PYY levels at both early (4 weeks) and late (12 weeks) stages of HFHSD-feeding. This is likely to underpin the anorexigenic effect of the bacterium. The early effect of the bacterium as a PYY enhancer and, thus, as an appetite suppressor could

have reduced the intraluminal exposure to dietary lipids, which are responsible for the duodenal hypersecretion of GIP in diet-induced obesity [42] and associated with adiposity [24], hypothalamic leptin resistance and hyperphagia [43]. We could also postulate that propionate, the main *P. faecium* by-product generated through succinate consumption [44], could be a key metabolite contributing to the enhanced PYY circulating levels [24], although direct evidence should be provided in further studies.

A high intake of dietary fat represents an immune challenge that can compromise the intestinal immune homeostasis, furthermore its breakdown could lead to systemic inflammation and thus to insulin resistance [9]. The vast majority of immune cells within the intestinal epithelium are lymphocytes, referred as IELs, which are considered sentinels of mucosal barrier integrity with a crucial function in the maintenance of intestinal immune homeostasis [45]. TCR+ IELs can be further divided into induced or conventional IELs (TCRαβ IELs), which are activated on recognition of foreign antigens in the periphery, and natural or unconventional IELs (TCRγδ IELs) that respond to self-ligands in the thymus or periphery tissue. Our results indicate that HFHSD causes an increase in the proportion of induced IELs TCRαβ. These IELs are reported to promote epithelial damage in response to inflammatory signals, for example of dietary or microbial origin, which seem to be counteracted by *P. faecium* in HFHSD-fed mice. *P. faecium* also increases the abundance of natural TCRγδ IELs in HFHSD-fed mice, in line with an increased expression of the gut-homing receptor αEβ7 integrin, involved in the recruitment of natural IEL to the small intestinal epithelium [46]. Although the exact functions and behavior of natural TCRγδ IELs have yet to be elucidated, their primary role seems to be in ensuring the integrity of the intestinal epithelium and maintaining local immune homeostasis. The natural γδ IELs cells have been shown to stimulate AMP production by Paneth and epithelial cells, which are crucial in maintaining intestinal immune homeostasis, and increasing IgA production levels [47]. Our results show that oral supplementation of *P. faecium* to HFHSD-fed mice increases the abundance of TCRγδ IEL which, in turn, could activate the protective functions of AMP and IgA, in obese mice. Accordingly, *P. faecium* administration stimulated primary intestinal defenses such as the expression of AMPs, Reg3ɤ and Pla2g2a, and cecal IgA concentrations, which may explain its ability to modulate the gut microbiota composition, adversely affected by the HFHSD. Furthermore, the increased production of IgA by *P. faecium* could also play a beneficial role in restoring glucose metabolism in obese subjects given that high-fat diet-induced IgA-deficiency is causally involved in glucose metabolic dysfunction in obese mice [48].

Intraepithelial innate ILC1s, a recently identified subset of TCR-IELs, are a unique subset of cytokine responsive interferon-γ-producing cells that facilitate immune responses during exposure to infections, but that also contribute to chronic intestinal inflammatory conditions when dysregulated [49]. Our results have shown that HFHSD-feeding increases the abundance of intestinal ILC1s and that their levels were fully normalized by *P. faecium*. In the context of obesity, these cells have mainly been studied in adipose tissue where their dysregulation promotes obesity in response to local proinflammatory cytokine production [50]. We have also shown a positive correlation between the abundance of ILC1 and caloric intake in obese mice, which does not remain significant after *P. faecium* administration, suggesting that this bacterium reduces the exposure of these immune cells to dietary insults activating ILC1s. Although the interplay between ILC1 and macrophages in the intestine has not been investigated yet, we hypothesize that, as occurs in adipose tissue, ILC1 may promote inflammation and, thus, polarize macrophages toward the M1 type. The increase in the latter could contribute to impaired intestinal immune homeostasis and insulin resistance [50]. In fact, our study shows that HFHSD-feeding increased the abundance of M1 compared to M2 macrophages. *P. faecium* reduced the abundance of M1, alone with ILCs, whereas it enhanced that of anti-inflammatory and regulatory M2. Additionally, P*. faecium* triggered Treg cell production, which could also be a mechanism whereby the bacterium promotes phenotypical and functional changes of macrophages towards the M2-type [51,52]. In line with this, *P. faecium* increased Gata3 expression, a transcription factor that controls Treg physiology during inflammation and their accumulation at inflamed sites, thus exerting a protective effect [53].

Pattern recognition receptors, such as TLRs, provide a critical link between innate and adaptive immunity. In particular, the innate immune receptor TLR5, located in intestinal epithelial cells and immune cells, modulates local immunity by secreting cytokines and chemo-attracting different immune cells, such as macrophages and T cells, once activated by bacterial flagellin.

Here, we have demonstrated that oral administration of *P. faecium* to HFHSD-fed mice strongly increased TLR5 expression in the epithelium of the small intestine compared with both CD- and HFHSD-fed mice, suggesting its involvement in the immune-mediated effects of the bacterium. Given that the co-stimulation of T cells with TLR5-ligand flagellin increases the suppressive capacity of Treg [54] and taking into account that *P. faecium* does not produce flagellin, we suggest that *P. faecium*-induced gut microbiota changes underlie the upregulation of TLR5 signaling, which could contribute to Treg [54] and, then, to M2-induction [55] and, thus, to restoring intestinal immune homeostasis. Remarkably, the altered gut microbiota from TLR5-deficient mice was sufficient

to develop low-grade inflammation and metabolic syndrome associated with hyperphagia [56,57], supporting a key role of TLR5 signaling in the host metabolism.

We also investigated whether the administration of *P. faecium* to HFHSD-fed mice influenced gut microbiota composition. Our findings revealed that *P. faecium* modified the HFHSD-altered microbiota structure and enhanced *Akkermansia muciniphila* abundance. This bacterial species has been shown to promote a healthy metabolic phenotype in both mice and humans [58,59], partly by protecting the mucosal barrier under a high-fat diet in rodents [60]. It is possible that *P. faecium*-associated benefits could be due not only to the direct effects of this bacterium but also to the indirect effects exerted on the gut ecosystem, involving other species like *A. muciniphila* [61]. Our findings suggest a novel cross-feeding-based synergy between *P. faecium* and *A. muciniphila*, which is a succinate producer. *A. muciniphila* might favor *P. faecium* growth through succinate production, which is consumed by *P. faecium*, generating propionate. It is this metabolite that might ultimately exert beneficial effects on obesity by reducing appetite [25] and obesity-associated inflammation [26]. Similar cross-feeding mechanisms have been identified in co-cultures between the succinate-producer *Bacteroides thetaiotaomicron* and *P. faecium* [44].

Taken together, the results of our study show that the administration of *P. faecium* DSM 32890 exerts beneficial effects on obesity and metabolic dysfunction. This takes place via a reduction in hypercaloric diet-induced hyperphagia and the restoration of intestinal immune homeostasis through the activation of anti-inflammatory immune cells, such as M2 and Tregs, and primary defensive mechanisms, like AMPs and IgA production, in the intestine. Further studies are warranted to identify the specific bacterial components and/or derived-metabolites that mediate the action of *P. faecium* DSM 32890 as PYY-enhancer and immune-modulator, and their respective contribution to restoring the metabolic phenotype in obesity.

Material and methods

Bacterial strain isolation, identification and culture conditions

Phascolarctobacterium faecium DSM 32890 was isolated from stools of healthy volunteers. Feces were diluted in PBS with 0.05% of cysteine and 130mM of NaCl, homogenized in a stomacher Lab-Blender 400 (Seward Medical, UK) and inoculated (1:5) into intestinal bacteria medium [27,28] with some modifications (0.5% starch; 0.4% mucin; 0.3% casein; 0.2% peptone, 0.2% NaHCO3, 0.2% pectin, 0.2% xylan and 0.2% wheat bran extract; 0.1% arabinogalactans, 0.1% arabic gum and 0.1% inulin; 0.05% cysteine; 0.01% NaCl; 0.005% hemin; 0.004% K2HPO4; 0.001% CaCl2 and MgSO4; and 0.0001% menadione) and incubated at 37°C with stirring, pH control (6.9–7.0) and under anaerobic conditions (Whitley DG250 Workstation, Don Whitley Scientific Ltd., Shipley, UK). After 24h, serial dilutions of fermented feces were spread on plates of a refined anaerobic agar medium supplemented with 0.5% of defibrinated sheep blood and fermented medium, used as nutritional supplement (0.1 mL of medium per agar plate). Then, dilutions were incubated in an anaerobic chamber at 37°C for 72 hours. Pure colonies were suspended in sterile PBS and incubated at 100°C for 10 minutes to obtain bacterial DNA. The isolates were identified by partial 16S rRNA gene sequencing through PCR amplification using the universal primers 27f (5'–AGAGTTTGATCCTGGCTCAG-3') and 1401r (5'- CGGTGTGTACAAGACCC-3'). Ilustra GFX PCR DNA and Gel Band Purification Kits (GE Healthcare, Madison, WI) were used to clean PCR products and Sanger technology in an ABI 3730XL sequencer (Stabvida, Portugal) was employed for DNA sequencing. *Phascolarctobacterium faecium* was identified with an identity of 99% using BLASTn algorithm and the NCBI database. The strain was deposited in the German Collection of Microorganisms and Cell Cultures (DSMZ), with the reference number DSM 32890. For the in vivo experiments with mice, *P. faecium* was grown in PyG medium (DSMZ, Braunschweig, Germany) supplemented with 0.8% of succinate at 37°C under anaerobiosis for 48h. Cells were harvested by centrifugation (7500rpm, 10 min, 4°C), washed twice in PBS and finally re-suspended in PBS with 0.05% cysteine and 10% glycerol. After freezing and thawing, the number of viable bacteria per milliliter was calculated using BD TrucountTM Tubes (BD) in a BD LSRFortessa (Becton Dickinson, Franklin Lakes, NJ) flow cytometer running FACS Diva software v.7.0.

Animals, diets and experimental design

Adult C57BL/6 mice (6-8 weeks old), purchased from Charles River Laboratories (Les Oncins, France), were housed in ventilated racks under controlled conditions of temperature (23±2°C), relative humidity (40-50%) and under 12-hour-light/dark cycle. Animals had *ad-libitum* access to water and food except where stated otherwise. Mice were divided into three experimental groups: (1) a lean group (CD-Veh; n=15) fed a control diet (CD, D12450K Research Diet NJ, USA; 10% of energy from fat and without sucrose) and vehicle (PBS with 0.05% cysteine and 10% glycerol) by gavage daily; (2) an obese group (HFHSD-Veh; n=15) fed a high-fat high-sugar diet (HFHSD, D12451 Research Diet NJ, USA; 45% of energy from fat and 35% from sucrose) and vehicle by gavage daily; and (3) an obese experimental group (HFHSD-*P.fae*; n=15) fed both the HFHSD and a daily dose of *P. faecium* (1-5x10^8 live cells in vehicle) by gavage for 12 weeks.

The experimental procedure is schematically represented in **Figure S1**. In brief, body weight was recorded once weekly and individual food intake was measured after 3, 4 and 12 weeks of the intervention. At week 4, the regulation of body weight variations was assessed in mice that were submitted to a nutritional challenge consisting of 12h of fasting followed by 2h of refeeding to measure body weight loss, body weight-gain and food intake. Fasting glycaemia was measured at week 8 and 10 and an oral glucose tolerance test was performed at week 10.

Cardiac puncture was conducted in anaesthetized mice (isofluorane) at week 4 (n=5-6 mice per group) and week 12 (n=9-10 mice per group) for blood sample extraction. Animals were then sacrificed by cervical dislocation. The whole small intestine (except the ileum: the 5 cm-long distal fragment) was immersed in cold FACS buffer (containing 0.5% FBS) and immediately processed for flow cytometry analysis. Epididymal and inguinal white adipose tissue were weighed. Samples of intestine (ileum and epithelial cells from the small intestine isolated as detailed below in flow cytometry description), cecal content and feces were collected and snap-frozen in liquid nitrogen and kept at -80°C until use.

All experimental procedures were evaluated and approved by the Ethics Committee of the University of Valencia (Animal Production, Central Service of Support to Research [SCSIE], University of Valencia, Spain). Dirección General de Agricultura, Ganadería y Pesca (Generalidad Valenciana" (approval ID 2017/VSC/PEA/00015) authorized the procedure. This was carried out

according to the European Union 2010/63/UE and the Spanish RD53/2013 regulation.

Oral glucose tolerance test

At week 10 an oral glucose tolerance test was conducted by administering an oral glucose load (2g/kg of body weight) to mice previously fasted for 4 hours. Blood from the saphenous vein was collected at 0, 15, 30, 60 and 120 min of the oral glucose load and glycaemia was determined in these samples with a Contour® XT glucometer (Bayer, Barcelona, Spain).

Blood metabolic parameters

Blood was collected into microfuge tubes with K3 EDTA (Sarstedt, Nümbrecht Germany) and centrifuged at 2500 rpm for 15 minutes at 4ºC for plasma collection, which was stored at −80°C until use. The multiplex assay Milliplex MAP Mouse Metabolic Hormone Magnetic Bead Panel kit (Merck Chemicals and Life Science, Madrid, Spain) was used to measured plasma levels of GLP-1 (7-36) and total PYY in samples collected at week 4, and insulin, GIP, GLP-1 (7-36) and total PYY levels in samples collected at week 12, according to the manufacturer's instructions. Triglycerides and cholesterol levels in plasma samples collected at week 12 were quantified with Triglyceride Colorimetric Assay Kit (Elabscience, USA) and cholesterol Liquid kit (Química Analítica Aplicada SA, Spain), respectively, according to manufacturer´s instruction.

IgA measurement in cecal content

Fecal cecum content was harvested and frozen after mice were sacrificed. Approximately 100 mg of the fecal content were 10-fold diluted in PBS and homogenized in the Lysing Matrix D tubes (MP biomedicals, USA). Homogenates were then centrifuged at 700 rpm and 4ºC for 5 min and the supernatant further diluted (1/100) in assay buffer to quantify IgA levels by ELISA, according to the manufacturer´s instructions (Invitrogen, USA).

Intestinal immune cells isolation and flow cytometry analysis

Small intestine was cleaned with cold PBS, opened longitudinally and cut into small pieces. Cells from the intestinal epithelium were isolated by incubating tissue twice in Hansk´s balanced salt solution (HBSS) with calcium and magnesium (ThermoFisher Scientific, Massachusetts, USA) containing

5mM EDTA (Scharlab), 1mM DTT, 100 µg/mL streptomycin and 100 U/mL penicillin (Merck, Darmstadt, Germany) in an orbital shaker for 30 minutes at 37°C. Supernatant fractions were filtrated with 100µm nylon cell strainers (Biologix, Shandong, China) and centrifuged to harvest cell suspensions. Thereafter, tissue was washed with PBS and incubated twice in HBSS supplemented with 0.5 mg/mL collagenase D (Roche Diagnostics GmbH, Mannheim, Germany), 3 mg/mL dispase II (Sigma-Aldrich), 1 mg/mL DNase I (Roche Diagnostics GmbH), and 100 µg/ml streptomycin and 100 U/ml penicillin, under orbital agitation at 37°C for 30 minutes. Cells from the lamina propria were collected by filtrating supernatant fractions with 70µm nylon cell strainers that were then centrifuged to harvest cell suspensions. Isolated cells in FACS buffer were incubated with different immune markers (see **Table 1** for details). Type 1 innate lymphoid cells (ILC1) and intraepithelial lymphocytes (IEL), induced (indIEL) and natural (natIEL) were analyzed in the epithelium, while type 2 and 3 ILC (ILC2 and ILC3), macrophages, CD4+ naïve T cells, regulatory T cells (Treg) and T helper 17 cells (Th17) were analyzed in the lamina propria. Additionally, when detection of intracellular markers was required, previously stained cells were permeabilized and fixed (fixation/permeabilization solution kit, BD Bioscience, USA). Data acquisition and analysis were performed using a BD LSRFortessa (Becton Dickinson, USA) flow cytometer operated by FACS Diva software v.7.0 (BD Biosciences, USA).

RT-qPCR

RNA isolation from ileum and epithelial cells from the whole small intestine was performed using TRIsure™ lysis reagent (Bioline, London, United Kingdom) according to the manufacturer's instructions. For cDNA transcription, 1-2 µg of total RNA, measured with NanoDropTM 2000c Spectrophotometer (Thermo Fisher Scientific, Waltham, MA, USA), were incubated with random primers, 4mM dNTPs, reverse transcription buffer and MultiScribeTM Reverse Transcriptase (50 units) (Reverse Transcription Kit, Thermo Fisher Scientific®) at 25°C for 10 min, followed by incubation at 37°C for 120 min and at 85°C for 5 min, including a final cooling step at 4°C. mRNA levels for the following genes were measured by qPCR: regenerating islet-derived protein 3 gamma (*Reg3g*), phospholipase A2 group IIA (*Pla2g2a*), defensin alpha 1 (*DefA)*, lisozyme 1 (*Lyz1*), claudin 3 (*Cldn3*) and occludin (*ocln*) in ileum and integrin αEβ7 (αEβ7) and granzyme B (*GrB*) in intestinal epithelial cells.

The qPCR mixture contained cDNA, 300 nM of gene-specific primer pairs (**Table 2**) and SYBR® Green Master Mix (1X SYBR® Green PCR kit, Eurogentec, Angers, France). Amplification was performed on a LightCycler® 480 Instrument (Roche, Boulogne-Billancourt, France) and with the following

PCR program: 10 min at 95°C for polymerase activation; 45 amplification cycles (95°C for 10 s; 60°C for 30 s and at 72°C for 5 sec); extension at 95°C for 5 s and at 65°C for 1 min and final cooling at 4°C. All reactions were carried out in duplicate. A negative control with no cDNA was included in each assay run for each primer. Relative mRNA levels were calculated by the double-delta Ct ($2^{-\Delta\Delta Ct}$) method and were normalized with the ribosomal protein L19 (*Rpl19*) mRNA levels. Data were expressed as mRNA fold-change compared to the control.

Microbiota analysis

Feces were collected at the end of the intervention and ~60 mg were used to isolate microbial DNA using the QIAamp PowerFecal DNA kit (Qiagen, Hilden, Germany) following the manufacturer's instructions. DNA concentration was measured using UV methods (Nanodrop, Thermo Scientific, Wilmington, USA). The V3-V4 hypervariable regions of the 16S ribosomal ribonucleic acid (rRNA) gene were amplified using 1 µL DNA (~20 ng) and 25 PCR cycles consisting of the following steps: 95 ºC for 20 sec., 55 ºC for 20 sec. and 72 ºC for 20 sec. Phusion High-Fidelity Taq Polymerase (Thermo Scientific, Wilmington, USA) and the 6-mer barcoded primers, S-D-Bact-0341-b-S-17 (TAGCCTACGGGNGGCWGCAG) and S-D-Bact-0785-a-A-21 (ACTGACTACHVGGGTATCTAATCC) that target a wide repertoire of bacterial 16S rRNA genes [29] were used for PCR. Dual barcoded PCR products, consisting of ~500 bp, were purified from triplicate reactions with the Illustra GFX PCR DNA and Gel Band Purification Kit (GE Healthcare, UK) and quantified through Qubit 3.0 and the Qubit dsDNA HS Assay Kit (Thermo Fisher Scientific, Waltham, MA, USA). The samples were multiplexed in one sequencing run by combining equimolar quantities of amplicon DNA (~50 ng per sample) and sequenced in one lane of the Illumina MiSeq platform with 2x300 PE configuration (Eurofins Genomics GmbH, Germany). Raw data were delivered in fastq files and pair ends with quality filtering were assembled using Flash software11 [30]. Sample de-multiplexing was carried out using sequence information from forward/reverse primers, the respective DNA barcodes, and the SeqKit suite of analysis [31]. After demultiplexing, the barcodes/primers were removed and sequences were processed for chimera removal using UCHIME algorithm [32] and the SILVA reference set of 16S sequences (Release 128) [33]. Operational Taxonomic Unit (OTU) information was retrieved by using a rarefied subset of 10,000 sequences per sample, randomly selected after multiple shuffling (10,000X) from the original dataset, and the UCLUST algorithm implemented in USEARCH v8.0.1623 [34]. Common alpha diversity descriptors including the Observed OTUs, Reciprocal Simpson's index, Simpson's evenness, dominance, and phylogenetic distance (PD) were computed using QIIME v1.9.1. For phylogenetic-based metrics the OTUs sequences were

aligned using the PyNAST algorithm implemented in QIIME and the SILVA aligned reference database and the tree topology reconstruction was completed with the FastTree algorithm [35] using the generalized time-reversible (GTR) model and gamma-based likelihood. The evaluation of the community structure across the sample groups was performed with the Vegan R package v2.5-6 through multivariate and constrained appraisal based on a distance-based redundancy analysis (dbRDA) (*vegan::dbrda* function and "bray" method). Taxonomic identification of differentially abundant OTUs was achieved by submitting respective sequences to the SINA aligner web server (https://www.arb-silva.de/aligner/) and using the SILVA database for classification.

Statistical analysis

Statistical analyses were performed using GraphPad Prism 8. One-way ANOVA followed by Tukey's *post-hoc* test was conducted to compare data among the three independent groups (CD-Veh, HFHSD-Veh and HFHSD-*P. fae*). Two-way ANOVA followed by Bonferroni's post-hoc test was used to evaluate the interaction between the two independent variables (time and body weight follow up or time and glycaemia after an oral glucose load). Correlations were calculated with the Pearson test. Differences were considered significant at $p<0.05$. All data are shown as mean ± standard error of the mean (SEM). Statistical analyses of microbiota data were performed applying non-parametric methods such as Kruskal-Wallis and pairwise Wilcoxon Rank Sum tests (for unpaired samples) with Benjamini-Hochberg *post hoc* correction for multiple group comparison across the alpha diversity descriptors. Statistical robustness for differences of the microbial community structure assessed by interpretative approaches was completed using the permutation-based *vegan::adonis* function. Differential abundance of OTUs across groups was calculated by the Kruskal-Wallis test with Benjamini-Hochberg *post hoc* correction. Highly divergent OTUs in terms of abundance were selected when Kruskal-Wallis corrected p-value were ≤ 0.01. Graphs and plots were drawn using ggplot2 and grid R v3.6 packages. Heatmap hierarchical clustering of OTUs (scaled DNA read counts) was achieved using euclidean distance and the complete clustering method.

Acknowledgments

This study received funding from the European Union 7th Framework Program through the MyNewGut project (Grant agreement No. 613979) and the European Union Horizon 2020 Marie Sklodowska-Curie program (Grant agreement No. 797297). The FPI grant of I.L.-A. from the Ministry of Science, Innovation and Universities (MCIU; Spain) and the contract of C. B-V for promotion of youth employment in R+D+I from MCIU (Spain) are fully acknowledged.

References

1 Yue JTY, Lam TKT. Lipid Sensing and Insulin Resistance in the Brain. *Cell Metabolism* 2012;15:646–55. doi:10.1016/j.cmet.2012.01.013

2 Cone RD. Anatomy and regulation of the central melanocortin system. *Nat Neurosci* 2005;8:571–8. doi:10.1038/nn1455

3 Færch K, Torekov SS, Vistisen D, *et al*. GLP-1 Response to Oral Glucose Is Reduced in Prediabetes, Screen-Detected Type 2 Diabetes, and Obesity and Influenced by Sex: The ADDITION-PRO Study. *Diabetes* 2015;64:2513–25. doi:10.2337/db14-1751

4 Batterham RL, Cohen MA, Ellis SM, *et al*. Inhibition of Food Intake in Obese Subjects by Peptide YY 3–36. *N Engl J Med* 2003;349:941–8. doi:10.1056/NEJMoa030204

5 de Lartigue G, Ronveaux CC, Raybould HE. Deletion of leptin signaling in vagal afferent neurons results in hyperphagia and obesity. *Molecular Metabolism* 2014;3:595–607. doi:10.1016/j.molmet.2014.06.003

6 Daly DM, Park SJ, Valinsky WC, *et al*. Impaired intestinal afferent nerve satiety signalling and vagal afferent excitability in diet induced obesity in the mouse: Impaired afferent satiety signalling in obesity. *The Journal of Physiology* 2011;589:2857–70. doi:10.1113/jphysiol.2010.204594

7 Sáinz N. Leptin Resistance and Diet-Induced Obesity: Central and Peripheral Actions of Leptin. ;:34.

8 Benítez-Páez A, Pugar EMG del, López-Almela I, *et al*. Depletion of Blautia Species in the Microbiota of Obese Children Relates to Intestinal Inflammation and Metabolic Phenotype Worsening. *mSystems* 2020;5. doi:10.1128/mSystems.00857-19

9 Winer DA, Luck H, Tsai S, *et al.* The Intestinal Immune System in Obesity and Insulin Resistance. *Cell Metabolism* 2016;23:413–26. doi:10.1016/j.cmet.2016.01.003

10 Sanz Y, Moya-Pérez A. Microbiota, Inflammation and Obesity. In: Lyte M, Cryan JF, eds. Microbial Endocrinology: The Microbiota-Gut-Brain Axis in Health and Disease. New York, NY: : *Springer New York* 2014. 291–317. doi:10.1007/978-1-4939-0897-4_14

11 Turnbaugh PJ, Ley RE, Mahowald MA, *et al.* An obesity-associated gut microbiome with increased capacity for energy harvest. *Nature* 2006;444:1027–31. doi:10.1038/nature05414

12 Turnbaugh PJ, Bäckhed F, Fulton L, *et al*. Diet-induced obesity is linked to marked but reversible alterations in the mouse distal gut microbiome. *Cell Host Microbe* 2008;3:213–23. doi:10.1016/j.chom.2008.02.015

13 Ridaura VK, Faith JJ, Rey FE, *et al*. Gut Microbiota from Twins Discordant for Obesity Modulate Metabolism in Mice. *Science* 2013;341:1241214. doi:10.1126/science.1241214

14 Grasset E, Puel A, Charpentier J, *et al*. A Specific Gut Microbiota Dysbiosis of Type 2 Diabetic Mice Induces GLP-1 Resistance through an Enteric NO-Dependent and Gut-Brain Axis Mechanism. *Cell Metabolism* 2017;25:1075-1090.e5. doi:10.1016/j.cmet.2017.04.013

15 Lobionda S, Sittipo P, Kwon HY, *et al.* The Role of Gut Microbiota in Intestinal Inflammation with Respect to Diet and Extrinsic Stressors. *Microorganisms* 2019;7:271. doi:10.3390/microorganisms7080271

16 Moya-Pérez A, Neef A, Sanz Y. *Bifidobacterium pseudocatenulatum* CECT 7765 Reduces Obesity-Associated Inflammation by Restoring the Lymphocyte-Macrophage Balance and Gut Microbiota Structure in High-Fat Diet-Fed Mice. *PLoS ONE* 2015;10:e0126976. doi:10.1371/journal.pone.0126976

17 Romaní-Pérez M, Agusti A, Sanz Y. Innovation in microbiome-based strategies for promoting metabolic health. *Current Opinion in Clinical Nutrition & Metabolic Care* 2017;20:484–91. doi:10.1097/MCO.0000000000000419

18 Rampelli S, Guenther K, Turroni S, *et al*. Pre-obese children's dysbiotic gut microbiome and unhealthy diets may predict the development of obesity. *Commun Biol* 2018;1:222. doi:10.1038/s42003-018-0221-5

19 Zhang X, Zhao Y, Xu J, *et al*. Modulation of gut microbiota by berberine and metformin during the treatment of high-fat diet-induced obesity in rats. *Sci Rep* 2015;5:14405. doi:10.1038/srep14405

20 Bajer L, Kverka M, Kostovcik M, *et al*. Distinct gut microbiota profiles in patients with primary sclerosing cholangitis and ulcerative colitis. *WJG* 2017;23:4548. doi:10.3748/wjg.v23.i25.4548

21 Morgan XC, Tickle TL, Sokol H, *et al*. Dysfunction of the intestinal microbiome in inflammatory bowel disease and treatment. *Genome Biol* 2012;13:R79. doi:10.1186/gb-2012-13-9-r79

22 Panasevich MR, Morris EM, Chintapalli SV, *et al.* Gut microbiota are linked to increased susceptibility to hepatic steatosis in low-aerobic-capacity rats fed an acute high-fat diet. *American Journal of Physiology-Gastrointestinal and Liver Physiology* 2016;311:G166–79. doi:10.1152/ajpgi.00065.2016

23 Wu F, Guo X, Zhang J, *et al. Phascolarctobacterium faecium* abundant colonization in human gastrointestinal tract. *Exp Ther Med* 2017;14:3122–6. doi:10.3892/etm.2017.4878

24 Chambers ES, Viardot A, Psichas A, *et al*. Effects of targeted delivery of propionate to the human colon on appetite regulation, body weight maintenance and adiposity in overweight adults. *Gut* 2015;64:1744–54. doi:10.1136/gutjnl-2014-307913

25 Guida C, Stephen SD, Watson M, *et al*. PYY plays a key role in the resolution of diabetes following bariatric surgery in humans. *EBioMedicine* 2019;40:67–76. doi:10.1016/j.ebiom.2018.12.040

26 Serena C, Ceperuelo-Mallafré V, Keiran N, *et al.* Elevated circulating levels of succinate in human obesity are linked to specific gut microbiota. *ISME J* 2018;12:1642–57. doi:10.1038/s41396-018-0068-2

27 Gibson GR, Cummings JH, Macfarlane GT. Use of a three-stage continuous culture system to study the effect of mucin on dissimilatory sulfate reduction and methanogenesis by mixed populations of human gut bacteria. *Appl Environ Microbiol* 1988;54:2750–5.

28 Lesmes U, Beards EJ, Gibson GR, *et al*. Effects of Resistant Starch Type III Polymorphs on Human Colon Microbiota and Short Chain Fatty Acids in Human Gut Models. *J Agric Food Chem* 2008;56:5415–21. doi:10.1021/jf800284d

29 Klindworth A, Pruesse E, Schweer T, *et al.* Evaluation of general 16S ribosomal RNA gene PCR primers for classical and next-generation sequencing-based diversity studies. *Nucleic Acids Research* 2013;41:e1–e1. doi:10.1093/nar/gks808

30 Magoc T, Salzberg SL. FLASH: fast length adjustment of short reads to improve genome assemblies. *Bioinformatics* 2011;27:2957–63. doi:10.1093/bioinformatics/btr507

31 Shen W, Le S, Li Y, *et al*. SeqKit: A Cross-Platform and Ultrafast Toolkit for FASTA/Q File Manipulation. *PLoS ONE* 2016;11:e0163962. doi:10.1371/journal.pone.0163962

32 Edgar RC, Haas BJ, Clemente JC, *et al.* UCHIME improves sensitivity and speed of chimera detection. *Bioinformatics* 2011;27:2194–200. doi:10.1093/bioinformatics/btr381

33 Quast C, Pruesse E, Yilmaz P, *et al*. The SILVA ribosomal RNA gene database project: improved data processing and web-based tools. *Nucleic Acids Research* 2012;41:D590–6. doi:10.1093/nar/gks1219

34 Edgar RC. Search and clustering orders of magnitude faster than BLAST. *Bioinformatics* 2010;26:2460–1. doi:10.1093/bioinformatics/btq461

35 Price MN, Dehal PS, Arkin AP. FastTree: Computing Large Minimum Evolution Trees with Profiles instead of a Distance Matrix. *Molecular Biology and Evolution* 2009;26:1641–50. doi:10.1093/molbev/msp077

36 Pereira S, O'Dwyer SM, Webber TD, *et al.* Metabolic effects of leptin receptor knockdown or reconstitution in adipose tissues. *Sci Rep* 2019;9:3307. doi:10.1038/s41598-019-39498-3

37 Park H-K, Ahima RS. Physiology of leptin: energy homeostasis, neuroendocrine function and metabolism. *Metabolism* 2015;64:24–34. doi:10.1016/j.metabol.2014.08.004

38 El-Haschimi K, Pierroz DD, Hileman SM, *et al*. Two defects contribute to hypothalamic leptin resistance in mice with diet-induced obesity. *J Clin Invest* 2000;105:1827–32. doi:10.1172/JCI9842

39 Lin S, Thomas T, Storlien L, *et al*. Development of high fat diet-induced obesity and leptin resistance in C57Bla6J mice. *International Journal of Obesity*;:8.

40 Breton J, Tennoune N, Lucas N, *et al*. Gut Commensal *E. coli* Proteins Activate Host Satiety Pathways following Nutrient-Induced Bacterial Growth. *Cell Metabolism* 2016;23:324–34. doi:10.1016/j.cmet.2015.10.017

41 Tennoune N, Chan P, Breton J, *et al.* Bacterial ClpB heat-shock protein, an antigen-mimetic of the anorexigenic peptide α-MSH, at the origin of eating disorders. *Translational Psychiatry* 2014;:11.

42 Miyawaki K, Yamada Y, Ban N, *et al*. Inhibition of gastric inhibitory polypeptide signaling prevents obesity. *Nat Med* 2002;8:738–42. doi:10.1038/nm727

43 Kaneko K, Fu Y, Lin H-Y, *et al*. Gut-derived GIP activates central Rap1 to impair neural leptin sensitivity during overnutrition. *J Clin Invest* 2019;129:3786–91. doi:10.1172/JCI126107

44 Ikeyama N, Murakami T, Toyoda A, *et al.* Microbial interaction between the succinate-utilizing bacterium *Phascolarctobacterium faecium* and the gut

commensal *Bacteroides thetaiotaomicron*. *MicrobiologyOpen* 2020;9. doi:10.1002/mbo3.1111

45 Olivares-Villagómez D, Van Kaer L. Intestinal Intraepithelial Lymphocytes: Sentinels of the Mucosal Barrier. *Trends Immunol* 2018;39:264–75. doi:10.1016/j.it.2017.11.003

46 Staton TL, Habtezion A, Winslow MM, *et al.* CD8+ recent thymic emigrants home to and efficiently repopulate the small intestine epithelium. *Nat Immunol* 2006;7:482–8. doi:10.1038/ni1319

47 Cheroutre H, Lambolez F, Mucida D. The light and dark sides of intestinal intraepithelial lymphocytes. *Nat Rev Immunol* 2011;11:445–56. doi:10.1038/nri3007

48 Luck H, Khan S, Kim JH, *et al*. Gut-associated IgA+ immune cells regulate obesity-related insulin resistance. *Nat Commun* 2019;10:3650. doi:10.1038/s41467-019-11370-y

49 Bernink JH, Peters CP, Munneke M, *et al*. Human type 1 innate lymphoid cells accumulate in inflamed mucosal tissues. *Nature Immunology* 2013;14:221–9. doi:10.1038/ni.2534

50 O'Sullivan TE, Rapp M, Fan X, *et al.* Adipose-Resident Group 1 Innate Lymphoid Cells Promote Obesity-Associated Insulin Resistance. *Immunity* 2016;45:428–41. doi:10.1016/j.immuni.2016.06.016

51 Liu G, Ma H, Qiu L, *et al*. Phenotypic and functional switch of macrophages induced by regulatory CD4 + CD25 + T cells in mice. *Immunol Cell Biol* 2011;89:130–42. doi:10.1038/icb.2010.70

52 Vieira-Potter VJ. Inflammation and macrophage modulation in adipose tissues: Adipose tissue macrophage modulation. *Cell Microbiol* 2014;16:1484–92. doi:10.1111/cmi.12336

53 Wohlfert EA, Grainger JR, Bouladoux N, *et al*. GATA3 controls Foxp3+ regulatory T cell fate during inflammation in mice. *J Clin Invest* 2011;121:4503–15. doi:10.1172/JCI57456

54 Crellin NK, Garcia RV, Hadisfar O, *et al.* Human CD4 + T Cells Express TLR5 and Its Ligand Flagellin Enhances the Suppressive Capacity and Expression of FOXP3 in CD4 + CD25 + T Regulatory Cells. *J Immunol* 2005;175:8051–9. doi:10.4049/jimmunol.175.12.8051

55 Lacavé-Lapalun J-V, Benderitter M, Linard C. Flagellin or lipopolysaccharide treatment modified macrophage populations after colorectal radiation of rats. *J Pharmacol Exp Ther* 2013;346:75–85. doi:10.1124/jpet.113.204040

56 Vijay-Kumar M, Aitken JD, Carvalho FA, *et al*. Metabolic Syndrome and Altered Gut Microbiota in Mice Lacking Toll-Like Receptor 5. *Science* 2010;328:228–31. doi:10.1126/science.1179721

57 Chassaing B, Ley RE, Gewirtz AT. Intestinal Epithelial Cell Toll-like Receptor 5 Regulates the Intestinal Microbiota to Prevent Low-Grade Inflammation and Metabolic Syndrome in Mice. *Gastroenterology* 2014;147:1363-1377.e17. doi:10.1053/j.gastro.2014.08.033

58 Depommier C, Everard A, Druart C, *et al*. Supplementation with *Akkermansia muciniphila* in overweight and obese human volunteers: a proof-of-concept exploratory study. *Nat Med* 2019;25:1096–103. doi:10.1038/s41591-019-0495-2

59 Cani PD, de Vos WM. Next-Generation Beneficial Microbes: The Case of *Akkermansia muciniphila*. *Front Microbiol* 2017;8:1765. doi:10.3389/fmicb.2017.01765

60 Everard A, Belzer C, Geurts L, *et al.* Cross-talk between *Akkermansia muciniphila* and intestinal epithelium controls diet-induced obesity. *Proceedings of the National Academy of Sciences* 2013;110:9066–71. doi:10.1073/pnas.1219451110

61 Gould AL, Zhang V, Lamberti L, *et al*. Microbiome interactions shape host fitness. *Proc Natl Acad Sci USA* 2018;115:E11951–60. doi:10.1073/pnas.1809349115

Supplemental figures

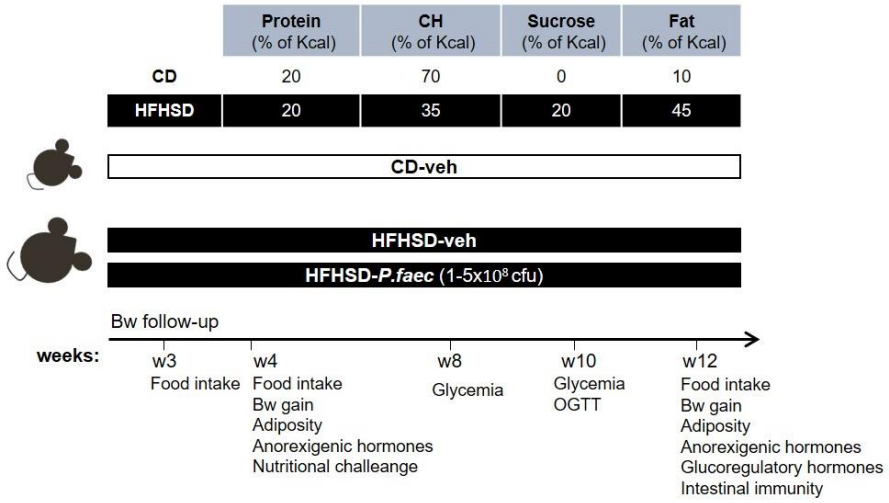

Figure S1. Schematic representation of the experimental design to evaluate the effects of *P. faecium* in obese mice.

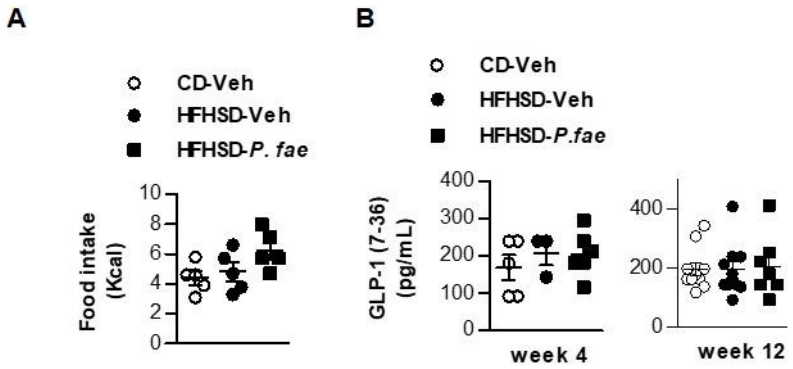

Figure S2. Food intake after fasting and GLP-1 plasma levels in HFHSD-mice fed or unfed on *P. faecium* and CD-mice. (**A**) 2h of food intake (Kcal) after fasting (n=5-6). (**B**) Plasma levels (pg/mL) of GLP-1 at week 4 (n=5-6) and 12 (n=9-10). Experimental groups abbreviations: CD-Veh, mice fed control diet and vehicle; HFHSD-Veh, obese mice fed on the high-fat-high sucrose diet (HFHSD) and receiving vehicle; HFHSD-*P. fae*, mice receiving (HFHSD) and 1-5x10^8 live cells of *P. faecium*. Data represent the mean ± SEM. Significant differences were assessed by one-way ANOVA followed by Tukey *post hoc* test.

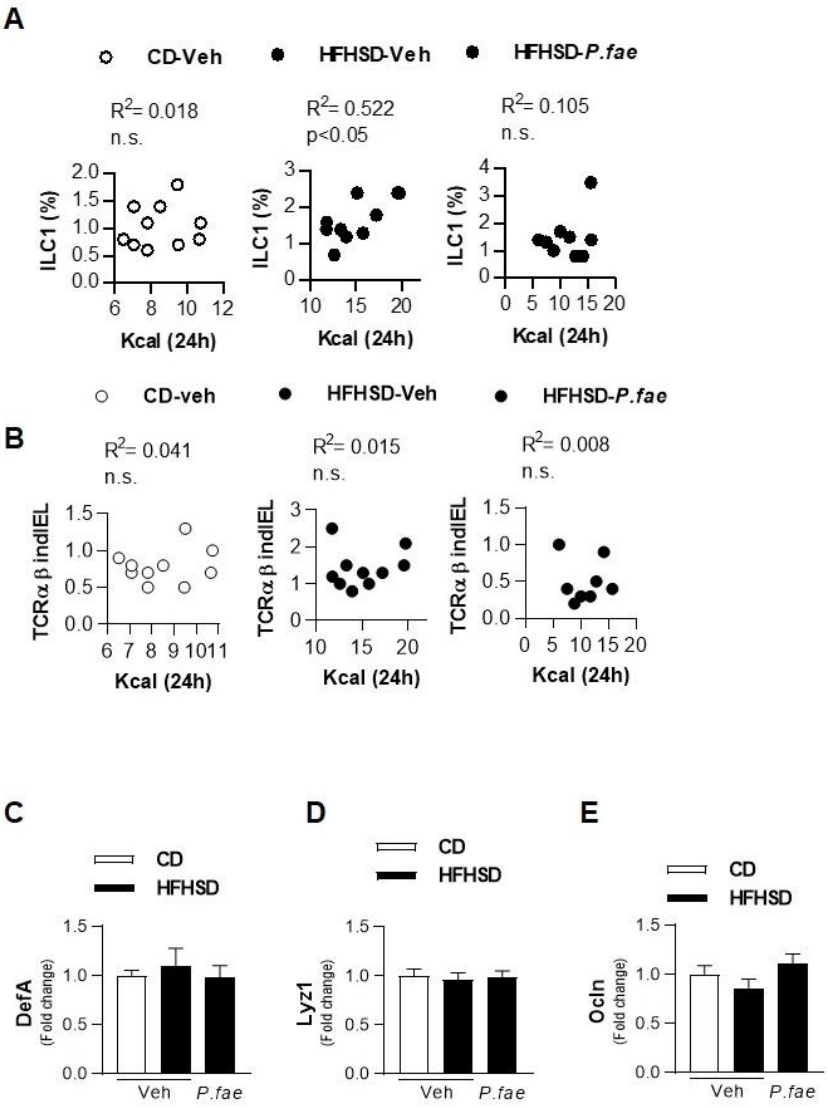

Figure S3. Evaluation of potential associations between immune cells in the intestinal epithelium and food intake and expression of molecular markers of intestinal epithelial defense and integrity. (**A**) Correlation between ILC1 percentages in epithelium and food intake (Kcal) for 24h (n=9-10)**.** (**B**) Correlation between TCRαβ induced IEL percentages in epithelium and food intake (Kcal) for 24h (n=9-10)**.** (**C-E**) mRNA levels of *DefA*, *Lyz1* and *Cldn3* in ileum (n=9-10). Experimental groups abbreviations: control mice (CD-fed mice receiving vehicle) and obese mice (HFHSD-fed mice receiving either vehicle or 1-5x10^8 live cells of *P. faecium)* at 12 weeks. Data represent the

mean ± SEM. Statistical significance was assessed by one-way ANOVA followed by Tukey *post hoc* test.

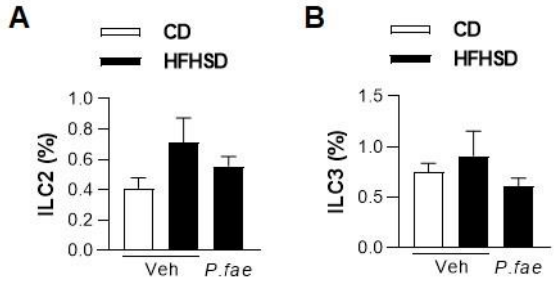

Figure S4. Levels of innate lymphoid cells type 2 and type 3 in the lamina propria. (**A**) ILC2 (percentage of ILC2+ cells of the total lamina propria cells) in the small intestine (n=9-10). (**B**) ILC3 (percentage of ILC3+ cells of the total lamina propria cells) in the small intestine (n=9-10). Data represent the mean ± SEM. Statistical significance was assessed by one-way ANOVA followed by Tukey *post hoc* test.

DISCUSIÓN GENERAL

Discusión general

Los resultados de esta tesis doctoral, presentados en los dos capítulos previos, responden al objetivo general de identificar nuevas estrategias basadas en la manipulación de la microbiota intestinal eficaces contra la obesidad, así como sus mecanismos de acción a través de interacciones con el huésped y la dieta.

La siguiente figura muestra un resumen de los diferentes estudios llevados a cabo durante la tesis, así como los principales resultados y contribuciones científicas realizadas.

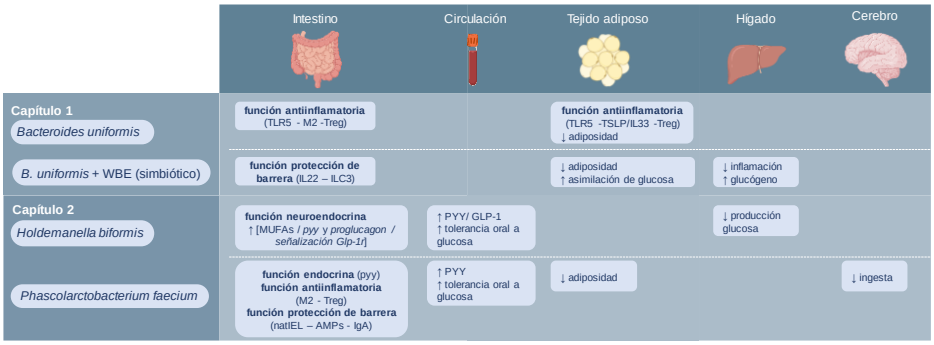

Figura 2: Representación esquemática de los principales resultados de los estudios incluidos en la tesis doctoral.

El primer capítulo de la tesis engloba dos estudios preclínicos que describen los mecanismos de acción de *Bacteroides uniformis* CECT 7771 sobre el sistema inmune y los efectos de una intervención combinando dicha bacteria y una fibra dietética (simbiótico) para mejorar su eficacia en el tratamiento de la obesidad y sus comorbilidades.

El primer estudio del capítulo 1 deriva de la necesidad de profundizar en los mecanismos de acción de *B. uniformis* CECT 7771 cuyos efectos anti-obesigénicos fueron previamente demostrados por nuestro grupo en un ensayo preclínico [227]. En este estudio previo se demuestra la capacidad de *B. uniformis* para mejorar la respuesta *in vitro* de macrófagos aislados del peritoneo al LPS y la de células dendríticas derivadas de la médula ósea en ratones obesos.

En base a estas evidencias y al importante papel de la inmunidad en mantener la función barrera intestinal y la sensibilidad a insulina, desarrollamos

el primer estudio de esta tesis en el que evaluamos la función de *B. uniformis* CECT 7771 en la regulación de la inmunidad en el eje intestino-tejido adiposo, como posible mecanismo de acción que subyace a sus efectos beneficiosos frente a la obesidad y el metabolismo de la glucosa.

Este estudio aporta nuevas evidencias a las ya proporcionadas por Gauffin y colaboradores [227] ya que, mediante el análisis de poblaciones celulares de las placas de Peyer, por citometría de flujo, hemos identificado tipos celulares específicamente influidos por *B. uniformis* CECT 7771. En particular, esta cepa de *B. uniformis* reduce el estado proinflamatorio intestinal asociado a la ingesta de la dieta rica en grasa y azúcares simples y caracterizado por un aumento de macrófagos de tipo M1, la citocina efectora IFNγ y las células B, al promover una respuesta antiinflamatoria mediada principalmente por marófagos de tipo M2, células Treg y la producción de la citocina IL-10. Curiosamente, este efecto se reproduce en el tejido adiposo visceral sugiriendo un papel clave de *B. uniformis* en la regulación del tono inflamatorio a lo largo del eje intestino-tejido adiposo. Un análisis más específico de componentes inmunes en el tejido adiposo destaca que *B. uniformis* incrementa la señalización mediada por TSLP e IL-33, citocinas directamente involucradas en la activación y proliferación de Treg e ILC2 [240–242]. Esta respuesta de tipo 2 podría ser la responsable de inhibir las señales inflamatorias producidas por la dieta rica en grasa, como la mediada por M1, y como consecuencia mejorar la sensibilidad a la insulina [243].

Este estudio también destaca el papel de TLR5 como mediador de la señalización inmune en el eje intestino-tejido adiposo, al demostrar que tanto los metabolitos fecales asociados a la intervención con *B. uniformis* como la propia bacteria activan el TLR5, que está inhibido en obesidad.

Además, en línea con los estudios de Gauffin y colaboradores y en una intervención más larga (14 semanas frente a 8 semanas de Gauffin *et al*) hemos reproducido los beneficios de *B. uniformis* sobre el fenotipo metabólico en el contexto de la obesidad, incluyendo la reducción de la ganancia de peso corporal, los niveles de colesterol, triglicéridos, glucosa y leptina; y la mejora de la tolerancia oral a glucosa.

Finalmente, este estudio genera nuevas cuestiones por resolver como la identificación del componente de *B. uniformis* que actúa como agonista de TLR5, ya que su genoma no contiene genes que codifiquen flagelina, así como la demostración de que *B. uniformis* requiere TLR5 como señal esencial para mantener la comunicación inmune entre el intestino y el tejido adiposo responsable de mantener la sensibilidad a insulina y por tanto prevenir el desarrollo de obesidad.

El segundo estudio del capítulo 1 se centra en mejorar la eficacia de la cepa *B. uniformis* CECT 7771 y facilitar su uso reduciendo la dosis necesaria y, por tanto, los esfuerzos necesarios para su producción.

Para ello, se realizó una intervención simbiótica integrada por dicha bacteria y una fibra para promover su crecimiento y potenciar su actividad metabólica. En comparación con otras fuentes de carbono, *B. uniformis* CECT 7771 presenta un crecimiento *in vitro* más rápido en presencia de extracto de salvado de trigo (WBE), el cual contiene un alto contenido en oligosacáridos de arabinoxilano (AXOS) [244]. En estudios de intervención en humanos este tipo de fibra presenta efectos metabólicos beneficiosos, principalmente sobre la homeostasis de la glucosa, y promueve el crecimiento de bacterias productoras de butirato [201,245].

Los resultados de este estudio demuestran que la combinación de *B. uniformis* y WBE produce beneficios aditivos en la ganancia de peso y la adiposidad en ratones obesos en relación a los efectos de las intervenciones con *B. uniformis* o con la fibra, administrados de manera individual. En este sentido, se destaca que la fórmula combinada restaura las rutas metabólicas insulinodependientes. En particular, en el tejido adiposo promueve la lipogénesis de novo consumiendo glucosa, tal y como indican marcadores lipogénicos (*Acc* y *Fas*) y el factor de transcripción que regula su expresión y que es activado por glucosa (*Chrebpα*) [246]. En el hígado, incrementa los depósitos de glucógeno. Sin embargo, esta señalización más bien explicaría la mejor asimilación de glucosa por los tejidos y no tanto una menor adiposidad. La combinación simbiótica parece impedir la absorción intestinal del ácido esteárico (18:0), uno de los ácidos grasos saturados más abundantes de la dieta, lo cual podría estar implicado en la menor adiposidad asociada, ya que no estimula las rutas de degradación de ácidos grasos como la termogénesis o la β-oxidación que, sin embargo, están activadas por la dieta rica en grasa, posiblemente como mecanismo para contrarrestar el exceso de energía.

Por otra parte, este estudio también indica que la cepa *B. uniformis* CECT 7771 es la principal responsable de los efectos de las distintas intervenciones en la homeostasis de glucosa, ya que, a pesar de ser administrada a una dosis más baja (una unidad logarítmica menor respecto al estudio anterior), es capaz de mejorar la tolerancia oral a glucosa, así como la expresión de *Gck* y su producto enzimático G6P en hígado, paso clave en la captación de glucosa y su incorporación en rutas metabólicas.

Además, *B. uniformis* y WBE aumentan los niveles de butirato en el contenido del ciego; este metabolito está involucrado, tanto en la mejora del metabolismo, como en la inmunidad. De hecho, *B. uniformis* combinado con

WBE contribuye a mantener y reforzar la homeostasis inmune intestinal al restaurar la proporción de IEL inducidos e ILC3 en el epitelio. Como consecuencia, esta intervención también atenúa la inflamación hepática al reducir la producción de la citocina inflamatoria IFNγ, posible factor causal de la resistencia a insulina, a través de una mejor señalización de IL22.

En conclusión, este estudio revela que la combinación de *B. uniformis* y WBE pueden ayudar al tratamiento de la obesidad al reforzar la primera línea de defensa inmunológica en el intestino, que protege contra las dietas poco saludables y la disbiosis asociada. Además, proporciona bases científicas que suponen un progreso en el diseño de intervenciones dietéticas más eficaces y específicas, potencialmente aplicables al manejo clínico de la obesidad.

El segundo capítulo de la tesis engloba dos estudios preclínicos que describen los efectos de *Holdemanella biformis* CECT 9752 y *Phascolarctobacterium faecium* DSM 32890, dos bacterias intestinales aisladas de heces de humanos metabólicamente sanos, como potenciales probióticos para el tratamiento de la obesidad y sus co-morbilidades.

Los resultados del primer estudio del capítulo 2 indican que la administración de *Holdemanella biformis* CECT 9752 reduce la hiperglucemia y favorece la tolerancia oral a la glucosa en ratones obesos, de manera independiente a insulina y al peso corporal. Se demuestra que *H. bifomis* actúa por mecanimos neuroendocrinos y no inmunes ya que no restaura el incremento de los niveles de linfocitos T citotóxicos inducidos por la dieta en la lámina propia y en la sangre periférica; sin embargo, la bacteria mejora los niveles circulantes de PYY y GLP-1, hormonas intestinales clave en el control de las variaciones postprandiales de la glucemia. Además, se demuestra que la intervención con *H. biformis* tiene un impacto significativo sobre las células L del colón, y no sobre las del íleon. En concreto, en el colon contribuye a estimular la expresión de *pyy* y *proglucagon* y, a través de este mecanismo, parece restaurar las concentraciones de PYY y GLP-1 en plasma. A pesar de que el efecto glucorregulador de GLP-1 se ha atribuido a la secreción de la hormona en el intestino delgado, un estudio reciente demuestra que la secreción selectiva de GLP-1 por las células L del colon también mejora la tolerancia a glucosa [247]. Además, la administración de *H. biformis* incrementa la abundancia de ácido oleico y α-linoleico en el contenido del ciego, ácidos grasos insaturados que, de manera preabsortiva, pueden actuar como secretagogos de GLP-1 [248–250]. Previamente se ha demostrado que los ácidos grasos detectados en la parte superior del intestino delgado, antes de ser absorbidos, aumentan la tolerancia a glucosa al reducir su producción endógena de manera independiente a insulina [251]. El aumento de ácidos grasos insaturados en el ciego podría deberse a una reducción en su absorción

en la parte proximal del intestino por un mecanismo todavía desconocido, directamente mediado por *H. biformis* o indirectamente favorecido por sus efectos en el ecosistema intestinal (sobre otras especies bacterianas, metabolitos, etc.). En particular, Paige V.Bauer y colaboradores revelaron un papel glucorregulador de *Lactobacillus gasseri* en la parte alta del intestino delgado, al favorecer la vía de detección de ácidos grasos dependiente de la enzima ACSL3 (Long-chain acyl-CoA synthetase 3) [251].

Por otra parte, evidencias científicas indican que el GLP-1 influye en el metabolismo de la glucosa, mediante su papel en la transmisión de señales a nivel del sistema nervioso central [252] y que sus efectos endocrinos en el cerebro pueden verse limitados debido a su rápida degradación [253]. Por ello, también exploramos la señalización paracrina de GLP-1 en el intestino delgado distal y el colon mediada por las aferencias vagales [52]. *H. biformis* parece modular la señalización de GLP-1, tanto en el íleon como en el colon, ya que influye en la expresión del receptor de GLP-1 y la periferina, marcador del sistema nervioso periférico en ambas regiones. Es destacable el efecto de *H. biformis* potenciando la señalización de GLP-1 en el íleon, el cual presenta inervaciones vagales aferentes a diferencia del colon, mostrando, al menos a nivel transcripcional, un incremento de la expresión de ambos genes. En línea con la estimulación paracrina de las aferencias vagales, en cultivos *in vitro* demostramos que *H. biformis* desporaliza neuronas del ganglio nodoso e incrementa la sensibilidad de estas neuronas a GLP-1.

Estudios previos han demotrado que GLP-1 puede reducir la producción endógena de glucosa independientemente de los niveles plasmáticos de insulina y glucagón [254,255] y mejorar la sensibilidad a la insulina [256].

Al explorar las vías metabólicas que median la homeostasis de glucosa, observamos que *H. biformis* mejora la ruta de señalización de insulina en el hígado, lo que está en concordancia con la reducción de la expresión y actividad de la G6Pasa [257], enzima limitante de la gluconeogénesis. Además, la administración de esta bacteria reduce la expresión de *Cpt1a*, gen que codifica la enzima que regula la β-oxidación y con ello los niveles de acetil-CoA, el producto final de la β-oxidación y un activador alostérico que potencia la gluconeogénesis a través de la piruvato carboxilasa [258,259]. Puesto que los hepatocitos no expresan el receptor de GLP-1, postulamos una conexión intestino-hígado mediada por la señalización vagal aferente de GLP-1 [53,260,261].

Por último, al evaluar los cambios en la comunidad microbiana intestinal observamos que el tratamiento con *H. biformis* aumenta la abundancia de especies del género *Akkermansia* y *Blautia*, relacionadas previamente con un

fenotipo metabólico saludable [164,223,224,262,263]. Además, parece reforzar la integridad de la barrera intestinal, ya que restaura las alteraciones en la expresión de proteínas de unión estrecha en el colon observadas en la obesidad.

A partir de estos resultados se plantea la necesidad de futuras investigaciones para (i) determinar si *H. biformis* indirectamente incrementa la secreción de GLP-1, al reducir la absorción en el intestino distal de sus secretagogos lipídicos y, por tanto, aumentar sus niveles preabsortivos; (ii) caracterizar en profundidad la activación de las aferencias vagales intestinales favorecida por la intervención con *H. biformis* en condiciones postprandiales, así como identificar núcleos del tronco cerebral implicados en la reducción de la producción endógena de glucosa, y (iii) explorar cual es el potential componente celular neuroactivo que actúa como modulador de la conexión intestino-cerebro a través de la vía vagal aferente. Un potencial candidato es el muramil dipéptido (MDP), componente abundante en la pared celular de bacterias Gram positivas como *H. biformis*. Cavallari y colaboradores demostraron que la inyección de MDP a ratones obesos mejora, a través de NOD2, la resistencia a la insulina y la tolerancia a la glucosa independientemente de cambios en el peso corporal [99]. Además, se ha demostrado *in vitro* que el MDP mejora la sensibilidad a GLP-1 de las neuronas entéricas [100] .

En conclusión, el efecto glucorregulador de *H. biformis* CECT 9752 a través del aumento de la sensibilidad y secreción de GLP-1, que demuestra nuestro estudio, sugiere su posible aplicación para la mejora de la diabetes tipo 2.

En el segundo estudio del capítulo 2 demostramos que *Phascolarctobacterium faecium* DSM32890 confiere resistencia a la obesidad inducida por la dieta al reducir la ingesta de alimentos y activar mecanismos anti-inflamatorios e inmunoprotectores en el intestino. Las evidencias mostradas en este trabajo resultan de gran interés, ya que la hiperfagia y la inflamación son unos de los principales procesos que contribuyen a agravar la obesidad y sus complicaciones metabólicas [27,262,264,265].

La administración diaria de *P. faecium* reduce la ingesta de alimentos tras un período corto (4 semanas) y largo (12 semanas) de exposición a la dieta hipercalórica. Debido a que estudios previos en roedores demuestran que 4 semanas de ingesta de HFD es insuficiente para desarrollar resistencia a leptina en el hipotálamo [266,267], este no parece ser el mecanismo que explique el efecto de *P. faecium* en la hiperfagia a corto plazo. Los efectos detectados a las 4 semanas probablemente se deben a una mejora en la detección de las señales activadas por los lípidos de la dieta en el hipotálamo

en el modelo de obesidad al que se administra *P. faecium* [268]. De hecho, esta bacteria tras 4 semanas de administración, ya incrementa los niveles circulantes de PYY siendo superiores a los del grupo control y dicho incremento se mantiene a las 12 semanas. Por tanto, *P. faecium* podría reducir la hiperfagia al promover la secreción de PYY en etapas tempranas de la exposición a la dieta hipercalórica, lo que a su vez supondría una mejor señalización de ácidos grasos en el hipotálamo al no haber un exceso de ingesta de lípidos. Por otro lado, el propionato podría ser un potencial ligando a través del cual *P.faecium* promueve la secreción de PYY [269] ya que es el principal producto que genera al consumir succinato [270] . Por otra parte, la supresión de la ingesta asociada a la intervención con *P. faecium* se hace evidente en la fase activa de ingesta (fase oscura), lo que sugiere que el efecto anorexigénico requiere de la interacción con los macronutrientes de la dieta.

Además, la ingesta excesiva de lípidos en la dieta induce la hipersecreción de GIP, lo que se asocia a una mayor acumulación de triglicéridos en los adipocitos y al desarrollo de resistencia a leptina a largo plazo [271]. El efecto temprano de la bacteria como supresora del apetito a través del aumento de PYY también podría ser el responsable de la reducción de los niveles de GIP y de la adiposidad observados en la semana 12 de tratamiento, como consecuencia de una reducción en la exposición a los lípidos de la dieta.

Por otra parte, *P. faecium* normaliza la inmunidad intestinal alterada por la dieta rica en grasa, reduciento la proporción de las células linfoides innatas proinflamatorias (ILC1) y de los linfocitos intraepiteliales TCRαβ (TCRαβ indIEL) y aumentando la de los macrófagos antiinflamatorios (M2).

La correlación positiva entre los niveles de ILC1 y la ingesta calórica en los ratones obesos se pierde tras la administración de la bacteria, lo que sugiere que *P. faecium* mediante el control de ingesta también modula la concentración de componentes de la dieta que activan estas células. Estos cambios también podrían ser los responsables de la reducción de los niveles de células TCRαβ indIEL, que se activan por el reconocimiento de antígenos exógenos en la periferia [272].

Estudios previos han demostrado que la desregulación de ILC1 en el tejido adiposo contribuye al desarrollo de obesidad como consecuencia de un aumento en la producción local de citocinas proinflamatorias y la polarización de los macrófagos hacia el tipo M1 [273]. En cambio, en el intestino estos cambios se han asociado con un estado proinflamatorio en pacientes con enfermedad de Crohn y enfermdad inflamatoria intestinal [274,275].

En este estudio observamos que la dieta rica en grasa aumenta la relación M1/M2 al reducir principalmente los niveles de M2; sin embargo, *P. faecium* reduce los niveles de M1 y aumenta los de M2 en la lámina propia. Por otra parte, la bacteria fortalece la función barrera intestinal y restablece la homeostasis inmunológica al aumentar los niveles de TCRγδ natIEL, la expresión de péptidos antimicrobianos, la concentración de IgA y la proporción de las células Treg, marcadores que se encuentran alterados por la dieta rica en grasa [276–279].

Con el fin de valorar la implicación de la inmunidad innata y adaptativa en los efectos inmunes de *P. faecium* sería interesante realizar estudios preclínicos con animales que carezcan de inmunidad adaptativa o de las principales células innatas implicadas, las ILC1 y los M2.

Uno de los vínculos de unión entre la inmunidad innata y adaptativa son los receptores de reconocimiento de moléculas microbianas llamados Toll-like receptors (TLR). La activación de estos receptores media una gran variedad de respuestas inflamatorias, además, estudios realizados en ratones deficientes en TLR5 respaldan su papel en el metabolismo del hospedador [175,280]. En este estudio, observamos que la admistración oral de *P. faecium* aumenta significativamente la expresión del TLR5 en el intestino delgado en comparación con ratones controles y obesos. Este podría ser el mediador molecular por el que la bacteria regula los niveles de Treg [281] y M2 [282] y, por lo tanto, restaura la homeostasis inmunitaria.

El receptor inmune innato TLR5 se activa por flagelina bacteriana, la secuenciación del genoma completo de *P. faecium* ha confirmado que carece de genes que codifiquen para esta proteína [283] por lo que sugerimos que el aumento en los niveles de TLR5 se deben a los cambios en el ecosistema intestinal. La administración de *P.faecium* modifica la composición de la microbiota alterada por la dieta rica en grasa y aumenta la concentación de especies bacterianas asociadas a un fenotipo metabólico sano y a la protección de la barrera intestinal, como *Akkermansia muciniphila* [222,224,284]. Además, la producción de succinado por *A.muciniphila* [285] podría estar favoreciendo el crecimiento de *P.faecium* y sus efectos sobre la obesidad. Por ello, resutaría de gran interés determinar la existencia de rutas metabólicas que expliquen una posible simbiosis entre estas especies bacterianas y que, a su vez, puedan mediar efectos sinérgicos o aditivos en el metabolismo del huésped.

En conclusión, los dos estudios del capítulo 2 aportan nueva información sobre cepas de dos especies bacterianas del intestino humano nunca estudiadas hasta la fecha en el contexto de la obesidad. Además, los resultados mostrados evidencian la especificidad de las bacterias en su

interacción con el huésped y su modo de acción y sugieren la posibilidad de utilizarlas como suplemento para preventir o mitigar la obesidad y condiciones clínicas asociadas. En este sentido, nuestros resultados sugieren que *H. biformis* podría ser adecuada para la prevención o tratamiento de la diabetes tipo 2, especialmente en aquellos pacientes que muestren una señalización defectuosa por GLP-1. Por otro lado, *P. faecium* podría ser apropiada para sujetos con sobrepeso y/u obesidad con patrones de ingesta y marcadores inflamatorios alterados.

CONCLUSIONES

Conclusiones

1. *Bacteroides uniformis* CECT 7771 reduce la obesidad y las alteraciones metabólicas (intolerancia a glucosa) inducidas por una dieta hipercalórica en ratones, en parte, a través de sus propiedas inmunoreguladoras. En el intestino esta cepa aumenta la proporción de macrófagos antiinflamatorios (M2) con respecto a los proinflamatorios (M1) y las Treg y la citocina antiinflmatoria IL-10; y en el tejido adiposo incrementa la concentración de TSLP e IL-33, implicadas en la activación y proliferación de Treg e ILC2 y reducción de la activación de macrófagos M1, reduciendo el estado de inflamación asociado a la obesidad. El TLR5 parece ser el mediador molecular que podría explicar la activación de esta respuesta antiinflamatoria, en la vía de comunicación entre el intestino y el tejido adiposo.

2. La combinación de *Bacteroides uniformis* CECT 7771 con una fibra dietética, rica en arabinoxilanos de salvado de trigo, amplia los efectos inmunometabólicos en relación a los que ejercen individualmente. Esta combinación de ingredientes produce beneficios metabólicos aditivos en: (i) la reducción del peso y la adiposidad en ratones obesos; (ii) la lipogénesis de novo en el tejido adiposo y (iii) el almacenamiento de glucosa en forma de glucógeno en el hígado. La combinación de la bacteria y la fibra también permite recuperar la homeostasis inmunológica en el intestino, al restaurar la proporción de IEL inducidos e ILC3, mecanismo en el que puede estar implicado el butirato. Esta intervención también atenúa la inflamación hepática al reducir la producción de IFNγ, factor causante de la resistencia a insulina, a través de una mejora en la señalización de IL22.

3. *Holdemanella biformis* CECT9752 mejora la tolerancia oral a glucosa en ratones alimentados con una dieta hipercalórica de forma independiente a la insulina. Este efecto parece estar mediado por aumentos en los niveles plasmáticos de las hormonas gastrointestinales GLP-1 y PYY, necesarias para el mantenimiento de las variaciones postprandiales de glucosa y la sensibilidad a insulina. El aumento de ácidos grasos monoinsaturados detectado en el ciego, que podrían actuar como secretagogos de GLP-1, podría explicar el incremento de esta hormona en plasma. Además, en el intestino delgado distal, la bacteria promueve la señalización paracrina de GLP-1 en las inervaciones aferentes, mecanismo implicado en la comunicación intestino-cerebro de control de la producción endógena de glucosa. *H. biformis* CECT9752 también incrementa la abundancia de especies de los géneros *Akkermansia* o *Blautia,*

asociadas a una mejor salud metabólica, que podrían ser mediadores de parte de sus efectos en la obesidad.

4. *Phascolarctobacterium faecium* DSM32890 mitiga la obesidad y sus complicaciones metabólicas mediante mecanismos enteroendocrinos e inmunitarios en ratones alimentados con una dieta hipercalórica. Los efectos enteroendocrinos de *P. faecium* se relacionan con su capacidad para reducir la hiperfagia de los ratones obesos a través de un aumento de la concentración plasmática de PYY, que se observa en etapas tempranas de exposición a la dieta. En relación a su capacidad inmunomoduladora *P. faecium:* (i) normaliza la inmunidad intestinal alterada por la dieta rica en grasa al restaurar los niveles de ILC1, los M2 y los TCRαβ indIEL y (ii) fortalece la función barrera intestinal y restablece la homeostasis inmunológica al aumentar los niveles de TCRγδ natIEL, la expresión de péptidos antimicrobianos, la concentración de IgA y las células Treg. Por último, *P. faecium* aumenta los niveles *Akkermansia muciniphila,* que a su vez pueden estar contribuyendo en sus beneficios metabólicos.

BIBLIOGRAFÍA
(Introducción y Discusión General)

Bibliografía (Introducción y discusión general)

1 Hruby A, Hu FB. The Epidemiology of Obesity: A Big Picture. *PharmacoEconomics* 2015;**33**:673–89. doi:10.1007/s40273-014-0243-x

2 Andolfi C, Fisichella PM. Epidemiology of Obesity and Associated Comorbidities. *Journal of Laparoendoscopic & Advanced Surgical Techniques* 2018;**28**:919–24. doi:10.1089/lap.2018.0380

3 World Health Organization (WHO). Global Strategy on Diet, Physical Activity and Health. 2004.https://www.who.int/dietphysicalactivity/strategy/eb11344/strategy_english_web.pdf

4 Statistical Office of the European Communities. *Sustainable development in the European Union: overview of progress towards the SDGs in an EU context.* 2019.

5 Romieu I, Dossus L, Barquera S, *et al.* Energy balance and obesity: what are the main drivers? *Cancer Causes Control* 2017;**28**:247–58. doi:10.1007/s10552-017-0869-z

6 Heymsfield SB, Wadden TA. Mechanisms, Pathophysiology, and Management of Obesity. *N Engl J Med* 2017;**376**:254–66. doi:10.1056/NEJMra1514009

7 González-Muniesa P, Mártinez-González M-A, Hu FB, *et al.* Obesity. *Nat Rev Dis Primers* 2017;**3**:17034. doi:10.1038/nrdp.2017.34

8 Frayling TM, Timpson NJ, Weedon MN, *et al.* A Common Variant in the FTO Gene Is Associated with Body Mass Index and Predisposes to Childhood and Adult Obesity. 2007;**316**:7.

9 Pigeyre M, Yazdi FT, Kaur Y, *et al.* Recent progress in genetics, epigenetics and metagenomics unveils the pathophysiology of human obesity. *Clinical Science* 2016;**130**:943–86. doi:10.1042/CS20160136

10 El-Sayed Moustafa JS, Froguel P. From obesity genetics to the future of personalized obesity therapy. *Nat Rev Endocrinol* 2013;**9**:402–13. doi:10.1038/nrendo.2013.57

11 Nicolaidis S. Environment and obesity. *Metabolism Clinical and Experimental* 2019;:5.

12 Aygun AD, Gungor S, Ustundag B, *et al.* Proinflammatory Cytokines and Leptin Are Increased in Serum of Prepubertal Obese Children. *Mediators of Inflammation* 2005;**2005**:180–3. doi:10.1155/MI.2005.180

13 Deshmane SL, Kremlev S, Amini S, *et al.* Monocyte chemoattractant protein-1 (MCP-1): an overview. *J Interferon Cytokine Res* 2009;**29**:313–26. doi:10.1089/jir.2008.0027

14 Goyal R, Faizy AF, Siddiqui SS, *et al.* Evaluation of TNF-α and IL-6 Levels in Obese and Non-obese Diabetics: Pre- and Postinsulin Effects. *N Am J Med Sci* 2012;**4**:180–4. doi:10.4103/1947-2714.94944

15 Jung C, Gerdes N, Fritzenwanger M, *et al.* Circulating Levels of Interleukin-1 Family Cytokines in Overweight Adolescents. *Mediators of Inflammation* 2010;**2010**:1–6. doi:10.1155/2010/958403

16 Poitou C, Dalmas E, Renovato M, *et al.* CD14dimCD16+ and CD14+CD16+ monocytes in obesity and during weight loss: relationships with fat mass and subclinical atherosclerosis. *Arterioscler Thromb Vasc Biol* 2011;**31**:2322–30. doi:10.1161/ATVBAHA.111.230979

17 Schmidt FM, Weschenfelder J, Sander C, *et al.* Inflammatory Cytokines in General and Central Obesity and Modulating Effects of Physical Activity. *PLoS ONE* 2015;**10**:e0121971. doi:10.1371/journal.pone.0121971

18 Chan KL, Pillon NJ, Sivaloganathan DM, *et al.* Palmitoleate Reverses High Fat-induced Proinflammatory Macrophage Polarization via AMP-activated Protein Kinase (AMPK). *Journal of Biological Chemistry* 2015;**290**:16979–88. doi:10.1074/jbc.M115.646992

19 Kim K-A, Gu W, Lee I-A, *et al.* High Fat Diet-Induced Gut Microbiota Exacerbates Inflammation and Obesity in Mice via the TLR4 Signaling Pathway. *PLoS ONE* 2012;**7**:e47713. doi:10.1371/journal.pone.0047713

20 Nunemaker CS, Chung HG, Verrilli GM, *et al.* Increased serum CXCL1 and CXCL5 are linked to obesity, hyperglycemia, and impaired islet function. *Journal of Endocrinology* 2014;**222**:267–76. doi:10.1530/JOE-14-0126

21 Athie-Morales V, Smits HH, Cantrell DA, *et al.* Sustained IL-12 Signaling Is Required for Th1 Development. *The Journal of Immunology* 2004;**172**:61–9. doi:10.4049/jimmunol.172.1.61

22 Martinez FO, Gordon S. The M1 and M2 paradigm of macrophage activation: time for reassessment. *F1000Prime Rep* 2014;**6**. doi:10.12703/P6-13

23 Lumeng CN, Bodzin JL, Saltiel AR. Obesity induces a phenotypic switch in adipose tissue macrophage polarization. *J Clin Invest* 2007;**117**:175–84. doi:10.1172/JCI29881

24 McLaughlin T, Liu L-F, Lamendola C, *et al.* T-Cell Profile in Adipose Tissue is Associated with Insulin Resistance and Systemic Inflammation in Humans. *Arterioscler Thromb Vasc Biol* 2014;**34**:2637–43. doi:10.1161/ATVBAHA.114.304636

25 Delano MJ, Kelly-Scumpia KM, Thayer TC, *et al.* Neutrophil Mobilization from the Bone Marrow during Polymicrobial Sepsis Is Dependent on CXCL12 Signaling. *JI* 2011;**187**:911–8. doi:10.4049/jimmunol.1100588

26 Shi C, Pamer EG. Monocyte recruitment during infection and inflammation. *Nat Rev Immunol* 2011;**11**:762–74. doi:10.1038/nri3070

27 Sanz Y, Moya-Pérez A. Microbiota, Inflammation and Obesity. In: Lyte M, Cryan JF, eds. *Microbial Endocrinology: The Microbiota-Gut-Brain Axis in Health and Disease*. New York, NY: : Springer New York 2014. 291–317. doi:10.1007/978-1-4939-0897-4_14

28 Kojta I, Chacińska M, Błachnio-Zabielska A. Obesity, Bioactive Lipids, and Adipose Tissue Inflammation in Insulin Resistance. *Nutrients* 2020;**12**:1305. doi:10.3390/nu12051305

29 Jansen HJ, Vervoort GM, van der Graaf M, *et al.* Liver fat content is linked to inflammatory changes in subcutaneous adipose tissue in type 2 diabetes patients. *Clin Endocrinol* 2013;:n/a-n/a. doi:10.1111/cen.12105

30 Lackey DE, Olefsky JM. Regulation of metabolism by the innate immune system. *Nat Rev Endocrinol* 2016;**12**:15–28. doi:10.1038/nrendo.2015.189

31 Miller AA, Spencer SJ. Obesity and neuroinflammation: A pathway to cognitive impairment. *Brain, Behavior, and Immunity* 2014;**42**:10–21. doi:10.1016/j.bbi.2014.04.001

32 Bonaz B, Bazin T, Pellissier S. The Vagus Nerve at the Interface of the Microbiota-Gut-Brain Axis. *Front Neurosci* 2018;**12**:49. doi:10.3389/fnins.2018.00049

33 Waise TMZ, Dranse HJ, Lam TKT. The metabolic role of vagal afferent innervation. *Nature Reviews Gastroenterology & Hepatology* 2018;**15**:625–36. doi:10.1038/s41575-018-0062-1

34 Coll AP, Farooqi IS, O'Rahilly S. The Hormonal Control of Food Intake. *Cell* 2007;**129**:251–62. doi:10.1016/j.cell.2007.04.001

35 Nogueiras R, Wiedmer P, Perez-Tilve D, *et al.* The central melanocortin system directly controls peripheral lipid metabolism. *J Clin Invest* 2007;**117**:3475–88. doi:10.1172/JCI31743

36 de Lartigue G. Role of the vagus nerve in the development and treatment of diet-induced obesity: The role of the vagus nerve in obesity. *J Physiol* 2016;**594**:5791–815. doi:10.1113/JP271538

37 Daly DM, Park SJ, Valinsky WC, *et al.* Impaired intestinal afferent nerve satiety signalling and vagal afferent excitability in diet induced obesity in the mouse: Impaired afferent satiety signalling in obesity. *The Journal of Physiology* 2011;**589**:2857–70. doi:10.1113/jphysiol.2010.204594

38 Kentish S, Li H, Philp LK, *et al.* Diet-induced adaptation of vagal afferent function: Adaptation of afferent function. *The Journal of Physiology* 2012;**590**:209–21. doi:10.1113/jphysiol.2011.222158

39 Gribble FM, Reimann F. Enteroendocrine Cells: Chemosensors in the Intestinal Epithelium. *Annu Rev Physiol* 2016;**78**:277–99. doi:10.1146/annurev-physiol-021115-105439

40 Rasoamanana R, Darcel N, Fromentin G, *et al.* Nutrient sensing and signalling by the gut. *Proc Nutr Soc* 2012;**71**:446–55. doi:10.1017/S0029665112000110

41 Martin AM, Sun EW, Rogers GB, *et al.* The Influence of the Gut Microbiome on Host Metabolism Through the Regulation of Gut Hormone Release. *Front Physiol* 2019;**10**:428. doi:10.3389/fphys.2019.00428

42 Bauer PV, Hamr SC, Duca FA. Regulation of energy balance by a gut–brain axis and involvement of the gut microbiota. *Cell Mol Life Sci* 2016;**73**:737–55. doi:10.1007/s00018-015-2083-z

43 Kreymann B, Ghatei MA, Williams G, *et al.* GLUCAGON-LIKE PEPTIDE-1 7-36: A PHYSIOLOGICAL INCRETIN IN MAN. *The Lancet* 1987;**330**:1300–4. doi:10.1016/S0140-6736(87)91194-9

44 Turton MD, O'Shea D, Gunn I, *et al.* A role for glucagon-like peptide-1 in the central regulation of feeding. *Nature* 1996;**379**:69–72. doi:10.1038/379069a0

45 Fonseca FR de, Navarro M, Alvarez E, *et al.* Peripheral versus central effects of glucagon-like peptide-1 receptor agonists on satiety and body weight loss in Zucker obese rats. *Metabolism - Clinical and Experimental* 2000;**49**:709–17. doi:10.1053/meta.2000.6251

46 Phillips LK, Deane AM, Jones KL, *et al.* Gastric emptying and glycaemia in health and diabetes mellitus. *Nat Rev Endocrinol* 2015;**11**:112–28. doi:10.1038/nrendo.2014.202

47 Deane AM, Nguyen NQ, Stevens JE, *et al.* Endogenous Glucagon-Like Peptide-1 Slows Gastric Emptying in Healthy Subjects, Attenuating Postprandial Glycemia. *The Journal of Clinical Endocrinology & Metabolism* 2010;**95**:215–21. doi:10.1210/jc.2009-1503

48 Mannucci E, Ognibene A, Cremasco F, *et al.* Glucagon-like peptide (GLP)-1 and leptin concentrations in obese patients with Type 2 diabetes mellitus. *Diabet Med* 2000;**17**:713–9. doi:10.1046/j.1464-5491.2000.00367.x

49 Vilsbøll T, Krarup T, Deacon CF, *et al.* Reduced Postprandial Concentrations of Intact Biologically Active Glucagon-Like Peptide 1 in Type 2 Diabetic Patients. 2001;**50**:5.

50 Duca FA, Katebzadeh S, Covasa M. Impaired GLP-1 signaling contributes to reduced sensitivity to duodenal nutrients in obesity-prone rats during high-fat feeding: Intestinal Nutrients and Obesity. *Obesity* 2015;**23**:2260–8. doi:10.1002/oby.21231

51 Duca FA, Sakar Y, Covasa M. Combination of Obesity and High-Fat Feeding Diminishes Sensitivity to GLP-1R Agonist Exendin-4. *Diabetes* 2013;**62**:2410–5. doi:10.2337/db12-1204

52 Krieger J-P, Langhans W, Lee SJ. Vagal mediation of GLP-1's effects on food intake and glycemia. *Physiology & Behavior* 2015;**152**:372–80. doi:10.1016/j.physbeh.2015.06.001

53 Yang M, Wang J, Wu S, *et al.* Duodenal GLP-1 signaling regulates hepatic glucose production through a PKC-δ-dependent neurocircuitry. *Cell Death Dis* 2017;**8**:e2609–e2609. doi:10.1038/cddis.2017.28

54 Madsbad S. The role of glucagon-like peptide-1 impairment in obesity and potential therapeutic implications. *Diabetes Obes Metab* 2014;**16**:9–21. doi:10.1111/dom.12119

55 Abbott CR, Monteiro M, Small CJ, *et al.* The inhibitory effects of peripheral administration of peptide YY3–36 and glucagon-like peptide-1 on food intake are attenuated by ablation of the vagal–brainstem–hypothalamic pathway. *Brain Research* 2005;**1044**:127–31. doi:10.1016/j.brainres.2005.03.011

56 Sanz Y, De Palma G. Gut microbiota and probiotics in modulation of epithelium and gut-associated lymphoid tissue function. *Int Rev Immunol* 2009;**28**:397–413. doi:10.3109/08830180903215613

57 Mann T, Tomiyama AJ, Westling E, *et al.* Medicare's search for effective obesity treatments: Diets are not the answer. *American Psychologist* 2007;**62**:220–33. doi:10.1037/0003-066X.62.3.220

58 Pories WJ. Bariatric Surgery: Risks and Rewards. *J Clin Endocrinol Metab* 2008;**93**:S89–96. doi:10.1210/jc.2008-1641

59 Schacke H, Docke W-D, Asadullah K. Mechanisms involved in the side effects of glucocorticoids. 2002;:21.

60 Shoelson SE, Lee J, Goldfine AB. Inflammation and insulin resistance. *J Clin Invest* 2006;**116**:1793–801. doi:10.1172/JCI29069

61 Drucker DJ, Habener JF, Holst JJ. Discovery, characterization, and clinical development of the glucagon-like peptides. *Journal of Clinical Investigation* 2017;**127**:4217–27. doi:10.1172/JCI97233

62 Juhl CB, Hollingdal M, Sturis J, *et al.* Bedtime Administration of NN2211, a Long-Acting GLP-1 Derivative, Substantially Reduces Fasting and Postprandial Glycemia in Type 2 Diabetes. *Diabetes* 2002;**51**:424–9. doi:10.2337/diabetes.51.2.424

63 Madsbad S, Schmitz O, Ranstam J, *et al.* Improved Glycemic Control With No Weight Increase in Patients With Type 2 Diabetes After Once-Daily Treatment With the Long-Acting Glucagon-Like Peptide 1 Analog Liraglutide (NN2211): A 12-week, double-blind, randomized, controlled trial. *Diabetes Care* 2004;**27**:1335–42. doi:10.2337/diacare.27.6.1335

64 Sisley S, Gutierrez-Aguilar R, Scott M, *et al.* Neuronal GLP1R mediates liraglutide's anorectic but not glucose-lowering effect. *J Clin Invest* 2014;**124**:2456–63. doi:10.1172/JCI72434

65 Astrup A, Rössner S, Van Gaal L, *et al.* Effects of liraglutide in the treatment of obesity: a randomised, double-blind, placebo-controlled study. *The Lancet* 2009;**374**:1606–16. doi:10.1016/S0140-6736(09)61375-1

66 Quarta C, Clemmensen C, Zhu Z, *et al.* Molecular Integration of Incretin and Glucocorticoid Action Reverses Immunometabolic Dysfunction and Obesity. *Cell Metabolism* 2017;**26**:620-632.e6. doi:10.1016/j.cmet.2017.08.023

67 Drucker DJ. Mechanisms of Action and Therapeutic Application of Glucagon-like Peptide-1. *Cell Metab* 2018;**27**:740–56. doi:10.1016/j.cmet.2018.03.001

68 Rothschild D, Weissbrod O, Barkan E, *et al.* Environment dominates over host genetics in shaping human gut microbiota. *Nature* 2018;**555**:210–5. doi:10.1038/nature25973

69 Sonnenburg JL, Bäckhed F. Diet–microbiota interactions as moderators of human metabolism. *Nature* 2016;**535**:56–64. doi:10.1038/nature18846

70 Martinez KB, Leone V, Chang EB. Western diets, gut dysbiosis, and metabolic diseases: Are they linked? *Gut Microbes* 2017;**8**:130–42. doi:10.1080/19490976.2016.1270811

71 Zeng MY, Inohara N, Nuñez G. Mechanisms of inflammation-driven bacterial dysbiosis in the gut. *Mucosal Immunol* 2017;**10**:18–26. doi:10.1038/mi.2016.75

72 Clarke G, Stilling RM, Kennedy PJ, *et al.* Minireview: Gut Microbiota: The Neglected Endocrine Organ. *Molecular Endocrinology* 2014;**28**:1221–38. doi:10.1210/me.2014-1108

73 Gill SR, Pop M, DeBoy RT, *et al.* Metagenomic Analysis of the Human Distal Gut Microbiome. *Science* 2006;**312**:1355–9. doi:10.1126/science.1124234

74 Qin J, Li R, Raes J, *et al.* A human gut microbial gene catalogue established by metagenomic sequencing. *Nature* 2010;**464**:59–65. doi:10.1038/nature08821

75 Sanz Y. Microbiome and Gluten. *Ann Nutr Metab* 2015;**67**:27–42. doi:10.1159/000440991

76 Claesson MJ, Cusack S, O'Sullivan O, *et al.* Composition, variability, and temporal stability of the intestinal microbiota of the elderly. *Proceedings of the National Academy of Sciences* 2011;**108**:4586–91. doi:10.1073/pnas.1000097107

77 Donaldson GP, Lee SM, Mazmanian SK. Gut biogeography of the bacterial microbiota. *Nat Rev Microbiol* 2016;**14**:20–32. doi:10.1038/nrmicro3552

78 Tropini C, Earle KA, Huang KC, *et al.* The Gut Microbiome: Connecting Spatial Organization to Function. *Cell Host & Microbe* 2017;**21**:433–42. doi:10.1016/j.chom.2017.03.010

79 Valdes AM, Walter J, Segal E, *et al.* Role of the gut microbiota in nutrition and health. *BMJ* 2018;:k2179. doi:10.1136/bmj.k2179

80 Cani PD, Everard A, Duparc T. Gut microbiota, enteroendocrine functions and metabolism. *Current Opinion in Pharmacology* 2013;**13**:935–40. doi:10.1016/j.coph.2013.09.008

81 Belkaid Y, Harrison OJ. Homeostatic Immunity and the Microbiota. *Immunity* 2017;**46**:562–76. doi:10.1016/j.immuni.2017.04.008

82 Louis P, Hold GL, Flint HJ. The gut microbiota, bacterial metabolites and colorectal cancer. *Nat Rev Microbiol* 2014;**12**:661–72. doi:10.1038/nrmicro3344

83 Flint HJ, Scott KP, Duncan SH, *et al.* Microbial degradation of complex carbohydrates in the gut. *Gut Microbes* 2012;**3**:289–306. doi:10.4161/gmic.19897

84 Woo V, Alenghat T. Host–microbiota interactions: epigenomic regulation. *Current Opinion in Immunology* 2017;**44**:52–60. doi:10.1016/j.coi.2016.12.001

85 Sleeth ML, Thompson EL, Ford HE, *et al.* Free fatty acid receptor 2 and nutrient sensing: a proposed role for fibre, fermentable carbohydrates and short-chain fatty acids in appetite regulation. *Nutr Res Rev* 2010;**23**:135–45. doi:10.1017/S0954422410000089

86 Byndloss MX, Olsan EE, Rivera-Chávez F, *et al.* Microbiota-activated PPAR-g signaling inhibits dysbiotic Enterobacteriaceae expansion. 2017;:7.

87 Cani PD, Knauf C. How gut microbes talk to organs: The role of endocrine and nervous routes. *Mol Metab* 2016;**5**:743–52. doi:10.1016/j.molmet.2016.05.011

88 Weitkunat K, Stuhlmann C, Postel A, *et al.* Short-chain fatty acids and inulin, but not guar gum, prevent diet-induced obesity and insulin resistance through differential mechanisms in mice. *Sci Rep* 2017;**7**:6109. doi:10.1038/s41598-017-06447-x

89 Canfora EE, Jocken JW, Blaak EE. Short-chain fatty acids in control of body weight and insulin sensitivity. *Nat Rev Endocrinol* 2015;**11**:577–91. doi:10.1038/nrendo.2015.128

90 Hu J, Lin S, Zheng B, *et al.* Short-chain fatty acids in control of energy metabolism. *Crit Rev Food Sci Nutr* 2018;**58**:1243–9. doi:10.1080/10408398.2016.1245650

91 Li Z, Yi C-X, Katiraei S, *et al.* Butyrate reduces appetite and activates brown adipose tissue via the gut-brain neural circuit. *Gut* 2018;**67**:1269–79. doi:10.1136/gutjnl-2017-314050

92 Sahuri-Arisoylu M, Brody LP, Parkinson JR, *et al.* Reprogramming of hepatic fat accumulation and “browning” of adipose tissue by the short-chain fatty acid acetate. *Int J Obes* 2016;**40**:955–63. doi:10.1038/ijo.2016.23

93 De Vadder F, Kovatcheva-Datchary P, Goncalves D, *et al.* Microbiota-Generated Metabolites Promote Metabolic Benefits via Gut-Brain Neural Circuits. *Cell* 2014;**156**:84–96. doi:10.1016/j.cell.2013.12.016

94 De Vadder F, Kovatcheva-Datchary P, Zitoun C, *et al.* Microbiota-Produced Succinate Improves Glucose Homeostasis via Intestinal Gluconeogenesis. *Cell Metabolism* 2016;**24**:151–7. doi:10.1016/j.cmet.2016.06.013

95 Dalile B, Van Oudenhove L, Vervliet B, *et al.* The role of short-chain fatty acids in microbiota–gut–brain communication. *Nat Rev Gastroenterol Hepatol* 2019;**16**:461–78. doi:10.1038/s41575-019-0157-3

96 Chimerel C, Emery E, Summers DK, *et al.* Bacterial Metabolite Indole Modulates Incretin Secretion from Intestinal Enteroendocrine L Cells. *Cell Reports* 2014;**9**:1202–8. doi:10.1016/j.celrep.2014.10.032

97 Lund ML, Sorrentino G, Egerod KL, *et al.* L-Cell Differentiation Is Induced by Bile Acids Through GPBAR1 and Paracrine GLP-1 and Serotonin Signaling. *Diabetes* 2020;**69**:614–23. doi:10.2337/db19-0764

98 Lebrun LJ, Lenaerts K, Kiers D, *et al.* Enteroendocrine L Cells Sense LPS after Gut Barrier Injury to Enhance GLP-1 Secretion. *Cell Reports* 2017;**21**:1160–8. doi:10.1016/j.celrep.2017.10.008

99 Cavallari JF, Fullerton MD, Duggan BM, *et al.* Muramyl Dipeptide-Based Postbiotics Mitigate Obesity-Induced Insulin Resistance via IRF4. *Cell Metabolism* 2017;**25**:1063-1074.e3. doi:10.1016/j.cmet.2017.03.021

100 Grasset E, Puel A, Charpentier J, *et al.* A Specific Gut Microbiota Dysbiosis of Type 2 Diabetic Mice Induces GLP-1 Resistance through an Enteric NO-Dependent and Gut-Brain Axis Mechanism. *Cell Metabolism* 2017;**25**:1075-1090.e5. doi:10.1016/j.cmet.2017.04.013

101 Tolhurst G, Heffron H, Lam YS, *et al.* Short-Chain Fatty Acids Stimulate Glucagon-Like Peptide-1 Secretion via the G-Protein-Coupled Receptor FFAR2. *Diabetes* 2012;**61**:364–71. doi:10.2337/db11-1019

102 Harach T, Pols TWH, Nomura M, *et al.* TGR5 potentiates GLP-1 secretion in response to anionic exchange resins. *Sci Rep* 2012;**2**:430. doi:10.1038/srep00430

103 Buckley MM, O'Brien R, Brosnan E, *et al.* Glucagon-Like Peptide-1 Secreting L-Cells Coupled to Sensory Nerves Translate Microbial Signals to the Host Rat Nervous System. *Front Cell Neurosci* 2020;**14**:95. doi:10.3389/fncel.2020.00095

104 Barrett E, Ross RP, O'Toole PW, *et al.* γ-Aminobutyric acid production by culturable bacteria from the human intestine. *J Appl Microbiol* 2012;**113**:411–7. doi:10.1111/j.1365-2672.2012.05344.x

105 Bravo JA, Forsythe P, Chew MV, *et al.* Ingestion of Lactobacillus strain regulates emotional behavior and central GABA receptor expression in a mouse via the vagus nerve. *Proceedings of the National Academy of Sciences* 2011;**108**:16050–5. doi:10.1073/pnas.1102999108

106 Asano Y, Hiramoto T, Nishino R, *et al.* Critical role of gut microbiota in the production of biologically active, free catecholamines in the gut lumen of mice. *American Journal of Physiology-Gastrointestinal and Liver Physiology* 2012;**303**:G1288–95. doi:10.1152/ajpgi.00341.2012

107 Pokusaeva K, Johnson C, Luk B, *et al.* GABA-producing Bifidobacterium dentium modulates visceral sensitivity in the intestine. *Neurogastroenterol Motil* 2017;**29**. doi:10.1111/nmo.12904

108 Tsavkelova EA, Botvinko IV, Kudrin VS, *et al.* Detection of neurotransmitter amines in microorganisms with the use of high-performance liquid chromatography. *Dokl Biochem* 2000;**372**:115–7.

109 Reigstad CS, Salmonson CE, Iii JFR, *et al.* Gut microbes promote colonic serotonin production through an effect of short-chain fatty acids on enterochromaffin cells. *FASEB j* 2015;**29**:1395–403. doi:10.1096/fj.14-259598

110 Yano JM, Yu K, Donaldson GP, *et al.* Indigenous Bacteria from the Gut Microbiota Regulate Host Serotonin Biosynthesis. *Cell* 2015;**161**:264–76. doi:10.1016/j.cell.2015.02.047

111 Nankova BB, Agarwal R, MacFabe DF, *et al.* Enteric Bacterial Metabolites Propionic and Butyric Acid Modulate Gene Expression, Including CREB-Dependent Catecholaminergic Neurotransmission, in PC12 Cells - Possible Relevance to Autism Spectrum Disorders. *PLoS ONE* 2014;**9**:e103740. doi:10.1371/journal.pone.0103740

112 Frost G, Sleeth ML, Sahuri-Arisoylu M, *et al.* The short-chain fatty acid acetate reduces appetite via a central homeostatic mechanism. *Nat Commun* 2014;**5**:3611. doi:10.1038/ncomms4611

113 van den Pol AN. Weighing the Role of Hypothalamic Feeding Neurotransmitters. *Neuron* 2003;**40**:1059–61. doi:10.1016/S0896-6273(03)00809-2

114 Tecott LH. Serotonin and the orchestration of energy balance. *Cell Metab* 2007;**6**:352–61. doi:10.1016/j.cmet.2007.09.012

115 Berglund ED, Liu C, Sohn J-W, *et al.* Serotonin 2C receptors in pro-opiomelanocortin neurons regulate energy and glucose homeostasis. *J Clin Invest* 2014;**124**:1868. doi:10.1172/JCI75669

116 Mao Y-K, Kasper DL, Wang B, *et al.* Bacteroides fragilis polysaccharide A is necessary and sufficient for acute activation of intestinal sensory neurons. *Nat Commun* 2013;**4**:1465. doi:10.1038/ncomms2478

117 Collins J, Borojevic R, Verdu EF, *et al.* Intestinal microbiota influence the early postnatal development of the enteric nervous system. *Neurogastroenterol Motil* 2014;**26**:98–107. doi:10.1111/nmo.12236

118 Arrieta M-C, Stiemsma LT, Amenyogbe N, *et al.* The Intestinal Microbiome in Early Life: Health and Disease. *Front Immunol* 2014;**5**. doi:10.3389/fimmu.2014.00427

119 Martin R, Nauta A, Ben Amor K, *et al.* Early life: gut microbiota and immune development in infancy. *Beneficial Microbes* 2010;**1**:367–82. doi:10.3920/BM2010.0027

120 McLoughlin K, Schluter J, Rakoff-Nahoum S, *et al.* Host Selection of Microbiota via Differential Adhesion. *Cell Host & Microbe* 2016;**19**:550–9. doi:10.1016/j.chom.2016.02.021

121 Sicard J-F, Le Bihan G, Vogeleer P, *et al.* Interactions of Intestinal Bacteria with Components of the Intestinal Mucus. *Front Cell Infect Microbiol* 2017;**7**:387. doi:10.3389/fcimb.2017.00387

122 Gallo RL, Hooper LV. Epithelial antimicrobial defence of the skin and intestine. *Nat Rev Immunol* 2012;**12**:503–16. doi:10.1038/nri3228

123 Pabst O, Slack E. IgA and the intestinal microbiota: the importance of being specific. *Mucosal Immunol* 2020;**13**:12–21. doi:10.1038/s41385-019-0227-4

124 Wells JM, Rossi O, Meijerink M, *et al.* Epithelial crosstalk at the microbiota-mucosal interface. *Proceedings of the National Academy of Sciences* 2011;**108**:4607–14. doi:10.1073/pnas.1000092107

125 Shi C, Jia T, Mendez-Ferrer S, *et al.* Bone Marrow Mesenchymal Stem and Progenitor Cells Induce Monocyte Emigration in Response to Circulating Toll-like Receptor Ligands. *Immunity* 2011;**34**:590–601. doi:10.1016/j.immuni.2011.02.016

126 Trompette A, Gollwitzer ES, Yadava K, *et al.* Gut microbiota metabolism of dietary fiber influences allergic airway disease and hematopoiesis. *Nat Med* 2014;**20**:159–66. doi:10.1038/nm.3444

127 Iwamura C, Bouladoux N, Belkaid Y, *et al.* Sensing of the microbiota by NOD1 in mesenchymal stromal cells regulates murine hematopoiesis. *Blood* 2017;**129**:171–6. doi:10.1182/blood-2016-06-723742

128 Belkaid Y, Hand TW. Role of the Microbiota in Immunity and Inflammation. *Cell* 2014;**157**:121–41. doi:10.1016/j.cell.2014.03.011

129 Weiner HL, da Cunha AP, Quintana F, *et al.* Oral tolerance: Basic mechanisms and applications of oral tolerance. *Immunological Reviews* 2011;**241**:241–59. doi:10.1111/j.1600-065X.2011.01017.x

130 Chistiakov DA, Bobryshev YV, Kozarov E, *et al.* Intestinal mucosal tolerance and impact of gut microbiota to mucosal tolerance. *Front Microbiol* 2015;**5**. doi:10.3389/fmicb.2014.00781

131 Round JL, Mazmanian SK. Inducible Foxp3+ regulatory T-cell development by a commensal bacterium of the intestinal microbiota. *Proceedings of the National Academy of Sciences* 2010;**107**:12204–9. doi:10.1073/pnas.0909122107

132 Kawamoto S, Maruya M, Kato LM, *et al.* Foxp3+ T Cells Regulate Immunoglobulin A Selection and Facilitate Diversification of Bacterial Species Responsible for Immune Homeostasis. *Immunity* 2014;**41**:152–65. doi:10.1016/j.immuni.2014.05.016

133 Jeon SG, Kayama H, Ueda Y, *et al.* Probiotic Bifidobacterium breve Induces IL-10-Producing Tr1 Cells in the Colon. *PLoS Pathog* 2012;**8**:e1002714. doi:10.1371/journal.ppat.1002714

134 Fanning S, Hall LJ, Cronin M, *et al.* Bifidobacterial surface-exopolysaccharide facilitates commensal-host interaction through immune modulation and pathogen protection. *Proceedings of the National Academy of Sciences* 2012;**109**:2108–13. doi:10.1073/pnas.1115621109

135 Ivanov II, Atarashi K, Manel N, *et al.* Induction of Intestinal Th17 Cells by Segmented Filamentous Bacteria. *Cell* 2009;**139**:485–98. doi:10.1016/j.cell.2009.09.033

136 Littman DR, Rudensky AY. Th17 and Regulatory T Cells in Mediating and Restraining Inflammation. *Cell* 2010;**140**:845–58. doi:10.1016/j.cell.2010.02.021

137 Tan TG, Sefik E, Geva-Zatorsky N, *et al.* Identifying species of symbiont bacteria from the human gut that, alone, can induce intestinal Th17 cells in mice. *Proc Natl Acad Sci USA* 2016;**113**:E8141–50. doi:10.1073/pnas.1617460113

138 Chelakkot C, Choi Y, Kim D-K, *et al.* Akkermansia muciniphila-derived extracellular vesicles influence gut permeability through the regulation of tight junctions. *Exp Mol Med* 2018;**50**:e450–e450. doi:10.1038/emm.2017.282

139 Wesemann DR, Portuguese AJ, Meyers RM, *et al.* Microbial colonization influences early B-lineage development in the gut lamina propria. *Nature* 2013;**501**:112–5. doi:10.1038/nature12496

140 Fransen F, Zagato E, Mazzini E, *et al.* BALB/c and C57BL/6 Mice Differ in Polyreactive IgA Abundance, which Impacts the Generation of Antigen-Specific IgA and Microbiota Diversity. *Immunity* 2015;**43**:527–40. doi:10.1016/j.immuni.2015.08.011

141 Arpaia N, Campbell C, Fan X, *et al.* Metabolites produced by commensal bacteria promote peripheral regulatory T-cell generation. *Nature* 2013;**504**:451–5. doi:10.1038/nature12726

142 Smith PM, Howitt MR, Panikov N, *et al.* The Microbial Metabolites, Short-Chain Fatty Acids, Regulate Colonic Treg Cell Homeostasis. *Science* 2013;**341**:569–73. doi:10.1126/science.1241165

143 Corrêa-Oliveira R, Fachi JL, Vieira A, *et al.* Regulation of immune cell function by short-chain fatty acids. *Clin Trans Immunol* 2016;**5**:e73. doi:10.1038/cti.2016.17

144 Zelante T, Iannitti RG, Cunha C, *et al.* Tryptophan Catabolites from Microbiota Engage Aryl Hydrocarbon Receptor and Balance Mucosal Reactivity via Interleukin-22. *Immunity* 2013;**39**:372–85. doi:10.1016/j.immuni.2013.08.003

145 Hepworth MR, Fung TC, Masur SH, *et al.* Group 3 innate lymphoid cells mediate intestinal selection of commensal bacteria–specific CD4+ T cells. *Science* 2015;**348**:1031–5. doi:10.1126/science.aaa4812

146 Wang L, Zhu L, Qin S. Gut Microbiota Modulation on Intestinal Mucosal Adaptive Immunity. *Journal of Immunology Research* 2019;**2019**:1–10. doi:10.1155/2019/4735040

147 McDonald BD, Jabri B, Bendelac A. Diverse developmental pathways of intestinal intraepithelial lymphocytes. *Nat Rev Immunol* 2018;**18**:514–25. doi:10.1038/s41577-018-0013-7

148 Cervantes-Barragan L, Chai JN, Tianero MD, *et al.* Lactobacillus reuteri induces gut intraepithelial CD4+CD8aa+ T cells. 2017;:6.

149 Ismail AS, Behrendt CL, Hooper LV. Reciprocal Interactions between Commensal Bacteria and γδ Intraepithelial Lymphocytes during Mucosal Injury. *J Immunol* 2009;**182**:3047–54. doi:10.4049/jimmunol.0802705

150 Ismail AS, Severson KM, Vaishnava S, *et al.* intraepithelial lymphocytes are essential mediators of host-microbial homeostasis at the intestinal mucosal surface. *Proceedings of the National Academy of Sciences* 2011;**108**:8743–8. doi:10.1073/pnas.1019574108

151 Erny D, Hrabě de Angelis AL, Jaitin D, *et al.* Host microbiota constantly control maturation and function of microglia in the CNS. *Nat Neurosci* 2015;**18**:965–77. doi:10.1038/nn.4030

152 Xu H, Liu M, Cao J, *et al.* The Dynamic Interplay between the Gut Microbiota and Autoimmune Diseases. *Journal of Immunology Research* 2019;**2019**:1–14. doi:10.1155/2019/7546047

153 Wostmann BS, Larkin C, Moriarty A, *et al.* Dietary intake, energy metabolism, and excretory losses of adult male germfree Wistar rats. *Lab Anim Sci* 1983;**33**:46–50.

154 Bäckhed F, Manchester JK, Semenkovich CF, *et al.* Mechanisms underlying the resistance to diet-induced obesity in germ-free mice. *Proc Natl Acad Sci U S A* 2007;**104**:979–84. doi:10.1073/pnas.0605374104

155 Ellekilde M, Selfjord E, Larsen CS, *et al.* Transfer of gut microbiota from lean and obese mice to antibiotic-treated mice. *Sci Rep* 2014;**4**:5922. doi:10.1038/srep05922

156 Ridaura VK, Faith JJ, Rey FE, *et al.* Gut Microbiota from Twins Discordant for Obesity Modulate Metabolism in Mice. *Science* 2013;**341**:1241214. doi:10.1126/science.1241214

157 Ley RE, Bäckhed F, Turnbaugh P, *et al.* Obesity alters gut microbial ecology. *PNAS* 2005;**102**:11070–5. doi:10.1073/pnas.0504978102

158 Ravussin Y, Koren O, Spor A, *et al.* Responses of gut microbiota to diet composition and weight loss in lean and obese mice. *Obesity (Silver Spring)* 2012;**20**:738–47. doi:10.1038/oby.2011.111

159 Ley RE, Turnbaugh PJ, Klein S, *et al.* Human gut microbes associated with obesity. *Nature* 2006;**444**:1022–3. doi:10.1038/4441022a

160 Sze MA, Schloss PD. Looking for a Signal in the Noise: Revisiting Obesity and the Microbiome. *mBio* 2016;**7**. doi:10.1128/mBio.01018-16

161 Armougom F, Henry M, Vialettes B, *et al.* Monitoring bacterial community of human gut microbiota reveals an increase in Lactobacillus in obese

patients and Methanogens in anorexic patients. *PLoS One* 2009;**4**:e7125. doi:10.1371/journal.pone.0007125

162 Million M, Thuny F, Angelakis E, *et al.* Lactobacillus reuteri and Escherichia coli in the human gut microbiota may predict weight gain associated with vancomycin treatment. *Nutr Diabetes* 2013;**3**:e87. doi:10.1038/nutd.2013.28

163 Million M, Angelakis E, Paul M, *et al.* Comparative meta-analysis of the effect of Lactobacillus species on weight gain in humans and animals. *Microb Pathog* 2012;**53**:100–8. doi:10.1016/j.micpath.2012.05.007

164 Dao MC, Everard A, Aron-Wisnewsky J, *et al.* Akkermansia muciniphila and improved metabolic health during a dietary intervention in obesity: relationship with gut microbiome richness and ecology. *Gut* 2016;**65**:426–36. doi:10.1136/gutjnl-2014-308778

165 Mulders RJ, de Git KCG, Schéle E, *et al.* Microbiota in obesity: interactions with enteroendocrine, immune and central nervous systems. *Obes Rev* 2018;**19**:435–51. doi:10.1111/obr.12661

166 Turnbaugh PJ, Ley RE, Mahowald MA, *et al.* An obesity-associated gut microbiome with increased capacity for energy harvest. 2006;**444**:5.

167 Semova I, Carten JD, Stombaugh J, *et al.* Microbiota Regulate Intestinal Absorption and Metabolism of Fatty Acids in the Zebrafish. *Cell Host & Microbe* 2012;**12**:277–88. doi:10.1016/j.chom.2012.08.003

168 Araújo JR, Tazi A, Burlen-Defranoux O, *et al.* Fermentation Products of Commensal Bacteria Alter Enterocyte Lipid Metabolism. *Cell Host & Microbe* 2020;**27**:358-375.e7. doi:10.1016/j.chom.2020.01.028

169 Lin H, An Y, Hao F, *et al.* Correlations of Fecal Metabonomic and Microbiomic Changes Induced by High-fat Diet in the Pre-Obesity State. *Scientific Reports* 2016;**6**:21618. doi:10.1038/srep21618

170 Chakaroun RM, Massier L, Kovacs P. Gut Microbiome, Intestinal Permeability, and Tissue Bacteria in Metabolic Disease: Perpetrators or Bystanders? *Nutrients* 2020;**12**. doi:10.3390/nu12041082

171 Lee MS, Kim Y-J. Signaling pathways downstream of pattern-recognition receptors and their cross talk. *Annu Rev Biochem* 2007;**76**:447–80. doi:10.1146/annurev.biochem.76.060605.122847

172 Cani PD, Amar J, Iglesias MA, *et al.* Metabolic endotoxemia initiates obesity and insulin resistance. *Diabetes* 2007;**56**:1761–72. doi:10.2337/db06-1491

173 Poggi M, Bastelica D, Gual P, *et al.* C3H/HeJ mice carrying a toll-like receptor 4 mutation are protected against the development of insulin resistance in white adipose tissue in response to a high-fat diet. *Diabetologia* 2007;**50**:1267–76. doi:10.1007/s00125-007-0654-8

174 Ehses JA, Meier DT, Wueest S, *et al.* Toll-like receptor 2-deficient mice are protected from insulin resistance and beta cell dysfunction induced by a high-fat diet. *Diabetologia* 2010;**53**:1795–806. doi:10.1007/s00125-010-1747-3

175 Vijay-Kumar M, Aitken JD, Carvalho FA, *et al.* Metabolic Syndrome and Altered Gut Microbiota in Mice Lacking Toll-Like Receptor 5. *Science* 2010;**328**:228–31. doi:10.1126/science.1179721

176 Hong C-P, Yun CH, Lee G-W, *et al.* TLR9 regulates adipose tissue inflammation and obesity-related metabolic disorders: TLR9 Regulates Obesity-Associated Inflammation. *Obesity* 2015;**23**:2199–206. doi:10.1002/oby.21215

177 Braniste V, Al-Asmakh M, Kowal C, *et al.* The gut microbiota influences blood-brain barrier permeability in mice. *Science Translational Medicine* 2014;**6**:263ra158-263ra158. doi:10.1126/scitranslmed.3009759

178 D'Mello C, Le T, Swain MG. Cerebral Microglia Recruit Monocytes into the Brain in Response to Tumor Necrosis Factorα Signaling during Peripheral Organ Inflammation. *J Neurosci* 2009;**29**:2089–102. doi:10.1523/JNEUROSCI.3567-08.2009

179 Waise TMZ, Toshinai K, Naznin F, *et al.* One-day high-fat diet induces inflammation in the nodose ganglion and hypothalamus of mice. *Biochem Biophys Res Commun* 2015;**464**:1157–62. doi:10.1016/j.bbrc.2015.07.097

180 Le Thuc O, Stobbe K, Cansell C, *et al.* Hypothalamic Inflammation and Energy Balance Disruptions: Spotlight on Chemokines. *Front Endocrinol* 2017;**8**. doi:10.3389/fendo.2017.00197

181 de Git KCG, Adan R a. H. Leptin resistance in diet-induced obesity: the role of hypothalamic inflammation. *Obes Rev* 2015;**16**:207–24. doi:10.1111/obr.12243

182 de La Serre CB, de Lartigue G, Raybould HE. Chronic exposure to low dose bacterial lipopolysaccharide inhibits leptin signaling in vagal afferent neurons. *Physiol Behav* 2015;**139**:188–94. doi:10.1016/j.physbeh.2014.10.032

183 Blüher M. Obesity: global epidemiology and pathogenesis. *Nat Rev Endocrinol* 2019;**15**:288–98. doi:10.1038/s41574-019-0176-8

184 Gérard P. Gut microbiota and obesity. *Cell Mol Life Sci* 2016;**73**:147–62. doi:10.1007/s00018-015-2061-5

185 Gibson GR, Roberfroid MB. Dietary Modulation of the Human Colonic Microbiota: Introducing the Concept of Prebiotics. *The Journal of Nutrition* 1995;**125**:1401–12. doi:10.1093/jn/125.6.1401

186 Benítez-Páez A, Gómez Del Pulgar EM, Kjølbæk L, *et al.* Impact of dietary fiber and fat on gut microbiota re-modeling and metabolic health. *Trends in Food Science & Technology* 2016;**57**:201–12. doi:10.1016/j.tifs.2016.11.001

187 Gibson GR, Hutkins R, Sanders ME, *et al.* Expert consensus document: The International Scientific Association for Probiotics and Prebiotics (ISAPP) consensus statement on the definition and scope of prebiotics. *Nat Rev Gastroenterol Hepatol* 2017;**14**:491–502. doi:10.1038/nrgastro.2017.75

188 Portune KJ, Benítez-Páez A, Del Pulgar EMG, *et al.* Gut microbiota, diet, and obesity-related disorders-The good, the bad, and the future challenges. *Mol Nutr Food Res* 2017;**61**:1600252. doi:10.1002/mnfr.201600252

189 Paulina Markowiak, Katarzyna Śliżewska. Effects of Probiotics, Prebiotics, and Synbiotics on Human Health. *Nutrients* 2017;**9**:1021. doi:10.3390/nu9091021

190 Quigley EMM, Gajula P. Recent advances in modulating the microbiome. *F1000Res* 2020;**9**:46. doi:10.12688/f1000research.20204.1

191 Davani-Davari D, Negahdaripour M, Karimzadeh I, *et al.* Prebiotics: Definition, Types, Sources, Mechanisms, and Clinical Applications. *Foods* 2019;**8**:92. doi:10.3390/foods8030092

192 Shokryazdan P, Faseleh Jahromi M, Navidshad B, *et al.* Effects of prebiotics on immune system and cytokine expression. *Med Microbiol Immunol* 2017;**206**:1–9. doi:10.1007/s00430-016-0481-y

193 Flint HJ, Duncan SH, Scott KP, *et al.* Links between diet, gut microbiota composition and gut metabolism. *Proc Nutr Soc* 2015;**74**:13–22. doi:10.1017/S0029665114001463

194 Scientific Opinion on the substantiation of health claims related to konjac mannan (glucomannan) and reduction of body weight (ID 854, 1556, 3725), reduction of post-prandial glycaemic responses (ID 1559), maintenance of normal blood glucose concentrations (ID 835, 3724), maintenance of normal (fasting) blood concentrations of triglycerides (ID 3217), maintenance of normal blood cholesterol concentrations (ID 3100, 3217), maintenance of normal bowel function (ID 834, 1557, 3901) and decreasing

potentially pathogenic gastro-intestinal microorganisms (ID 1558) pursuant to Article 13(1) of Regulation (EC) No 1924/2006. *EFSA Journal* doi:10.2903/j.efsa.2010.1798

195 Dewulf EM, Cani PD, Claus SP, *et al.* Insight into the prebiotic concept: lessons from an exploratory, double blind intervention study with inulin-type fructans in obese women. *Gut* 2013;**62**:1112–21. doi:10.1136/gutjnl-2012-303304

196 Hume MP, Nicolucci AC, Reimer RA. Prebiotic supplementation improves appetite control in children with overweight and obesity: a randomized controlled trial. *Am J Clin Nutr* 2017;**105**:790–9. doi:10.3945/ajcn.116.140947

197 Vulevic J, Juric A, Tzortzis G, *et al.* A Mixture of trans-Galactooligosaccharides Reduces Markers of Metabolic Syndrome and Modulates the Fecal Microbiota and Immune Function of Overweight Adults. *The Journal of Nutrition* 2013;**143**:324–31. doi:10.3945/jn.112.166132

198 Canfora EE, van der Beek CM, Hermes GDA, *et al.* Supplementation of Diet With Galacto-oligosaccharides Increases Bifidobacteria, but Not Insulin Sensitivity, in Obese Prediabetic Individuals. *Gastroenterology* 2017;**153**:87-97.e3. doi:10.1053/j.gastro.2017.03.051

199 Lefranc-Millot C, Guérin-Deremaux L, Wils D, *et al.* Impact of a Resistant Dextrin on Intestinal Ecology: How Altering the Digestive Ecosystem with NUTRIOSE®, a Soluble Fibre with Prebiotic Properties, May Be Beneficial for Health. *J Int Med Res* 2012;**40**:211–24. doi:10.1177/147323001204000122

200 Aliasgharzadeh A, Dehghan P, Gargari BP, *et al.* Resistant dextrin, as a prebiotic, improves insulin resistance and inflammation in women with type 2 diabetes: a randomised controlled clinical trial. *Br J Nutr* 2015;**113**:321–30. doi:10.1017/S0007114514003675

201 Kjølbæk L, Benítez-Páez A, Gómez del Pulgar EM, *et al.* Arabinoxylan oligosaccharides and polyunsaturated fatty acid effects on gut microbiota and metabolic markers in overweight individuals with signs of metabolic syndrome: A randomized cross-over trial. *Clinical Nutrition* 2020;**39**:67–79. doi:10.1016/j.clnu.2019.01.012

202 Hill C, Guarner F, Reid G, *et al.* The International Scientific Association for Probiotics and Prebiotics consensus statement on the scope and appropriate use of the term probiotic. *Nat Rev Gastroenterol Hepatol* 2014;**11**:506–14. doi:10.1038/nrgastro.2014.66

203 Neef A, Sanz Y. Future for probiotic science in functional food and dietary supplement development: *Current Opinion in Clinical Nutrition and Metabolic Care* 2013;**16**:679–87. doi:10.1097/MCO.0b013e328365c258

204 Kadooka Y, Sato M, Imaizumi K, *et al.* Regulation of abdominal adiposity by probiotics (Lactobacillus gasseri SBT2055) in adults with obese tendencies in a randomized controlled trial. *Eur J Clin Nutr* 2010;**64**:636–43. doi:10.1038/ejcn.2010.19

205 Sharafedtinov KK, Plotnikova OA, Alexeeva RI, *et al.* Hypocaloric diet supplemented with probiotic cheese improves body mass index and blood pressure indices of obese hypertensive patients - a randomized double-blind placebo-controlled pilot study. *Nutr J* 2013;**12**:138. doi:10.1186/1475-2891-12-138

206 Sáez-Lara M, Robles-Sanchez C, Ruiz-Ojeda F, *et al.* Effects of Probiotics and Synbiotics on Obesity, Insulin Resistance Syndrome, Type 2 Diabetes and Non-Alcoholic Fatty Liver Disease: A Review of Human Clinical Trials. *IJMS* 2016;**17**:928. doi:10.3390/ijms17060928

207 O'Toole PW, Marchesi JR, Hill C. Next-generation probiotics: the spectrum from probiotics to live biotherapeutics. *Nat Microbiol* 2017;**2**:17057. doi:10.1038/nmicrobiol.2017.57

208 Romaní-Pérez M, Agusti A, Sanz Y. Innovation in microbiome-based strategies for promoting metabolic health. *Current Opinion in Clinical Nutrition & Metabolic Care* 2017;**20**:484–91. doi:10.1097/MCO.0000000000000419

209 Duncan SH. Growth requirements and fermentation products of Fusobacterium prausnitzii, and a proposal to reclassify it as Faecalibacterium prausnitzii gen. nov., comb. nov. *INTERNATIONAL JOURNAL OF SYSTEMATIC AND EVOLUTIONARY MICROBIOLOGY* 2002;**52**:2141–6. doi:10.1099/ijs.0.02241-0

210 Tremaroli V, Bäckhed F. Functional interactions between the gut microbiota and host metabolism. *Nature* 2012;**489**:242–9. doi:10.1038/nature11552

211 Sokol H, Pigneur B, Watterlot L, *et al.* Faecalibacterium prausnitzii is an anti-inflammatory commensal bacterium identified by gut microbiota analysis of Crohn disease patients. *Proceedings of the National Academy of Sciences* 2008;**105**:16731–6. doi:10.1073/pnas.0804812105

212 Qiu X, Zhang M, Yang X, *et al.* Faecalibacterium prausnitzii upregulates regulatory T cells and anti-inflammatory cytokines in treating TNBS-induced colitis. *Journal of Crohn's and Colitis* 2013;**7**:e558–68. doi:10.1016/j.crohns.2013.04.002

213 Munukka E, Rintala A, Toivonen R, *et al.* Faecalibacterium prausnitzii treatment improves hepatic health and reduces adipose tissue inflammation in high-fat fed mice. *ISME J* 2017;**11**:1667–79. doi:10.1038/ismej.2017.24

214 Martín R, Chain F, Miquel S, *et al.* The Commensal Bacterium Faecalibacterium prausnitzii Is Protective in DNBS-induced Chronic Moderate and Severe Colitis Models: *Inflammatory Bowel Diseases* 2014;**20**:417–30. doi:10.1097/01.MIB.0000440815.76627.64

215 Martín R, Miquel S, Chain F, *et al.* Faecalibacterium prausnitzii prevents physiological damages in a chronic low-grade inflammation murine model. *BMC Microbiol* 2015;**15**:67. doi:10.1186/s12866-015-0400-1

216 Carlsson AH, Yakymenko O, Olivier I, *et al. Faecalibacterium prausnitzii* supernatant improves intestinal barrier function in mice DSS colitis. *Scandinavian Journal of Gastroenterology* 2013;**48**:1136–44. doi:10.3109/00365521.2013.828773

217 Wrzosek L, Miquel S, Noordine M-L, *et al.* Bacteroides thetaiotaomicron and Faecalibacterium prausnitzii influence the production of mucus glycans and the development of goblet cells in the colonic epithelium of a gnotobiotic model rodent. *BMC Biol* 2013;**11**:61. doi:10.1186/1741-7007-11-61

218 Xu Y, Wang N, Tan H-Y, *et al.* Function of Akkermansia muciniphila in Obesity: Interactions With Lipid Metabolism, Immune Response and Gut Systems. *Front Microbiol* 2020;**11**:219. doi:10.3389/fmicb.2020.00219

219 Belzer C, de Vos WM. Microbes inside—from diversity to function: the case of Akkermansia. *ISME J* 2012;**6**:1449–58. doi:10.1038/ismej.2012.6

220 Ouwerkerk JP, de Vos WM, Belzer C. Glycobiome: Bacteria and mucus at the epithelial interface. *Best Practice & Research Clinical Gastroenterology* 2013;**27**:25–38. doi:10.1016/j.bpg.2013.03.001

221 Derrien M, Belzer C, de Vos WM. Akkermansia muciniphila and its role in regulating host functions. *Microbial Pathogenesis* 2017;**106**:171–81. doi:10.1016/j.micpath.2016.02.005

222 Everard A, Belzer C, Geurts L, *et al.* Cross-talk between Akkermansia muciniphila and intestinal epithelium controls diet-induced obesity. *Proceedings of the National Academy of Sciences* 2013;**110**:9066–71. doi:10.1073/pnas.1219451110

223 Plovier H, Everard A, Druart C, *et al.* A purified membrane protein from Akkermansia muciniphila or the pasteurized bacterium improves metabolism in obese and diabetic mice. *Nat Med* 2017;**23**:107–13. doi:10.1038/nm.4236

224 Depommier C, Everard A, Druart C, *et al.* Supplementation with Akkermansia muciniphila in overweight and obese human volunteers: a proof-of-concept exploratory study. *Nat Med* 2019;**25**:1096–103. doi:10.1038/s41591-019-0495-2

225 Sánchez E, De Palma G, Capilla A, *et al.* Influence of Environmental and Genetic Factors Linked to Celiac Disease Risk on Infant Gut Colonization by Bacteroides Species. *Appl Environ Microbiol* 2011;**77**:5316–23. doi:10.1128/AEM.00365-11

226 Owen CG. Effect of Infant Feeding on the Risk of Obesity Across the Life Course: A Quantitative Review of Published Evidence. *PEDIATRICS* 2005;**115**:1367–77. doi:10.1542/peds.2004-1176

227 Gauffin Cano P, Santacruz A, Moya Á, *et al.* Bacteroides uniformis CECT 7771 Ameliorates Metabolic and Immunological Dysfunction in Mice with High-Fat-Diet Induced Obesity. *PLoS ONE* 2012;**7**:e41079. doi:10.1371/journal.pone.0041079

228 Fernández-Murga ML, Sanz Y. Safety Assessment of Bacteroides uniformis CECT 7771 Isolated from Stools of Healthy Breast-Fed Infants. *PLoS ONE* 2016;**11**:e0145503. doi:10.1371/journal.pone.0145503

229 Gómez del Pulgar EM, Benítez-Páez A, Sanz Y. Safety Assessment of Bacteroides Uniformis CECT 7771, a Symbiont of the Gut Microbiota in Infants. *Nutrients* 2020;**12**:551. doi:10.3390/nu12020551

230 Żółkiewicz J, Marzec A, Ruszczyński M, *et al.* Postbiotics-A Step Beyond Pre- and Probiotics. *Nutrients* 2020;**12**. doi:10.3390/nu12082189

231 Cencic A, Chingwaru W. The Role of Functional Foods, Nutraceuticals, and Food Supplements in Intestinal Health. *Nutrients* 2010;**2**:611–25. doi:10.3390/nu2060611

232 Hadi A, Mohammadi H, Miraghajani M, *et al.* Efficacy of synbiotic supplementation in patients with nonalcoholic fatty liver disease: A systematic review and meta-analysis of clinical trials: Synbiotic supplementation and NAFLD. *Critical Reviews in Food Science and Nutrition* 2019;**59**:2494–505. doi:10.1080/10408398.2018.1458021

233 Khalesi S, Johnson DW, Campbell K, *et al.* Effect of probiotics and synbiotics consumption on serum concentrations of liver function test enzymes: a systematic review and meta-analysis. *Eur J Nutr* 2018;**57**:2037–53. doi:10.1007/s00394-017-1568-y

234 Tabrizi R, Moosazadeh M, Lankarani KB, *et al.* The Effects of Synbiotic Supplementation on Glucose Metabolism and Lipid Profiles in Patients with Diabetes: a Systematic Review and Meta-Analysis of Randomized

Controlled Trials. *Probiotics & Antimicro Prot* 2018;**10**:329–42. doi:10.1007/s12602-017-9299-1

235 Ke X, Walker A, Haange S-B, *et al.* Synbiotic-driven improvement of metabolic disturbances is associated with changes in the gut microbiome in diet-induced obese mice. *Molecular Metabolism* 2019;**22**:96–109. doi:10.1016/j.molmet.2019.01.012

236 Swanson KS, Gibson GR, Hutkins R, *et al.* The International Scientific Association for Probiotics and Prebiotics (ISAPP) consensus statement on the definition and scope of synbiotics. *Nat Rev Gastroenterol Hepatol* 2020;**17**:687–701. doi:10.1038/s41575-020-0344-2

237 McLoughlin RF, Berthon BS, Jensen ME, *et al.* Short-chain fatty acids, prebiotics, synbiotics, and systemic inflammation: a systematic review and meta-analysis. *Am J Clin Nutr* 2017;:ajcn156265. doi:10.3945/ajcn.117.156265

238 Hibberd AA, Yde CC, Ziegler ML, *et al.* Probiotic or synbiotic alters the gut microbiota and metabolism in a randomised controlled trial of weight management in overweight adults. *Beneficial Microbes* 2019;**10**:121–35. doi:10.3920/BM2018.0028

239 Stenman LK, Lehtinen MJ, Meland N, *et al.* Probiotic With or Without Fiber Controls Body Fat Mass, Associated With Serum Zonulin, in Overweight and Obese Adults—Randomized Controlled Trial. *EBioMedicine* 2016;**13**:190–200. doi:10.1016/j.ebiom.2016.10.036

240 Mosconi I, Geuking MB, Zaiss MM, *et al.* Intestinal bacteria induce TSLP to promote mutualistic T-cell responses. *Mucosal Immunol* 2013;**6**:1157–67. doi:10.1038/mi.2013.12

241 Negishi H, Miki S, Sarashina H, *et al.* Essential contribution of IRF3 to intestinal homeostasis and microbiota-mediated Tslp gene induction. *Proceedings of the National Academy of Sciences* 2012;**109**:21016–21. doi:10.1073/pnas.1219482110

242 Molofsky AB, Savage AK, Locksley RM. Interleukin-33 in Tissue Homeostasis, Injury, and Inflammation. *Immunity* 2015;**42**:1005–19. doi:10.1016/j.immuni.2015.06.006

243 Bénézech C, Jackson-Jones LH. ILC2 Orchestration of Local Immune Function in Adipose Tissue. *Front Immunol* 2019;**10**:171. doi:10.3389/fimmu.2019.00171

244 Benítez-Páez A, Gómez del Pulgar EM, Sanz Y. The Glycolytic Versatility of Bacteroides uniformis CECT 7771 and Its Genome Response to Oligo

and Polysaccharides. *Front Cell Infect Microbiol* 2017;**7**:383. doi:10.3389/fcimb.2017.00383

245 Boll EVJ, Ekström LMNK, Courtin CM, *et al.* Effects of wheat bran extract rich in arabinoxylan oligosaccharides and resistant starch on overnight glucose tolerance and markers of gut fermentation in healthy young adults. *Eur J Nutr* 2016;**55**:1661–70. doi:10.1007/s00394-015-0985-z

246 Herman MA, Peroni OD, Villoria J, *et al.* A novel ChREBP isoform in adipose tissue regulates systemic glucose metabolism. *Nature* 2012;**484**:333–8. doi:10.1038/nature10986

247 Lewis JE. Selective stimulation of colonic L cells improves metabolic outcomes in mice. 2020;:12.

248 Hirasawa A, Tsumaya K, Awaji T, *et al.* Free fatty acids regulate gut incretin glucagon-like peptide-1 secretion through GPR120. *Nat Med* 2005;**11**:90–4. doi:10.1038/nm1168

249 Iakoubov R, Ahmed A, Lauffer LM, *et al.* Essential Role for Protein Kinase Cζ in Oleic Acid-Induced Glucagon-Like Peptide-1 Secretion in Vivo in the Rat. *Endocrinology* 2011;**152**:1244–52. doi:10.1210/en.2010-1352

250 Rocca AS, Lagreca J, Kalitsky J, *et al.* Monounsaturated Fatty Acid Diets Improve Glycemic Tolerance through Increased Secretion of Glucagon-Like Peptide-1. 2001;**142**:8.

251 Bauer PV, Duca FA, Waise TMZ, *et al.* Lactobacillus gasseri in the Upper Small Intestine Impacts an ACSL3-Dependent Fatty Acid-Sensing Pathway Regulating Whole-Body Glucose Homeostasis. *Cell Metabolism* 2018;**27**:572-587.e6. doi:10.1016/j.cmet.2018.01.013

252 Sandoval D, Sisley SR. Brain GLP-1 and insulin sensitivity. *Molecular and Cellular Endocrinology* 2015;**418**:27–32. doi:10.1016/j.mce.2015.02.017

253 Gilbert MP, Pratley RE. GLP-1 Analogs and DPP-4 Inhibitors in Type 2 Diabetes Therapy: Review of Head-to-Head Clinical Trials. *Frontiers in Endocrinology* 2020;**11**:13.

254 Sandhu H, Wiesenthal SR, MacDonald PE, *et al.* Glucagon-like peptide 1 increases insulin sensitivity in depancreatized dogs. *Diabetes* 1999;**48**:1045–53. doi:10.2337/diabetes.48.5.1045

255 Seghieri M, Rebelos E, Gastaldelli A, *et al.* Direct effect of GLP-1 infusion on endogenous glucose production in humans. *Diabetologia* 2013;**56**:156–61. doi:10.1007/s00125-012-2738-3

256 Ayala JE, Bracy DP, James FD, *et al.* The Glucagon-Like Peptide-1 Receptor Regulates Endogenous Glucose Production and Muscle Glucose Uptake Independent of Its Incretin Action. *Endocrinology* 2009;**150**:1155–64. doi:10.1210/en.2008-0945

257 Hatting M, Tavares CDJ, Sharabi K, *et al.* Insulin regulation of gluconeogenesis: Insulin regulation of gluconeogenesis. *Ann NY Acad Sci* 2018;**1411**:21–35. doi:10.1111/nyas.13435

258 Petersen MC, Vatner DF, Shulman GI. Regulation of hepatic glucose metabolism in health and disease. *Nat Rev Endocrinol* 2017;**13**:572–87. doi:10.1038/nrendo.2017.80

259 Perry RJ, Camporez J-PG, Kursawe R, *et al.* Hepatic acetyl CoA links adipose tissue inflammation to hepatic insulin resistance and type 2 diabetes. *Cell* 2015;**160**:745–58. doi:10.1016/j.cell.2015.01.012

260 Krieger J-P, Arnold M, Pettersen KG, *et al.* Knockdown of GLP-1 Receptors in Vagal Afferents Affects Normal Food Intake and Glycemia. *Diabetes* 2016;**65**:34–43. doi:10.2337/db15-0973

261 Gaykema RP, Newmyer BA, Ottolini M, *et al.* Activation of murine pre-proglucagon–producing neurons reduces food intake and body weight. *Journal of Clinical Investigation* 2017;**127**:1031–45. doi:10.1172/JCI81335

262 Benítez-Páez A, Pugar EMG del, López-Almela I, *et al.* Depletion of Blautia Species in the Microbiota of Obese Children Relates to Intestinal Inflammation and Metabolic Phenotype Worsening. *mSystems* 2020;**5**. doi:10.1128/mSystems.00857-19

263 Depommier C, Van Hul M, Everard A, *et al.* Pasteurized *Akkermansia muciniphila* increases whole-body energy expenditure and fecal energy excretion in diet-induced obese mice. *Gut Microbes* 2020;**11**:1231–45. doi:10.1080/19490976.2020.1737307

264 Yue JTY, Lam TKT. Lipid Sensing and Insulin Resistance in the Brain. *Cell Metabolism* 2012;**15**:646–55. doi:10.1016/j.cmet.2012.01.013

265 Winer DA, Luck H, Tsai S, *et al.* The Intestinal Immune System in Obesity and Insulin Resistance. *Cell Metabolism* 2016;**23**:413–26. doi:10.1016/j.cmet.2016.01.003

266 El-Haschimi K, Pierroz DD, Hileman SM, *et al.* Two defects contribute to hypothalamic leptin resistance in mice with diet-induced obesity. *J Clin Invest* 2000;**105**:1827–32. doi:10.1172/JCI9842

267 Lin S, Thomas TC, Storlien LH, *et al.* Development of high fat diet-induced obesity and leptin resistance in C57Bl/6J mice. *International Journal of Obesity* 2000;**24**:639–46. doi:10.1038/sj.ijo.0801209

268 Pocai A. Restoration of hypothalamic lipid sensing normalizes energy and glucose homeostasis in overfed rats. *Journal of Clinical Investigation* 2006;**116**:1081–91. doi:10.1172/JCI26640

269 Chambers ES, Morrison DJ, Frost G. Control of appetite and energy intake by SCFA: what are the potential underlying mechanisms? *Proc Nutr Soc* 2015;**74**:328–36. doi:10.1017/S0029665114001657

270 Ikeyama N, Murakami T, Toyoda A, *et al.* Microbial interaction between the succinate-utilizing bacterium *Phascolarctobacterium faecium* and the gut commensal *Bacteroides thetaiotaomicron*. *MicrobiologyOpen* 2020;**9**. doi:10.1002/mbo3.1111

271 Miyawaki K, Yamada Y, Ban N, *et al.* Inhibition of gastric inhibitory polypeptide signaling prevents obesity. *Nat Med* 2002;**8**:738–42. doi:10.1038/nm727

272 Olivares-Villagómez D, Van Kaer L. Intestinal Intraepithelial Lymphocytes: Sentinels of the Mucosal Barrier. *Trends Immunol* 2018;**39**:264–75. doi:10.1016/j.it.2017.11.003

273 O'Sullivan TE, Rapp M, Fan X, *et al.* Adipose-Resident Group 1 Innate Lymphoid Cells Promote Obesity-Associated Insulin Resistance. *Immunity* 2016;**45**:428–41. doi:10.1016/j.immuni.2016.06.016

274 Fuchs A, Vermi W, Lee JS, *et al.* Intraepithelial Type 1 Innate Lymphoid Cells Are a Unique Subset of IL-12- and IL-15-Responsive IFN-γ-Producing Cells. *Immunity* 2013;**38**:769–81. doi:10.1016/j.immuni.2013.02.010

275 Bernink JH, Peters CP, Munneke M, *et al.* Human type 1 innate lymphoid cells accumulate in inflamed mucosal tissues. *nature immunology* 2013;**14**:10.

276 Cheroutre H, Lambolez F, Mucida D. The light and dark sides of intestinal intraepithelial lymphocytes. *Nat Rev Immunol* 2011;**11**:445–56. doi:10.1038/nri3007

277 Everard A, Lazarevic V, Gaïa N, *et al.* Microbiome of prebiotic-treated mice reveals novel targets involved in host response during obesity. *The ISME Journal* 2014;**8**:2116–30. doi:10.1038/ismej.2014.45

278 Luck H, Khan S, Kim JH, *et al.* Gut-associated IgA+ immune cells regulate obesity-related insulin resistance. *Nat Commun* 2019;**10**:3650. doi:10.1038/s41467-019-11370-y

279 Eller K, Kirsch A, Wolf AM, *et al.* Potential Role of Regulatory T Cells in Reversing Obesity-Linked Insulin Resistance and Diabetic Nephropathy. *Diabetes* 2011;**60**:2954–62. doi:10.2337/db11-0358

280 Chassaing B, Ley RE, Gewirtz AT. Intestinal Epithelial Cell Toll-like Receptor 5 Regulates the Intestinal Microbiota to Prevent Low-Grade Inflammation and Metabolic Syndrome in Mice. *Gastroenterology* 2014;**147**:1363-1377.e17. doi:10.1053/j.gastro.2014.08.033

281 Crellin NK, Garcia RV, Hadisfar O, *et al.* Human CD4 $^{+}$ T Cells Express TLR5 and Its Ligand Flagellin Enhances the Suppressive Capacity and Expression of FOXP3 in CD4 $^{+}$ CD25 $^{+}$ T Regulatory Cells. *J Immunol* 2005;**175**:8051–9. doi:10.4049/jimmunol.175.12.8051

282 Lacavé-Lapalun J-V, Benderitter M, Linard C. Flagellin or lipopolysaccharide treatment modified macrophage populations after colorectal radiation of rats. *J Pharmacol Exp Ther* 2013;**346**:75–85. doi:10.1124/jpet.113.204040

283 Rachek S, Nikpoor N, Pulgar EMG del, *et al.* Complete Genome Sequence of Phascolarctobacterium faecium G 104, Isolated from the Stools of a Healthy Lean Donor. *Microbiol Resour Announc* 2021;**10**. doi:10.1128/MRA.01054-20

284 Cani PD, de Vos WM. Next-Generation Beneficial Microbes: The Case of Akkermansia muciniphila. *Front Microbiol* 2017;**8**:1765. doi:10.3389/fmicb.2017.01765

285 Chia LW, Hornung BVH, Aalvink S, *et al.* Deciphering the trophic interaction between Akkermansia muciniphila and the butyrogenic gut commensal Anaerostipes caccae using a metatranscriptomic approach. *Antonie van Leeuwenhoek* 2018;**111**:859–73. doi:10.1007/s10482-018-1040-x

ABREVIATURAS
(Introducción y Discusión General)

Abreviaturas

5HT	Serotonina	Serotonine
Acc	Acetil-CoA carboxilasa	acetyl-CoA carboxylase
ACSL3	Acil-CoA sintetasa 3 de cadena larga	Long-chain acetyl-CoA synthetase 3
AgRP	proteína relacionada con Agouti	Agouti-related protein
AHR	Receptor de hidrocarburo de arilo	Aryl hydrocarbon receptor
AMP	Péptidos antimicrobianos	Antimicrobial peptides
AMPc	Adenosín monofosfato cíclico	Cyclic adenosine monophosphate
ATCC	Colección americada de cultivos tipo	American type culture collection
AX	Arabinoxilanos	Arabinoxylans
AXOS	Arabinoxilo-oligosacaridos	Arabinoxylan-oligosacarides
CART	Péptido regulado por la cocaína y la anfetamina	Cocaine and amphetamine regulated transcript peptide
CCK	Colecistoquinina	Cholecystokinin
CECT	Colección Española de Cultivos tipo	Spanish type culture collection
CEEs	Células enteroendocrinas	Enteroendocrine cells
Chrebpα	Proteina de union a elementos sensiblesa carbohidratos alpha	carbohydrate responsive-element-binding protein alpha
Cpt1a	Carnitina palmitoil transferasa	Carnitine palmitoyltransferase 1a
CXCL-1	Quimiocinas con motivo C-X-C	C-X-C Motif Chemokine Ligand 1
DA	Dopamina	Dopamine
DIO	Obesidad inducida por dieta	Diet-induced obesity
EFSA	Autoridad Europea de Seguridad Alimentaria	European Food Safety Authority
Fas	Ácido graso sintetasa	Fatty acid synthase

FDA	Administración de Medicamentos y Alimentos	Food and Drug Administration
FOS	Fructooligosacáridos	Fructooligosaccharides
FTO	Proteina asociada a la masa grasa y la obesidad	Fat mass and obesity-associated protein
G6Pasa	Glucosa 6 fosfatasa	Glucose-6-phosphatase
GABA	ácido gamma aminobutírico	Gamma-aminobutyric acid
Gck	Glucoquinasa	Glucokinase
GF	Libres de gérmenes	Germ-free
GIP	Polipéptido inhibidor gástrico	Gastric inhibitory polypeptide
GLP-1	Péptido 1 similar al glucagón	Glucagón like peptide 1
GLP-1R	Receptor de GLP-1	GLP-1 receptor
GLP-2	Péptido 2 similar al glucagón	Glucagón like peptide 2
Glut4	Transportador de glucose 4	glucose transporter 4
GOS	Galactooligosacáridos	Galactooligosaccharides
GPR	Receptor acoplado a proteínas G	G protein-coupled receptors
GRAS	Generalmente reconocido como seguro	Generally Recognized as Safe
GWAS	Estudios de asociación del genoma completo	Large-scale genome wide association studies
GWAS	Estudios de asociación del genoma completo	Genome Wide Association Studies
HDAC	Histona deacetilasa	Histone deacetylases
HFD	Dieta rica en grasa	High fat diet
IELs	Linfocitos intraepiteliales intestinales	Intraepithelial lymphocytes
IFN-γ	Interferón gamma	Interferon-gamma
IgA	Inmunoglobulina A	Immunoglobulin A
IL	Ácido gamma-aminobutírico	Gamma-aminobutyric acid
ILC	Innate lymphoid cells	Células linfoides innatas

IMC	Índice de masa corporal	Body mass index
ISAPP	Asociación Científica Internacional para probióticos y prebióticos	International Scientific Asociation for Probiotics and Prebotics
JNK	Quinasa c-Jun N-terminal	C-Jun N-terminal kinase
Lep	Leptina	Leptine
Lepr	Receptor de leptina	Leptine receptor
LPS	Lipopolisacarido	Lipopolysaccharide
M1	Macrófagos proinflamatorios	Por-inflammatory macrophages
M2	Macrófagos Antiinflamatorios	Anti-inflammatory macrophages
MAPKs	Protenina quinasa activada por mitógenos	Mitogen-Activated Protein Kinases
Mc4r	Receptor 4 de melanocortina	Melanocortin-4-receptor
MCP-1	Proteina quimioatrayente de monocitos 1	Monocyte chemoattractant protein-1
MDP	Muramil dipéptido	Muramyl dipeptide
MDP	Muramil dipéptido	Muramyl dipeptide
MHCII	Complejo mayor de histocompatibilidad clase II	Mayor histocompatibility complex cass II
MSC	células mesenquimales	Mesenchymal stem cell
MUFAs	Ácidos grasos monoinsaturados	Monounsaturated fatty acids
NA	Noradrenalina	Noradrenaline
NF-κB	Factor nuclear potenciador de las cadenas ligeras kappa de las células B activadas	Nuclear factor kappa-light-chain-enhancer of activated B cells
NLR	Receptores tipo NOLL	NOLL-like receptors
NO	Óxido nítrico	Nitric oxide
NOD2	Dominio de oligomerización de unión a nucleótidos	Nucleotide-binding oligomerizacion domain containing protein 2
NPY	Neuropéptido Y	Neuropeptide Y
NTS	Núcleo del tracto solitario	Nucleus solitary tract

OXM	Oxintomodulina	Oxyntomodulin
PH	Potencial de hidrógeno	Hydrogen potencial
PMAM	Patrones moleculares asociados a microorganismos	Microorganisms associated molecular patterns
Pomc	Pro-opiomelanocortina	Proopiomelanocortin
PSA	Polisacarido A	Polysaccharide A
PYY	Péptido YY	YY peptide
QPS	Presupción calificada como segura	Qualified Presuption as Safe
RegIIIγ	Proteina de regeneración derivada de islotes III-gamma	Regenerating islet-derived protein III-gamma
RHM	Macrófagos hepáticos reclutados	Recruited hepatic macrophages
RRP	Receptores de reconocimiento de patrones	Pattern recognition receptors
SBT	Estructura basa en secuencia	Sequence-based typing
SCFA	Ácidos grasos de cadena corta	Short chain fatty acids
SFB	Bacterias filamentosas segmentadas	Segmented filamentous bacteria
SGTL1	Proteínas de transporte sodio-glucosa 1	Sodium-glucose linked transporter-1
TCR	Receptor de células T	T cell receptor
TGR5	Receptor de acidos biliares acoplado a proteínas G (GPBAR1)	G protein-coupled bile acid receptor (GPBAR1)
Th17	Células T 17 auxiliares	T helper 17 cells
TLR	Receptores tipo TOLL	TOLL-like receptors
TNF-α	Factor de necrosis tumoral alpha	Tumor necrosis factor alpha
TOS	Trans-galactooligosacáridos	Trans- galactooligosaccharides
Treg	Célula T reguladora	T regulatory cell
TSLP	O-desmetilangolensina	O-desmetylangolensin
WBE	Extracto de salvado de trigo	wheat bran extract

Lista de Publicaciones

Lista de Publicaciones

Esta tesis doctoral comprende **cuatro artículos**; uno de ellos publicado en una revista indexada (segundo artículo del capítulo 1 de la tesis), otros dos en revisión enviados a revistas indexadas (primer artículo del capítulo 1 y 2) y otro que será enviado en breve para su publicación (segundo artículo del capitulo 2 de la tesis). Además, durante el período de desarrollo de la tesis doctoral se ha contribuído también en las siguientes **publicaciones científicas**, aparte de las incluídas en la presente tesis:

- Agusti A, Garcia-Pardo MP, **Lopez-Almela I**, Campillo I, Maes M, Romani-Perez M, Sanz Y. Interplay Between the Gut-Brain Axis, Obesity and Cognitive Function. Frontiers in neuroscience. 2018;12:155.

- Benítez-Páez A, Gómez del Pugar EM, **López-Almela I**, Moya-Pérez A, Codoñer-Franch P, Sanz Y. Depletion of *Blautia* species in the microbiota of obese children relates to intestinal inflammation and metabolic phenotype worsening. mSystems.2020; 5:e00857-19.

- Liébana-García R, Olivares M, Bullich-Vilarrubias C, **López-Almela I**, Romaní-Pérez M, Sanz Y. The gut microbiota as a versatile immunomodulator in obesity and associated metabolic disorders. Best Pract Res Clin Endocrinol Met. *In Press*.

-Romaní-Pérez M, Bullich-Vilarrubias C, **López-Almela I**, Liébana R, Olivares M, Sanz Y. The microbiota and the gut-brain axis in controlling food intake and energy homeostasis. International Journal of Molecular Sience. *Under review.*

Patentes:

- Sanz Y; **López-Almela, I**; Gómez del Pulgar, Eva Mª; Benítez-Páez, A; Romaní-Pérez, M. “Bacteria de holdemanella sp. y uso de la misma”. 201831282. 26/12/2018. Consejo Superior de Investigaciones Científicas, CSIC.

- Sanz Y; **López-Almela, I**; Gómez del Pulgar, Eva Mª; Benítez-Páez, A; Romaní-Pérez, M; “*Phascolarctobacterium faecium* para la prevención y tratamiento de la obesidad y sus comorbilidades”. P201831166. 30/11/2018. Consejo Superior de Investigaciones Científicas, CSIC.

AGRADECIMIENTOS

Agradecimientos

Antes de empezar la tesis tenía claro que no iba a ser un camino sencillo, me había informado, todo el mundo me decía: “Tendrás que trabajar duro, pero aprenderás mucho y valdrá la pena”. Tenían toda la razón, pero las personas que me conocen y me han acompañado en el camino saben que esta tesis doctoral significa mucho más que eso.

Han sido 5 años intensos en los que me he formado como persona y profesional dentro del mundo apasionante de la investigación. No solo he conocido un poco más sobre mí y de lo que soy capaz, sino que también he conocido a gente increíble que me ha ayudado, enseñado y acompañado en este largo camino.

Intentaré no olvidarme de nadie…

Yolanda, gracias por darme la oportunidad de formar parte de este gran grupo, por confiar en mí y por hacerme ver que todo es posible si se tienen las ganas y la valentía de hacerlo.

A mi tutor JM Mulet y a Belén Picó, gracias por estar siempre dispuestos a ayudarme y a resolverme las dudas burocráticas.

A ti Marina, gracias por aguantarme en los días y noches de experimentos, por apoyarme en todo momento y por hacer posible que este trabajo haya salido adelante, no me cansaré de decirte que sin ti esto no hubiera sido posible.

A mi querida Mamen, gracias por estar a mi lado desde el primer momento y por estar dispuesta a escucharme y a ayudarme incondicionalmente. Has sido, eres y serás imprescindible en mi vida.

A Clara, gracias por aparecer en el 114 y querer formar parte de nuestra locura. Ha sido un placer trabajar contigo y poder aportar mi granito de arena en tu formación como investigadora.

A Claudia, gracias por nuestras confesiones en los pasillos de la primera planta y nuestras largas llamadas de teléfono. Ya sabes que siempre estaré para recordarte que todo tiene una parte positiva.

A vosotras, las chicas del lab 114-116, gracias por compartir conmigo momentos de risas y lloros, por hacerme sentir una más y por vuestra gran

contribución en el desarrollo de esta tesis. Con l@s que he compartido bancada y momentos increíbles en el IATA durante estos años (Isa, Kevin, Eva, Emanuel, Zoran, Alfonso, Victor, Marta Teresa, Marta, Lorena, Vero, Rebeca, Ana, Ana L, Gara, María Roca, Carmen, Irene, Sonia, Aitor, Miguel, Sergio….)

A Sandra (la del citómetro) por su paciencia y profesionalidad, gracias a ella, en parte, me he convertido en "la loca de los tubos". Y a todas las personas que forman el Servicio de citometría y Animalario de la Universidad de Valencia, en especial a Ana Flores e Inma Noguera.

A mis chicas del CEU, de mis principios en la investigación. Pili, mi primera compañera de bancada, gracias por enseñarme tantas cosas en el laboratorio y en la pista de baile. A Cristina, nos bastaron tres días de laboratorio para convertirnos en amigas, gracias por aconsejarme y apoyarme en esta carrera de fondo.

A Paula, la universidad nos unió y te convertiste en mi hermana "mayor". Gracias por guiarme y ayudarme en todo momento, siempre serás un pilar imprescindible en mi vida.

A mis amigas, las que desde antes de empezar esta andadura han estado a mi lado y me han animado a perseguir mis sueños. Gracias por darme las fuerzas para continuar.

A mi familia, los que han vivido de cerca todo el esfuerzo y dedicación con los que he hecho posible esta tesis. Gracias por vuestro apoyo, vuestros consejos y por todo el amor que me habéis dado. Estos 5 años nos han unido y nos han hecho mucho más fuertes. ¡Os quiero ¡

Y, por último, gracias a LAS ESTRELLAS DE MI VIDA, a mi iaio que se fue muy orgulloso al saber que había conseguido la beca para poder hacer el doctorado y a ti mamá, mi guerrera, por enseñarme que rendirse no es una opción, hay que luchar siempre.

Mi lema: Todas las dificultades, por muy malas que parezcan, tiene algo positivo, y es que te están volviendo más fuerte.